Table of Contents

Appendices

List of Abbreviations

~	Approximately
α-2-M	Alpha-2-Macroglobulin
ACN	Acetonitrile
ACV	Articular cartilage vesicle
ApoA-I	Apolipoprotein A-I
APS	Ammonium persulphate
BGE	Background Electrolyte
BGH3	Transforming growth factor-beta-induced protein ig-h3
BH_4	Tetra hydrobiopterin
BP	Bound protein
BSA	Bovine Serum Albumin
CB	Cibacron Blue
CE	Capillary Electrophoresis
CHAPS	3-[(3-cholamidopropyl)dimethylammonio]-1-propanesulfonate
COX	Cyclooxygenase
COMP	Cartilage Oligomeric Matrix Protein
CPPD	Calcium Pyrophosphate dihydrate Disease
Da	Dalton
DAMP	Damage-Associated Molecular Patterns
DAN	Diaminonaphthalene
DDR2	Discordin Domain Receptor 2
DTT	Dithiothreitol
ECM	Extracellular Matrix
EDTA	Ethylenediaminetetraacetic Acid
ELISA	Enzyme-Linked ImmunoSorbant Assay
ELLA	Ezyme-Linked Lectin Assays
EM	Electro-Microscopy
ER	Endoplasmic Reticulum
ESCRT	Endosomal Sorting Complex Required For Transport
ESI	Electro-spray ionisation
FAD	Flavin Adenine Dinucleotide
Fc	Fragment, crystallisable
FMN	Flavin Mononucleotide
FT	Flow-through
GAG	Glycosaminoglycan
HA	Hyaluronan/Hyaluronic Acid

HAase	Hyaluronidase
Hb	Hemoglobin
HDL	High Density Lipoprotein
HSA	Human serum albumin
HSP	Heat Shock Protein
HtrA1	High-temperature requirement A serine peptidase 1
IA	Inflammatory Arthritis
IAP	Inhibitor of Apoptosis
IC	Immune Complex
IDL	Intermediate-Density Lipoprotein
IFN	Interferon
IgG	Immunoglobulin isotype G
Il	Interleukin
ILV	Intralumenal Vesicles
IPA	Isopropyl Alcohol
kDa	Kilodalton
LAC	Lectin affinity chromatography
LBPA	Lipid Lysobisphosphatidic Acid
LPS	Lipopolysaccharide
mAb	Monoclonal Antibody
MAC	Membrane Attack Complex
MECC	Micellar Eectro kinetic Cpillary Chromatography
MeOH	Methanol
Met	Methionine
MMP	Matrix Metalloproteinase
MP	Microparticle
MRI	Magnetic Resonance Imaging
MV	Microvesicle
MVB	Multivesicular Body
MWCO	Molecular Weight “Cut-Off”
MWM	Molecular Weight Marker
NAT	2,3-Naphthotriazole
NO	Nitric Oxide
NO_2^-	Nitrite
NO_3^-	Nitrate
NOS	Nitric Oxide Synthase
OA	Osteoarthritis
OG	β-octlyglucopyranoside
PAGE	Polyacrylamide gel electrophoresis

PBS	Phosphate buffered saline solution
PBST	Phosphate buffered saline solution with Tween
PCM	PeriCellular Matrix
PCR	Polymerase Chain Reaction
PE	Phosphatidylethanolamine
Pl(3)P	Phosphatidylinositol 3-phosphate
Pro	Proline
PS	Phosphatidylserine
PSA	Psoriatic arthritis
RA	Rheumatoid Arthritis
RAGE	Receptor for Advanced Glycation End Products
RNS	Reactive Nitrogen Species
RP-HPLC	Reverse Phase High Performance Liquid Chromatography
SCX	Strong Cation Exchange
SDS	Sodium Dodecyl Sulphate
SELDI	Surface Enhanced Laser Desorption Ionisation-time
SF	Synovial Fluid
SLE	Systemic Lupus Erythematosus
SN	Supernatant
TBAHS	Tetrabutylammonium Hydrogensulphate
TCEP	Tris(2-carboxyethyl)phosphinehydrochloride
TEM	Transmission Election Microscopy
TEMED	Tetramethylethylenediamine
TGF-β	Transforming Growth Factor β
TGFBIp	Transforming growth factor-beta-induced protein ig-h3 protein
Thr	Threonine
TLR	Toll-Like Receptor
TNF	Tumour Necrosis Factor
TOF	Time of Flight
Tsg101	Tumor susceptibility gene 101
UV	Ultraviolet
VLDL	Very Low-Density Lipoprotein
WB	Western Blot

Chapter 1

Literature Review

1.0 Introduction to Arthritis

1.0.1 Prelimary Statistics

Arthritis is defined as any limb, joint or spine condition associated with inflammation or structural change [1]. Symptoms of arthritis in general include pain, swelling, warmth and restricted movement of the joint [2].

There are in excess of 200 types of arthritic disease but the two most common forms are osteoarthritis (OA) and rheumatoid arthritis (RA) [1]. Other forms of the disease include gout, pseudogout (PS), psoriatic arthritis, Reiter's syndrome, colitic arthritis and Behçet's syndrome.

A common misconception held by many is the association of arthritis solely with old age. Juvenile idiopathic arthritis (JIA) occurs in one in every thousand children in the UK. This particular disease varies on a geographical basis e.g. 0.7 per 1000 in USA to 4 per 1000 in Australia [3]. Figures released by *Arthritis Ireland* [4] reveal that currently;

1. One in six people in Ireland i.e. three quarters of a million men and women, suffer from some form of arthritis.
2. 1,000 of these are children.
3. 34% of women and 23% of men are affected by arthritis in Ireland.
4. Over 30% of GP visits are arthritis related.
5. 18% of arthritis patients are less than 55 years old.
6. It is estimated that the cost of arthritis to the state due to lost working hours is €1.6 billion per annum.
7. The majority of arthritis patients suffer from OA.
8. 40,000 people suffer from RA. 70% of these are women.

Further statistical data show that in Europe, a joint is replaced every 1.5 minutes due to OA. In the USA a total of around 500,000 joint replacements are performed each year [5]. Table 1.1 highlights that the number of individuals suffering form osteoarthritis (OA) and rheumatoid arthritis (RA) is steadily increasing on a global scale and it has been postulated that this is due to increasing population longevity. However, it is also believed that obesity is a major risk factor for developing OA and Allman-Farinelli *et al*.

[6] suggest that there will be an epidemic of obesity-related OA in the general population, particularly among the 45-54 age-group in the coming years. Significantly, even though RA accounts for a small number of cases relative to OA (less than one for every 10), its mechanism of disease and potential cures are better understood. This is due in part to the fact that RA attracts more scientific and public attention than OA [5].

Osteoarthritis Epidemiology			
Country	*2002*	*2007*	*2012*
United States	13.2	14.4	15.5
Europe	14.5	15.2	15.8
Japan	6.6	6.9	7.2
Total OA Cases	34.3	36.5	38.6
Total RA Cases	2.8	3.1	3.4

Table 1.1: *Number (in millions) of people already diagnosed with OA and a projected figure for 2012. Included for comparison are the corresponding figures for RA. Data taken from Arthritis Ireland website* [4]

1.0.2 Osteoarthritis (OA)

As mentioned, OA is the most common form of arthritis and is characterised by the progressive degeneration of articular cartilage [7]. It is also defined as *"a loss of homeostasis in the maintenance of healthy articular cartilage"* [8]. The American College of Rheumatology define OA as a *"heterogeneous group of conditions that leads to joint symptoms and signs which are associated with defective integrity of articular cartilage, in addition to related changes in the underlying bone at the joint margins"* [9]. A schematic representation of a normal versus an osteoarthritic knee may be seen in Figure 1.1 [10]. It is clear from this that OA does not have a single pathology and indeed, clinical heterogeneity is a feature of OA.

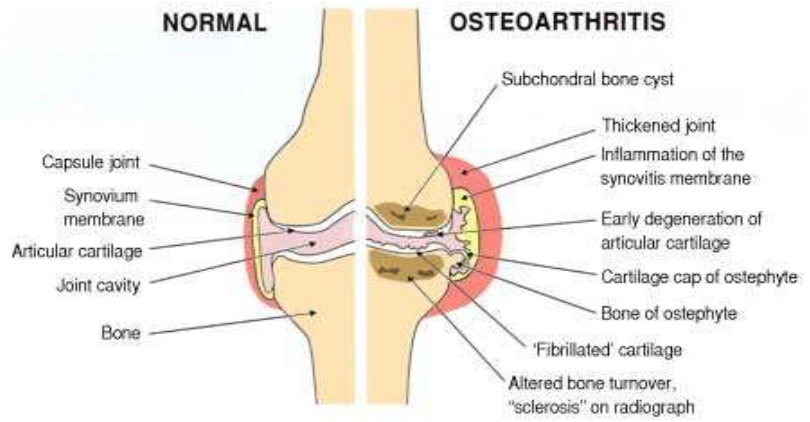

Figure 1.1: *Schematic diagram of contrasting a normal knee versus an osteoarthritic knee. This illustrates that OA is a multi-symptomatic and complex disease. The schematic diagram was sourced from* [10]

An important and notable point in the definition given above is that OA is a multifactorial disease, i.e. there is no one, unique attributable cause for the onset of OA in any particular individual. Coupled to this is the fact that not only are the initiating factors of the disease poorly understood, but so also are the relative contributions of each to joint damage in individual patients at specific stages of disease [11]. By extension, this could mean that there is unlikely to be any single species that may be hypothesised to be the cause of this disease and thus the render the causative agent in turn to become a therapeutic target. Therefore, to gain a firm understanding of the pathophysicological causes of OA, it has come to be recognised that a multidisciplinary approach is required. Indeed, it is argued [12] that pooling knowledge obtained from recent advances in phosphoproteomics (the analysis of phosphorylated proteins), glycoproteomics (the analysis of glycosylated proteins), glycomics (the analysis of sugars), lipidomics (the analysis of lipids) and degradomics (the analysis of protein degradation products) is the way forward.

1.0.3 Cartilage Composition

It is interesting to note that in the embryo, cartilage initially develops along the same pathway as bone [13]. However, at the onset of endochrondral bone formation, cartilage development diverges and becomes an independent entity. Cartilage is a layered structure consisting mainly of cartilage cells (chondrocytes), cartilage tissue (the Extra Cellular Matrix - ECM) and a collagen network. A schematic diagram of articular cartilage may be seen in Figure 1.2.

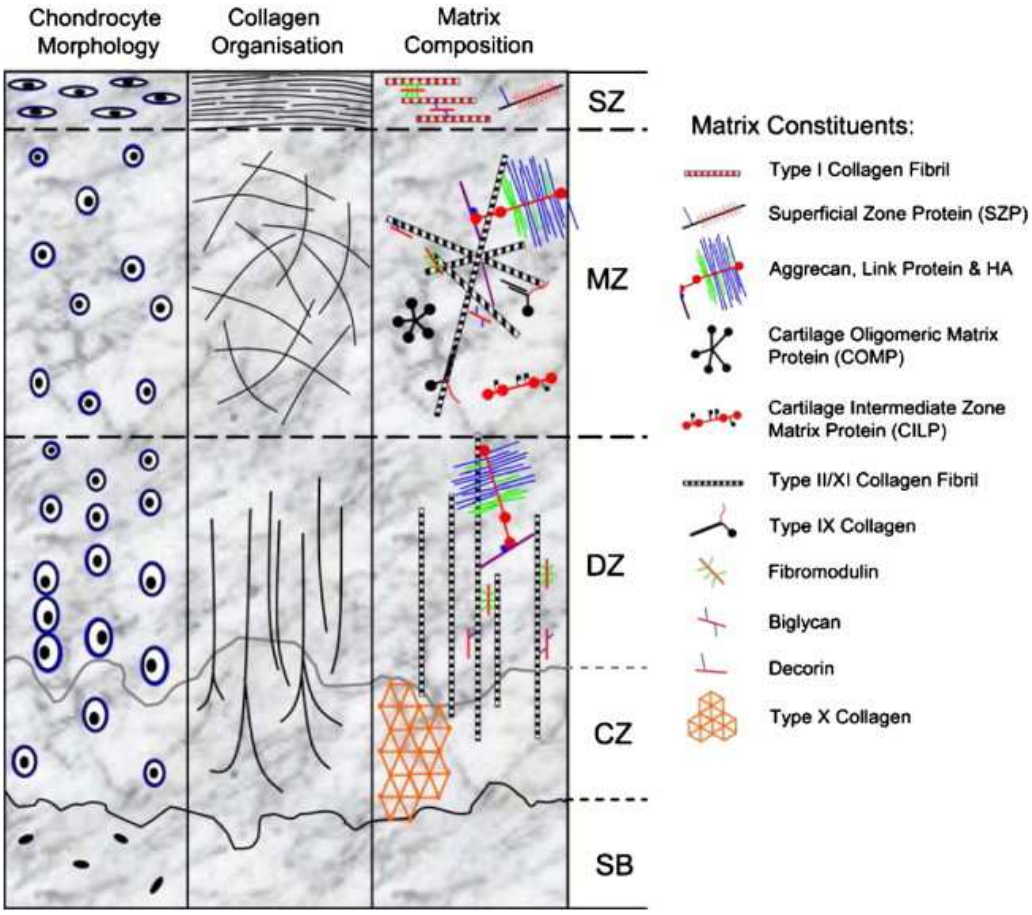

Figure 1.2: *Schematic representation of articular cartilage showing four main zones; superficial (SZ), middle (MZ), deep (DZ) and calcified cartilage matrix (CZ) plus the underlying subchondral bone (SB). The figure shows that each zone differs in cell morphology (left), collagen fibre organisation (middle) and ECM molecular composition. Figure from Wilson et al.* [14]

Surprisingly, cartilage has relatively few chondrocytes with only 5% of cartilage consisting of cells. The remaining 95% consists of the ECM, which is a cell-free matrix. This scarcity of cells may explain why cartilage cannot regenerate by means of cell turnover. Effectively, each cell is a completely independent entity and only gains information through mechanical forces and molecular mediators e.g. cytokines and growth factors. Structurally, approximately 5% of the wet weight of cartilage is composed of highly-sulphated proteoglycans. The two major proteoglycans are aggrecan and the glucuronic acid polymer, hyaluron [15]. The aggrecan entities, however, do not exist in isolation but instead, they bind in their hundreds to a central hyaluronic acid (HA) filament. HA is a polysaccharide composed of repeating units of glucuronic acid and *N*-acetyl glucosamine. Its monomer structure may be seen in Figure 1.3.

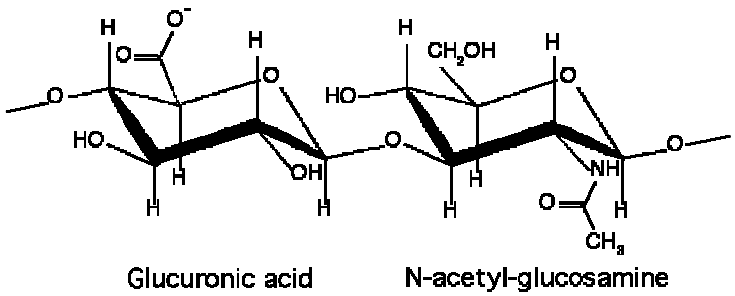

Figure 1.3: *A monomer unit of the polysaccharide hyaluronic acid (HA). The two subunits glucuronic acid and N-acetyl-glucosamine are also labelled.*

Hyaluronic Acid is the component of synovial fluid that imparts viscosity and gives the joint fluid an "egg-like" appearance and consistency. It is believed that the size of the HA entity decreases while its actual abundance increases with age [16] and with the onset of arthritic diseases[17]. This decrease in size is attributed to degradation and is thought to involve the action of hyaluronidases or free radicals. The increase in the volume of HA produced is offset by a dilution of the synovial fluid. A study completed by Lenormand *et al.* [18] concluded that HA can complex with proteins at various conditions of pH, ionic strength and protein over HA ratios. Therefore, an analysis of synovial fluid necessarily involves the hydrolysis of HA by hyaluronidase (HAase). Furthermore, the high viscosity of synovial fluid due to HA is problematic when it comes to instrumental analysis.

Proteoglycans are located between the collagen fibres in fixed locations. An interesting feature of these is that they are only 40 – 60% hydrated. This is due to the restrictive network of collagen network fibres i.e. there is a swelling pressure generated [15]. As a result, this imparts a degree of stiffness to the cartilage. However in OA, proteolytic enzymes degrade both the proteoglycans (aggrecanases) and collagen (collagenases)[19, 20]. Though the entire process is quite complex, the net manifestation is eventual cartilage degradation.

Horton *et al.* [21] propose that chondrocyte apoptosis is more prevalent in OA. They further advance that chondrocyte cloning is evident and this may be interpreted as a localised attempt at cartilage repair and regeneration. Poole and colleagues believe there is evidence of increased chondrocyte synthetic activity in early OA [22]. They interpret this as an attempt by the chondrocytes to regenerate the matrix components e.g. collagens and aggrecans. This attempt at repair by the chondrocytes manifests itself in the appearance of fibres, matrix depletion, cell clusters and above all, as changes in the quantity, distribution and/or composition of matrix proteins [23]. Therefore, the simultaneous but opposing processes of cartilage degradation and cartilage repair are at work in the very early stages of OA. Abramson [11] also supports this theory, stating that the chondrocyte undergoes a series of complex changes, including hypertrophy (an increase in volume), proliferation, catabolic alterations and finally, death. Eventually, as the disease and/or ageing process progresses, the catabolic processes overcome their anabolic counterparts. Sarzi-Puttini *et al.* [9] concur that the degradation of the ECM exceeds its synthesis and this leads to a decrease in the amount of cartilage matrix and eventually, to the complete erosion of the cartilage thus exposing the underlying bone. Eventually a stage is reached where once the cartilage is severely degraded, the chondrocyte is unable to replicate the very complex collagen network structure and total cartilage destruction is certain.

1.0.4 Osteoarthritis – Diagnosis and Prognosis

OA has been described as the "silent plague" of the 21st century [24]. It is a degenerative disease and a consequence of many factors including natural age-related changes, genetic predisposition and abnormal biomechanical forces that alter metabolic processes and destruction of articular cartilage [25]. Not only is the cartilage affected but also the entire joint structure, including the synovial membrane, bone, ligaments and the periarticular muscles. In spite of the compelling statistical data presented above relating to its prevelance, there is currently no prevention or cure for OA. Though the American College of Rheumatism has published criteria for the diagnosis and classification of OA, these are not convenient for the early detection of the disease [26]. It is also stated that evaluation of OA progression is equally uncertain, and lacks coherent, standardised criteria. For the most part, the seriousness and progression of the disease are evaluated based on the pain experienced by the patient at the time. Cushnaghan [27] states that the cardinal symptom of OA is pain, which occurs with joint use and is only relieved by rest. It is usually aching in character and it is often difficult to locate the site of origin. Rheumatologists ascertain the severity of the disease by employing the Kellgren/Lawrence scoring system to knee joint x-rays. However, it has also been shown that some patients who experience moderate to severe pain may actually have very little bone damage (by radiography) and only a third of patients with x-ray evidence of OA complain of pain at the relevant site [9]. The author goes on to state that not only is there "*no gold standard diagnostic test for OA"*, but also current radiographic diagnosis may be non-specific. This renders the early detection of OA extremely difficult as the progression of the disease is already underway before intervention can be affected should a cure be eventually found. Moreover, to date there is no specific diagnostic laboratory-detectable abnormality in primary OA [9]

The natural aging process also frustrates any attempted OA diagnosis [28]. Major components of the ECM e.g. type II collagen and proteoglycans, undergo structural and compositional changes during the natural aging process. Gobezie *et al.* [29] offer a number of reasons for the difficulties in developing diagnostic and treatment solutions for OA (Figure 1.4).

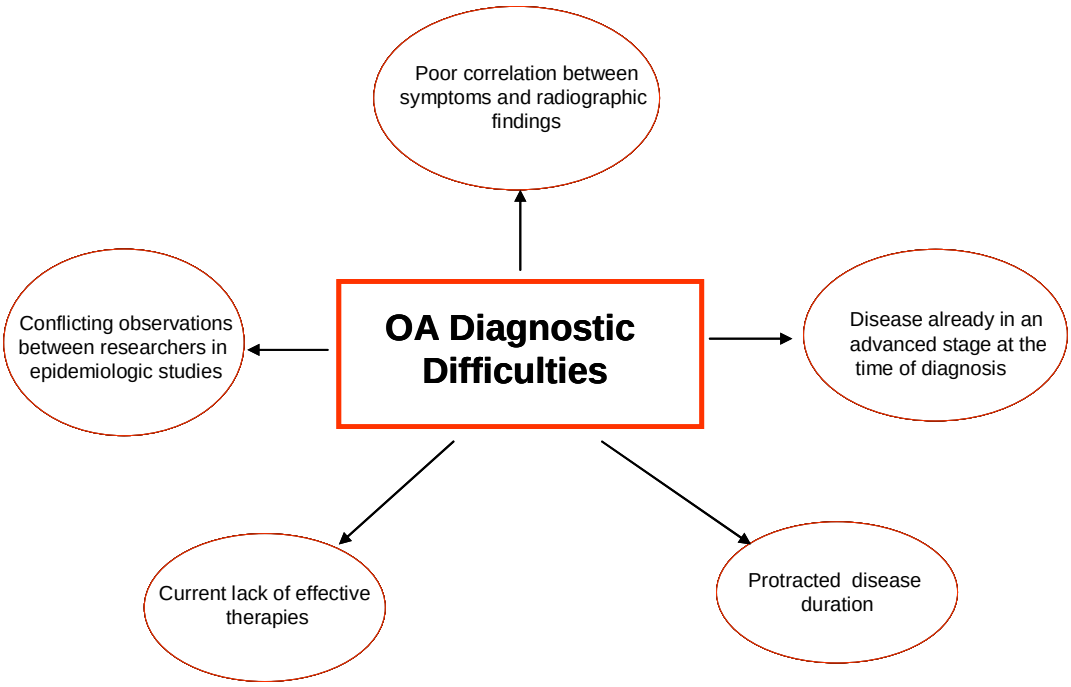

Figure 1.4: *Confounding factors in the development of diagnostic and treatment solutions for OA.*

Coupled to these difficulties is the realisation that cartilage deterioration is non-uniform in terms of disease progression with time as there are intermittent episodes of inflammatory attacks and remission periods. Regan *et al* [30] support this hypothesis by claiming that radiographic evidence often occurs late after significant loss of cartilage has already taken place. Indeed, by the time OA is positively diagnosed, the deterioration of cartilage has reached the point of no return and the patient is already undergoing symptomatic treatment with anti-inflammatory drugs or analgesics [12].

Though the early detection of OA is problematic and intervention is limited to pain relief, the prognosis is all too clear. Should the symptoms not be effectively controlled, the suffering patients' fate is likely to be total joint failure leading to eventual joint replacement [31].

1.0.5 Traditional methodologies for OA diagnosis

In 1985, Fawthrop *et al.* [32] undertook an investigation to identify particulate matter in synovial fluid (SF). In particular, they sought to examine the specificity and sensitivity of routine techniques available at the time in order to differentiate between normal and pathological SF. The authors noted that prior to this, other work had been done employing light microscopy for the identification of urate (in gout), pyrophosphate and cholesterol crystals. They were however, unaware of any previous study of normal, healthy fluid for these crystals. Their findings revealed that crystals were present in some normal fluids from young patients with no clinical evidence of joint disease, which cast doubts on the specificity of the technique. Moreover, the alizarin red assay used to detect hydroxyapatite particles also lacked specificity as particles in normal fluid were also stained. The effects of exercise and the levels of lactate were also examined in this study. It was concluded that all the techniques examined, lacked disease specificity. Finally, it was recommended to interpret synovial fluid microscopy with caution.

More recently however, Yavorskyy *et al.* [33] countered this assertion by stating that basic calcium phosphate crystals are unique to OA and may represent a therapeutic target. Rosenthal [34] supports this claim and found that 60% of synovial fluids from patients with severe OA contain calcium pyrophosphate (CPPD) or basic calcium phosphate crystals. Sinz *et al.* [35] also expressed reservations concerning the ability of current routine clinical tests on synovial fluid to offer a precise description of particular disease states. These tests include measurement of synovial fluid transparency, viscosity, glucose and protein concentrations as well as the quantity and morphology of any cells present. Though the synovial fluid from RA patients has been found to be increased in volume, cloudy from suspended cells, less viscous than normal SF and liable to clot on standing (due to higher fibrinogen content), the fluid from OA patients retains normal colour, clarity and high viscosity with an only increase in volume [17].

Joint imaging with conventional radiography, arthroscopy and magnetic resonance imaging (MRI) are also routinely used to monitor pathologic changes in the osteoarthritic joint. These methods are the current diagnostic tools. The severity of OA is assessed by measuring cartilage thickness and evaluating osteophytes and any ulceration of the

cartilage surface. However, it is believed that these methods fail to provide a sensitive assessment of disease progression [36].

It would appear then, that the more traditional diagnostic methodologies are limited in terms of early disease diagnosis, disease specificity and monitoring disease progression. Even with the availability of these limited methods, the primary manifestation of OA is the presence of pain, despite the poor correlation between level of pain and severity of OA. However, breakthroughs and developments in molecular and cell biology in the latter part of the 20th century have increased our understanding of many diseases e.g. cancer [37]. Specifically, disruption to cellular networks is now believed to be the consequence of genetic changes and/or environmental factors. These changes are manifested through altered mRNA transcriptions and subsequent modifications to protein profiles. In addition, the up or down regulation of other molecules that have a role in metabolic processes e.g. reactive oxygen species, cytokines, proteases and enzyme inhibitors are also useful biomarker candidates [38]. Thus, the phenomenon of body fluid proteomics, peptideomics, glycomics, metabolomics and the search for disease biomarkers has begun in earnest.

1.0.6 Biomarker classification and a system approach to biomarker discovery

In 2001 the Biomarker's Definitions Working Group defined a biomarker as a *"characteristic that is objectively measured and evaluated as an indicator of normal biological processes or pharmacological responses to therapeutic intervention"* [39].

Bauer *et al.* [40] sought to classify osteoarthritis biomarkers in particular, on the basis of function. The BIPED classification scheme was introduced in 2006. A single biomarker may be classified in one or more of the following categories;

Burden of disease; **I**nvestigative; **P**rognostic; **E**fficacy of intervention; **D**iagnostic

Burden of disease biomarkers ascertain the severity or extent of the disease at a particular point in time. This determination can be in just a single joint or a group of joints

simultaneously. The authors stress that this classification has nothing to do with the economic or social "burden" of the disease.

Investigative biomarkers are the least precisely defined class. In brief, they are markers where the relationship to various normal and abnormal parameters of cartilage turnover has not yet been established. They are listed in this category to stimulate further research.

The main feature of a *prognostic* marker is to predict the future onset of OA among "healthy" individuals or the progression of OA among those already with the disease. This generally requires a longitudinal study in order to track the levels of a particular marker over time.

Efficacy of intervention markers may be measured prior to therapy to predict treatment efficacy, or may be measured more than once to assess short-term changes that occur as a result of pharmacologic or other interventions. Finally, diagnostic makers are usually employed in a dichotomous manner - diseased or non-diseased, OA or RA etc.

In the last decade it has been recognised that a "systems biology" approach towards elucidating the cause of a disease is required [41]. This has generally been defined as a broad study of the components of biological processes e.g. proteins, reactive oxygen species, glycosylation entities and nucleic acids (e.g. ribonucleic acid; RNA). The study of these various components is believed to lead to a greater and deeper understanding of the dynamic biological processes at the cellular and tissue levels. It is widely accepted that this systems methodology will eventually lead to the identification of the most important moieties that differentiate between health and disease and could become primary targets for therapeutic intervention.

1.0.7 Body fluids as a source of OA biomarkers

Over recent years a number of review papers have been published [42] [37] relating to human bodyfluid analysis in the search for protein biomarkers. They outline the unique features and challenges in the analysis of each particular biofluid as well as the applications of each to human disease biomarker discovery. An extensive list was reviewed and included: plasma/serum, urine, cerebrospinal fluid, saliva, bronchoalveolar lavage fluid, synovial fluid, nipple aspirate, tears fluid and amniotic fluid. All research papers studied related to the search for biomarkers for arthritis in general and OA in particular,

discussed the analysis of just three of these biofluids i.e. serum/plasma, urine and synovial fluid.

The scope of this project is limited to the analysis of synovial fluid. Therefore, a detailed description of the composition and sample treatment of serum/plasma and urine will not be discussed here. However, confining research to one biofluid i.e. synovial fluid is not without some merit. Indeed, Gibson *et al.*[17] advise caution against the simultaneous analysis of synovial fluid and plasma/serum stating that at present, there is no evidence of any correlation between the two fluids. It is now believed [43] that what are termed "proximal fluids" of which synovial fluid is a good example, increase the probability of finding new biomarker molecules for OA. The reasoning behind this is that blood, though readily obtained, may contain potential disease biomarkers at such low concentrations due to dilution effects, that detection may be difficult. Felson *et al.* [44] also expressed concern about OA biomarkers derived from blood or urine. Their reasoning was as follows: A cartilage degradation marker is released into the synovial fluid where it is potentially diluted by a large volume of SF. It then travels through the synovial membrane at a rate dependant on a concentration gradient between synovial fluid and blood. Leaving the joint cavity, the biomarker may be metabolised by synovial cells, lymph nodes etc. with the result that the epitopes that originally identified it are altered, and any assays that were developed to detect it, are no longer effective. Finally further dilution and metabolism will take place in the kidney. Yamagiwa *et al.* [45] agreed, stating that ECM proteins, ECM degradation products, proteins from the synovium, ligament, meniscus, joint capsule and bone, all accumulate in the synovial fluid. Though there is protein exchange between synovial fluid and the systemic circulation, it is known that the protein concentration in the former is approximately three and a half times that of the latter. This may be seen in Table 1.2.

Protein	Molecular Weight (kDa)	Synovial Fluid			Serum/Plasma		
		Normal	OA	RA	Normal	OA	RA
Hyaluronan	$2x10^6$	3.2	1.5	0.17-2.0			
Fibrinogen	340		0.15-2.10	0.25-0.55	3		7.0
Albumin	69	12.0 - 20.0	11.0-34.0	8.0-35.0	32.7	26.0	29.2-44.0
Haptoglobin	100	0.1	0.2	0.9-4.0	1.8	2	2.4-6.0
IgG	156		4.0-30.0	10.3-11.0		4.0-12.0	11.0-20.1
Total Protein		**19**	**40.0-68.0**	**38.0-84.0**	**67.7**		**70.0**

Table 1.2: *Comparison in protein concentration between SF and serum/plasma. All concentrations are in mg/mL. In addition a comparison between healthy and arthritic synovial is made. The molecular weight of each protein is included. This data was taken from Gibson et al.*[17]

A further merit to synovial fluid analysis is that information relevant to the specific joint may be obtained. Therefore biofluids in direct contact with the diseased site may contain interesting and potentially useful biomarkers at a concentration that renders detection possible. Sarzi-Puttini [9] concluded that the use of serum markers for diagnostic and prognostic purposes remains investigational. In a recent review [46] it was stated, that although serum and urine biomarkers for diagnosis and prognosis have been found, none of them can yet be used in clinical practice because of large inter-patient variations. However, the same author did concede that synovial fluid analysis may be impractical for large-scale clinical diagnosis and monitoring. Courtney *et al.* [47] state that aspiration of synovial fluid from a joint can quickly relieve severe pain by reducing intra-articular pressure and therefore the aspiration of synovial fluid from the joint is routinely employed at the clinic. For proteomic analysis in particular, it was stated that the high abundance of hyaluronan is extremely problematic for biomarker detection and so this anionic macromolecule needs to be removed prior to analysis. A further and not insignificant confounding factor with the analysis of synovial fluid is the difficulty in securing normal or healthy samples. Therefore, any biofluid being mined for diagnostic, prognostic markers with a view to therapeutic targeting is not without some inherent challenges.

1.0.8 Properties of Synovial Fluid (SF)

Synovial fluid is a viscous liquid that lubricates the joints of the body. Its physical characteristics are similar to egg white in being clear yellow, transparent and highly viscous due to the high content of hyaluronic acid which is synthesised locally within the joint. One of its functions is to provide a cushion around the joint cartilage in order to reduce friction. It has a coefficient of friction of 0.002 – which is about 25 times less than steel on ice or that of an artificial joint replacement [48]. Normal healthy knee joints contain a small amount of synovial fluid, approximately 0.5mL whereas other joints contain a few drops [47]. A photograph of normal, healthy synovial fluid can be seen in Figure 1.5.

Figure 1.5: *Synovial fluid aspirated from a normal, healthy knee. Note the small volume of the clear, slightly yellow viscous fluid. Photograph taken from Courtney et al.* [47]

SF is not a static pool within the joint. A dynamic situation exists, whereby the synovial lining of the joint cavity (see Figure 1) continually absorbs and replenishes joint fluid [49]. Fluid turnover is governed by three elements – the synovial capillary system, the synovial interstitium and the lymphatic drainage system. Normal, healthy synovium contains a row of capillaries approximately 30μm below the surface. These capillaries in turn, possess fenestrations (membranes with a high permeability to water), often on the side of

the joint cavity that are the sites of synovial fluid formation and nutrient supply [50-52]. SF is a plasma dialysate whereby plasma undergoes a filtration process by this capillary network embedded in the synovial membrane. This is the second function of synovial fluid and serves to facilitate the transport of essential nutrients to the cartilage. At the sub-synovium-synovium border there is a network of terminal lymph vessels which drains away fluid, macromolecules, and particles that leave the joint cavity [53]. Generally speaking, the onset of inflammatory conditions changes the appearance from a clear to a cloudy, cell packed fluid. A contrast between the appearance of non-inflammatory and inflammatory SF may be seen in Figure 1.6.

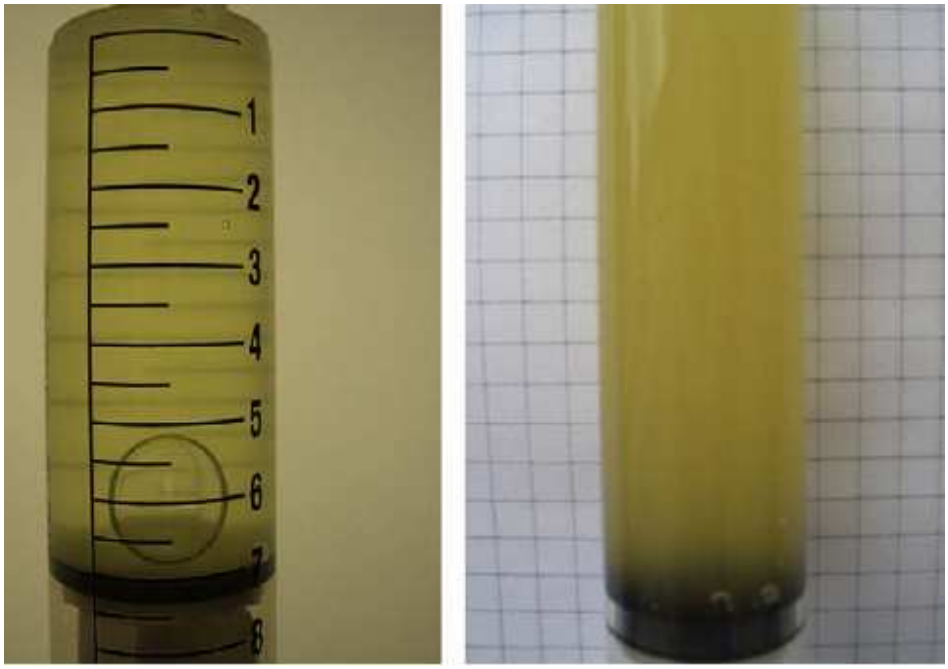

Figure 1.6: *A comparison in the appearance between non-inflammatory (left) and inflammatory SF. Note the increase in volume compared to normal SF in Figure 4. Also the cloudy appearance is evident in inflammatory SF. Picture taken from Courtney et al.* [47]

Finally, Figure 1.7 shows an example of SF that was inadvertently contaminated with blood during aspiration. Blood contaminated samples were omitted from all studies in this project.

Figure 1.7: *A specimen of blood tinged SF. Picture taken from Courtney et al.* [47]

1.0.9 Overarching project aim

As discussed above, osteoarthritis is an extremely complex and heterogeneous pathology. In this project it is hoped to apply a suite of techniques to the characterisation of both whole synovial fluid and the micro/nano-vesicular sub- component.

1.1 References

References

(1) Macpherson, G. In *Black's medical dictionary;* A & C Black: London, 1992; .

(2) Anonymous In *Harrap's dictionary of medicine & health;* Harrap Reference: London, 1988; .

(3) Gibson, D. S.; Blelock, S.; Curry, J.; Finnegan, S.; Healy, A.; Scaife, C.; McAllister, C.; Pennington, S.; Dunn, M.; Rooney, M. Comparative analysis of synovial fluid and plasma proteomes in juvenile arthritis - Proteomic patterns of joint inflammation in early stage disease. *Journal of Proteomics* **2009**, *72*, 656-676.

(4) AnonymousArthritis Ireland http://www.arthritisireland.ie/sitemap.php. *http://www.arthritisireland.ie/sitemap.php* (accessed 11/10/2010, 2010).

(5) Wieland, H. A.; Michaelis, M.; Kirschbaum, B. J.; Rudolphi, K. A. Osteoarthritis - an untreatable disease? *Nature Reviews Drug Discovery* **2005**, *4*, 331-344.

(6) Allman-Farinelli, M. A.; Aitken, R. J.; King, L. A.; Bauman, A. E. Osteoarthritis - the forgotten obesity-related epidemic with worse to come. *Medical Journal of Australia* **2008**, *188*, 317-317.

(7) Felson, D. T.; Chaisson, C. E.; Hill, C. L.; Totterman, S. M. S.; Gale, M. E.; Skinner, K. M.; Kazis, L.; Gale, D. R. The Association of Bone Marrow Lesions with Pain in Knee Osteoarthritis. *Annals of Internal Medicine* **2001**, *134*, 541-549.

(8) Poole, A. R. Can serum biomarker assays measure the progression of cartilage degeneration in osteoarthritis? *Arthritis & Rheumatism* **2002**, *46*, 2549-2552.

(9) Sarzi-Puttini, P.; Cimmino, M. A.; Scarpa, R.; Caporali, R.; Parazzini, F.; Zaninelli, A.; Atzeni, F.; Canesi, B. Osteoarthritis: An Overview of the Disease and Its Treatment Strategies. *Seminars in Arthritis and Rheumatism* **2005**, *35*, 1-10.

(10) AnonymousMendMeShop.com | knee osteoarthritis causes *http://www.mendmeshop.com/knee/knee_osteoarthritis_causes.php* (accessed 11/10/2010, 2010).

(11) Abramson, S. B.; Yazici, Y. Biologics in development for rheumatoid arthritis: Relevance to osteoarthritis. *Advanced Drug Delivery Reviews* **2006**, *58*, 212-225.

(12) De Ceuninck, F. The application of proteomics to articular cartilage: A new hope for the treatment of osteoarthritis. *Joint Bone Spine* **2008**, *75*, 376-378.

(13) Pacifici, M.; Koyama, E.; Shibukawa, Y.; Wu, C.; Tamamura, Y.; Enomoto-Iwamoto, M.; Iwamoto, M. Cellular and Molecular Mechanisms of Synovial Joint and Articular Cartilage Formation. *Annals of the New York Academy of Sciences* **2006**, *1068*, 74-86.

(14) Wilson, R.; Whitelock, J. M.; Bateman, J. F. Proteomics makes progress in cartilage and arthritis research. *Matrix Biology* **2009**, *28*, 121-128.

(15) Mollenhauer, J. A. Perspectives on articular cartilage biology and osteoarthritis. *Injury* **2008**, *39*, 5-12.

(16) Holmes, M. W. A.; Bayliss, M. T.; Muir, H. Hyaluronic-Acid in Human Articular-Cartilage - Age-Related-Changes in Content and Size. *Biochemical Journal* **1988**, *250*, 435-441.

(17) Gibson, D. S.; Rooney, M. E. The human synovial fluid proteome: A key factor in the pathology of joint disease. *Proteomics Clinical Applications* **2007**, *1*, 889-899.

(18) Lenormand, H.; Deschrevel, B.; Tranchepain, F.; Vincent, J. Electrostatic Interactions Between Hyaluronan and Proteins at pH 4: How Do They Modulate Hyaluronidase Activity. *Biopolymers* **2008**, *89*, 1088-1103.

(19) Knäuper, V.; López-Otin, C.; Smith, B.; Knight, G.; Murphy, G. Biochemical Characterization of Human Collagenase-3. *Journal of Biological Chemistry* **1996**, *271*, 1544-1550.

(20) Tetlow, L. C.; Adlam, D. J.; Woolley, D. E. Matrix metalloproteinase and proinflammatory cytokine production by chondrocytes of human osteoarthritic cartilage: Associations with degenerative changes. *Arthritis & Rheumatism* **2001**, *44*, 585-594.

(21) W.E. Horton Jr; R. Yagi; . Laverty D; S. Weiner Overview of studies comparing human normal cartilage with minimal and advanced osteoarthritic cartilage. *Clinical and Experimental Rheumatology* **2005**, *23*, 103.

(22) Poole A.R.; Guilak F.; Abramson S.B. In *Etiopathogenesis of osteoarthritis;* Moskowitz RW, Altman RW, Hochberg MC, Buckwalter JA, Goldberg VM, Ed.; Osteoarthritis: Diagnosis and medical/surgical management; Lippincott, Williams and Wilkins: Philadelphia, 2007; pp 27.

(23) Pritzker, K. P. H.; Gay, S.; Jimenez, S. A.; Ostergaard, K.; Pelletier, J. -.; Revell, P. A.; Salter, D.; van den Berg, W. B. Osteoarthritis cartilage histopathology: grading and staging, *Osteoarthritis and Cartilage* **2006**, *14*, 13-29.

(24) Jaovisidha K, R. A. Calcium crystals in osteoarthritis. *Current Opinion in Rheumatology* **2002**, *14*, 298.

(25) Rogers, J.; Shepstone, L.; Dieppe, P. Is osteoarthritis a systemic disorder of bone? *Arthritis and Rheumatism* **2004**, *50*, 452-457.

(26) Pavelka, K.; Forejtová, S.; Olejárová, M.; Gatterová, J.; Senolt, L.; Spacek, P.; Braun, M.; Hulejová, M.; Stovícková, J.; Pavelková, A. Hyaluronic acid levels may have predictive value for the progression of knee osteoarthritis. *Osteoarthritis and Cartilage* **2004**, *12*, 277-283.

(27) Cushnaghan, J.; Dieppe, P. Study of 500 patients with limb joint osteoarthritis. I. Analysis by age, sex, and distribution of symptomatic joint sites. *Annals of the Rheumatic Diseases* **1991**, *50*, 8-13.

(28) Goldring, M.; Goldring, S. Osteoarthritis. *Journal of Cellular Physiology* **2007**, *213*, 626-634.

(29) Gobezie, R.; Kho, A.; K., B.; Thornhill, T.; Chase, M.; Millett, P.; Lee, D. High abundance synovial fluid proteome: distinct profiles in health and osteoarthritis. *Arthritis Research & Therapy* **2007**, *9*, R36.

(30) Regan, E. A.; Bowler, R. P.; Crapo, J. D. Joint fluid antioxidants are decreased in osteoarthritic joints compared to joints with macroscopically intact cartilage and subacute injury. *Osteoarthritis and Cartilage* **2008**, *16*, 515-521.

(31) Hochberg, M. C. Opportunities for the Prevention of Osteoarthritis. *Seminars in Arthritis and Rheumatism* **2010**, *39*, 321-322.

(32) Fawthrop F.; Hornby J.; Swan A.; Hutton C.; Doherty M.; Dieppe P. A comparasion of normal and pathological synovial fluid. *British Journal of Rheumatology* **1985**, *24*, 61.

(33) Yavorskyy A.; Hernandez-Santana A.; McCarthy G.; McMahon G. Detection of calcium phosphate crystals in the joint fluid of patients with osteoarthritis - analytical approaches and challenges. *The Analyst* **2008**, *133*, 302.

(34) Rosenthal, A. K.; Mattson, E.; Gohr, C. M.; Hirschmugl, C. J. Characterization of articular calcium-containing crystals by synchrotron FTIR. *Osteoarthritis and Cartilage* **2008**, *16*, 1395-1402.

(35) Sinz, A.; Bantscheff, M.; Mikkat, S.; Ringel, B.; Drynda, S.; Kekow, J.; Thiesen, H.; Glocker, M. O. Mass spectrometric proteome analyses of synovial fluids and plasmas from patients suffering from rheumatoid arthritis and comparison to reactive arthritis or osteoarthritis. *Electrophoresis* **2002**, *23*, 3445-3456.

(36) Yamagiwa H.; Sarkar G.; Charlesworth M.C.; McCormack D.J.; Bolander M.E. Two-dimensional gel electrophoresis of synovial fluid: method for detecting

candidate protein markers for osteoarthritis. *Journal of Orthopaedic Science* **2003**, *8*, 482.

(37) Ahn, S.; Simpson, R. J. Body fluid proteomics: Prospects for biomarker discovery. *Proteomics - Clinical Applications* **2007**, *1*, 1004-1015.

(38) Rousseau, J.; Delmas, P. D. Biological markers in osteoarthritis. *Nature Clinical Practice Rheumatology* **2007**, *3*, 346.

(39) Biomarkers Definitions Working Group Biomarkers and surrogate endpoints; Preferred definitions and conceptual framework. *Clinical Pharmacological Therapy* **2001**, *69*, 89.

(40) Bauer, D. C.; Hunter, D. J.; Abramson, S. B.; Attur, M.; Corr, M.; Felson, D.; Heinegård, D.; Jordan, J. M.; Kepler, T. B.; Lane, N. E.; Saxne, T.; Tyree, B.; Kraus, V. B.; Chair),For the Osteoarthritis Biomarkers Network (V.Kraus Classification of osteoarthritis biomarkers: a proposed approach. *Osteoarthritis and Cartilage* **2006**, *14*, 723-727.

(41) Smith, J. C.; Lambert, J.; Elisma, F.; Figeys, D. Proteomics in 2005/2006: Developments, Applications and Challenges. *Analytical Chemistry* **2007**, *79*, 4325-4344.

(42) Hu, S.; Loo, J. A.; Wong, D. T. Human body fluid proteome analysis. *Proteomics* **2006**, *6*, 6326-6353.

(43) Ruiz-Romero, C.; Blanco, F. J. Proteomics role in the search for improved diagnosis, prognosis and treatment of osteoarthritis. *Osteoarthritis and Cartilage* **2010**, *18*, 500-509.

(44) Felson, D. T.; Lohmander, L. S. Whither osteoarthritis biomarkers? *Osteoarthritis and Cartilage* **2009**, *17*, 419-422.

(45) Hiroshi Y.; Sarkar G.; Charlesworth C.; McCormick D.; Bolander M. Two-dimensional gel electrophoresis of synovial fluid: method for detecting candidate protein markers for osteoarthritis. *Journal of Orthopaedic Science* **2003**, *8*, 482.

(46) De Ceuninck, F.; Berenbaum, F. Proteomics: addressing the challenges of osteoarthritis. *Drug Discovery Today* **2009**, *14*, 661-667.

(47) Courtney, P.; Doherty, M. Joint aspiration and injection and synovial fluid analysis. *Best Practice & Research Clinical Rheumatology* **2009**, *23*, 161-192.

(48) Guilak, F. The slippery slope of arthritis. *Arthritis & Rheumatism* **2005**, *52*, 1633.

(49) Levick JR; McDonald JN Fluid Movement Across Synovium in Healthy Joints - Role of Synovial-Fluid Macromolecules. *Annals of the Rheumatic Diseases* **1995**, *54*, 417-423.

(50) Stevens, C.; Blake, D.; Merry, P.; Revell, P.; Levick, J. A Comparative-Study by Morphometry of the Microvasculature in Normal and Rheumatoid Synovium. *Arthritis and Rheumatism* **1991**, *34*, 1508-1513.

(51) Levick, J.; Smaje, L. An Analysis of the Permeability of a Fenestra. *Microvascular Research* **1987**, *33*, 233-256.

(52) Knight, A.; Levick, J.; McDonald, J. Relation between Trans-Synovial Flow and Plasma Osmotic-Pressure, with an Estimation of the Albumin Reflection Coefficient in the Rabbit Knee. *Quarterly Journal of Experimental Physiology and Cognate Medical Sciences* **1988**, *73*, 47-65.

(53) Jensen, L.; Henriksen, J.; Olesen, H.; Risteli, J.; Lorenzen, I. Lymphatic Clearance of Synovial-Fluid in Conscious Pigs - the Aminoterminal Propeptide of Type-Iii Procollagen. *European Journal of Clinical Investigation* **1993**, *23*, 778-784.

Chapter 2

Proteomic profiling of synovial fluid by high performance liquid chromatography and capillary electrophoresis

2.0 Introduction

2.0.1 Proteomics

Proteomics is a relatively new and exciting field of study that has enabled the discovery of biomarkers for disease and has helped the elucidation and understanding of disease mechanisms. Proteomics has been defined as *"the study of the set of proteins expressed by a tissue or cell, and the changes in protein expression patterns in health and disease or in different environments."* [1]. It is also believed that proteomic studies offer a more useful insight than the previous genomic RNA systems studies. The reasons for this include the fact that RNA levels do not accurately predict protein levels and/or post-translational modifications of proteins which are often an indicator of their biological activities. It is further hypothesised that protein expression profiles of diseased tissue or biological fluids can effectively function as a disease "fingerprint" that reflects the onset or progression of a particular pathologic disease. Body fluids are now being conceptualised as *"windows into health and disease"* and there are aspirations that these fluids may be mined for markers that ascertain the onset of disease, the monitoring of disease progression and drug efficacy in various conditions [2].

2.0.2 Proteomic Methodologies

Traditional proteome analysis generally commences with 2D polyacrylamide gel electrophoresis (2D-PAGE) separation of proteins. Spots or bands of interest are then excised from the gel and digested by an enzyme with particular cleavage specificity and the resulting peptide mixture is introduced into a mass spectrometer (MS). For each mixture, the data obtained for the peptide masses, protein molecular mass, cleavage specificity and isoelectric point are all compared with data in a protein sequence database, and the output is the identity of the proteins selected on a "best match" basis. The confidence of identification is increased with the increasing selection of more peptides from the same protein(s) in MS analysis. An advantage of this methodology is that the researcher can effectively hand pick spots of interest (including those not highly expressed) for further investigation [3]. The strengths of the 2-D PAGE technique include

its ability to separate and quantify thousands of intact proteins in a single run [4]. Quantification is a relatively new step forward in this technique and is achieved through multi-colour fluorescent labeling techniques analogous to those used in mRNA analysis.

The 2D-PAGE proteomic analysis of biological fluids is recognised as a slow and labour intensive protocol due to the 2D gel electrophoresis and enzymatic digestion steps. These shortcomings in 2D PAGE have prompted an upsurge in the development of gel-free approaches and quantification [5]. Though 2D PAGE is a powerful and widely employed technique, some of the limitations of the technique cited include labor-intensive preparation procedures (often requiring hours or days for a single analysis) and stringent demands on reproducibility of experimental procedures and reagents in order to effect the high reproducibility required in any proteomic study. Shi *et al.* [6] stated that though there are recent improvement in 2D-PAGE techniques, reproducibility was still an issue. This view was also taken up by Bodzon-Kulalowska *et al*. [7] in their review paper who stated that reproducibility of protein patterns between laboratories is difficult to achieve due to protocol variations, artifacts and technology. There are also technical difficulties with on-line coupling to MS. Further, classical Coomassie-stained gels display at most four orders of magnitude in protein concentration [4]. Finally, proteins with a molecular mass of less than approximately (~) 20kDa, highly acidic or basic proteins and hydrophobic (membrane) proteins are not well resolved by gel electrophoresis [8]. This potentially leads to the loss of important biological information [9]. Gygi *et al.* [8] estimate that more than half of all proteins in the yeast proteome are not detectable by 2D-PAGE analysis.

An increasingly attractive alternative to 2D-PAGE is high performance liquid chromatography (HPLC). This is due to its high resolving power, high reproducibility and its on-line compatibility with electrospray MS. In addition, there is a broad range of mobile and stationary phase combinations available. In recent years a number of HPLC methods have appeared for the analysis of both peptides and intact proteins. Another major benefit of chromatographic techniques in a proteomic study, is the range of modes available e.g. reversed-phase, ion chromatography, affinity chromatography and size exclusion. These have been employed either alone or in combination with each other. When two or more different, orthogonal modes of chromatography are employed (e.g. 2D

or 3D LC), then superior resolution may be achieved. Relative to the 2D-PAGE approach, sample handling and preparation are minimal. Furthermore, automation is possible and this results in a high sample throughput, thus making it ideal for a clinical laboratory. It is also known that because of the high resolving power of LC, ion suppression effects in MS can be reduced or even eliminated. In short, chromatography in proteomics can provide high resolution, high speed, good sensitivity and specific separation of very complex matrices i.e. biological fluids. Finally, this kind of separation facilitates on-line MS detection and quantification.

2.0.3 A critique of "Top-Down" versus "Bottom-Up" or "Shotgun" Approach

Bottom-up (or shotgun) proteomics generally refers to the enzymatic digestion of intact proteins into a peptide mix that is injected into a MS for protein elucidation and identification. This approach is undoubtedly the most widely used approach in proteomic literature today. Peptides possess greater solubility, are stable in a wider range of solvents and are therefore easier to separate than proteins [10]. There are however, some limitations associated with this approach. The peptide database mapping may be compromised due to insufficient search specificity, incomplete digestion, sample impurities, post-translational modifications and/or database sequence errors [11]. Following enzymatic digestion, the sample is rendered more complex with certainly thousands and possibly millions of peptides in solution. Tang *et al.* [10] advise that bottom-up approaches provide very limited "true" molecular information of intact proteins, in particular proteins that have undergone post-translational modifications. As a significant portion of disease biomarkers maybe among the very low abundant proteins, peptides of these interesting, low abundant species may be masked by those of the high abundant, ubiquitous proteins e.g. albumin. Intact protein analysis offers the advantage of the detection of post-translational modifications and it is possible that a top-down approach has the potential to enhance biomarker discovery research. Analysis of intact proteins by HPLC is however technically challenging and problematic. Difficulties experienced include carryover, multiple peak formation (splitting) and broad, poorly shaped peaks [12]. The reasons for these difficulties include, slow intra-pore diffusion times, unresolved structural micro-

heterogeneities and conformational isomers and finally secondary interactions with the stationary phase. To offset the effects of broad peaks, longer gradients are required which results in longer run times. Also, though the analysis of intact proteins has the potential to offer useful molecular level information, the process currently requires the use of Fourier transform ion cyclotron resonance (FTICR)-MS/MS for obtaining protein sequencing measurements [13]. Finally, positive protein identification is currently limited by the relative scarcity of bioinformatic tools to date to analyse intact protein data. Though these challenges may appear formidable, there is still merit to analysing whole, intact proteins via HPLC. On or off-line digestion of the resolved or even partially resolved eluted proteins, would greatly facilitate protein identification through peptide mass mapping. In this case, instead of performing enzyme digestion on the whole sample at once, fractions of interest could be collected and each aliquot digested separately before MS analysis. This method eliminates the relatively lengthy 2D-PAGE approach. Because there are significantly less peptides in each fraction, this approach may greatly increase the chances of securing correct identification of a protein in addition to a reduced chance of missing low abundant and potentially interesting species. The peak resolution could be further improved by removal of high abundant proteins prior to HPLC analysis.

Gillette *et al.* [14] published a review paper outlining the merits (and also the precautions) of pattern profiling in proteomic biomarker discovery. More specifically, they critiqued pattern profiles generated by MS as a reliable, legitimate and reproducible mode of analysis in the search for markers of disease. Two platforms are currently available for biomarker discovery; 1) pattern profiling and 2) protein identification. They reminded us that there is a broad consensus view that heterogeneity and complexity of the individual, environment and disease, imply that individual markers are rarely sufficient for establishing a diagnosis or prognosis. On the contrary, panels of biomarkers are typically required. This may be particularly true for a complex and heterogeneous pathology like OA. The author also commented on the time consuming nature of protein identification. Everley and co-workers [15] characterised the *Clostridium* species through the analysis of intact proteins employing LC/MS without identifying the individual proteins. They

justified this approach by claiming that reproducible biomarkers candidates had been observed allowing for characterisation at the strain level without actually knowing the identity of the proteins involved. Again they noted that the sequencing of intact proteins on a chromatographic time scale is extremely challenging and was not attempted.

Therefore, acknowledging the aforementioned difficulties with intact protein analysis – in particular the scarcity of algorithms for identifying intact proteins by MS – pattern profiling of intact proteins in SF may be instructive and informative. A thorough search of the literature showed that this work has not been attempted before. It was therefore the objective of the present study to separate intact, native SF proteins via reverse phase HPLC and then to compare the chromatographic and/or MS profiles generated for each of the various arthritic pathologies in the hope that this leads to a protein footprint that is indicative of a particular joint pathology. Knowing that no one single agent is wholly responsible for the onset of OA, establishing a footprint that characterises a particular arthritic pathology may merit further study.

2.0.4 Putative OA biomarkers found to date

A literature survey was carried out in order to ascertain what OA biomarkers have been discovered to date and what methodologies were used. Table 1 displays the findings of various research groups in the search for protein biomarkers that differentiates OA from the various controls and/or other arthritic pathologies. Inspection of Table 2.3 reveals a wide variety in the type and number of biomarkers found and the methodologies used. De Ceuninck *et al*. [16] advised caution concerning the application of proteomic techniques to OA in particular as it is not straightforward due to the inherent complexity of the disease, and they reiterated that the progression of OA is slow with sporadic episodes of inflammation and remission. This may be interpreted as a reminder that a single sample from a patient is just a snap-shot of the disease at a particular moment in time. Furthermore they advised that although serum and urine biomarkers for diagnosis and prognosis have been proposed, it is said that none of them can be used in actual clinical practice because of large inter-individual variation.

Year	Biofluid	Biomarker	Concentration change in OA relative to RA or Control	Mode of Analysis	Reference
1993	Plasma & Synovial Fluid	Substance-P	No change	HPLC & RIA	17
2002	Plasma & Synovial Fluid	(i) Calgranulin B (MRP14) (ii) Serum amyloid A	(i) Not observed in OA (ii) Not observed in OA	2-DE/MALDI-TOF MS	18
2003	Synovial Fluid (4 OA samples)	Haptoglobin	18 spots increased 5-fold between any two samples and 9 spots increased 100-fold between any two samples	2D-PAGE	19
2006	Synovial Fluid	(i) Superoxide dismutase (ii) Catalase (iii) glutathione reductase (iv) glutathione-S-transferase (v)Malondialdehyde (vi) Viscosity	Enzyme activities were elevated in the OA group relative to the control group. Glutathione reductase activity higher in secondary OA group. Viscosity lower in OA group.	Various kinetic methods. Viscosity measured on a viscometer	20
2006	Cartilage	100 proteins Identified	Carilage Characterisation	1-D-SDS PAGE MS/MS	21
2007	Articular Cartilage	59 proteins	Differentially expressed relative to control	SDS-PAGE/ nanoHPLC/ MS-MS	22
2007	Blood & Urine	(i) Epitopes of type II collagen (C2C, C1, C2) (ii) Aggrecan 846 epitope (CS846) (iii) Cartilage Oligomeric Matrix Protein (COMP)	COMP levels indicate cartilage loss. Upregulated in OA.	ELISA	23
2007	Urine	C-termina cross-linked telopeptide of type II collagen CTX-II	Up-regulated in OA	Not specified	24
2007	Synovial Fluid (1 control & 1 postmortem sample)	40 proteins identified	16 unique to OA	Reverse Phase nano-HPLC/ MS	25

2007	Synovial Fluid	135 proteins identified	18 proteins differentially expressed between OA and control - 3 down-regulated in OA & 15 up-regulated.	1D-PAGE/ MS/MS	26
2008	Serum	16 proteins identified	15 proteins up-regulated and 1 down-regulated in OA	Rolling circle amplification	27
2008	Synovial Fluid	(i) Extra-cellular superoxide dismutase (EC-SOD) (ii) Ascorbate (iii) Urate (iv) Glutathione (GSH) (v) Total Nitrates (vi) Cytokines IL-6 & TGF-β	(i) Decrease in late OA samples (ii) Decrease in late OA samples (iii) No difference (iv) Decrease in late OA samples (v) No difference (vi) No difference	(i) ELISA (ii) HPLC (iii) HPLC (iv) Colorimetric Assay (v) Greiss Assay (vi) ELISA	28
2009	Serum	Il-6	Up-regulated in OA	ELISA	29
2010	Serum & Synovial Fluid	(i) S100A8 (ii) S100A12 (iii) S100A9	10 fold higher in RA	SELDI-TOF MS Western Blot ELISA	30
2011	Serum & Synovial Fluid	(i) V65 vitronectin fragment (ii) C3f peptide (iii)Unknown protein @ m/z 3762 (iv) Connective tissue-activating peptide III protein	(i) Increase in OA patients relative to control (both fluids) (ii) Increased in OA patients relative to control (iii) Increased in OA patients relative to control and RA patients (iv) Decreased in OA relative to control patients	SELDI-TOF MS	31

Table 2.1: *A list of proposed biomarkers for OA found in a variety of biological fluids. Also shown is their relative abundance to other arthritic diseases or control samples. Finally, the analytical techniques employed are shown.*

2.0.5 Protein dynamic range in SF

Though the protein concentration of serum and plasma is relatively high (tens of mg/mL), 99% of the protein content is comprised of just 22 individual proteins e.g. albumin, IgG, fibrinogen and transferrin [32]. Albumin accounts for about 50% of the total protein concentration in blood. Though plasma proteins can enter the SF by passive diffusion - indeed SF is considered a dialysate of blood plasma – concentrations of larger proteins remain substantially less in SF than in plasma, 30% less in fact [33]. However, it is not correct to suggest that all proteins found in SF originated in the blood. Recent developments have shown that many of the constituents of SF present in disease e.g. cytokines, proteases and various antibodies, are produced locally in the joint [34] .

Albumin is the most abundant protein in SF, accounting for about 64% of the total protein load in normal SF. As mentioned already, the protein composition of SF is dominated by a relatively small group of proteins. Indeed, the dynamic range between potentially clinically useful proteins and the high abundant proteins may differ by a factor of 10^{10} in both SF [34] and plasma [32]. For example, albumin and the high abundant proteins are found in the mg/mL range, while a protein like the cytokine TNFα is present in the pg/mL range. Removal of the high abundant proteins would increase the sample loading capacity and hence improve the detection sensitivity of low abundant proteins [35].

2.0.6 Methods employed for removal of the most abundant proteins

In order to increase the chances of unearthing potentially insightful pattern profiles, it is now believed that the high abundant proteins should be removed from the matrix prior to any separation, whether by 2D-PAGE, chromatography, capillary electrophoresis or any other mode of analysis. It must be stressed that removal of the high abundant proteins is by no means a suggestion that they are uninteresting or an unfortunate inconvenience that must be overcome in order to reach the lower abundant species. It is known that the immunoglobins and albumin can act as carrier molecules by binding to other peptides and proteins. Indeed “albuminomics” has become a useful offshoot of depletion strategies,

where research has been conducted on the albumin fraction in order to investigate the entities that attach to this carrier molecule [36]. Moritz *et al.* [37] also found that abundant plasma proteins act as sponges for low molecular weight peptides. Examples of interesting potential biomarkers that have been found to associate with albumin and so have the potential to be removed during albumin depletion are peptides, C-reactive protein, cystatin, apolipoprotein CIII, lumican and angiotensinogen [38]. A more prudent strategy would be to analyse both the low and high abundant fractions as not only the lower abundant proteins, but also the proteins that are specifically or non-specifically removed may be analysed [4]. The author in this case discovered that 129 proteins were identified in the high abundant protein fraction. After identifying 40 of these proteins, it was discovered that 26 proteins were common to both the high and low abundant fractions, thus underlining the importance of keeping and analysing all fractions.

Several approaches exist for the removal of the most abundant proteins in biofluids. Some of the methods available to the researcher include, the removal of human serum albumin (HSA) by immunoaffinity columns based on HAS-specific antibodies [39], isoelectric trapping using albumin as a marker [40], peptide affinity chromatography [41], Cibacron Blue (CB) to remove albumin [42] and ultrafiltration [43]. More recently, immunoaffinity columns and cartridges have been developed for the removal of multiple abundant proteins [44] [45] [46]. Non-specific depletion of plasma proteins can also be accomplished by rivanol (2-ethoxy-6,9-diamino acridine, ammonium sulphate and caprylic acid [37]. Limitations of the CB method mentioned above include binding to the binding sites of proteins other than albumin [47]. Zolotarjova *et al.* [42] performed a study where the objective was to compare CB and IgG immunoaffinity methodologies for the removal of the must abundant protein, HSA, from serum. Their findings revealed that not only were other non-targeted proteins inadvertently removed, but that a significant amount of HSA was found in the depleted fraction. This compounds the difficulty in identifying very low abundant proteins, as these species are now placed in an even more concentrated solution of serum albumin which in turn increases the difficulty in identifying and quantifying these proteins of interest. On the other hand, the IgG system was observed to have no albumin, transferrin, alpha-1-antitrypsin or haptoglobin present

in the flow-through fraction. It was confirmed by ELISA assays that the depletion of the target proteins was typically greater than 98%. An immunoaffinity column was used by Liu *et al* [45] for the proteomic analysis of plasma. The author did note some non-specific binding to the column.

2.0.7 Project Aim

For this project it was decided to employ an affinity column consisting of avian IgY antibodies, in order to remove twelve high abundant proteins – albumin, IgG, α1-antitrypsin, IgA, IgM, transferrin, haptoglobin, α1-acid glycoprotein (orosomucoid), α2-macroglobin, HDL (apolipoproteins AI & AII) and fibronectin – from synovial fluid in a single step prior to reverse-phase high performance liquid chromatography (RP-HPLC) and/or capillary electrophoresis (CE). All fractions were analysed i.e. the non-bound, the non-specific binding and the bound fractions. On achieving a good separation in all fractions, peaks of interest would be characterised by LC-MS or CE-MS.

2.1 Materials and Methods

2.1.1 Reagents and materials

HPLC grade methanol (MeOH), Isopropyl alcohol (IPA) and water were purchased from Sigma Aldrich.

HPLC grade acetonitrile was obtained from Sigma or Fisher Scientific.

Reagent grade trifluoroacetic acid, formic acid (98%), acetic acid (99-100%) was obtained from Sigma for use as ion-pairing reagents.

Sodium Dodecyl Sulphate (≥99.0%) was purchased from Fluka.

Sodium Tetraborate was obtained from Sigma.

Peptide standards, protein standards, bovine serum albumin (BSA), human serum albumin (HSA), hyaluronidase from bovine testes were purchased from Sigma.

Triethylamine, urea, dimethylformamide & tetrahydrofuran were obtained from Sigma and used for column regeneration.

A Beckman Coulter ProteomeLab IgY-12 High Capacity Partitioning Kit was obtained from Phenomenex.

Amicon Ultra centrifugal filter units with a 3kDa cut-off were obtained from Millipore.

2.1.2 HPLC Instrumentation

A Waters HPLC modular system was used and comprised of the following:

1) 600E Powerline multisolvent delivery system with 100μL heads
2) 600E system controller
3) 717plus autosampler
4) 486 UV absorbance detector
5) 474 Fluorescence detector.

The instrument was controlled by Empower software.

2.1.3 Capillary Electrophoresis Instrumentation

Capillary electrophoresis (CE) was carried out using an Agilent H-P3D CE Instrument with a UV-Vis diode array detector.

The instrument was controlled by HP Chemstation software.

A roll of fused silica polyimide coated capillary was purchased from Composite Metal Services. The capillary for analysis was prepared as follows; a length of capillary, 48.6cm long was cut from the roll. A detection window was made by burning the polyimide coating 40cm from one end. Polyimide was also removed from both ends of the capillary to prevent capillary blockage.

2.1.4 Miscellaneous equipment

A Hettich Mikro120 centrifuge was used in the immunoaffinity protocol in order separate non-bound proteins from targeted, bound proteins.

A Gilson GV Lab vortex mixer was used mix sample and standard solutions.

2.1.5 Peptide Standard Preparation

The purchased five-peptide mixture (0.5mg of each peptide) was prepared by weighing out the compound mixture and diluting in water to a final concentration of (0.1mg/mL of each peptide). The mixture was stored in aliquots at -20ºC. The five peptides were:

1) Gly-Phe
2) Val-Tyr-Val
3) Met Enkephalin
4) Angiotensin
5) Leu-Enkephalin.

2.1.6 Protein Standard Preparation

A four protein mixture was prepared (1mg/mL of each protein) by weighing out the compound mixture and diluting in water. The mixture was stored in aliquots at -20ºC. The four proteins were:

1) Ribonuclease A (13.7kDa, pI 8.63)
2) Cytochrome C (12kDa, pI 10.0-10.5)
3) Holotransferrin (77kDa, pI 5.0-6.0)
4) Apomyglobin (17kDa, pI 7).

HSA and BSA standards were prepared by weighing out the appropriate quantity of each protein and diluting in water.

2.1.7 Synovial fluid preparation

Synovial fluid samples were obtained by informed consent from patients attending the Rheumatology Department of the Mater Hospital in Dublin. Samples were aspirated from the patient and placed in plastic sample containers containing 1mM EDTA and centrifuged at 2500g for 20 minutes to remove cells and cellular debris and then stored in aliquots at -80ºC. Only one freeze/thaw cycle was permitted.

In order to reduce the high viscosity of SF, each sample was treated with hyaluronidase from bovine testes (1mg hyaluronidase dissolved in 1mL phosphate buffer. 250mL added to each sample and incubated overnight at 37ºC).

2.1.8 Removal of high abundant proteins from synovial fluid

A Beckman Coulter Proteome Lab IgY-12 High Capacity Proteome Partitioning kit was purchased from Phenomenex. The kit consisted of two affinity columns containing beads (60μm polymeric microbeads) coated with avian antibody (IgY)-antigens for the 12 targeted proteins and three buffers to be used for sample loading, washing, eluting and regenerating the column. The buffer composition was:

- 10x Dilution Buffer: Tris buffered saline (100mM Tris-HCl, pH 7.4, 1.5M NaCl). This was used for sample dilution, washing and equilibrating the column.
- 1M Stripping Buffer: (1M glycine-HCl, pH 2.5). This was used for eluting the bound proteins from the column.
- 1M Neutralisation Buffer: (1M Tris-HCl, pH 8.0). This was used for neutralising column and also the eluted, bound proteins.

The manufacturer's instructions were followed throughout.
The immunodepletion process is outlined in Figure 2.1.

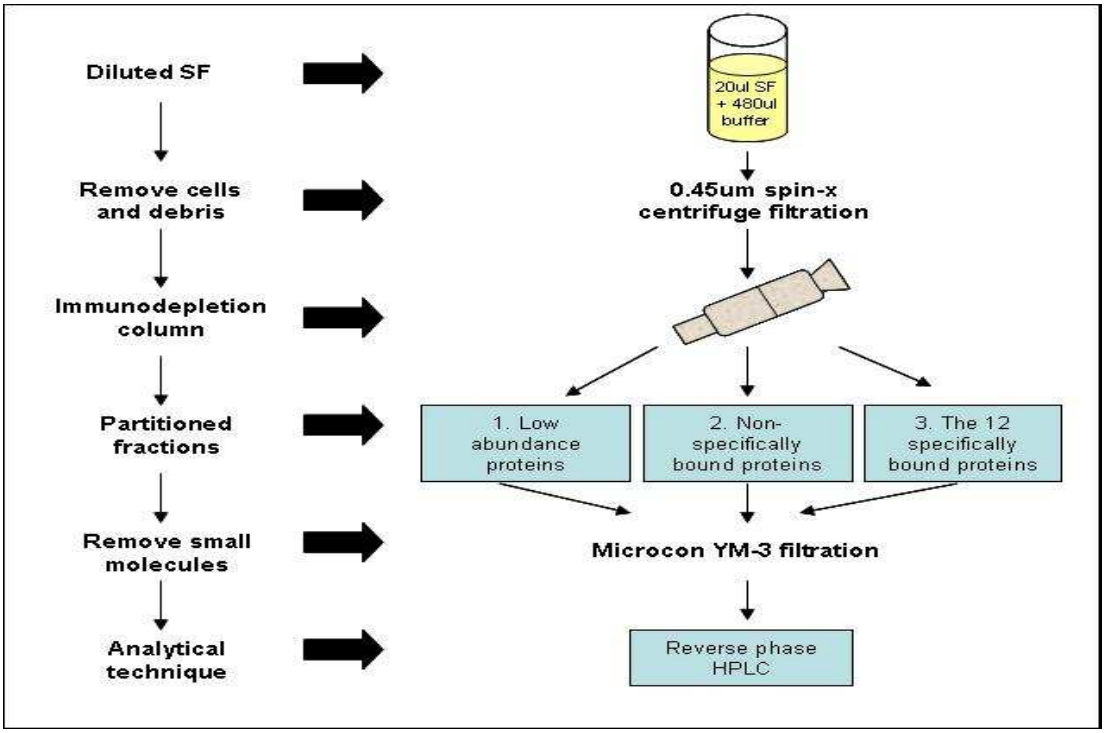

Figure 2.1: *A schematic work flow diagram of the immunoaffinity process*

2.1.9 HPLC Conditions

RP-HPLC columns: Phenomenex Jupiter C_{18} 300Å (150 x 3.0mm, 5µm)

Phenomenex Jupiter C4 300Å (150 x 4.5mm, 5µm).

No guard column was used.

A linear gradient elution was performed with two mobile phases; Mobile Phase A: 0.01% (v/v) aqueous TFA and Mobile Phase B: 0.01% (v/v) TFA in acetonitrile/water (60/40). The gradient elution was 100% mobile phase A to 100% mobile phase B over 80 minutes.

UV detection wavelength: 220nm

Fluorescence detection wavelength: λ_{ex} 280nm, λ_{em} 360nm

Injection volume: 50µL

Flow rate: 0.8mL/min

All mobile phases were vacumn filtered through 0.45µM filters and then sonicated in a water bath for 5 minutes before use.

2.1.10 Capillary Electrophoresis

All new capillaries were conditioned by first washing through with 0.1M NaOH for 10mins followed by distilled water for 5mins and finally with the background electrolyte (BGE) for 10mins. Between runs, the capillary was rinsed with 0.1M NaOH, distilled water, 0.1M HCl, distilled water and BGE for 5mins each. The BGE consisted of 10mM sodium tetraborate and 60mM sodium dodecylsulphate (SDS), pH 9.

The column was maintained at 25ºC.

Operating voltage was 15kV

Detection wavelength: 200nm, 220nm, 235nm and 280nm

2.2 Results

2.2.1 Standard peptide analysis with C_{18} column

A five peptide standard (0.1mg/mL of each peptide) was injected in order to establish retention times, peak shape and check the suitability of the system. Mobile phase was prepared as outlined by [48]. Briefly, mobile phase A was composed of 0.1% (v/v) formic acid and mobile phase B was 0.1% (v/v) formic acid in acetonitrile /water (60/40). A sample chromatogram can be seen in Figure 2.2. The peaks are identified from the supplier's datasheet.

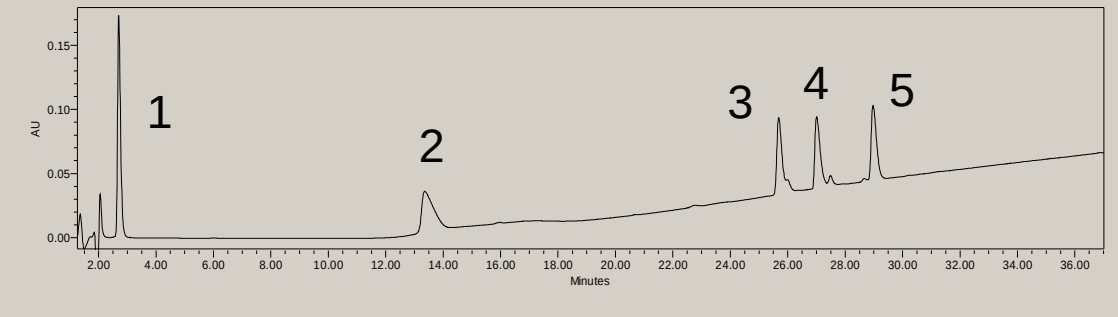

Figure 2.2: *A five peptide standard mix (0.1mg/mL of each); 1=Gly-Phe, 2= Val-Tyr-Val, 3= Met Enkephalin, 4= Angiotensin II, 5 Leu-Enkepalin. Detection wavelength 220nm. The column was a Phenomenex Jupiter C_{18} 300Å (150 x 3.0mm, 5µm).*

2.2.2 Standard protein analysis with C_{18} column

A four protein standard was then prepared and run under the same operating conditions as the peptide analysis. However, the quality of the separation was extremely poor, with broad, tailing peaks.

As a result of the poor chromatography obtained for the standard proteins, the formic acid was removed from the mobile phase. However, this made the chromatography worse. Acetic acid was then tried but again peak shape was problematic. Trifluoroacetic acid (TFA) is another wellknown ion pairing agent used in RP-HPLC. However, TFA is deemed unsuitable if the HPLC is to be coupled to electrospray MS [49], which was the ultimate aspiration of this study. This is because TFA forms very strong ion pairs with analytes that can not be easily broken apart in the conditions used in the electrospray

chamber which would hinder ionisation of the sample. Huber and Premstaller [50] compared the performance of acetic acid, formic acid and TFA for the analysis of proteins with molecular masses ranging from 14kDa to 80kDa. They found a 35 to 160-fold improvement in sensitivity when formic acid was used instead of TFA. However, Wang and colleagues [13] also conducted a study of ion pairing reagents and concluded TFA was the best choice for the HPLC analysis of *intact* proteins with MS. This was further supported by Corradini *et al.* [51] who studied TFA, formic acid and acetic acid for the analysis of membrane proteins by RP-HPLC-ESI-MS. Despite the fact that both formic acid and acetic acid showed less signal suppression than TFA, these acids resulted in poorer quality chromatography. The authors therefore, recommended TFA at a concentration of 0.05% (v/v) as the most suitable mobile phase additive. In this experiment 0.01% (v/v) trifluoroacetic acid (TFA) was added to each mobile phase and the chromatography dramatically improved (Figure 2.3).

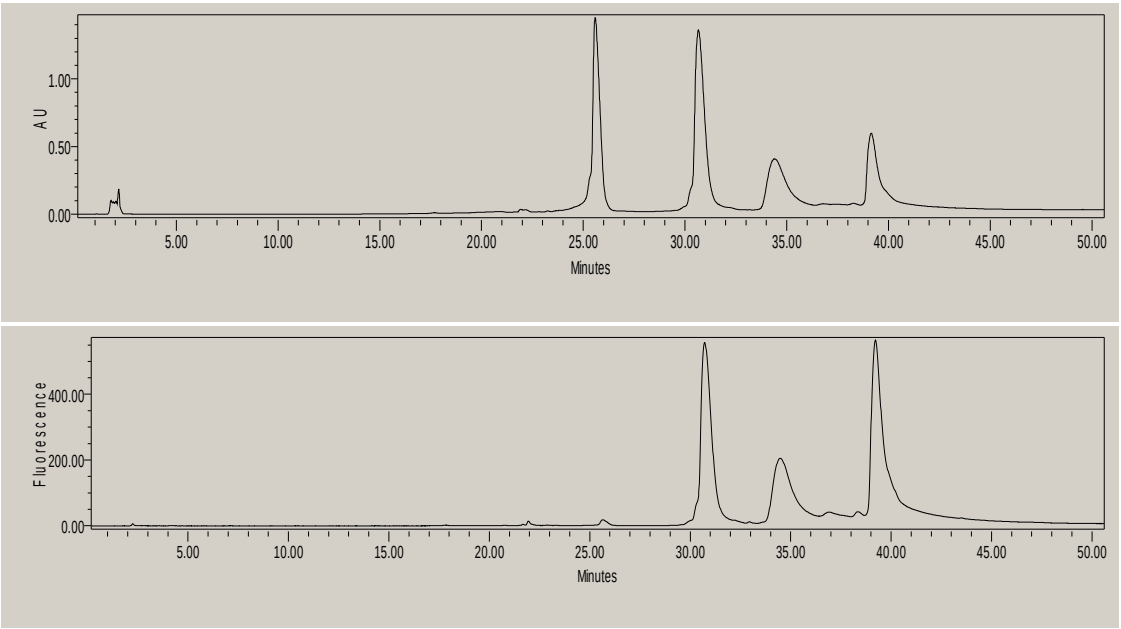

Figure 2.3: *Chromatograms of a 4 protein standard mixture and chromatographic conditions as in Figure 2.1 with the exception that the formic acid was replaced by 0.01%(v/v) TFA. The upper and lower chromatograms are for UV-Vis and fluorescence detection respectively. The column employed was a Phenomenex Jupiter C_{18} 300Å (150 x 3.0mm, 5µm)*

2.2.3 Immunodepletion of the 12 most abundant proteins

A "proof of concept" study was undertaken in order to assess the ability of the immunoaffinity column to extract albumin from samples. A human serum albumin (HSA) standard was prepared at approximately 15mg/mL- comparable to the concentration of albumin found in SF [34]. In addition, a bovine serum albumin (BSA) standard was also prepared at the same concentration for comparison. Each standard was analysed employing the immunoaffinity protocol supplied by the manufacturer, in order to assess the specificity of the method. All fractions was collected and analysed.

As expected, the immunoaffinity separation was specific for HSA as there was no protein peak found in either the "flow-through" or the non-specifically bound fractions. This demonstrates that the HSA present in SF will be fully removed thus potentially uncovering lower abundance proteins that may otherwise have been masked by the dominant HSA peak. However, the presence of some BSA in the bound fraction demonstrated that the immunoaffinity column may non-specifically remove proteins from the SF i.e. remove proteins other than the 12 listed by the manufacturer. A possible reason for this could be that BSA shares similar amino acid sequences as HSA, and these epitopes may be recognised by the HSA antibodies attached to the beads. Therefore, saving and analysing all three fractions would appear to be a prudent course of action.

2.2.4 Assessment of the effect of removing high abundant proteins on non-targeted proteins

Although the high abundant proteins, particularly albumin, will mask less abundant proteins with similar elution times, depletion columns may also bind proteins in a non-specific manner [52]. Whether bound directly to the column or indirectly through binding to a carrier protein e.g. albumin, lower abundant proteins may be inadvertently discarded. Albumin is a known carrier protein and an offshoot to proteomics – termed albuminomics – has emerged. It was decided to perform a study in order to determine if any of the four standard proteins would be non-specifically removed either by direct adhesion to the column or possibly through attachment to albumin. A mixture of HSA (20mg/mL) and the four protein standard mixture, (1mg/mL of each) was prepared and the mixture underwent the immunoaffinity protocol. The resulting chromatographs representing

analysis prior to and after employing the immunoaffinity protocol, are shown in Figures 2.4, 2.5 & 2.6.

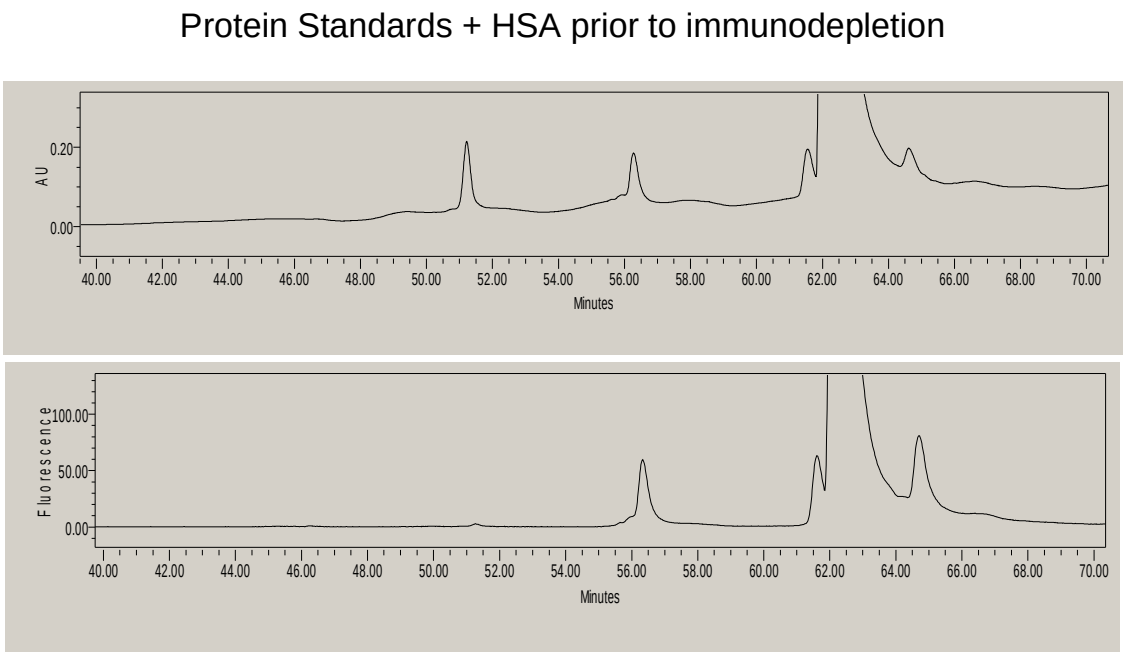

Figure 2.4: *Chromatograms depicting a mixture of four commercial, standard proteins(1mg/mL of each) plus HSA (20mg/mL) prior to the immunodepletion protocol. The upper chromatogram results from UV detection while the bottom chromatogram represents fluorescence detection. The column employed was a Phenomenex Jupiter C_{18} 300Å (150 x 3.0mm, 5μm)*

It can be seen from Figure 2.4 that the HSA peak eluted at the same retention time as one of the standard proteins and decreased the resolution of another.

Protein Standards + HSA after immunodepletion – FT fraction

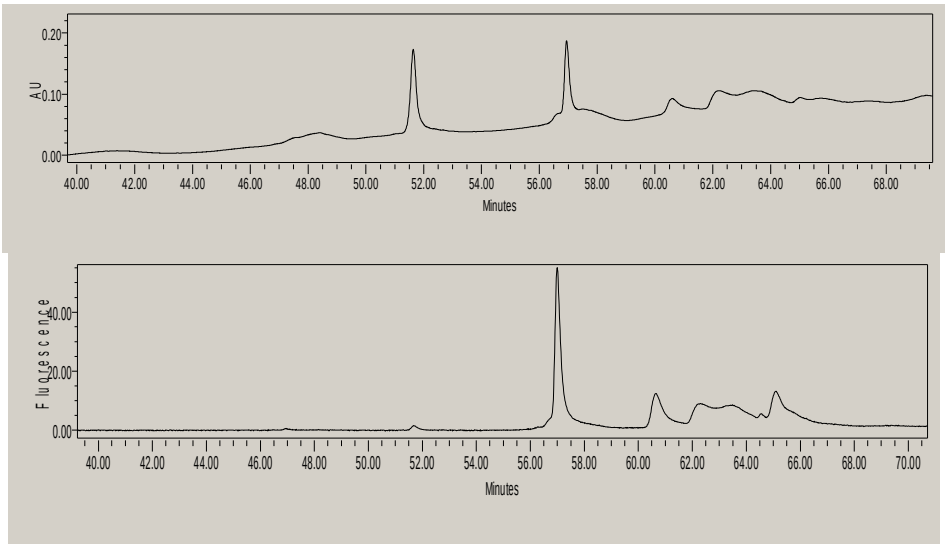

Figure 2.5: *Chromatograms depicting the flow-through (FT) fraction for a mixture of four commercial, standard proteins(1mg/mL of each) plus HSA (20mg/mL) after the immunodepletion protocol was employed. The upper chromatogram results from UV detection while the lower chromatogram represenst fluorescence detection. The column employed was a Phenomenex Jupiter C_{18} 300Å (150 x 3.0mm, 5µm)*

Protein Standards + HSA after immunodepletion – BP fraction

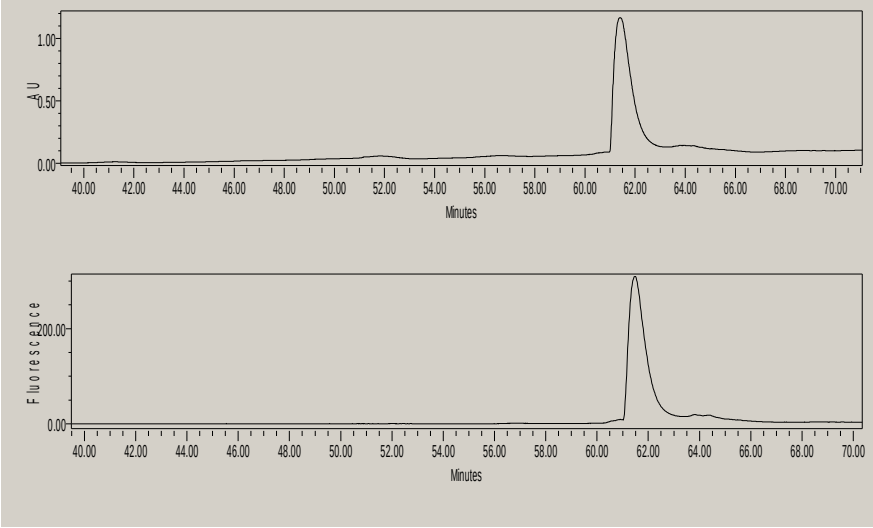

Figure 2.6: *Chromatograms depicting the flow-through (FT) fraction for a mixture of four commercial, standard proteins(1mg/mL of each) plus HSA (20mg/mL) after the immunodepletion protocol was employed. The upper chromatogram results from UV detection while the lower chromatogram represenst fluorescence detection. The column employed was a Phenomenex Jupiter C_{18} 300Å (150 x 3.0mm, 5µm)*

Comparing Figures 2.5 and 2.6 it can be appreciated that removal of albumin via immunodepletion resulted in the almost complete removal of the standard proteins that eluted at a similar retention time. Figure 2.6 confirmed albumin as the principal component of the bound fraction.

2.2.5 Analysis of synovial fluid prior to immunodepletion on C_{18} column

Prior to applying the immunodepletion procedure, it was decided to analyse one synovial fluid sample (1:25 dilution) in order to ascertain if proteins could be detected. Figure 2.7 shows that peaks are clearly evident and that both UV and fluorescence modes of detection are complimentary, with each chromatogram displaying peaks that are not evident in the other.

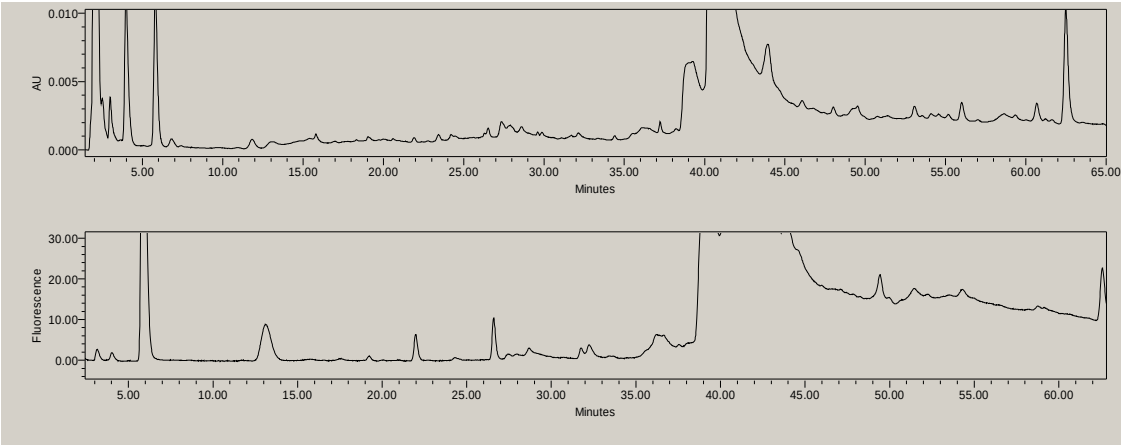

Figure 2.7: C*hromatograms for the analysis of a synovial fluid sample (1 in 25 dilution). The figure displays two modes of detection-UV (upper) and fluorescence (lower). Chromatography conditions were the same as those for the standard protein runs.*

2.2.6 Analysis of whole synovial fluid representing four different pathologies prior to immunodepletion

Four SF samples were chosen – each representing a different arthritic pathology – and analysed as before. The fluorescence chromatograms are displayed in Figure 2.8.

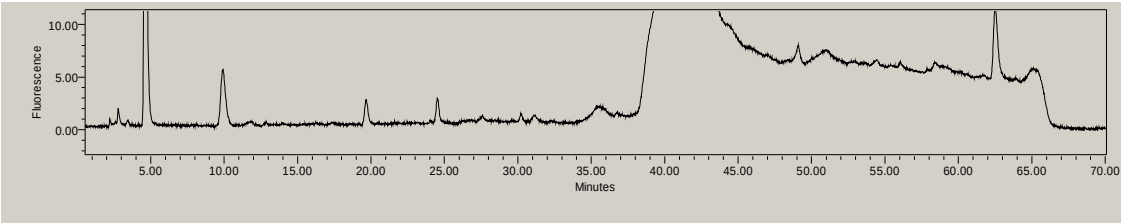

Osteoarthritis (OA)

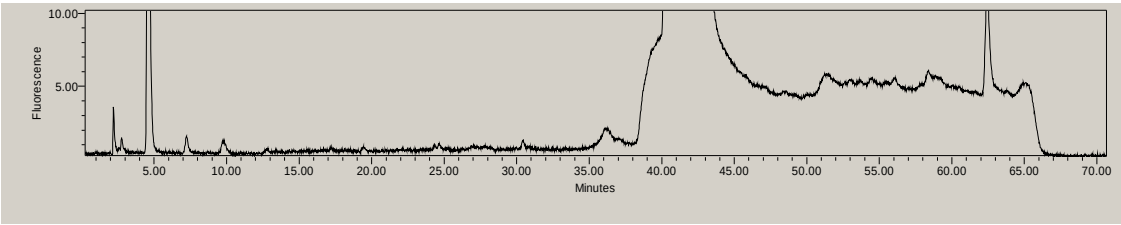

Rheumatoid Arthritis (RA)

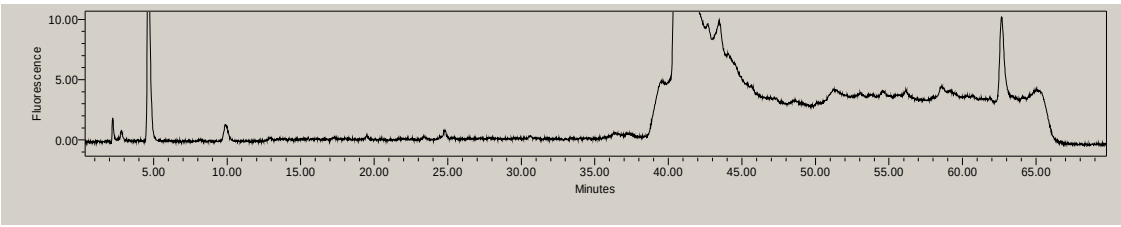

Calcium Pyrophosphate dihydrate Disease (CPPD)

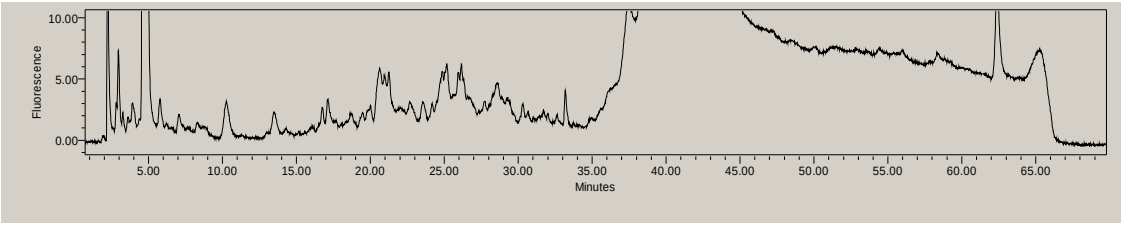

Gout

Figure 2.8: *Fluorescence detection chromatograms representing four arthritic diseases – OA, RA, CPPD and Gout. The chromatography conditions were as before.*

2.2.7 Analysis of synovial fluid after immunodepletion on C_{18} column

A SF sample was treated with dilution buffer (1:25 dilution) and the immunoaffinity protocol was employed, as described in the materials and methods section. All fractions were retained and analysed. However rather surprisingly, no protein peaks were evident in the chromatograms. Other SF samples were treated in the same way and analysed with the same. Increased injection volumes were tried in the hope that the sensitivity would increase, in addition to a number of changes to the mobile phase composition. Various alterations to the sample dilution stage were also tried. The manufacturer's standard operating procedure requires a 1:25 dilution of the sample with buffer. Various smaller dilution factors were also investigated. However, this resulted in some of the targeted proteins being found in the FT fraction. The most likely explanation for this is that all the antibody binding sites were saturated so that the excess proteins were eluted from the column with the first "wash-through".

2.2.8 Analysis of synovial fluid by 2D-PAGE

A sample of SF was sent to a colleague to confirm the protein complexity by 2D-PAGE. Approximately equal amounts of protein were loaded onto the gel as were loaded onto the HPLC. A complex proteome was confirmed (Figure 2.9). The protein complexity is comparable with that of plasma.

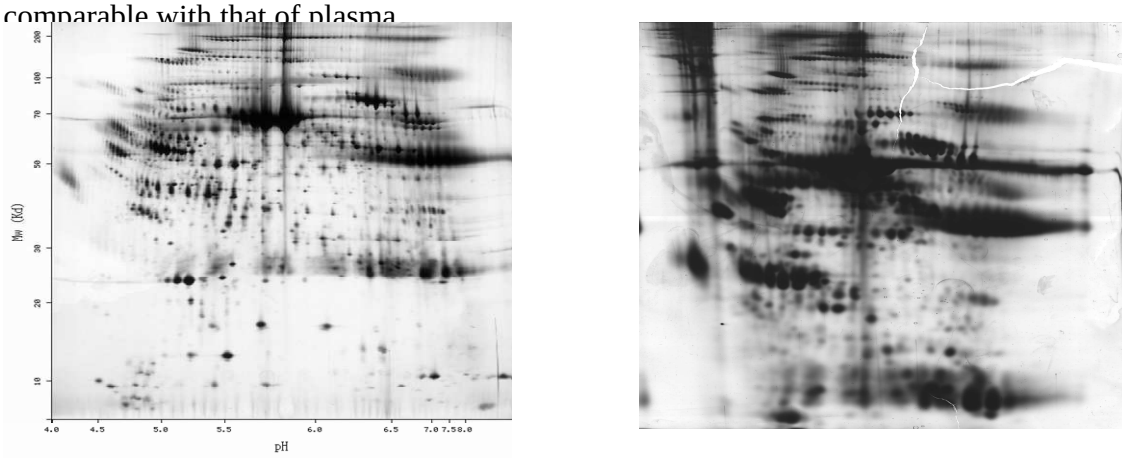

Figure 2.9: *A 2D-PAGE image of a synovial fluid sample (right). For comparison purposes a 2D-PAGE image of plasma taken from SwissProt is also displayed (left).*

2.2.9 Analysis of non-bound fraction employing a monolith capillary

A sample of the non-bound fraction containing the targeted, lower abundant proteins was sent to a protein separation specialist in Dionex (UK) Ltd to establish if proteins could be detected. Separation was performed on a monolith capillary employing UV detection. The resulting chromatogram is displayed in Figure 2.10.

Figure 2.10: *Chromatogram of a "non-bound" fraction following immunodepletion of the 12 most abundant proteins. Rather than employing a C18 reverse phase column, a capillary monolith column used. The sample was anlaysed in Dionex (UK) Ltd in order to establish if there was protein present in this fraction and that these proteins could be detected by UV detection .*

2.2.10 Synovial fluid sample analysis with immunodepletion on a C_4 column

Having proposed earlier that each arthritic pathology may have its own unique protein signature pattern, it was decided to select a number of samples of a single disease type in order investigate proteins that may be characteristic of that particular disease and determine inter-patient variability. Four OA samples were taken and the "non-bound"

fractions of each, following immunodepletion, were analysed on a C4 column. The chromatograms of the non-bound fraction of each can be seen in Figure 2.11.

OA sample 1

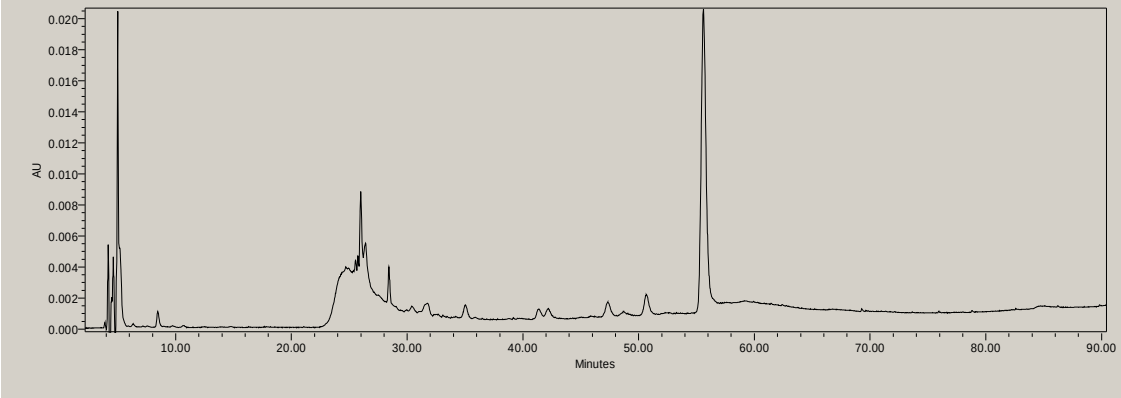

OA sample 2

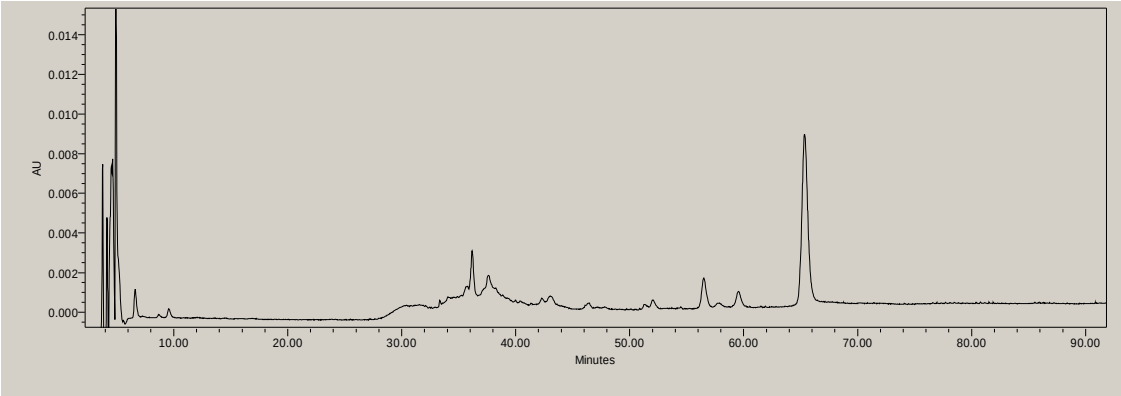

OA sample 3

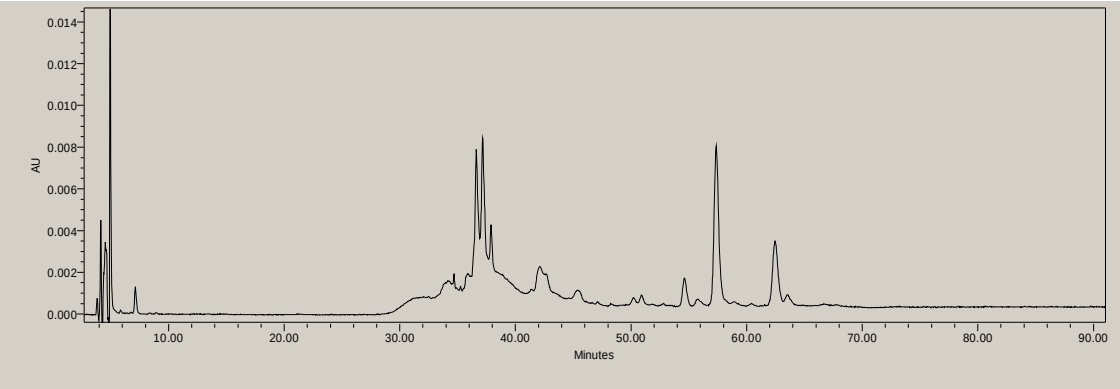

OA sample 4

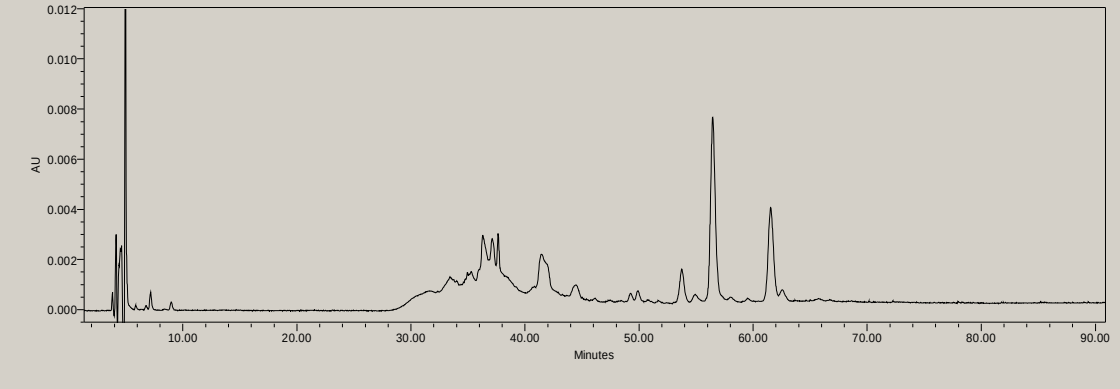

Figure 2.11: *Chromatograms of the non-bound fraction obtained after the immunoaffinity depletion of four OA samples. Separation was performed on a Phenomenex Jupiter C4 300Å (150 x 4.5mm, 5µm) column. The mobile phase and chromatographic conditions were as in the materials and methods section.*

2.2.11 Standard peptide analysis by CE

The same peptide mix that was used in the HPLC experiment was employed here. Following a good deal of method development a successful separation was obtained (Figure 2.12).

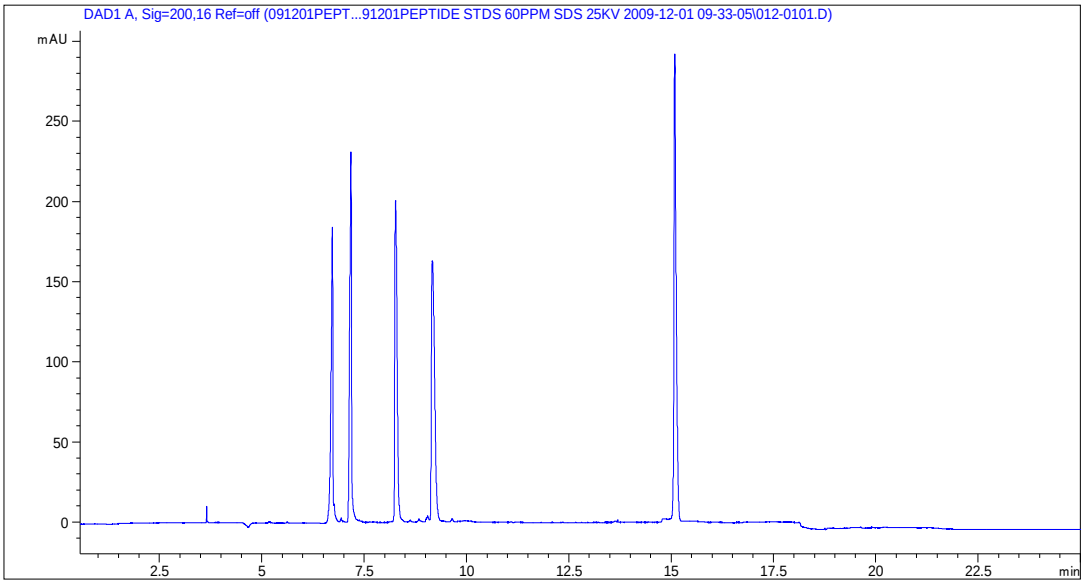

Figure 2.12: *Electropherogram of a standard five-peptide mixture. The applied voltage was 25kV and the background electrolyte consisted of 10mM sodium tetraborate containing 60ppm SDS.*

2.2.12 Standard protein analysis by CE

A mixture of four protein standards was run employing the same operating conditions. A sample electropherogram can be seen in Figure 2.13.

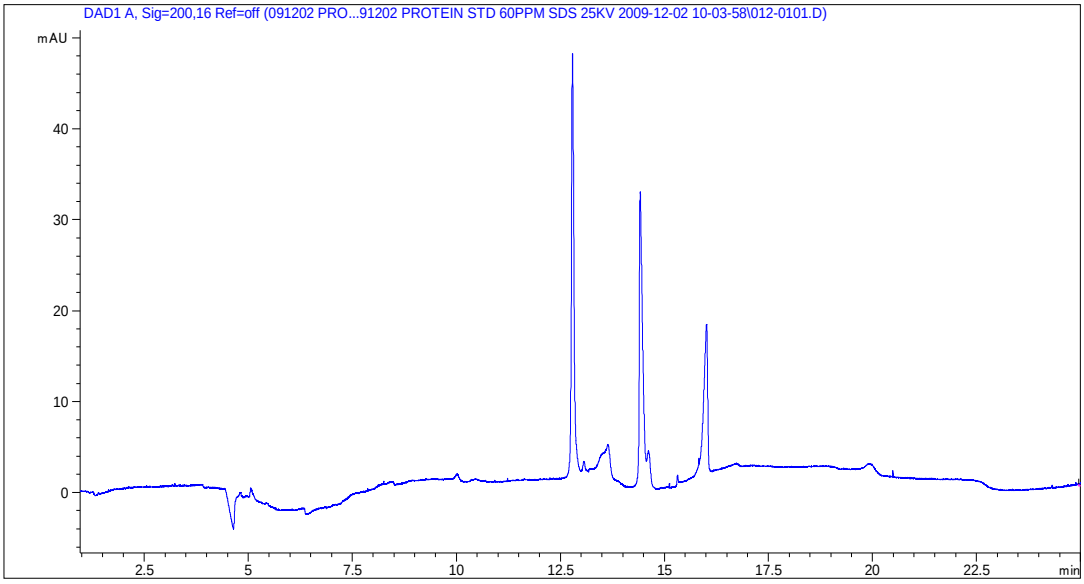

Figure 2.13: *Electropherogram of a four model-protein mixture. The applied voltage was 25kV and the background electrolyte consisted of 10mM sodium tetraborate containing 60ppm SDS. Detection was at 280nm employing UV.*

2.2.13 Analysis of synovial fluid by CE

A SF sample was filtered through a 3kDa spin filter in order to assess the low molecular weight protein/peptide/ion fraction and the high molecular weight protein fraction. An example of the low and high molecular weight fractions of a SF sample can be seen in Figure 2.14.

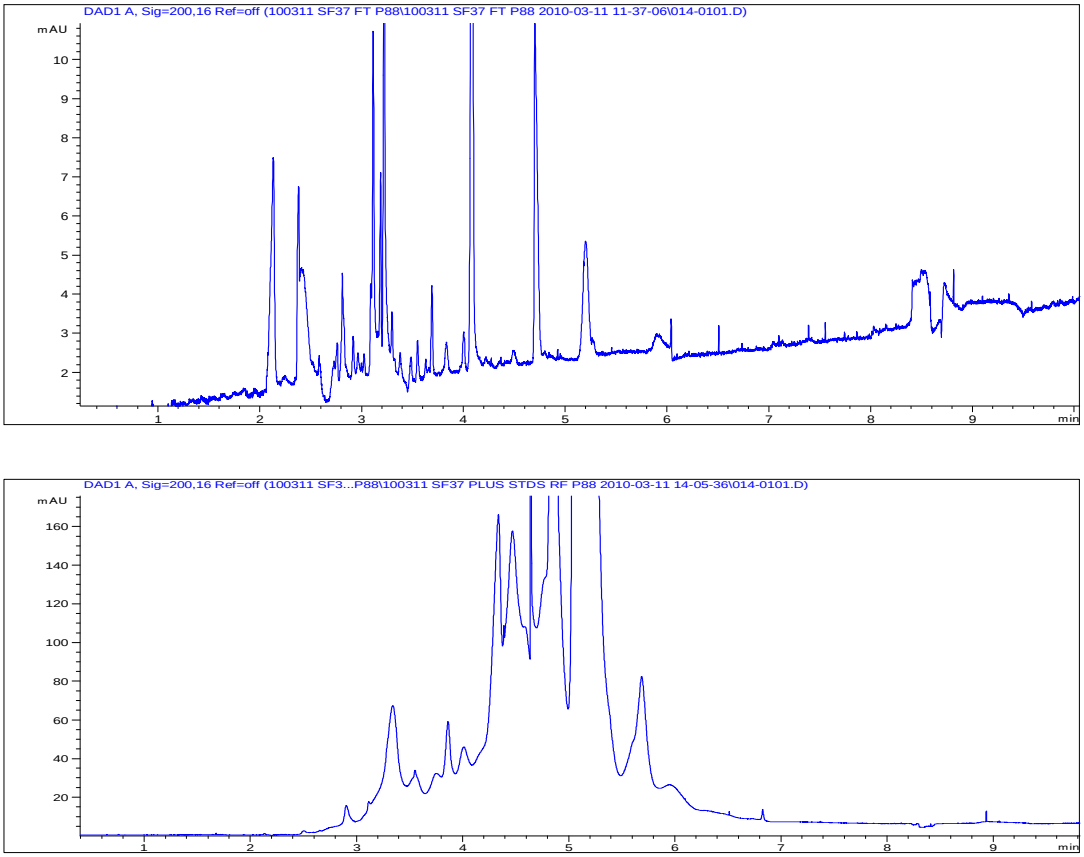

Figure 2.14: *Electropherograms for the low molecular weight (<3kDa upper) and high molecular weight (>3kDa lower) fractions of a synovial fluid sample after filtration through a 3kDa "cut-off" filter.*

2.2.14 Reproducibility of CE separations

To date, CE is not regarded as a routine tool in proteomics research due to the tendency of proteins to strongly adsorb onto the capillary wall which causes serious peak tailing, low efficiency and poor reproducibility and recovery [53]. It is said that in order to make CE as a proteomic technique more acceptable for routine analysis, improving the reproducibility in terms of peak migration time and peak area is still a major issue [54]. Capillary blockage with proteins, even over short sample sets, is another limitation. To determine if any of these issues were likely to be problematic here, a synovial fluid sample was prepared and five successive injections were performed. Three of resulting

electropherograms are displayed in Figure 2.15. Following the third run, the current dropped to zero and no separation took place.

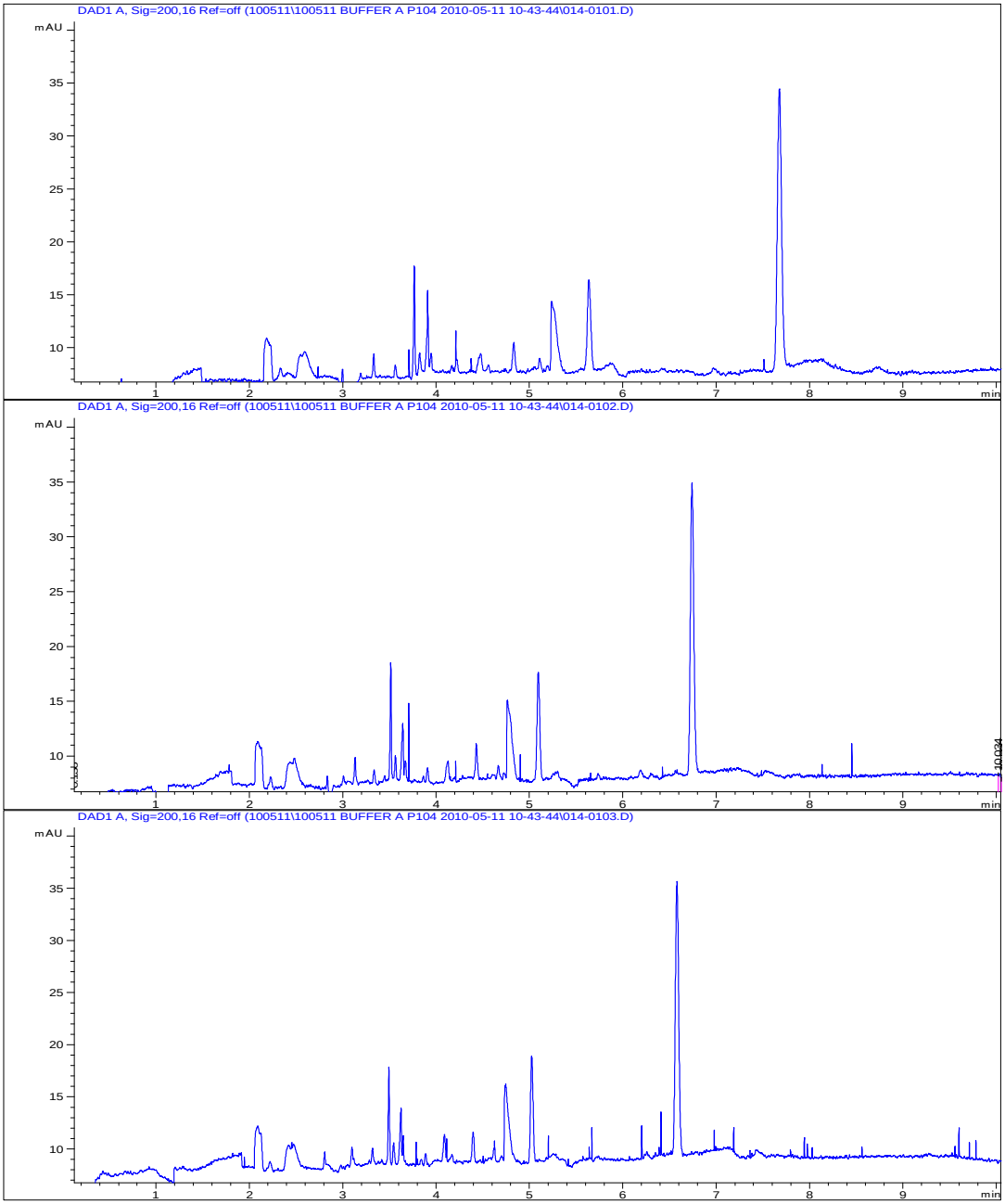

Figure 2.13: *Electropherograms for successive injections of the same synovial fluid sample. The applied voltage was 25kV and the background electrolyte consisted of 10mM sodium tetraborate containing 60ppm SDS. Detection was at 280nm employing UV.*

2.3 Discussion

2.3.1 Analysis of intact proteins in SF by HPLC

A good separation was obtained for the five standard peptide mixture (Figure 2.2). A small impurity was noted at peak number 4.

On substituting TFA for formic acid in the mobile phase, the resolution and peak shape of the four standard protein mixture improved dramatically. It is interesting to note in Figure 2.3 that the peak at 25mins is virtually absent in the fluorescence chromatogram. Only three of the twenty amino acids are naturally capable of fluorescence – tryptophan, tyrosine and phenylalanine – due to the fact that these are the only amino acids to possess aromatic side chains. Tryptophan is the most sensitive UV-absorbing amino acid, followed by tyrosine, while phenylalanine is the least [55]. The fluorescence of tryptophan is about ten times that of tyrosine, while that of phenylalanine is negligible due to its low absorbtivity and quantum efficiency. However, unlike absorption measurements, the fluorescence of proteins is not linearly proportional to the number of aromatic residues [55]. This would imply that more that one mode of detection is beneficial in complex sample analysis.

On assessing the specificity of the immunoaffinity it was found that some BSA remained in the bound fraction. This may be the effect of non-specific binding to the beads. It was concluded that the analysis of both bound and unbound fractions is necessary.

Figures 2.4, 2.5 & 2.6 demonstrate the effect of removing a high abundant protein like albumin from other less abundant proteins. The first point to note here is that all the HSA (retention time ~ 63 minutes) was successfully removed (Figure 2.5). However, comparing Figure 2.4 and 2.5, it may be argued that some of standard proteins close in retention time to HSA (protein standard number 4 ~ 65 minutes) were also removed. A possible explanation for this phenomenon, is that these proteins either remained non-specifically bound on the beads, or were attached to albumin. Gundry *et al.* [56] in their study of an albumin-enriched fraction of human serum, found 35 proteins, of which 24

were intact, were associated with albumin and included both known high and low abundance proteins. This confirms the necessity to analyse all fractions.

This importance of more that one mode of detection was again highlighted in the analysis of synovial fluid prior to immunodepletion (Figure 2.7). Here it is clear that both UV-Vis and fluorescence detection yield chromatograms with entirely different features. Both modes of detection display unique information. This could be extremely important for any 'pattern recognition' experiment where positive identification by MS may not be feasible or even required.

Encouraged by these initial results, it was decided to analyse whole synovial fluid representing a number of arthritic pathologies – OA, RA, CPPD and Gout. Inspection of Figure 2.8 clearly highlights striking differences between each of the four pathologies in the 0 – 35 minute window. The gout sample has a markedly different protein profile to the other three diseases. The OA sample also displays unique features at retention times of 20 and 25 minutes. Collection of fractions at these times and analysis by MS may prove fruitful. However, from 35 minutes on, a large and relatively featureless 'mass' is evident. It is hypothesised that a highly complex series of proteins are eluting here. In order to confirm this, a colleague performed a 2D-PAGE analysis of synovial fluid (Figure 2.9). This revealed that synovial fluid is plasma-like in terms of protein complexity and established that in order to unearth lower abundant species, removal of high abundant protein is necessary.

Following immunodepletion of the most abundant proteins, all fractions were analysed. Disappointingly, no peaks were observed in the HPLC chromatograms. Suspecting a sensitivity issue, the injection volumes were increased. In addition, changes to the sample dilution stage were also implemented. The manufacturer's standard operating procedure recommends a 1:25 dilution of the sample with buffer. Various smaller dilution factors were investigated. However, this resulted in some of the targeted proteins being found in the non-bound fraction. A possible explanation for this is that all the antibody binding sites were occupied so that the excess proteins were eluted from the column with the first wash-through.

Two possible reasons for this lack of chromatographic information were postulated;

1. The interesting peaks found in Figure 2.8 were captured on the immunoaffinity column and that the protein concentration of the unbound fraction is so low as to be undetected by both modes of detection. This would signify insufficient sensitivity.
2. There was protein adhesion to the head of the C_{18} column.

To test the insufficient sensitivity hypothesis, a sample of the unbound fraction was sent to Dionex (UK) Ltd. for analysis by HPLC employing a capillary monolith column and UV detection. A sample chromatogram may be seen in Figure 2.10. There are clearly peaks evident, thus nullifying the lack of sensitivity hypothesis.

Another reason for the scarcity of peaks in the chromatograms may be that the C18 column is too hydrophobic and that there is a build up of proteinaceous matter on the head of the column. Therefore a C_4 column was procured and the experiments repeated. Figure 2.11 displays the chromatograms of the "non-bound" fractions from four different OA patients and peaks are evident. The C_4 is less hydrophobic and exhibits less affinity for proteins. On close inspection of the four chromatograms in Figure 2.11, it can be seen that patient samples 3 and 4 are remarkably similar with some inter-patient variability within 0-10 minutes and 36-40 minutes. There are a number of peaks that share the same retention times. Other peaks are upregulated e.g. the peak at 56 minutes in sample 1.

These initial studies we deemed encouraging and the next phase of the project was to dramatically increase the sample cohort and generate a large volume of data on all the various disease subtypes in order to afford a meaningful comparison that would highlight both similarities and differences in the pattern profiles. The final stage was to identify particular proteins of interest by mass spectrometry.

2.3.2 Column Issues

As more SF samples were injected, the backpressure of the HPLC system steadily increased. Checking through the instrument logs revealed that when the C_4 column was first installed, the back pressure was around 500psi. After a number repeated injections with SF, the backpressure was over 3500psi. Various column cleaning/regenerating protocols were sought and tried. Back-flushing with all of these made no impact on column regeneration. Dowell *et al.* [3]suggested that due to the inherent complexity of their structures, proteins exhibit very unpredictable interactions with the stationary phase in the column. The primary mode of separation in RP-HPLC is due to the partitioning effect, whereby analytes constantly partition themselves between the stationary and mobile phases as they progress down the column. By contract, proteins stick to the stationary phase due to hydrophobic interactions – the greater the number of exposed hydrophobic residues, the stronger the adhesion to the column. Wang *et al.* [13] compared C_4 and C_{18} columns for protein separations using the same model proteins that were used in this experiment and concluded that they experienced protein loss due to hydrophobic interactions with the C_{18} column. No such loss was found with the C_4 column. This study would appear to challenge that assertion when complex biological samples are being analysed. It would appear that the separation of intact proteins in a complex biological matrix such as SF could not be achieved by RP-HPLC without regular replacement of expensive columns. This was disappointing as there was great potential for intact protein pattern profiling in SF.

2.3.3 Analysis of intact proteins in SF by Capillary Electrophoresis (CE)

It was then decided to continue this area of research by CE. SF analysis by CE to date has been largely being carried by Grimshaw and co-workers[57-59] . These three studies involved the quantitative analysis of hyaluronic acid in SF, a qualitative comparison between control, OA and RA samples for non-protein moieties e.g. uric acid, and finally the identification of α_1- acid glycoprotein. These components of interest were positively identified through a series of spiking experiments. Inspection of the electropherograms generated in these studies, show these analytes eluted first, followed by a large protein mass. No further work on this broad protein peak was carried out. The authors

acknowledged that attaining reproducible migration times was extremely difficult during the electrophoresis of SF samples. They attribute protein adhesion to the capillary wall as the primary reason for this. In order to minimise protein adhesion, sodium dodecylsulphate (SDS) was included in a high pH phosphate background electrolyte (BGE) and micellar electro kinetic capillary chromatography (MECC) was employed as the mode of separation. SDS is a cationic surfactant that forms micelles, with which the proteins interact and thus effect a separation. However, a major drawback with the use of surfactants and other additives to the BGE is that coupling to mass spectrometry is not possible [60]. The technical difficulties of coupling CE to MS for proteome analysis remain a challenge [61] .

As a starting point, Grinshaws's work was repeated and similar electropherograms were obtained. However as the separation of the protein agglomerate was the principal aim of this project, a new CE method was required. As in the HPLC experiment, standard model peptides and proteins were used for method development. Satisfactory resolution and peak shape were obtained (Figures 2.12 and 2.13).

Prior to performing the immunodepletion protocol and then analysing bound and unbound fractions, SF was subdivided based on molecular weight. Samples were filtered through a 3kDa filter and both molecular weight categories were separately analysed. Figure 2.14 displays the electropherograms for each fraction. As can be seen, for the <3kDa subset, good separation was obtained and the potential for pattern profiling between pathologies is evident. The >3kDa fraction would require further method optimization before useful information could be extracted.

However, prior to expending time and resources on this, it was deemed prudent to assess the reproducibility of CE in separating biological fluids. To date, CE is not regarded as a routine tool in proteomics research due to the tendency of proteins to strongly adsorb onto the capillary wall which caused serious peak tailing, low efficiency and poor reproducibility and recovery [53]. It is said that in order to make CE as a proteomic technique more acceptable for routine analysis, improving the reproducibility in terms of peak migration time and peak area is still a major issue [54]. Capillary blockage with

proteins, even over short sample sets, is another limitation. To determine if any of these short-comings are likely to become an issue here, a synovial fluid sample was prepared and five successive injections were performed. The electropherograms are displayed in Figure 2.15. Examination of the electropherograms shows that the migration times are getting shorter with each successive run. More importantly though, is that this was a five injection run. After the third injection the current dropped from approximately 80μA to zero. Therefore no electrophoretic separation was possible. Up until that point, single injections were performed with relatively simple model proteins and peptides. On turning to complex matrices like SF, it was likely that protein adhesion to the capillary wall became a significant issue. In a quite detailed study of protein attachment onto silica surfaces, Stutz [62] distinguishes between two classes of proteins, which he termed *"hard"* and *"soft"*. Hard proteins, such as cytochrome C and ribonuclease A, have a rigid structure and undergo little or no conformational change at the capillary interface. On the contrary, what he termed soft proteins e.g. HSA, BSA, Hb and IgG, are prone to unfolding once attached to the capillary surface. As the proteins unfold, there are more positively charged sites available to electro-statically attach to the negatively charged capillary wall. As the number of attachment sites increase, it becomes ever increasingly more difficult to remove the proteinaceous matter from the capillary inner wall. This exasperates the problem because the adsorption of further proteins is influenced by the proteins already adsorbed onto the capillary wall. Soon the proteins interact with each other forming what are termed "protein clusters" and "multilayer formations".

It is interesting to note that all the literature encountered in this study employed the use of model proteins to demonstrate the benefits of various buffers, wall coatings etc. Indeed, the two *"hard"* proteins cited by Stutz, i.e. cytochrome C and ribonuclease A, were two of the four model proteins employed in this study. These were used in many different studies over relatively long time periods with no adverse consequences. However, on the analysis of SF samples which contain a high content of what Stutz termed *"soft"* proteins, capillary deterioration occurred after a small number of injections were performed.

2.4 Conclusions

The aim of this project was to mine the proteome of synovial fluid for potential biomarkers of OA. This necessitated the targeted removal of the 12 most abundant proteins and analysis of the remaining depleted fraction. Biomarker discovery would be achieved by comparing the intact protein profiles of the various arthritic diseases and noting interesting differences. Identification of promising moieties would then be carried out by MS. The merit to this study would be to offset some of the limitations inherent in traditional proteomic methodologies e.g. gel electrophoresis and bottom-up, shotgun proteomics, in terms of lengthy sample preparation times and the potential to overlook very low abundant, interesting species.

The HPLC study displayed real potential in the differential characterisation of SF. Notable differences were observed between various disease states, and collection and identification of peaks of interest could be achieved. Disappointingly though, the potentially high attrition rate of columns was cost prohibitive. Investigation into the use of capillary monolith columns for intact protein analysis should merit further investigation.

Interesting separations were also achieved with CE. However reproducibility and extremely short capillary lifetimes were an issue and rendered this mode of analysis unattractive. In addition CE-MS is still in its infancy and there was little chance in taking advantage of this technique for this project.

2.5 References

References

(1) De Ceuninck, F. The application of proteomics to articular cartilage: A new hope for the treatment of osteoarthritis. *Joint Bone Spine* **2008**, *75*, 376-378.

(2) Ahn, S.; Simpson, R. J. Body fluid proteomics: Prospects for biomarker discovery. *Proteomics - Clinical Applications* **2007**, *1*, 1004-1015.

(3) Dowell, J. A.; Frost, D. C.; Zhang, J.; Li, L. Comparison of Two-Dimensional Fractionation Techniques for Shotgun Proteomics. *Analytical Chemistry* **2008**, *80*, 6715-6723.

(4) Gong, Y.; Li, X.; Yang, B.; Ying, W.; Li, D.; Zhang, Y.; Dai, S.; Cai, Y.; Wang, J.; He, F.; Qian, X. Different Immunoaffinity Fractionation Strategies to Characterize the Human Plasma Proteome. *Journal of Proteome Research* **2006**, *5*, 1379-1387.

(5) Smith, J. C.; Lambert, J.; Elisma, F.; Figeys, D. Proteomics in 2005/2006: Developments, Applications and Challenges. *Analytical Chemistry* **2007**, *79*, 4325-4344.

(6) Shi, Y.; Xiang, R.; Horváth, C.; Wilkins, J. A. The role of liquid chromatography in proteomics. *Journal of Chromatography A* **2004**, *1053*, 27-36.

(7) Bodzon-Kulakowska, A.; Bierczynska-Krzysik, A.; Dylag, T.; Drabik, A.; Suder, P.; Noga, M.; Jarzebinska, J.; Silberring, J. Methods for samples preparation in proteomic research. *Journal of Chromatography B* **2007**, *849*, 1-31.

(8) Gygi, S. P.; Corthals, G. L.; Zhang, Y.; Rochon, Y.; Aebersold, R. Evaluation of two-dimensional gel electrophoresis-based proteome analysis technology. *Proceedings of the National Academy of Sciences of the United States of America* **2000**, *97*, 9390-9395.

(9) Wagner, K.; Racaityte, K.; Unger, K.; Miliotis, T.; Edholm, L.; Bischoff, R.; Marko-Varga, G. Protein mapping by two-dimensional high performance liquid chromatography. *Journal of Chromatography A* **2000**, *893*, 293-305.

(10) Tang, J.; Gao, M.; Deng, C.; Zhang, X. Recent development of multi-dimensional chromatography strategies in proteome research. *Journal of Chromatography B* **2008**, *866*, 123-132.

(11) Li, W.; Hendrickson, C. L.; Emmett, M. R.; Marshall, A. G. Identification of Intact Proteins in Mixtures by Alternated Capillary Liquid Chromatography Electrospray Ionization and LC ESI Infrared Multiphoton Dissociation Fourier Transform Ion

Cyclotron Resonance Mass Spectrometry. *Analytical Chemistry* **1999**, *71*, 4397-4402.

(12) Everley, R. A.; Croley, T. R. Ultra-performance liquid chromatography/mass spectrometry of intact proteins. *Journal of Chromatography A* **2008**, *1192*, 239-247.

(13) Wang, Y.; Balgley, B. M.; Rudnick, P. A.; Lee, C. S. Effects of chromatography conditions on intact protein separations for top-down proteomics. *Journal of Chromatography A* **2005**, *1073*, 35-41.

(14) Gillette, M. A.; Mani, D. R.; Carr, S. A. Place of Pattern in Proteomic Biomarker Discoveryâ€. *Journal of Proteome Research* **2005**, *4*, 1143-1154.

(15) Everley, R. A.; Mott, T. M.; Toney, D. M.; Croley, T. R. Characterization of Clostridium species utilizing liquid chromatography/mass spectrometry of intact proteins. *Journal of Microbiological Methods* **2009**, *77*, 152-158.

(16) De Ceuninck, F.; Berenbaum, F. Proteomics: addressing the challenges of osteoarthritis. *Drug Discovery Today* **2009**, *14*, 661-667.

(17) Joyce T.J., Wood R.A.,Carraway R.E. Quantitation of Substance-P and its metabolites in plasma and synovial fluid from patients with arthritis. *Journal of Clinical Endocrinology and Metabolism* **1993**, *77*, 632.

(18) Sinz, A.; Bantscheff, M.; Mikkat, S.; Ringel, B.; Drynda, S.; Kekow, J.; Thiesen, H.; Glocker, M. O. Mass spectrometric proteome analyses of synovial fluids and plasmas from patients suffering from rheumatoid arthritis and comparison to reactive arthritis or osteoarthritis. *Electrophoresis* **2002**, *23*, 3445-3456.

(19) Yamagiwa H.; Sarkar G.; Charlesworth M.C.; McCormack D.J.; Bolander M.E. Two-dimensional gel electrophoresis of synovial fluid: method for detecting candidate protein markers for osteoarthritis. *Journal of Orthopaedic Science* **2003**, *8*, 482.

(20) Ostalowska, A.; Birkner, E.; Wiecha, M.; Kasperczyk, S.; Kasperczyk, A.; Kapolka, D.; Zon-Giebel, A. Lipid peroxidation and antioxidant enzymes in synovial fluid of patients with primary and secondary osteoarthritis of the knee joint. *Osteoarthritis and Cartilage* **2006**, *14*, 139-145.

(21) Garcia, B. A.; Platt, M. D.; Born, T. L.; Shabanowitz, J.; Marcus, N. A.; Hunt, D. F. Protein profile of osteoarthritic human articular cartilage using tandem mass spectrometry. *Rapid Communications in Mass Spectrometry* **2006**, *20*, 2999-3006.

(22) Wu, J.; Liu, W.; Bemis, A.; Wang, E.; Qiu, Y.; Morris, E. A.; Flannery, C. R.; Yang, Z. Comparative proteomic characterization of articular cartilage tissue from normal

donors and patients with osteoarthritis. *Arthritis & Rheumatism* **2007**, *56*, 3675-3684.

(23) Hunter D.J., Li J., LaValley M., Bauer D.C. Nevitt M., De groot J., Poole R., Eyre D., Guermazi A., Gale D., Felson D.T. Cartilage markers and their association with cartilage loss on magnetic resonance imaging in knee osteoarthritis: the Boston Osteoarthritis Knee Study. *Arthritis Research & Therapy* **2007**, *9*, 108.

(24) Rousseau, J.; Delmas, P. D. Biological markers in osteoarthritis. *Nature Clinical Practice Rheumatology* **2007**, *3*, 346.

(25) Kamphorst, J. J.; van der Heijden, R.; DeGroot, J.; Lafeber, F. P. J. G.; Reijmers, T. H.; van El, B.; Tjaden, U. R.; van der Greef, J.; Hankemeier, T. Profiling of Endogenous Peptides in Human Synovial Fluid by NanoLC−MS: Method Validation and Peptide Identification. *Journal of Proteome Research* **2007**, *6*, 4388-4396.

(26) Gobezie, R.; Kho, A.; Krastins, B.; Sarracino, D.; Thornhill, T.; Chase, M.; Millett, P.; Lee, D. High abundance synovial fluid proteome: distinct profiles in health and osteoarthritis. *Arthritis Research & Therapy* **2007**, *9*, R36.

(27) Ling, S. M.; Patel, D. D.; Garnero, P.; Zhan, M.; Vaduganathan, M.; Muller, D.; Taub, D.; Bathon, J. M.; Hochberg, M.; Abernethy, D. R.; Metter, E. J.; Ferrucci, L. Serum protein signatures detect early radiographic osteoarthritis. *Osteoarthritis and Cartilage* **2009**, *17*, 43-48.

(28) Regan, E. A.; Bowler, R. P.; Crapo, J. D. Joint fluid antioxidants are decreased in osteoarthritic joints compared to joints with macroscopically intact cartilage and subacute injury. *Osteoarthritis and Cartilage* **2008**, *16*, 515-521.

(29) Livshits, G.; Zhai, G.; Hart, D. J.; Kato, B. S.; Wang, H.; Williams, F. M. K.; Spector, T. D. Interleukin-6 is a significant predictor of radiographic knee osteoarthritis: The Chingford study. *Arthritis & Rheumatism* **2009**, *60*, 2037-2045.

(30) Baillet, A.; Trocme, C.; Berthier, S.; Arlotto, M.; Grange, L.; Chenau, J.; Quetant, S.; Seve, M.; Berger, F.; Juvin, R.; Morel, F.; Gaudin, P. Synovial fluid proteomic fingerprint: S100A8, S100A9 and S100A12 proteins discriminate rheumatoid arthritis from other inflammatory joint diseases. *Rheumatology* **2010**, *49*, 671-682.

(31) de Seny, D.; Sharif, M.; Fillet, M.; Cobraiville, G.; Meuwis, M.; Maree, R.; Hauzeur, J.; Wehenkel, L.; Louis, E.; Merville, M.; Kirwan, J.; Ribbens, C.; Malaise, M. Discovery and biochemical characterisation of four novel biomarkers for osteoarthritis. *Ann. Rheum. Dis.* **2011**, *70*, 1144-1152.

(32) Issaq, H. J.; Xiao, Z.; Veenstra, T. D. Serum and Plasma Proteomics. *Chemical reviews* **2007**, *107*, 3601-3620.

(33) Levick, J. R. Permeability of Rheumatoid and Normal Human Synovium to Specific Plasma Proteins. *Arthritis & Rheumatism* **1981**, *24*, 1550-1560.

(34) Gibson, D. S.; Rooney, M. E. The human synovial fluid proteome: A key factor in the pathology of joint disease. *Proteomics Clinical Applications* **2007**, *1*, 889-899.

(35) Björhall, K.; Miliotis, T.; Davidsson, P. Comparison of different depletion strategies for improved resolution in proteomic analysis of human serum samples. *Proteomics* **2005**, *5*, 307-317.

(36) Smejkal, G. B. I'm an -omics, you're an -omics... *Expert Review of Proteomics* **2006**, *3*, 383-385.

(37) Moritz, R. L.; Clippingdale, A. B.; Kapp, E. A.; Eddes, J. S.; Ji, H.; Gilbert, S.; Connolly, L. M.; Simpson, R. J. Application of 2-D free-flow electrophoresis/RP-HPLC for proteomic analysis of human plasma depleted of multi high-abundance proteins. *Proteomics* **2005**, *5*, 3402-3413.

(38) Gundry, R. L.; White, M. Y.; Nogee, J.; Tchernyshyov, I.; Van Eyk, J. E. Assessment of albumin removal from an immunoaffinity spin column: Critical implications for proteomic examination of the albuminome and albumin-depleted samples. *Proteomics* **2009**, *9*, 2021-2028.

(39) Govorukhina, N. I.; Keizer-Gunnink, A.; van der Zee, A. G. J.; de Jong, S.; de Bruijn, H. W. A.; Bischoff, R. Sample preparation of human serum for the analysis of tumor markers: Comparison of different approaches for albumin and γ-globulin depletion. *Journal of Chromatography A* **2003**, *1009*, 171-178.

(40) Rothemund, D. L.; Locke, V. L.; Liew, A.; Thomas, T. M.; Wasinger, V.; Rylatt, D. B. Depletion of the highly abundant protein albumin from human plasma using the Gradiflow. *Proteomics* **2003**, *3*, 279-287.

(41) Sato, A. K.; Sexton, D. J.; Morganelli, L. A.; Cohen, E. H.; Wu, Q. L.; Conley, G. P.; Streltsova, Z.; Lee, S. W.; Devlin, M.; DeOliveira, D. B.; Enright, J.; Kent, R. B.; Wescott, C. R.; Ransohoff, T. C.; Ley, A. C.; Ladner, R. C. Development of Mammalian Serum Albumin Affinity Purification Media by Peptide Phage Display. *Biotechnology Progress* **2002**, *18*, 182-192.

(42) Zolotarjova, N.; Martosella, J.; Nicol, G.; Bailey, J.; Boyes, B. E.; Barrett, W. C. Differences among techniques for high-abundant protein depletion. *Proteomics* **2005**, *5*, 3304-3313.

(43) Georgiou, H. M.; Rice, G. E.; Baker, M. S. Proteomic analysis of human plasma: Failure of centrifugal ultrafiltration to remove albumin and other high molecular weight proteins. *Proteomics* **2001**, *1*, 1503-1506.

(44) Pieper, R.; Su, Q.; Gatlin, C. L.; Huang, S.; Anderson, N. L.; Steiner, S. Multi-component immunoaffinity subtraction chromatography: An innovative step towards a comprehensive survey of the human plasma proteome. *Proteomics* **2003**, *3*, 422-432.

(45) Liu, T.; Qian, W.; Mottaz, H. M.; Gritsenko, M. A.; Norbeck, A. D.; Moore, R. J.; Purvine, S. O.; Camp, D. G.,II; Smith, R. D. Evaluation of Multiprotein Immunoaffinity Subtraction for Plasma Proteomics and Candidate Biomarker Discovery Using Mass Spectrometry. *Mol Cell Proteomics* **2006**, *5*, 2167-2174.

(46) Brand, J.; Haslberger, T.; Zolg, W.; Pestlin, G.; Palme, S. Depletion efficiency and recovery of trace markers from a multiparameter immunodepletion column. *Proteomics* **2006**, *6*, 3236-3242.

(47) Prestera, T.; Prochaska, H. J.; Talalay, P. Inhibition of NAD(P)H:(quinone-acceptor) oxidoreductase by Cibacron Blue and related anthraquinone dyes: a structure-activity study. *Biochemistry* **1992**, *31*, 824-833.

(48) Carr C.D., M. R. L. In *Role of Reversed-phase High-performance Liquid Chromatography in Protein Isolation and Purification;* Richard J. Simpson, Ed.; Puryifying Proteins for Proteomics; Cold Spring Harbor Laboratory Press: 2004; pp 179.

(49) García, M. C. The effect of the mobile phase additives on sensitivity in the analysis of peptides and proteins by high-performance liquid chromatography–electrospray mass spectrometry. *Journal of Chromatography B* **2005**, *825*, 111-123.

(50) Huber, C. G.; Premstaller, A. Evaluation of volatile eluents and electrolytes for high-performance liquid chromatography–electrospray ionization mass spectrometry and capillary electrophoresis–electrospray ionization mass spectrometry of proteins: I. Liquid chromatography. *Journal of Chromatography A* **1999**, *849*, 161-173.

(51) Corradini, D.; Huber, C. G.; Timperio, A. M.; Zolla, L. Resolution and identification of the protein components of the photosystem II antenna system of higher plants by reversed-phase liquid chromatography with electrospray-mass spectrometric detection. *Journal of Chromatography A* **2000**, *886*, 111-121.

(52) Hiroshi Y.; Sarkar G.; Charlesworth C.; McCormick D.; Bolander M. Two-dimensional gel electrophoresis of synovial fluid: method for detecting candidate protein markers for osteoarthritis. *Journal of Orthopaedic Science* **2003**, *8*, 482.

(53) Liu, Q.; Yang, Y.; Yao, S. Enhanced stability of surfactant-based semipermanent wall coatings in capillary electrophoresis using oppositely charged surfactant. *Journal of Chromatography A* **2008**, *1187*, 260-266.

(54) Suratman, A.; Wätzig, H. Long-term precision in capillary isoelectric focusing for protein analysis. *Journal of Separation Science* **2008**, *31*, 1834-1840.

(55) Issaq, H. J.; Chan, K. C.; Blonder, J.; Ye, X.; Veenstra, T. D. Separation, detection and quantitation of peptides by liquid chromatography and capillary electrochromatography. *Journal of Chromatography A* **2009**, *1216*, 1825-1837.

(56) Gundry, R. L.; Fu, Q.; Jelinek, C. A.; Van Eyk, J. E.; Cotter, R. J. Investigation of an albumin-enriched fraction of human serum and its albuminome. *Proteomics - Clinical Applications* **2007**, *1*, 73-88.

(57) Duffy J.M., Grimshaw J., Kane A., Mollan R.A.B., Spedding P.L., Trocha-Grimshaw J. Capillary Electrophoresis of naormal human synovial fluid: comparasion with fluid from disease states of osteoarthritis and rheumatoid arthritis. *Analytical Proceedings Including Analytical Communications* **1994**, *31*, 257.

(58) Grimshaw J., Trocha-Grimshaw J., Fisher W., Rica A., Smith S., Spedding P., Duffy J., Mollan R. Quantitative analysis of hyaluronan in human synovial fluid using capillary electrophoresis. *Electrophoresis* **1996**, *17*, 396.

(59) Rice, A.; Grimshaw, J.; Trocha-Grimshaw, J.; McCarron, P.; Wisdom, G. B. Identification of α1-acid glycoprotein (orosomucoid) in human synovial fluid by capillary electrophoresis. *Journal of Chromatography A* **1997**, *772*, 305-311.

(60) Lamari, F. N.; Karamanos, N. K. Methodological Challenges of Protein Analysis in Blood Serum and Cerebrospinal Fluid by Capillary Electrophoresis. *Chromatographia* **2003**, *58*, 349-356.

(61) Ahmed, F. E. The role of capillary electrophoresis–mass spectrometry to proteome analysis and biomarker discovery. *Journal of Chromatography B* **2009**, *877*, 1963-1981.

(62) Stutz, H. Protein attachment onto silica surfaces - a survey of molecular fundamentals, resulting effects and novel preventive strategies in CE. *Electrophoresis* **2009**, *30*, 2032-2061.

Chapter 3

Isolation and characterisation of microvesicles in synovial fluid

3.0 Introduction

3.0.1 Microvesicle nomenclature

A relatively recent and interesting line of research into small vesicles s from most cell types, has contributed to an increase in understanding in signalling and molecular transfer mechanisms between cells [1]. Cell-to-cell communication is required to ensure a coordinated functionality among different cell types within the tissue. Modes of communication include (i) secretion of soluble species e.g. cytokines and hormones [2], (ii) cell-to-cell interaction via adhesion molecules which enable ligand-receptor mediated exchange of surface molecules e.g. the activation of T cells by antigen-presenting cells i.e. immunological synapse and (iii) the exchange of both membrane and cytosolic components (including organelles) via nanotubules [3, 4]. In addition to these communication lines, cells may transfer information via membrane-bound fragments which are generically termed microvesicles (MVs). MVs have been known to exist for quite some time. However, their role in cell-to-cell communication was not initially realised. It was thought that they were simple inert cell debris or plasma membrane turnover [5] or even artefacts [6]. It was De Broe *et al.* [7] who first suggested that these plasma membrane fragments result from a specific, biological process and also, that the enzyme composition of the vesicle membrane maintained the same ratio as that of the parent cell.

Subsequently, it was realised that the term *microvesicle* does not represent one, unique homogeneous entity. Indeed, the nomenclature in the field of membrane-bound small fragments remains controversial and confused. Terms such as microvesicle, microparticles (MPs), exosomes, ectosomes, shedding vesicles and even apoptotic blebs are often used interchangeably in the literature. In their review paper, Simpson *et al.* [8] observe that these entities share many similarities. For example, exosomes, apoptotic blebs and MPs exhibit the same membrane topology, i.e. the cytosolic side of the lipid bilayer is inside the vesicle while the luminal portion of the membrane is exposed with bound phosphatidylserine. The authors state that in the case of MPs and MVs, the variety of isolation schemes employed, and a lack of biochemical and biophysical validation

protocols leads one to ask if these vesicles represent discreet entities with specialised functions or are merely different sizes of the same thing. Further, the term MVs is often used to describe different species of vesicle, while at other times as a generic term for MPs and exosomes, thus using the terms interchangeably. Sadallah *et al.* [9] make no distinction between ectosomes and shedding vesicles. Johnstone [10] cites some examples of studies which produced conflicting results in the analysis of vesicles derived from tumour cells. It was concluded that a lack of information and a precise definition of terms may lie at the core of the discrepancy in the literature. The author further adds that a single cell may produce different populations of vesicles and that most investigators have harvested these as if they represented a single population of identical vesicles. Cocucci *et al.* [6] define a number of terms which may be useful in clarifying all subsequent discussion in this project, and is produced in Table 3.1.

Micro/Nano Vesicle Terminology
Ectosome: term used to indicate shedding vesicles of neutrophils and monocytes.
Endosome: small vesicle accumulated within MVBs and discharged upon their exocytosis.
Enlargesome: a non-secretory exocytic vesicle.
Endosomal sorting complexes required for transport (ESCRETs): multimolecular systems involved in the sorting of MVB vesicles.
Exosome: a vesicle contained in MVBs.
Microparticle: term used to define shedding vesicles of platelets and monocytes.
Microvesicle: term used to indicate exosomes and shedding vesicles together.
Multivesicular bodies (MVBs): intracellular organelles of the endosomal system that contain exosomes. MVBs can fuse with the plasma membrane, releasing exosomes from the cell.
Shedding vesicle: a vesicle that buds directly from the plasma membrane into the extracellular space.

Table 3.1: *A list of various micro/nano vesicles and their definitions as proposed by* [6]

With a defined vocabulary in place, a more detailed examination of micro/nano vesicles will follow. Regardless the vesicle type or its origin, there are but two distinct processes of vesicle release from cells. In broad terms these are;

1. Vesicles that are derived from the endosomal pathway which following subsequent fusion with the plasma membrane, are exocytosed as exosomes [11] .
2. Vesicles that originate by direct budding of the cell plasma membrane [6].

3.0.2 Microvesicle variety

A concern in the study of MVs lies in distinguishing one vesicle type from another. As mentioned above, the terminology and vocabulary employed does not enjoy universal agreement. Vesicle populations recovered from either cell incubation media or biofluids are inevitably of mixed origin. Théry *et al.*[12] provide a very useful table summarising the physicochemical characteristics of different types of secreted vesicle. This is shown in Table 3.2.

Feature	Exosomes	Microvesicles	Ectosomes	Membrane Particles	Exosome-like Vesicles	Apoptopic Vesicles
Size	50-100nm	100-1,000nm	50-200nm	50-80nm	20-50nm	50-500nm
Density in Sucrose	1.13-1.19g/mL	ND	ND	1.04-1.07g/mL	1.1g/mL	1.16-1.28g/mL
Appearance by electron microscopy	Cup shape	Irregular shape and electron-dense	Bilamellar and round	Round	Irregular shape	Heterogeneous
Sedimentation	100,000g	10,000g	160,000-200,000g	100,000-200,000g	175,000g	1,200g, 10,000g or 100,000g
Lipid Composition	Enriched in: Cholesterol, Sphingomyelin, Ceramide Contains lipid rafts; exposes phosphatidylserine	Exposes Phosphatidyl serine	Enriched in: Cholesterol, Diacylglycerol exposes phosphatidylserine	ND	Do not contain lipid rafts	ND
Main protein markers	Tetraspanins (CD63 & CD9) Alix Tsg101	Integrins, selectins and CD40 ligand	CR1 and proteolytic enzymes; no CD63	CD133; no CD63	TNFRI	Histones
Intracellular origin	Internal compartments (endosomes)	Plasma membrane	Plasma membrane	Plasma membrane	Internal compartments	ND

Table 3.2:*A summary of the physicochemical properties of secreted vesicles. Various differences and similarities are evident. ND=not determined. TNFRI=Tumour necrosis factor receptor 1. Information adapted from* [12].

The author however, cautions that all vesicle preparations are heterogeneous with different protocols allowing enrichment of one type over another. Also, it was stressed that electron microscopy is only an indication of vesicle type and should not be employed to define vesicle types. Cocucci *et al.* [6] advise that presently the most promising studies are those based on immunoprecipitation, using antibodies against antigens exposed at the vesicle surface. Recently Lee *et al.* [13] listed differentially expressed markers between ectosomes and exosomes. A modified list can be seen in Table 3.3.

Marker	Function
Ectosome/ Shedding Vesicle	
Tissue factor (TF)	Coagulation and angiogenesis
Flotillin-1	Lipid raft molecule
PSGL1	P selectin glycoprotein ligand 1 - cell adhesion
β1 integrin	Cell adhesion molecule
IL-1β	Cytokine involved in inflammation
MMP2	Matrix metalloproteinase involved in degradation of ECM
MMP9	Matrix metalloproteinase involved in degradation of ECM
EMMPRIN	ECM metalloproteinase inducer
ARF6	Remodelling of membrane lipids and actin
MUC1	Mucin associated with pathogen protection
CB1	Cannabinoid G protein coupled receptor
Lineage Markers	CD61; glycophorin A; CD66e; CD14; CD62e
Exosomes	
CD9	Tetraspanin - cell surface glycoprotein
CD37	Tetraspanin - cell surface glycoprotein
CD63	Tetraspanin - cell surface glycoprotein
CS81	Tetraspanin - cell surface glycoprotein
CD106	Tetraspanin - cell surface glycoprotein
Tspan8	Tetraspanin - cell surface glycoprotein
HSP70	Heat shock protein
HSP90	Heat shock protein
Caveolin-1	Scaffolding protein of lipid rafts
Rab-5a	GTPase involves in endocytosis
Rab-5b	GTPase involves in endocytosis
PLP	Proteolipid protein
Alix	Protein involved in late endocytosis
TSAP6	P53 transcriptional target involved in exocytosis
Tsg101	Protein involved in ubiquitination-dependent endocytosis
MHC ClassI/II	Immune recognition/regulation
Flotillin-1	Lipid raft molecule

Table 3.3: *Molecular markers believed to be associated with ectosomes/shedding vesicles and exosomes*

Recently, György *et al.* [14] published a paper cautioning against interfering species in the isolation of MVs. It was claimed that after comprehensive characterisation of MVs by electron microscopy, atomic force microscopy, dynamic light scattering and flow cytometry, protein complexes, especially insoluble immune complexes (IC) overlap in biophysical properties (size, light scattering and sedimentation) with MVs. The effect of this overlap is that purification and quantification of MVs is compromised as both ICs and free immunoglobulins may co-precipitate in the pellet. This is especially true in the case where ICs are common, including autoimmune diseases, hematologic disorders, infections and cancer. They conclude that "*Results obtained without MP-IC discrimination should be interpreted cautiously. This is also underlined by a previous work in which RA SF MPs were reported to carry IgG, IgM, complement components, serum amyloid P and C-reactive protein"*. A study by Mayr *et al.* [15] on microparticles, found that immunoglobulins were not surface labelled with the fluorescent tag CyDyes and suggested that these species might be entrapped within the vesicles. In light of these findings it may be important to establish the origin of any immunoglobulins present. Are they (i) free species within the matrix, (ii) associated on the microvesicle surface or (iii) entrapped within the vesicle? Could it be that they are present in all three locations?

Other potential "contaminants" in any MV-isolation protocol are high-density lipoproteins (HDLs). This is because due to considerable overlapping density ranges, HDLs will be potentially present if MV isolation is based on differential centrifugation or any variation thereof. From above, exosomes have a density range between 1.13-1.19g/mL, while HDLs fall within the 1.063-1.210g/mL range [16].

MVs are therefore, an assorted population of membrane-bound entities that differ in cellular origin, size and cargo composition and are shed in both physiological and pathological conditions [9]. Ratajczak and co-workers [17] state that MVs are released by cells upon activation by soluble agonists, by physical or chemical stress e.g. oxidative stress and hypoxia and also by shear stress.

It now follows to describe the biogenesis of the vesicles produced by these pathways.

3.0.3 Microvesicle Biogenesis

3.0.3.1 Exosomes - Microvesicles derived from the endosomal pathway

Exosomes are saucer-shaped vesicles, 30-100nm in diameter and are bound by a lipid bilayer [18]. In general, these vesicles have a density ranging from 1.13g/mL (for B cell derived) to 1.19g/mL (for intestinal derived) [19]. They are released into the extracellular matrix (ECM) upon fusion of multivesicular bodies (MVBs) with the cell surface. MVBs contain intralumenal vesicles (ILVs) that are released during exocytosis. These released or exocytosed ILVs are then termed exosomes. To date knowledge on the assembly mechanism of exosomes is still not complete [1]. However, what is known for certain is that exosomes are a product of the endosomal pathway.

Electrographs displaying the exocytosis of exosomes may be seen in Figure 3.1. In Figure 3.1a the MVBs from the endosomal pathway carrying ILVs can be seen approaching the cellular membrane. Following fusion of the MVB with the plasma membrane, The ILVs undergo exocytosis and are released into the ECM as exosomes (Figure 3.1B).

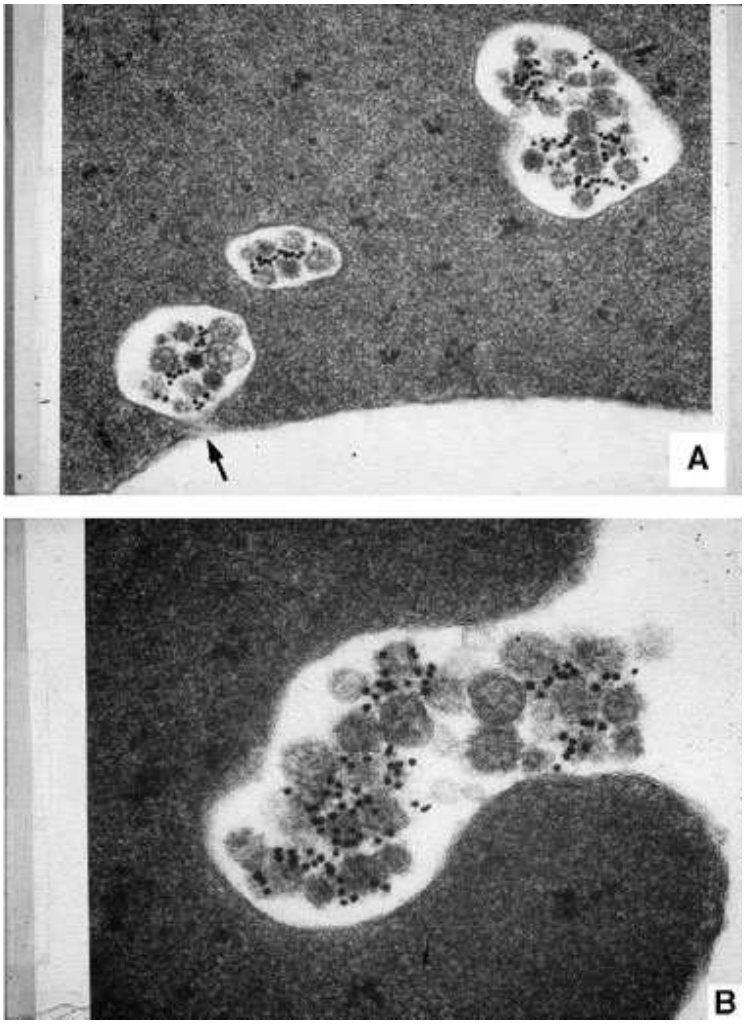

Figure 3.1: *Colloidal gold electron micrographs of maturing sheep reticulocyte exosomes at two different times. In (A) 18 hours post incubation with transferrin receptor mAb. The black arrow indicates the point of contact of the MVB with the plasma membrane. After 36 hours(B) the MVB cargo is shed into the ECM as exosomes. Picture taken from*[8]

3.0.3.2 Biogenesis of exosomes

Exosomes originate from the cell surface and their role is to ferry unneeded, damaged or dangerous plasma membrane protein cargo - either internalised from the cell membrane or through the Golgi network - to the lysosome for destruction [20 21] or to the cell surface for release as exosomes. Johnstone *et al*. [22] initially coined the term exosome for vesicles

produced by intracellular budding in the endosome while Harding *et al.* [23] first proposed a model for the secretion of entrapped vesicles within the endosome at the cell surface. This model was confirmed by Pan *et al.* [24]. Using immunoelectron microscopy, both groups studied the fate of an internalised anti-transferrin receptor antibody in reticulocytes. They also provided a chronological sequence of events culminating in the release of exosomes at the cell surface. This may be seen in Figure 3.2.

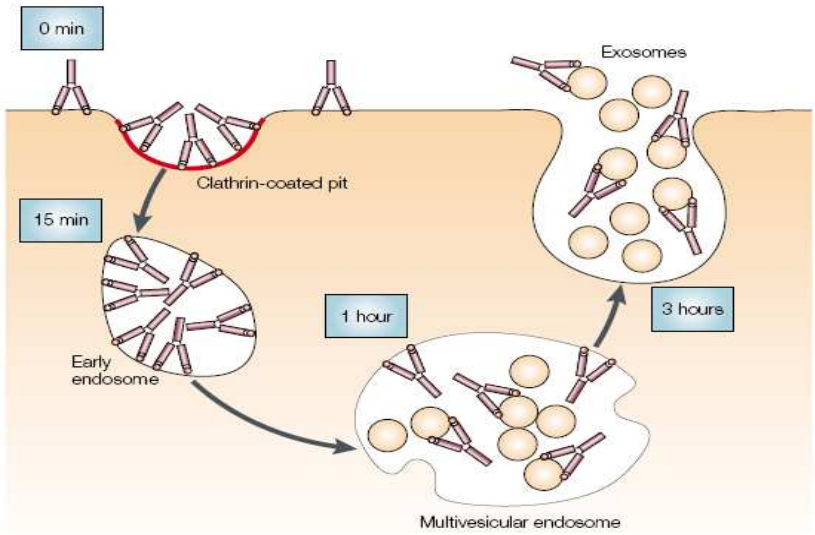

Figure 3.2: *The chronological pathway for the formation of exosomes as proposed by Harding [23] and Pan [24]. The pathway followed by internalised anti-transferrin-receptor antibody is outlined. Invagination or internal budding of the late endosome to for a MVB can be seen before final release to the ECM as exosomes. Image taken from [25]*

An overall schematic representation of the endocytic pathway outlining the fate of proteins can be seen in Figure 3.3.

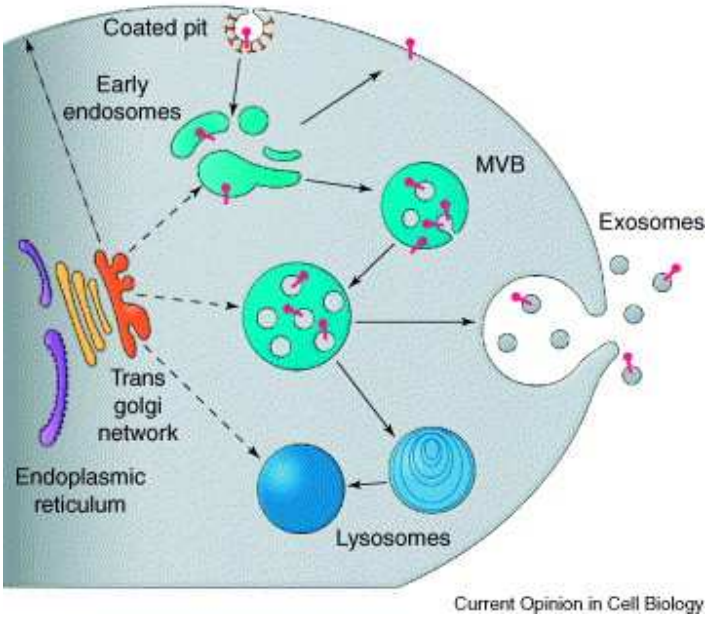

Figure 3.3: *A schematic diagram of the endosomal pathway. Proteins (in red) are entrapped inside the endosome. From there two destination routes are possible – destruction by fusion with a lysosome or exocytosis via fusion with the plasma membrane as exosomes. Diagram is taken from* [26].

From Figure 3.3 it may be seen that proteins which are delivered to the endosome become engulfed in vesicles which are generated by internal budding or invagination of the endosomal membrane to form ILVs. This MVB is then destined to fuse with the lysosome or with the plasma membrane. It is still not known how a decision at the cellular level is made determining which of the two routes the MVB embarks upon.

Though the presence of MVBs is now widely accepted, there are still significant gaps in the understanding of MVB biogenesis, in particular the budding or invagination mechanism and the protein cargo selection process [27].

Relating to the sorting of cargo, Katzmann *et al.* [28] proposed that protein sorting into MVBs involves monoubiquitination of endosomal proteins, while van Niel *et al.* [29] in their study of dendritic cells suggested that oligoubiquitination may also be a sorting mechanism for trafficking proteins into MVBs. It was proposed that oligoubiquitination

increases the cargo sorting efficiency. Finally, other studies [30, 31] provide evidence that proteins need not be ubiquitin labelled for inclusion in the MVB.

Hurley *et al.* [32] outline four membrane budding models which may be seen labelled A-D in Figure 3.4.

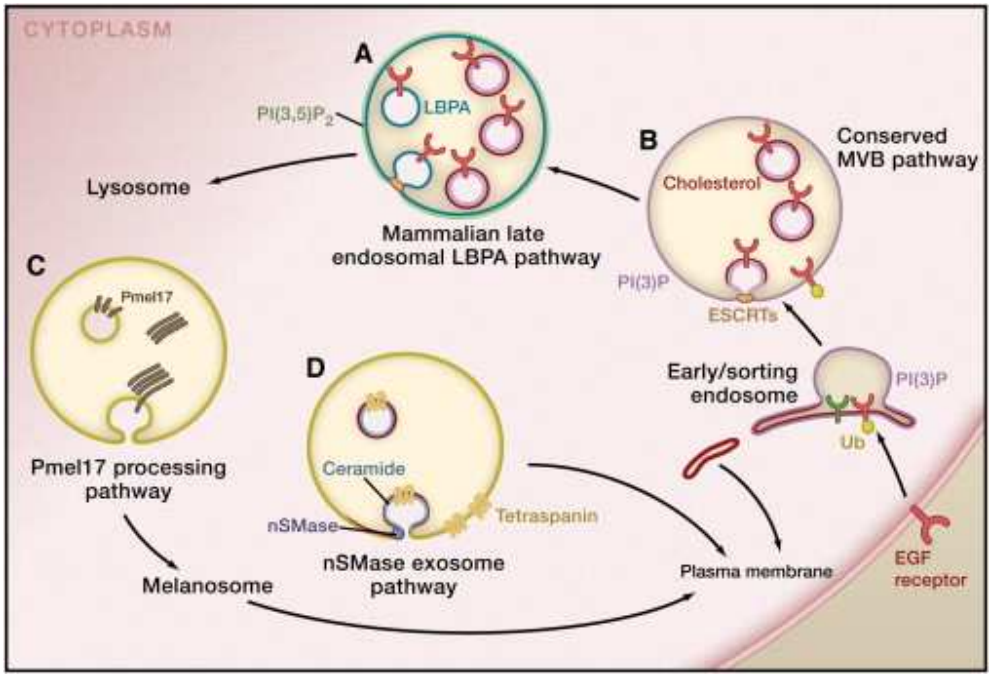

Figure 3.4: *Modes of endosomal membrane budding within the cell. Four separate mechanisms are known to exist, labelled A ,B, C and D. Diagram taken from* [32]

3.0.3.2.1 ESCRT Dependant Membrane Budding

A key promoter for protein inclusion in MVBs is the hetero-oligomeric protein complex, endosomal sorting complex required for transport (ESCRT) [27]. ESCRT-0, -I, -II and –III are believed to recognise ubiquitinated proteins and ensure their inclusion in MVBs. It is believed that once the cargo is delivered to the vesicle, the ESCRT complex dissociates from the membrane and is recycled for further cargo transport. Interestingly, Simpson *et al.* [8] include the ESCRT-I,-II and -III complexes in their list of proteins possessed by *all* exosomes. This conflicting data again highlights a lack of consensus within this current area of research.

The endosomal pathway is believed to begin with the presence of the lipid, phosphatidylinositol 3-phosphate (Pl(3)P) plus ubiquitin-labelled species on the surface

of the early endosome. This may be seen in the pathway labelled B in Figure 3.4. The Pl(3)P plus the ubiquitinated cargo form a docking site on the endosomal surface for the ESCRT complexes. The membrane budding process is quite complex and the fine detail is still not fully understood. Briefly ESCRT-0, which contains five ubiquitin-binding domains, binds to ubiquitinated cargo on the endosomal surface [32]. This initiates the recruitment of ESCRT –I, -II and –III [33, 34]. The ESCRT–I and –II complexes are believed to drive the budding process while the ESCRT-III unit cleaves the bud neck and so completes the formation of the ILV. It is hypothesised that as the ESCRT complexes are localised at the bud neck, budding proceeds away from the cytosol without the ESCRT complex being included in the ILV. Again, this would appear to conflict with Simpson *et al.* [8] who found ESCRT moieties engulfed within exosomes.

3.0.3.2.2 Lipid Lysobisphosphatidic Acid (LBPA) Dependant Membrane Budding

Matsuo *et al*. [35] proposed an alternative invagination model specific to the late endosomal pathway. They note that the late endosome contains approximately 15% LBPA and declare that this lipid is not present anywhere else in the cell. The authors conclude that LBPA is involved in the trafficking of proteins and lipids through late endosomes. Furthermore, they proposed that LBPA in conjunction with the Alix protein in an acid environment also produces ILVs. Alix is one of the proteins that are part of the endosomal machinery responsible for sorting proteins along the endocytic/degradative pathway [27]. This model is also ESCRT-dependent. Their studies have also shown that the absence of either LBPA or Alix disrupts the production of ILVs. This process is labelled A in Figure 3.4.

3.0.3.2.3 ESCRT and Ubiquitin Independent Membrane Budding

MVBs are also formed within lysosome-related organelles e.g. melanosomes, without requiring the ESCRT complex or ubiquitin labelling. Raposo *et al.* [36] studied the sorting

of the glycoprotein Pmel17 into ILVs in an ESCRT-independent reaction. This can be seen as pathway C in Figure 3.4.

3.0.3.2.4 Spingomyelinase Dependent Membrane Budding

Trajkovic *et al.* [37] discovered a further ESCRT-independent budding mechanism. Here, ILVs are produced by the hydrolysis of sphingomyelin by shingomyelinase to produce ceramide. However, it is not clear which properties of ceramide favour the budding mechanism. What is known though, is that exosomes produced by this mechanism are highly enriched in the tetraspanin CD63. CD63 is an exosomal marker (Tables 3.2 and 3.3) and will be used to confirm the presence of exosomes. This mechanism is shown as pathway D in Figure 3.4.

3.0.3.3 Biogenesis of ectosomes or shedding vesicles

Vesicles released directly from the cell surface are termed ectosomes or shedding microvesicles [6]. Stein and Luzio [38] first coined the term 'ectocytosis' for the release of vesicles from the cell membrane, though these microparticles were first reported by Wolf *et al.* in 1967 [39]. It was noticed that human plasma platelets shed particles that were small, membrane-coated vesicles. Hence the term *"platelet dust"* was coined. Further studies demonstrated that like the cells from which they were derived, these particles have a role in clotting and are not inert. Subsequently it was discovered that microparticles can be released from multiple cell types e.g. macrophages, monocytes, B and T cells, neutrophils, erythrocytes, endothelial cells, vascular smooth muscle cells, epithelial cells and tumour cell lines [40].

The cell membrane is composed of a lipid bilayer. However, each of the two leaves is quite different in terms of lipid composition i.e. there is lipid heterogeneity. The inner (cytosolic) membrane contains phosphatidylserine (PS) and phosphatidylethanolamine (PE), while the outer leaf is enriched in phosphatidylcholine and sphingomyelin. This asymmetric lipid composition of the cell membrane is maintained and controlled by three enzymes – flippase, floppase and scramblase [41]. In response to cell stimulation there is a

sustained increase in Ca^{2+} concentration in the cytoplasm and this is thought to lead to a breakdown in the asymmetric lipid composition of the outer membrane [42]. A notable feature of this remodelling is the surface exposure of the inner PS moiety. This is followed by MP release into the ECM by a Ca^{2+}-dependent proteolysis of the cellular membrane. These released vesicles are termed ectosomes or shedding vesicles. A schematic diagram of such vesicles may be seen in Figure 3.5. This representation does not display all the cargo species present in these vesicles.

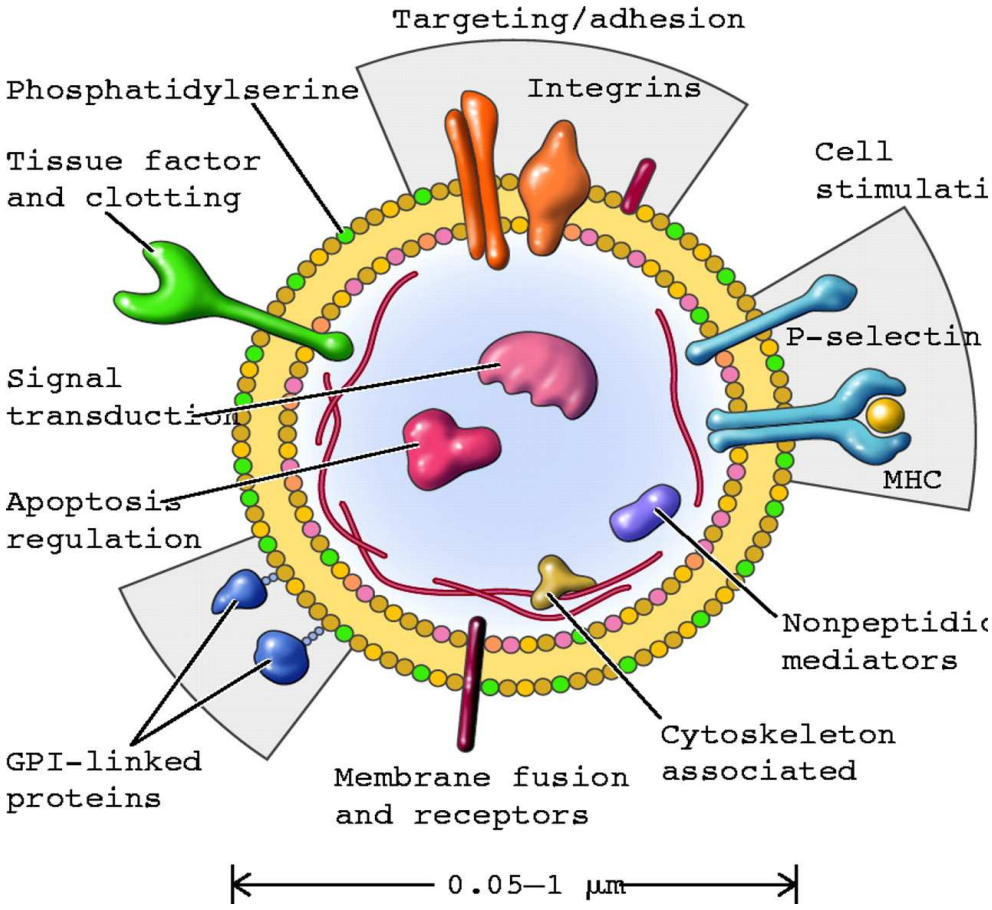

Figure 3.5: *A schematic representation of an ectosome/shedding vesicle released from the outer membrane of a stimulated cell. Different classes of protein and lipid effectors are displayed. Diagram taken from* [42]

Sadallah *et al.* [9] in their recent review, state that although the shedding process is the same in all cell types, the stimuli inducing the formation of ectosomes can differ from one cell type to another. They go on to list vesicle-release triggers for various cells.

3.0.4 Vesicle cargo composition

3.0.4.1 Exosome cargo composition

The membrane and internal composition of MVs depends on (i) the original cell type and (ii) the mechanism of MV release [1]. In the case of exosomes, the cargo is believed to consist of entities found in the cytoplasm and in the plasma membrane. They do not contain proteins belonging to the nucleus, mitochondria, Golgi or ER [43]. A review of the protein composition of exosomes classified by protein function and their location was provided by Schorey *et al.* [19]. A schematic summary is reproduced in Figure 3.6.

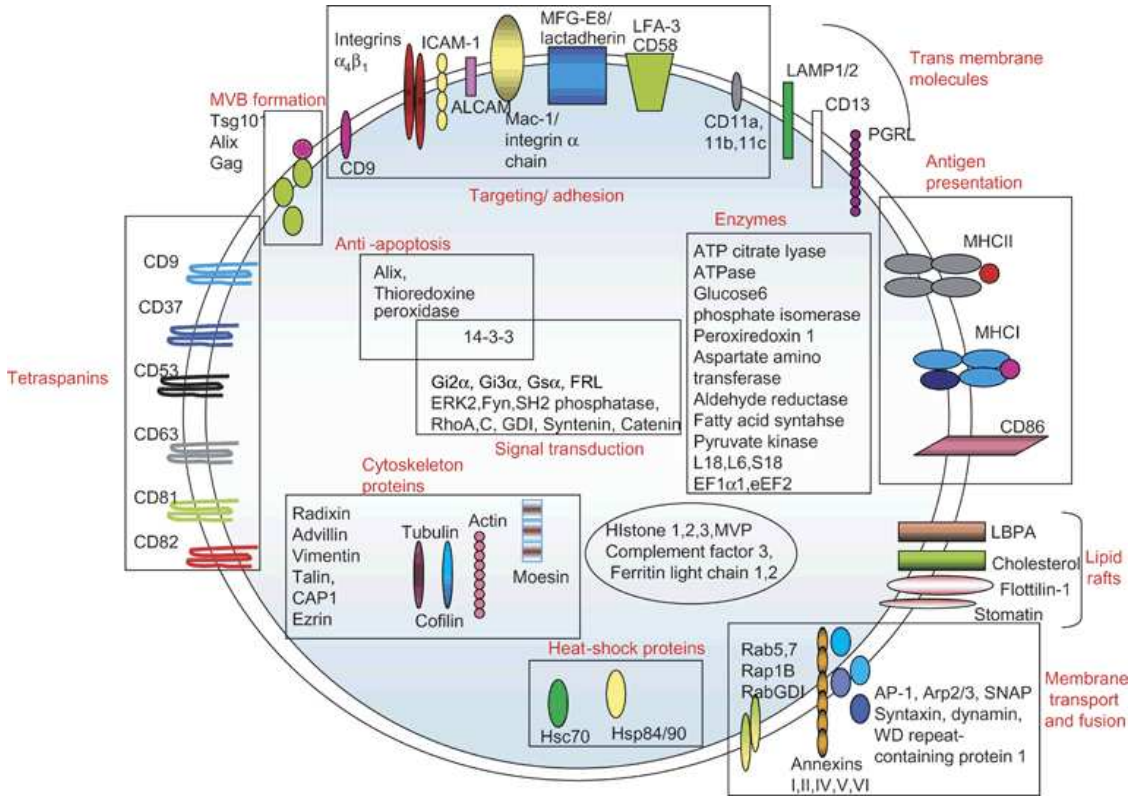

Figure 3.6: *A schematic diagram of an exosome displaying protein composition by name, function (in red) and location (i.e. membrane bound or soluble). Diagram taken from* [19]

Simpson *et al.* [8] in their recent review provide two tables listing proteins found in exosomes. In the first table (reproduced here to aid discussion, as Table 3.4) is a list of proteins reported to be found in *all* exosomes studied to date, while the second table provides a list of cell-type specific exosome proteins. Included in this list are some biofluids, though synovial fluid is not included.

Protein Category	Description
1 Antigen-presentation	HLA class 1 histocompatability antigen
2 Cell Adhesion	Lactadherin Thrombospondin-1 Integrins Claudin-1
3 Cell structure and motility	Actins α-Actinin-4 Cofilin-1 Erzin Moesin Myosin Radixin Tublins
4 Heat shock proteins & chaperones	Heat shock cognate 71kDa protein Heat shock protein hsp90β T-complex protein 1
5 Metabolic enzymes	α-Enolase Fatty acid synthase Glyceraldehyde-3-phosphate dehydrogenase Phosphoglycerate kinase 1 Phosphoglycerate mutase 1 Pyruvate kinase isozymes M1/M2
6 MVB biogenesis	Alix **ESCRT I complex** Tumour susceptibility gene 101 protein Vacuolar sorting protein 28 Vacuolar sorting-associated protein 37 **ESCRT II complex** Vacuolar sorting-associated protein 25 Vacuolar sorting-associated protein 36 Vacuolar sorting protein SNF8 **ESCRT III complex**

		Charged MVB proteins
7	Signaling proteins	14-3-3 Proteins GTPase Hras Rho GDP-dissociation inhibitor 1 Rho-related GTP-binding protein RhoC precurser Ras-related protein Rap-1b Ras-related protein Rap-2b Ras-related protein R-Ras2 Ras GTPase-activating-like protein IQGAP1 Syntenin-1 Transforming protein RhoA Guanine nucleotide-binding protein (G proteins)
8	Tetraspanins	CD9 antigen CD63 antigen CD81 antigen CD82 antigen
9	Transcription and protein synthesis	Histones Ribosomal proteins Ubiquitin Elongation factor 1-α 1
10	Trafficking and membrane fusion	Annexins ADP-ribosylation factor AP-2 complex subunit α-1 AP-2 complex subunit β-1 Clatherin heavy chain 1 Rab GDP dissociation inhibitor β Synaptosomal-associated protein 23 Syntaxin-3

Table 3.4: *List of proteins commonly found in all exosomes studied to date. Adapted from* [8]

3.0.4.2 Ectosome/Shedding vesicle cargo composition

Vesicles originating from the plasma membrane are now thought to contain some unique proteins and like exosomes, their cargo content reflects their cellular origin. Figure 3.5

displays the protein and lipid classes that are thought to comprise ectosomal cargo. For example, β1 integrin is concentrated in the membrane of all shedding vesicles investigated to date, while vesicles shed from tumors and neutrophils are enriched with metalloproteinases and other proteolytic enzymes [6]. The latter are believed to function in the digestion of the ECM necessary for the progress of inflammation and caner growth. Del Conde *et al*. [44] discovered that the vesicles shed from platelets also contain various integrins necessary for coagulation e.g. the glycoproteins GPIb and GPIIb-IIIa.

3.0.5 Microvesicle function

It has already been mentioned that cellular vesicle release is one mode of communication between cells. Figure 3.7 outlines the mechanisms involved in vesicle-mediated cell-to-cell communication.

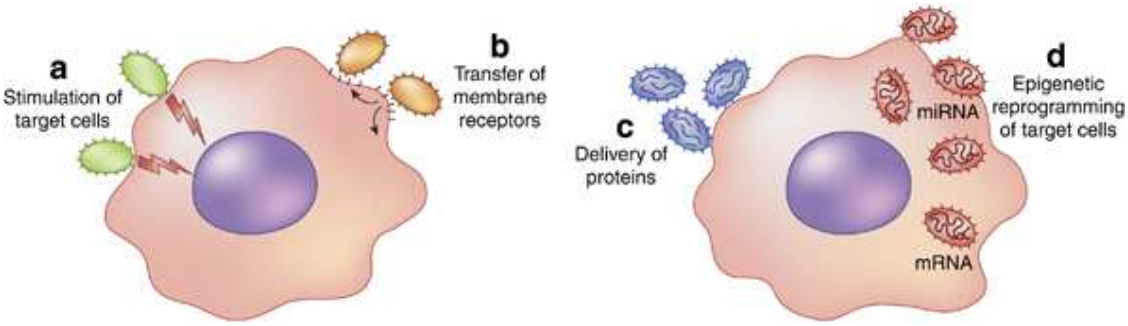

Figure 3.7: *Four mechanisms by which microvesicles can interact with target cells. Diagram is taken from [5] – MVs act as (a) signaling complexes, (b) receptor transferors, (c) delivery agents and (d) mediators in the transfer of genetic information between cells.*

Camussi *et al*. [5] provide detailed examples of each mechanism. In brief, MV function may influence the activity of target cells in four ways;

(a) Act as ***signaling*** complexes by directly stimulating target cells – e.g. in coagulation and clotting factors

(b) Act as ***receptor transferors*** between cells – e.g. (i) antigen presentation to T-cells, (ii) promotion of pro-adhesion properties through the transfer of CD41, (iii) removal of harmful molecules such as Fas or complement attack complexes and (iv) spreading infective agents such as HIV type I

(c) Act as ***delivery agents*** of proteins between cells – e.g. apoptosis induction molecules such as caspase-1 or the delivery of molecules that contribute to the destruction of certain infective agents e.g. prions. In addition, they act as vehicles for soluble (e.g. IL-1β) and insoluble (e.g. membrane antigens, transmembrane receptors and transmembrane ligands) proteins.

(d) Act as ***mediators*** in the transfer or shuttling of genetic information between cells – e.g. mRNA from tumour cells to monocytes or microRNAs (regulators of protein translation)

In the last year Lee *et al*. [13] stress the importance of intercellular communication via MVs to processes such as cell polarity, cell differentiation (e.g. from reticulocytes to mature red cells by the removal of transferrin), migration, chemotherapy resistance, immunoregulation, inflammation, coagulation, angiogenesis and cancer metastasis. In their study of cancer metastasis Hendrix *et al*. [45] postulate that MVs provide a platform for the controlled assembly of multimolecular complexes with a pre–programmed composition of proteins, lipids and nucleic acids. These inner vesicle assemblies are then delivered to the target cell. The term *"Trojan exosomes"* was coined to describe this phenomenon. Recently, Taylor *et al*. [46] described the immunosuppressive properties of exosomes of tumour origin both *in vivo* and *in vitro* e.g. their ability to mediate apoptosis of activated cytotoxic T-cells or the impairment of monocyte differentiation into dendritic cells.

3.0.5 Species present in biofluids which impact MV yield

Certain endogenous species present in the sample may interfere with the yield of MVs isolated and hence impact adversely on the sensitivity of low abundant species that may be present. In the isolation of exosomes from urine for example, the Tamm-Horsfall

protein was found to be an effective MV-trapping agent [47]. Its polymerisation entraps urinary exosomes as thus prevents their isolation during the ultracentrifugation stage. Therefore, it is necessary to depolymerise this protein before isolating exosomes and this was achieved by treatment with dithiothreitol (DTT). More recently, Musante *et al*.[48] improved on this method by employing the milder detergent 3-[3-clolamidopropyl)dimethylammino]-1propanesulfonic (CHAPS), which was found not to affect vesicle morphology or exosomal marker distribution.

For isolating exosomes from human plasma, Looze *et al*. [49] employed fast protein liquid chromatography to remove interfering very low-density lipoproteins (VLDL) and intermediate-density lipoproteins before ultracentrifugation.

With SF it may be the case that viscous hyaluronic acid may entrap MVs. This will be investigated in this project.

3.0.6 Microvesicle studies in synovial fluid

A search through PubMed yields surprisingly little concerning the study of microvesicles and the relationship to arthritis in synovial fluid. Those studies that were made were related to inflammation in RA. Boilard *et al*. [50] identified platelet microparticles in synovial fluid from patients with RA and other forms of inflammatory arthritis. No microparticles were detected in the synovial fluid of patients with OA. The platelets were pro-inflammatory and elicited cytokine responses from synovial fibroblasts via Il-1. However, Skriner *et al*. [18] also isolated exosomes from patients with RA, reactive arthritis and OA and this group found that citrullinated proteins (citrullination is a crucial step for changing a nonimmunogenic protein into an autoimmunogenic protein) are found in *all* synovial fluid exosomes, including OA. They acknowledge that further studies will need to be undertaken to reveal why the immune system in RA exclusively recognises these proteins (fibrin-derived molecules and Spα) as autoantigens. They did however; find that fibronectin and IgG were recovered only in RA exosomes.

3.0.7 Project aim

The overarching aim of this project is to characterise the proteome of MV in osteoarthritis SF.

The first objective is to establish a MV isolation protocol for synovial fluid and in particular to determine if hyaluronic acid entraps microvesicles in a manner similar to Tamm-Horsfall in urine or if ICs co-precipitate with MVs. This has not been established to date.

With a customised protocol established, isolated MV were prepared for MS analysis and the vesicle-associated proteome elucidated.

.

3.1 Materials & Methods

3.1.1 Reagents

All reagents were obtained from Sigma Aldrich except where noted.

Absolute Ethanol (HPLC Grade), Acetic Acid (reagent >99.7%), Acetronitrile (HPLC-grade), Acrylamide (molecular biology), Alcian Blue 8-GX (electrophoresis), Ammonium Bicarbonate (anhydrous), Ammonium persulphate (APS) (Ultra ~99%) (98%), β-mercaptoethanol (98%), Calcium Chloride (96%), CHAPS, Coomassie Brilliant Blur R, Coomassie Brilliant Blue G-250 (Merck), Dithiothreitol (DTT) (molecular biology), Ethylenediaminetetraacetic Acid (EDTA) Formic Acid (Fluka), Glycerol (molecular biology 99%), Glycine (electrophoresis 99%), Hyaluronadase (from bovine testes), Iodoacetamide, Methanol (Thermo Fischer), N-acetylcysteine, Nitric Acid (5% v/v), Ponceau Stain (electrophoresis), Sodium Chloride (molecular biology), Sodium Deoxycholate, Sodium Dodecyl Sulphate (SDS) (Fluka) (Ultra >99%), Sodium Formate, Tris(2-carboxyethyl)phosphinehydrochloride(TCEP), Tetra-methylethylene-diamine (TEMED), Tris-HCl, Tris pH 6.8, Tris pH 8.8, Triton x100; Trypsin (Promega), Tween-20, Urea

Odyssey blocking buffer and molecular weight standards were obtained from LI-COR Biosciences (Lincoln, New England, USA)

3.1.2 Antibodies

Primary Antibodies: Polyclonal Rabbit Anti-human Orosomucoid (α-1-Acid Glycoprotein), Polyclonal Rabbit Anti-human Apolipoprotein A-1, Polyclonal Rabbit Anti-human α-2-Macroglobulin, Polyclonal Rabbit Anti-human IgM and Polyclonal Rabbit Anti-human IgG were supplied by Dako (Denmark).

Polyclonal Rabbit Anti-human IgD was supplied by Dako (Denmark).

Polyclonal Rabbit Anti-human Tsg101 and Polyclonal Rabbit Anti-human CD63 were supplied by Sigma.

Secondary Antibodies: Goat anti-Rabbit IRDye®600CW & 800CW were supplied by Licor.

Protein A immobilised on agarose CL-4B from *Staphylococcus aureus* was purchased from Sigma.

3.1.3 Equipment

Nitrocellulose, with a membrane pore size of 0.22mm filter paper was purchased from Whatman (Springfield, United Kingdom)

Filter paper purchased from Whatman

Sep-Pak® cartridges were purchased from Waters Corporation.

Odyssey Infrared Laser Scanner (manufactured byLI-COR Biosciences, Lincoln, NE, USA)

Speed Vac: Model MiVac manufactured by GeneVac (Suffolk, Ipswich, UK)

Centrifuges:

Mikro 200R manufactured by Hettich

Avanti®J-26 XP centrifuge (Beckman Coulter, Fullerton, CA, USA)

OptimaTM L-90 K preparative ultracentrifuge (Beckman Coulter, Fullerton, CA, USA)

3.1.4 Synovial fluid sample preparation

Synovial fluid samples were obtained by informed consent from patients attending the Rheumatology Department of the Mater Hospital in Dublin. Samples were aspirated from the patient and placed in plastic sample containers containing 1mM EDTA and centrifuged at 2500g for 20 minutes to remove cells and cellular debris. To reduce the high viscosity of synovial fluid due to hyaluronic acid, each sample was treated with hyaluronidase from bovine testes (1mg/mL 20mM phosphate buffer pH 7) at 37ºC overnight. The requirement to perform this step is detailed in the results section. Samples were then stored in aliquots at -80ºC. Only one freeze/thaw cycle was permitted per aliquot.

3.1.5 Microvesicle purification from synovial fluid

A schematic representation of the initial differential centrifugation protocol that was employed is shown in Figure 3.8. Customisation of this protocol for MV analysis is developed in the results section.

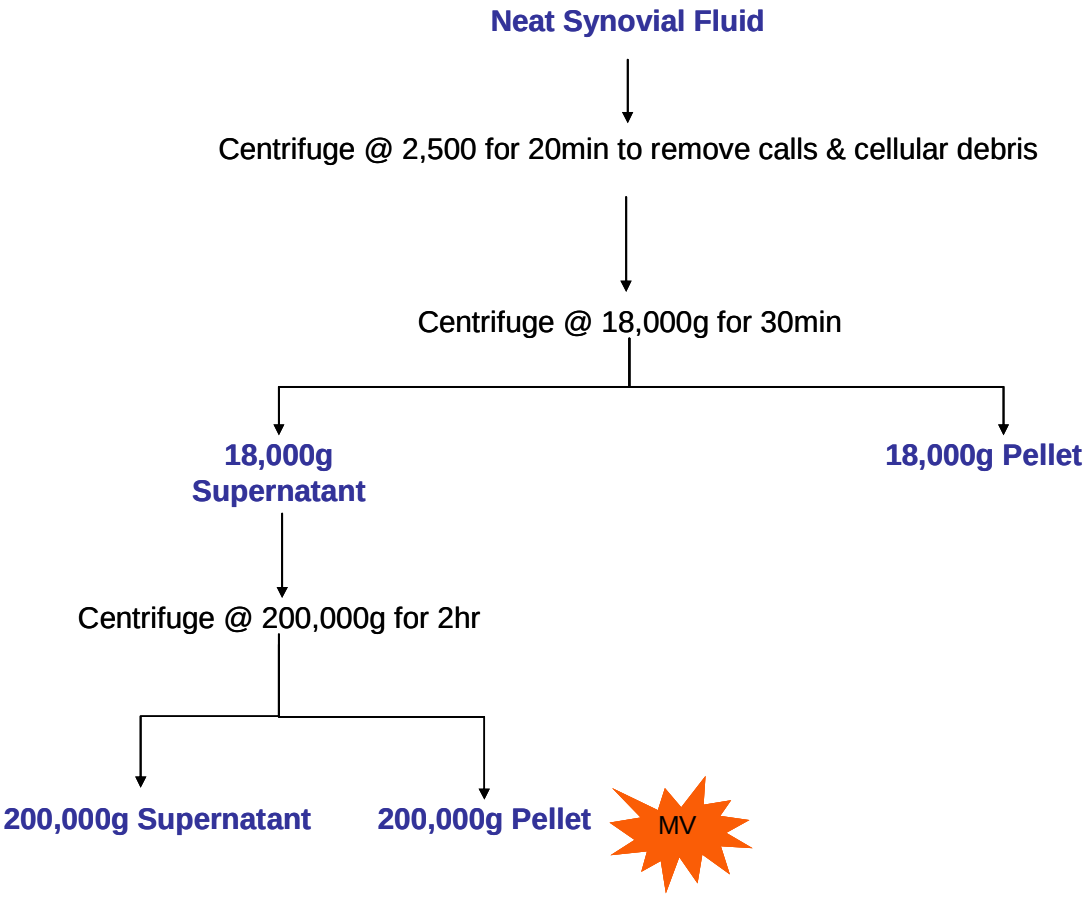

Figure 3.8: *Flow diagram outlining the standard differential centrifugation process for the isolation of microvesicles from biofluids.*

Following the initial centrifugation to remove cells and cellular debris, samples were then centrifuged in an Avanti®J-26 XP centrifuge (Beckman Coulter, Fullerton, CA, USA) at 18,000g for 30 minutes at room temperature in a fixed angle rotor (Beckman JA-20,

Fullerton, CA) with the brakes applied. The 18,000g pellet was resuspended in 1mL water and stored at -80ºC. Next the 18,000g SN fraction was then subjected to an ultracentrifugation step by an OptimaTM L-90 K preparative ultracentrifuge (Beckman Coulter) at 44,000 rpm for 2 hours at 4ºC in a fixed-angle rotor (Beckman 70Ti, Beckman) with braking applied. The 200,000g SN was then stored at -80ºC. 1mL of water was added to the crude 200,000g pellet.

3.1.6 Microvesicle lyses

The resuspended microvesicles were lyased by adding octyl β-D-glucopyrannoside (final concentration (1% w/v). Samples were mixed end-over-end overnight at 4ºC.

3.1.7 Protein assay

To ensure equal protein loading onto the gel, the protein concentration of each sample was carried out using the Bradford assay. A range of standards are made to generate a standard curve, these include the concentrations; 0 to 500µg/ml BSA. The Bradford reagent composition was: 100mg Coomassie Brilliant Blue G-250 in 50ml of 95% (v/v) ethanol and then mixed with 100ml of 85%(w/v) phosphoric acid [51]. The mixture was diluted to 1litre and allowed to dissolve. The dye is then filtered through Whatman filter (0.45µm) paper and stored at 4ºC. Each standard and sample was run in triplicate.

3.1.8 Sample preparation for electrophoresis

To 100µg protein (based on the Bradford assay), 40µL of x5 sample buffer (10% (w/v) SDS, 50% (v/v) glycerol, 5% (v/v) β- mercaptoethonal and 1M Tris-HCl, pH 6.8) was added and the final volume made up to 200µL. This yielded 100µg/200µL protein. 10µg (20µL) of protein was loaded into each lane. To complete protein denaturation, samples were boiled for 5 minutes. For non reducing conditions, omit β-mercaptoethonal from the sample buffer and also the boiling step.

3.1.9 Gel electrophoresis

Proteins were separated using SDS-PAGE employing 6-18% gradient resolving gel (80mm x 50mm x 1mm). Table 3.5 summarises the composition of each solution.

	Heavy Solution		**Light Solution**	
	Volume	Final Concentration	Volume	Final Concentration
30% (w/v) Acrylamide	3mL	18% (w/v)	1mL	6% (w/v)
1.5M Tris pH 8.8	1.25mL	0.375M	1.25 mL	0.375M
10% (w/v) SDS	0.05mL	0.1% (w/v)	0.05mL	0.1% (w/v)
100% (v/v) Glycerol	0.7mL	20% (v/v)	0mL	0% (w/v)
Water	0mL		0.7mL	
Total	**5mL**		**5mL**	

Table 3.5: *Composition of heavy and light solutions for the resolving gel*

2.4mL of each solution was added to each chamber.

Polymerisation was achieved by adding 22µL 10% (w/v) APS and 3.8µL TEMED.

The composition of the stacking gel is shown in Table 3.6.

	Volume	Final Concentration
30% (w/v) Acrylamide	0.23mL	3.50%
0.5M Tris pH 6.8	0.5mL	0.125M
10% (w/v) SDS	0.02mL	0.1% (w/v)
Water	1.25mL	
Total	2.0mL	

Table 3.6: *Composition of stacking gel*

Polymerisation was achieved by adding 45µL 10% (w/v) APS and 7.5µL TEMED.

Separation took place by applying 15mA per plate for 1 hour. The running buffer was 25mM Tris; 192mM glycine; 0.1% (w/v) SDS.

After electrophoresis the gels were either stained with Coomassie or transferred to a nitrocellulose membrane for Western Blot (WB) analysis.

3.1.10 Colloidal Coomassie Staining

Gels were removed from the plates and placed in a fixing solution (40% ethanol, 10% acetic acid) for 1 hour. Next, the gel was washed with Milli-Q water (6 x 5minutes). This removes SDS. Incubation in the Coomassie stain [80% Coomassie solution (10% (v/v) H_3PO_4, 10% (w/v) $(NH_4)_2SO_4$, 0.12% (w/v) brilliant blue coomassie G, water to final volume), 20% (v/v) methanol][52] took place overnight. Excess stain was removed using 10% (v/v) acetic acid. The gels were then stored in water.

Gels were imaged with an Odyssey Infrared Laser Scanner.

3.1.11Transfer to nitrocellulose membrane

Transfer to the nitrocellulose membrane was carried out using the 'wet' transfer method. Transfer took place in 25mM Tris, 190mM Glycine, 20% (v/v) ethanol buffer by applying 100mA for 1 hour at 4ºC [53]. To confirm if protein transfer took place, the membrane was stained with Ponceau and visually inspected before being de-stained with PBS. Membranes were blocked overnight at 4ºC or at room temperature for 1 hour with blocking buffer solution [Odyssey Blocking Buffer : PBS (1 : 1)].

3.1.12 Primary and secondary antibody incubation

Following the membrane blocking stage, the membrane was washed with PBST (PBS + 0.1% (v/v) Tween 20). Antibodies were diluted as per the supplier instructions in Odyssey blocking buffer/PBST 1:1. Incubation of the membrane took place for 90 minutes at room temperature. Excess antibody was removed employing a series of 4 x 10 minute washes with PBST. Next, the membrane was incubated with a secondary antibody (to the primary antibody) with a fluorescent tag (either green 680μm or red 700μm) in Odyssey blocking buffer/PBST 1:1 for 1 hour in the dark. Finally, washing 4 x 10mins with PBST took place before imaging with the Odyssey scanner.

3.1.13 Determination of proteases activity employing zymography with gelatin substrate

6-18% gradient gels (80mm x 50mm x 0.75mm) were prepared as before except gelatin was added to the heavy and light solution to a final concentration of 1mg/mL. Gelatin was dissolved into solution by heating to 50ºC for ~ 5 minutes.

10µg non-reduced total protein was loaded into each lane and protein separation performed as above.

Following electrophoresis, gels were placed into the following solution; 25mM Tris-HCl pH 7.8 made up in ice-cold water containing 2.5% (v/v) Triton x100. Mixture stirred at 4ºC until required. This was to remove the denaturing effects of SDS i.e. allow the proteins to return to their pseudo-native state.

Gels were then incubated in the triton x100 solution for 40 minutes at 4ºC

To activate any proteases present, 50mL 5mM $CaCl_2$ was added to each gel. Gels were then incubated in a water bath at 37ºC for 24 hours.

Stain with 2% (w/v) Coomassie solution followed by distaining with 40% (v/v) MeOH/10% (v/v) acetic acid solution, until clear bands are noted [54].

3.1.14 Determination of hyaluronidase (HAase) activity employing zymography with a hyaluronic acid (HA) substrate

The method developed by Miura et al.[54] was followed except instead of using a 7% (v/v) acrylamide gel, a 6-18% (v/v) gradient gel was prepared as outlined above.

HA was added to the heavy and light solution to a final gel concentration of 170µg/mL.

10µg non-reduced total protein was loaded into each lane and protein separation performed as above.

Following electrophoresis, gels were placed into the following solution; 25mM Tris-HCl pH 7.8 made up in ice-cold water containing 2.5% (v/v) Triton x100. Mixture stirred at 4ºC until required.

Gels were then incubated in the triton x100 solution for 40 minutes at 4ºC.

The gels were then incubated in 0.1M sodium formate and 0.15M NaCl at pH 3.5 for 16 hours at 37ºC.

In order to prevent artifact formation (i.e. unstained bands due to non-enzymatic proteins), the gels were incubated with 0.1mg/mL pronase solution (20mM Tris-HCl, pH 8.0) for 2 hours at 37ºC.

Following this, washing with 20% (v/v) ethanol/10% (v/v) acetic acid took place for 20 minutes.

The gels were then stained with 0.5% (w/v) alcian blue in 20% (v/v) ethanol/10% (v/v) acetic acid for 1 hour.

Finally, destaining took place in 20% (v/v) ethanol/10% (v/v) acetic acid.

HAase activity was detected a unstained bands which correspond to the positions of enzymes which had migrated.

3.1.15 Removal of immunoglobulins employing Protein A affinity chromatography

Column conditioning: Place 10mL Protein A beads (IgG binding capacity = 35mg/mL) into a syringe. Wash through with 10 column volumes PBS, followed by one column volume 0.1M glycine/0.15M NaCl solution. Finally wash again with 10 column volumes PBS.

Sample Loading: 10mL of SF (40-300mg IgG, Table 1.2) were loaded onto pre-conditioned Protein A beads and equilibrated for 10 minutes. Collect flow-through in a 50mL tube on ice.

Elution of unbound fraction: Wash column with PBS until no further protein is detected in the wash using a nano-drop. Dialyse against water overnight and SpeedVac to 10mL.

Elution of bound fraction: To the column add 0.1Mglycine/0.15M NaCl, pH 2.3. Continue to rinse column until no protein is detected using a nano-drop. Bring to physiological pH with tris-HCl. Dialyse against water overnight and SpeedVac to 10mL.

Carry out the MV-isolation protocol as detailed above.

3.1.16 Preparation of OA 200,000g CHAPS pellet for mass spectrometry

200μg of reconstituted 200,00g pellet was dried and then dissolved in 100μL of reducing solution (8M Urea, 5mM tris(2-carboxyethyl)phosphine (TCEP) (reducing agent), 1%(w/v) sodium deoxycholate (detergent that lyases MVs), 200mM Tris pH8.8, 0.2mM EDTA; final pH > 8.2) for one hour at room temperature. Alkylation followed with the addition of 10μL 420mM iodoacetamide (final concentration 20mM), mixed end-over-end in the dark for 90 minutes. Alkylation was quenched by the addition of 20mM N-acetylcysteine.

Proteins were precipitated as follows. To the above sample 600μL MeOH, 200μL chloroform and 600μL water was added. Vortex and centrifuge at 5000g for two minutes. Remove aqueous layer and save. To the organic layer add a further 800μL MeOH. Centrifuge at 14,000g for 40 minutes. Remove the SN and dry the pellet in the SpeedVac to remove residual organic solvent [55]. Reconstitute in 50μL HPLC grade water. Divide the sample - 25μL for in-gel and 25μL off-gel (shotgun) MS identification apprpach.

3.1.17 Preparation of polyacrylamide gel bands for mass spectrometry

Bands were cut into 1mm from the gel on a glass slide previously washed with 5% (v/v) HNO_3 to remove residual proteins and all traces of keratin. Gel slices were placed in PCR-grade eppendorfs previously washed with acetonitrile. The bands were destained with 0.5mL destaining solution (50% (v/v) H_2O, 5% (v/v) acetic acid) for 2 hours. Destaining was repeated a second time until the gel slices were completely clear.

Reduction and alkylation took place as follows. For reduction to occur, add 30μL 10mM Dithiothreitol (DTT) for 30 minutes at room temperature. Centrifuge and remove DTT solution. Alkylation took place with the addition of 30μL 50mM iodoacetamide in the dark at room temperature for 30 minutes. Centrifuge and remove iodoacetamide solution. Wash the gel slices with 100μL 100mM $(NH_4)HCO_3$ for 10 minutes and remove.

The gel slices were then dehydrated in 200μL acetonitrile for 5 minutes. This was repeated a second time. Rehydration with 100μL 100mM $(NH_4)HCO_3$ followed. Further dehydration of the samples took place with the addition of 200μL acetonitrile, followed by a second rehydration with 200μL 100mM $(NH_4)HCO_3$. The samples were

then centrifuged to remove $(NH_4)HCO_3$. A further dehydration step with 200µL acetronitrile took place before the gel slices were dried in the SpeedVac.

The trypsin solution was prepared as follows; 20µg Promega trypsin (Promega, Madison, WI) was added to 500µL ice-cold 50mM $(NH_4)HCO_3$ i.e. trypsin concentration = 10ng/µL. This was kept on ice. The gel slices were then covered with 50µL of the trypsin solution and rehydrated on ice for 30 minutes. Excess trypsin solution was removed by centrifugation before covering the slices with 50mM $(NH_4)HCO_3$. Incubation then took place overnight at 37ºC.

The resulting peptides were extracted with 30µL 5% (v/v) formic acid for 10 minutes. Following centrifugation, the supernatant (SN) was removed and placed into a fresh, acetonitrile-washed eppendorfs (Protein LoBind tube). Extraction of residual peptides from the gel slices took place by the addition of 50µL 5% formic acid in 50% acetonitrile. Following centrifugation, the SN was removed and placed into the same eppendorf as the first SN. To complete the peptide extraction process from the gel slices, the slices were washed with two cycles of 20µL 50mM $(NH_4)HCO_3$/20µL 5% (v/v) formic acid/50µL 5% (v/v) in 100% acetonitrile. All SNs were pooled before reducing to ~1µL and then reconstitute to 20µL total volume with 1% (v/v) acetic acid.

3.1.18 Preparation of microvesicles for separation by HPLC followed by mass spectrometry

To the second 25µL sample, add 5µL trypsin (i.e. 2µg trypsin/100µg protein) in 50mM Tris-HCl, pH 8.0 and 1% (w/v) sodium deoxycholate which is compatible with trypsin activity [56] . Incubate overnight at 37ºC.

Sodium deoxycholate was removed as follows. Add 1% (v/v) formic acid to the sample. Centrifuge at 24,000g for 15 minutes and save the SN. Resuspend pellet in 25mM Tris pH8.8 and acidify with 1% (v/v) formic acid. Repeat centrifugation. Pool all the SN fractions [57].

3.1.19 Purification of trypsin-digested peptides

Condition SepPak cartridge with 1mL 100% (v/v) MeOH followed by 2mL 80% (v/v) acetonitrile. Equilibrate with 4mL 0.1% formic acid. Acidify sample with 90μL 10% (v/v) formic acid to a final pH 2-3. Load acidified samples onto the cartridge. Wash cartridge with 6mL 0.1% (v/v) formic acid. Elute peptides into a clean tube with 1mL 0.1% (v/v) formic acid/80% (v/v) acetonitrile. Concentrate sample by SpeedVac to about 20 μL final volume.

3.1.20 Mass spectrometry using LC–MS/MS

All mass spectrometry analysis was carried out by the National Institute of Cellular (NICB) Biotechnology with whom a collaboration was obtained. The following protocol was supplied by NICB.

Nano LC–MS/MS analysis was carried out using an Ultimate 3000 nanoLC system (Dionex) coupled to a hybrid linear ion trap/Orbitrap mass spectrometer (LTQ Orbitrap XL; Thermo Fisher Scientific). Five microlitres of digest were loaded onto a C18 trap column (C18 PepMap, 300 μm ID × 5 mm, 5 μm particle size, 100 Å pore size; Dionex) and desalted for 10 min using a flow rate of 25 μL/min in 0.1% (v/v) TFA. The trap column was then switched online with the analytical column (PepMap C18, 75 μm ID × 250 mm, 3 μm particle and 100 Å pore size; (Dionex)) and peptides were eluted with the following binary gradients of solvent A and B: 0–25% solvent B in 120 min and 25–50% solvent B in a further 60 min, where solvent A consisted of 2% (v/v) acetonitrile (ACN) and 0.1% (v/v) formic acid in water and solvent B consisted of 80% (v/v) ACN and 0.08% (v/v) formic acid in water. Column flow rate was set to 350 nL/min.

Two-dimensional peptide separations in-line using an Ultimate 3000 nanoLC system (Dionex) coupled to a hybrid linear ion trap/Orbitrap mass spectrometer (LTQ Orbitrap XL; Thermo Fisher Scientific). 20μL of digest were loaded onto a BioX-Strong Cation Exchange (SCX) column (5μm. 500μm i.d. x 15mm μ-Precolumn™ Cartridge, Dionex) for 10 min using a flow rate of 25μL/min in 0.1% (v/v) TFA. Sample complexity was reduced by eluting small fractions of peptides from the SCX column with salt plugs at

concentrations of 0, 10, 25, 50, 100, 500, 1000mM ammonium formate containing 0.1% (v/v) TFA. The SCX fractions containing peptides were then subjected to reverse phase separation as described above.

Data were acquired with Xcalibur software, version 2.0.7 (Thermo Fisher Scientific). The mass spectrometer was operated in data-dependent mode and externally calibrated. Survey MS scans were acquired in the Orbitrap in the 400–1800 m/z range with the resolution set to a value of 60,000 at m/z 400. Lock mass was set at 445.120025 u (protonated $(Si(CH_3)_2O)_6$). Up to seven of the most intense ions (1+, 2+ and 3+) per scan were CID fragmented in the linear ion trap. A dynamic exclusion window was applied within 40 s. All tandem mass spectra were collected using a normalised collision energy of 35%, an isolation window of 3 m/z, and one microscan.

Proteins were identified using BioWorks 3.2 from Thermo Fisher Scientific using the HUPO criteria with XC scores of 1.8, 2.2, 3.75 for single, double and triple charged ions. A peptide probability score of 0.05 was also used. The database used was Human UniProt-SwissProt downloaded January 2012. Carboxymethylation of Cysteine was set as fixed and oxidation of methionine as a variable modification. Two missed cleavages were allowed. The mass tolerance for precursor ions was 20ppm and the mass tolerance for fragment ions was 0.5Da.

3.1.21 Comparison of proteome after three modes of analysis

Lists of proteins generated by MS were analysed using an on-line comparison tool - http://sablab.net/venn.php

3.1.22 Gene ontology classification analysis

The Panther (Protein ANalysis THrough Evolutionary Relationships) Classification System (www.pantherdb.org) was used to categorise the MV proteome as described by [58].

3.1.23 Transmission Electron Microscopy (TEM)

A sample of an OA 200,000g CHAPS pellet was sent to Trinity College Dublin for analysis by TEM. The following preparation procedure was supplied by the technician.

Instrument: Jeol 2100 TEM system (Joel Ltd., Tokyo, Japan)

The system was operated at 100kV to maximise contrast.

Sample preparation: Formavar carbon coated grids (Agar Scientific, Stansted, UK) were floated upside down on drops of solution

1. 50ul drops of sample. (60mins)
2. 3 washes of 0.1M phosphate buffer (3x10mins)
3. Transferred to 3% Gluteraldehyde solution. (30mins)
4. Then 3 washes of 0.1M phosphate buffer (3x10mins)
5. The 2% Osmium Tetroxide (30 mins)
6. 1 phospdate buffer wash
7. 2 dH2O washes.
8. Uranyl acetate. Drained with filter paper and allowed to dry over night.

Images were taken the next day.

3.2 Results

3.2.1 Optimisation of microvesicle harvesting protocol

3.2.1.1 Assessment of the distribution of protein in MV harvested at 18,000g and 200,000g

MVs from 4 patient samples were isolated as in the materials and methods section (Figure 3.8). The Coomassie gels (top panels) and antibody anti-Tsg101 Western Blots (bottom panels) can be seen in Figure 3.9. Tumour suppressing gene 101 (Tsg101) is a specific exosomal marker (Table 3.2). It is one of four components of the ESCRT I machinery and like ESCRT 0, its function is to bind to ubiquitinated proteins at the endosome surface. [59] It is located on the inner surface of the exosome.

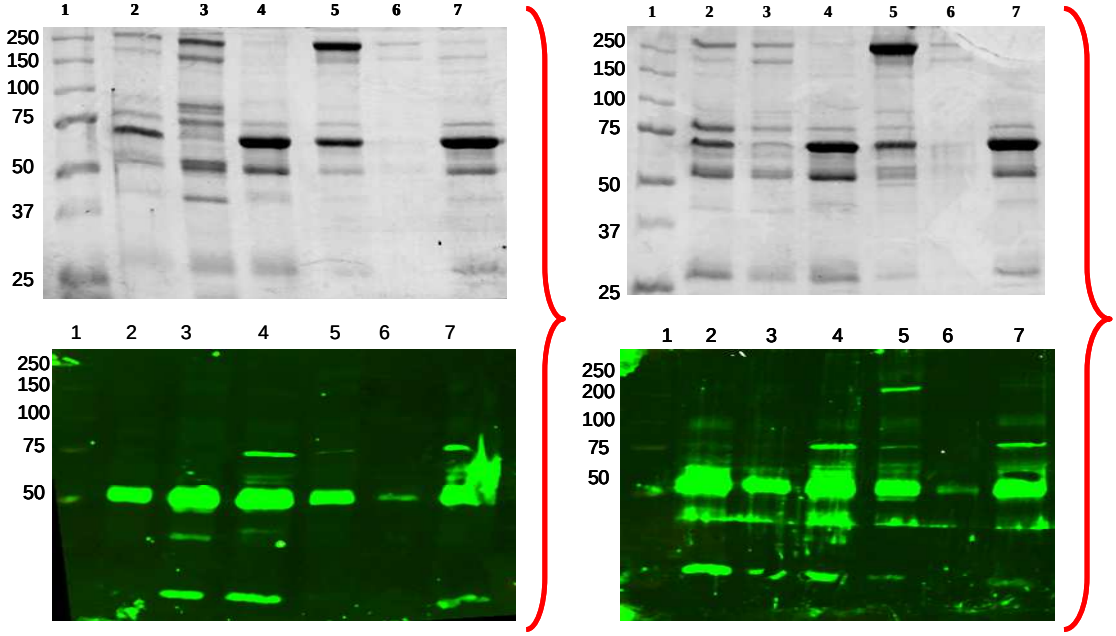

Lane 1: MWM
Lane 2: PSA 18,000g Crude Pellet
Lane 3: PSA 200,000g Crude Pellet
Lane 4: PSA 200,000g Crude SN
Lane 5: OA1 18,000g Crude Pellet
Lane 6: OA1 200,000g Crude Pellet
Lane 7: OA1 200,000g Crude SN

Lane 1: MWM
Lane 2: RA 18,000g Crude Pellet
Lane 3: RA 200,000g Crude Pellet
Lane 4: RA 200,000g Crude SN
Lane 5: OA2 18,000g Crude Pellet
Lane 6: OA2 200,000g Crude Pellet
Lane 7: OA2 200,000g Crude SN

Figure 3.9: *Coomassie and corresponding anti- Tsg101 WBs of four patient samples which were differentially centrifuged in order to isolate MVs*

From the coomassie images in Figure 3.9 above, it can be observed that for any particular patient sample, there are different protein patterns between 18,000g pellet, 200,000g pellet and 200,000g SN. A further observation is the remarkable similarity in the band profile between the two OA samples (Lanes 5, 6 & 7) and also the differences between these and both PSA (Lanes 1, 2, & 3 left) and RA (Lanes 1, 2 & 3 right). In addition a WB of these samples was performed after incubation with an exosomal marker, Tsg101. This has a molecular weight ~46kDa. From these WBs it can be seen that there are exosomes in all three fractions i.e. 18,000 g crude pellets, 200,000g crude pellet and the 200,000g crude SN. In the case of the OA samples in particular, the exosome yield in the targeted 200,000g pellet is poor relative to the other two fractions. In particular, there is a strong signal in the 200,000g SN, implying a less than satisfactory enrichment of exosomes in the targeted 200,000g pellet. Therefore, a method needs to be developed to maximise the exosome harvest in the 200,000g pellet and hence increase the sensitivity of any proteomic study.

3.2.1.2 Establishment of the effect of HAase treatment on the yield of MVs

The 200,000g SN of each sample from the previous study was taken and the following protocol was applied (Figure 3.10). This is an extension of the initial protocol displayed in Figure 8.

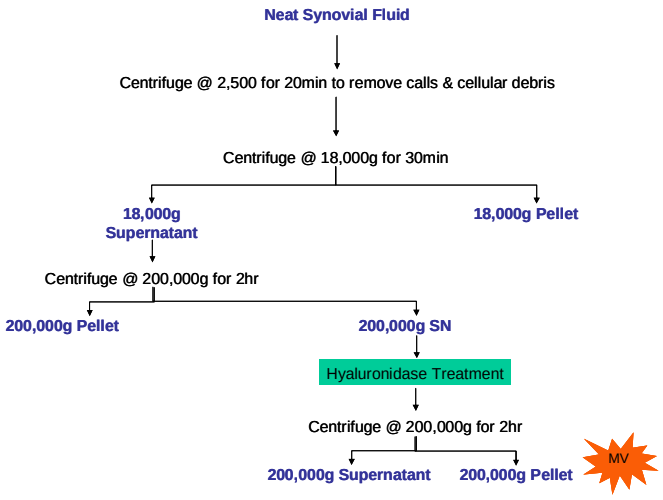

Figure 3.10: *Treatment of the 200,000g crude SN with HAase (as outlined in the materials and methods section) aimed at recovering additional MV that may be entrapped by HA.*

From Figure 3.10, the original 200,000g SN was treated with HAase followed by a second ultracentrifugation step at 200,000g. This yielded the HAase 200,000g pellet and SN. Proteins from the pallet and SN were separated by SDS-PAGE. The Coomassie stain can be seen in Figure 3.11. Comparing the 200,000g pellet lanes in Figures 3.9 and 3.11, it is can be seen that following treatment with HAase, there is considerable enrichment of protein in the 200,000g pellet fractions particularly albumin at ~ 60kDa. The two OA 200,000g pellet samples (Lanes 4 & 6) have similar band patterns. However, the RA and PSA 200,000g pellets (Lanes 2 & 9) have extra bands at ~40kDa, 80kDa and 90kDa.

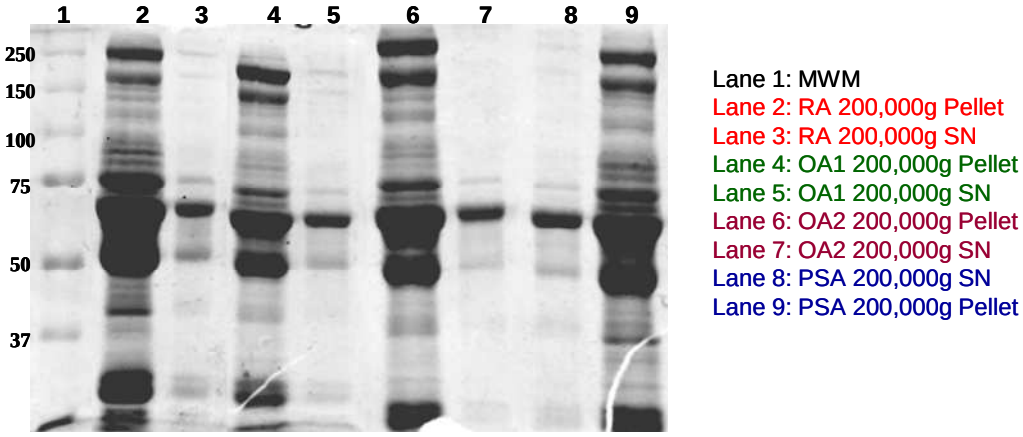

Figure 3.11: *Coomassie gel of the same samples run in Figure 3.9 following HAase treatment at 37ºC overnight.*

Following this, the HAase 200,000g pellet in turn, was treated with 1% (w/v) CHAPS and mixed end-over-end overnight at 4ºC as per Musante *et al.* [48] CHAPS is a non-denaturing zwitterionic detergent and is ideally suited to disrupt non-specific protein interactions, while at the same time preserving protein conformation [60]. A third ultracentrifugation at 200,000g was performed and both fractions were analysed by SDS-PAGE. The workflow is shown in Figure 3.12 and the resulting Coomassie gel is in Figure 3.13.

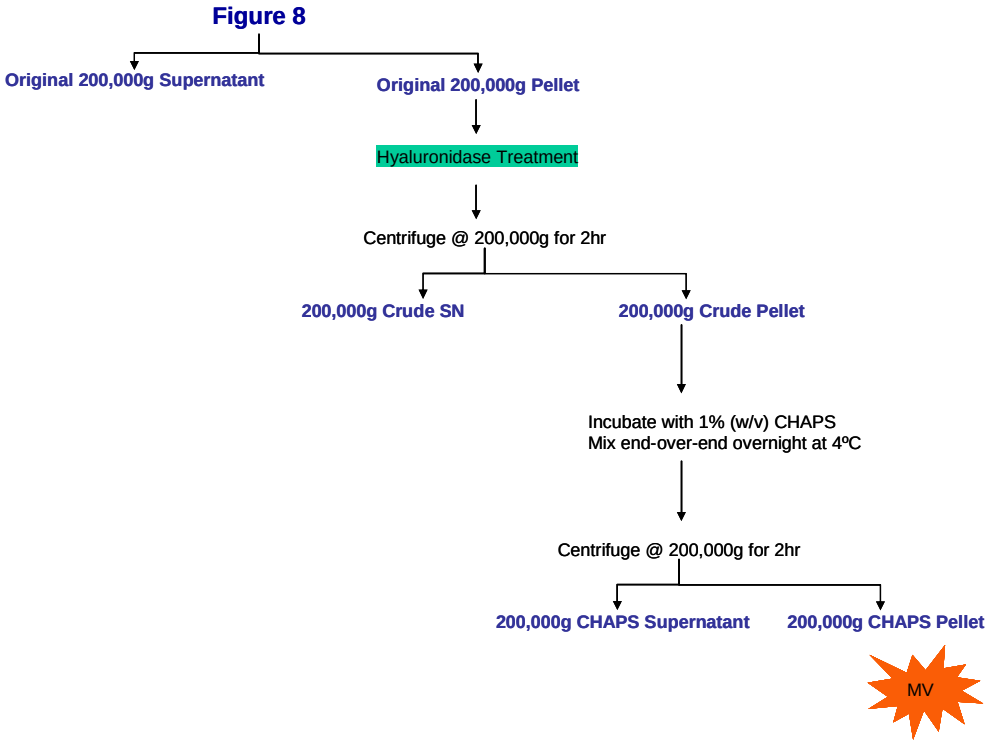

Figure 3.12: *An extension to the workflow outlined in Figure 3.10 aimed at further enhancing MV recovery by removing those proteins that are loosely associated with the vesicle surface, by incubating the original crude pellet with 1% (w/v) CHAPS overnight at 4ºC.*

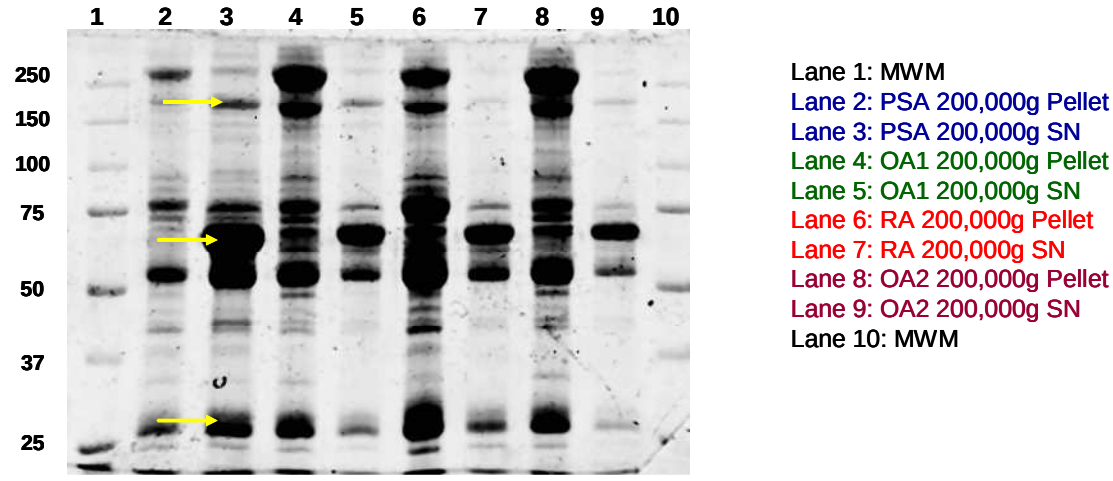

Figure 3.13: *Treatment of the previous crude 200,000g pellet with 1% (w/v) CHAPS solution.*

Comparing Figure 3.11 and 3.13, it is shown that for each sample, there is redistribution of protein from the pellet to the SN post-CHAPS treatment. For example, albumin at ~63kDa has mainly moved to the SN following CHAPS treatment. Other species are also

enriched in the SN in Figure 3.13 relative to Figure 3.11. Species that moved from the pellet to the SN following CHAPS treatment are indicated with a yellow arrow for one of patient samples. Examination of the 200,000g pellet fractions in Figure 3.13 also highlights an enrichment of protein following CHAPS treatment due to removal of high abundant, soluble/loosely bound protein into the SN.

To better evaluate the protein profiling pre and post HAase digestion, SDS-PAGE was performed, comparing CHAPS-treated 200,000g pellets pre- and post-digestion with HAase for each sample. These were loaded into adjacent lanes to aid comparison. Further, each fraction was incubated with antibodies against well known exosomal markers i.e. Actin β and CD63. CD63 is a tetraspanin protein associated with exosomes (Figure 3.6 and Table 3.3). As it is a membrane protein, it is an ideal species to act as a positive control to demonstrate that CHAPS, while removing loosely bound proteins from the vesicle surface, does not remove strongly associated proteins. Actin β was listed by Mathivanan *et al.*[61] as the third most often found protein in exosomes (behind heat shock protein 8 and CD63). The result of this study may be seen in Figure 3.14.

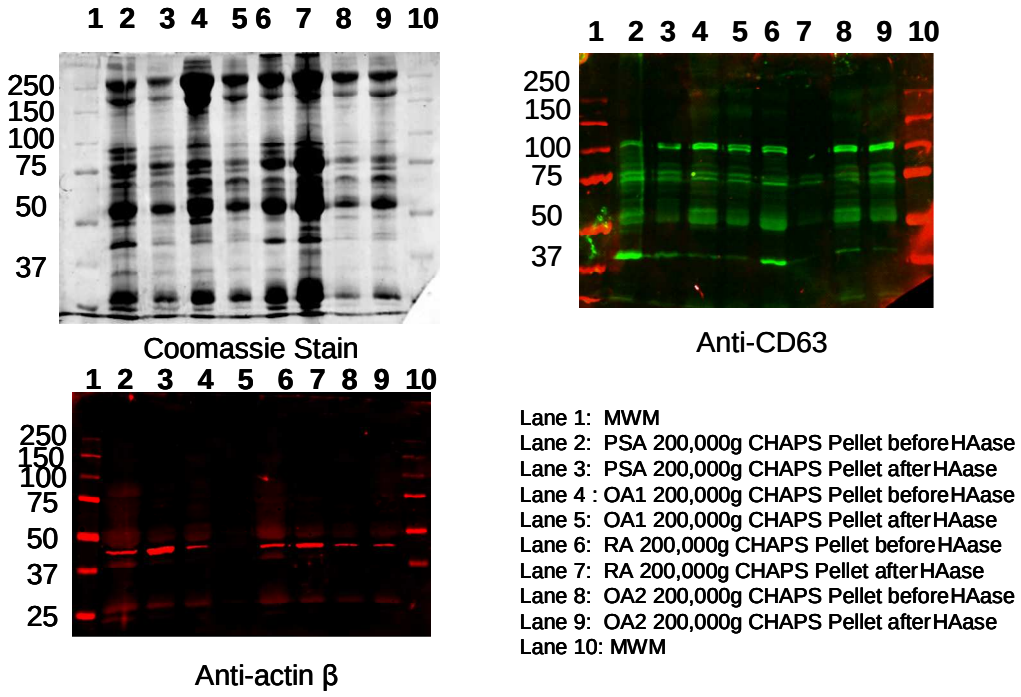

Figure 3.14: *Treatment of the same samples analysed in Figure 3.11 before and after HAase treatment. A Coomassie staining gel (upper left) and two WBs of known exosomal markers – anti-CD63 (upper right) and anti-actin β (lower left) – were prepared.*

The Coomassie image in Figure 3.13 clearly demonstrates that further treatment of the crude 200,000g SN with 1% (w/v) CHAPS, followed by another 200,000g ultracentrifugation step, resulted in further recovery of MV. That these "extra" acquired MVs contain exosomes was shown by performing a WB analysis with two well-known exosomal markers – actin β and CD63. Incubation with CD63 exhibited bands with a range of molecular weights. This species is known to be heavily glycosylated [62] and the bands in the 75 -100kDa region are due to a high degree of glycosylation by poly *N*-acetyl lactosamine [48].

3.2.1.3 Confirmation of the effectiveness of the HAase/CHAPS steps on MV recovery

Seven new patient samples were taken and the following expanded workflow was applied (Figure 3.15). This additional step (red box) was designed to establish if the 18,000g fractions merited further study. The crude 18,000g pellet was treated with CHAPS and centrifuged again at the same speed.

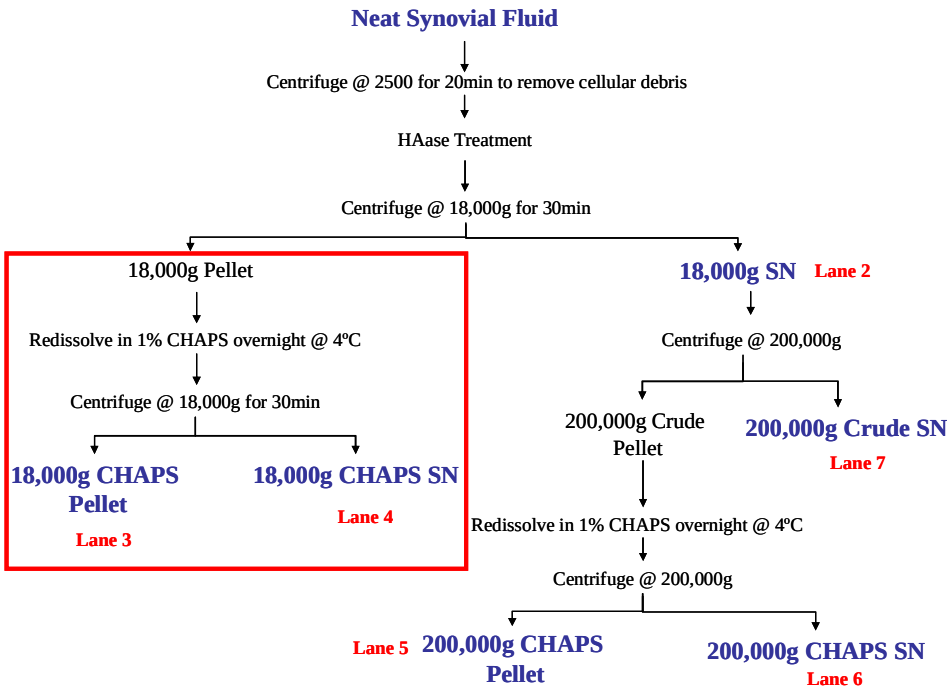

Figure 3.15: *The workflow employed to establish the repeatability of the previous study with new patient samples and ascertain if further analysis of the 18,000g pellet merits any further study.*

SDS-PAGE Coomassie gels for this study are displayed in Figure 3.16.

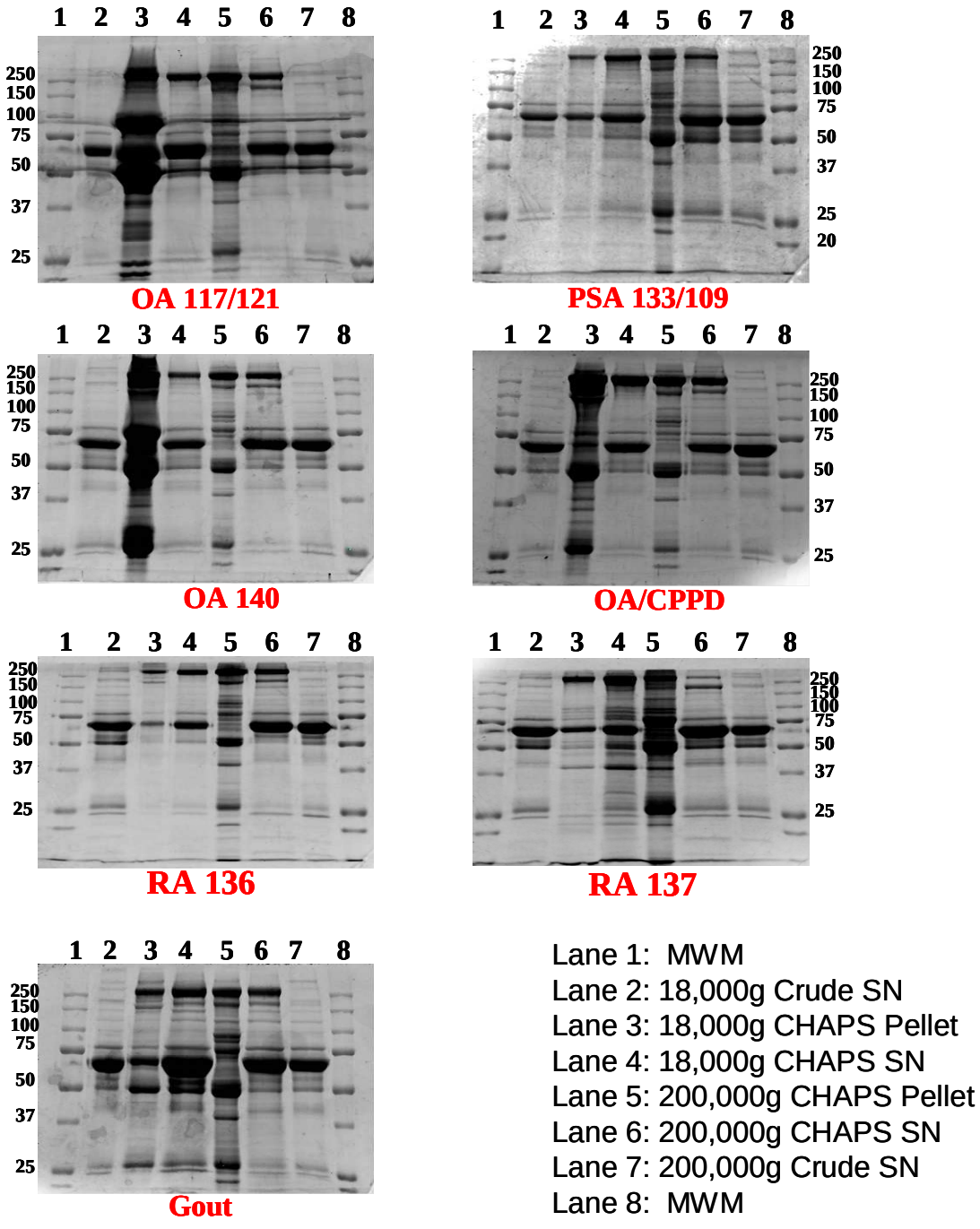

Figure 3.16: *Coomassie gels representing various differential centrifugation fractions as shown in the workflow in Figure 3.15, representing seven different patient samples.*

Examination of Lane 3 in each gel confirms that treatment of the crude SN (Lane 2) with CHAPS, followed by a further 18,000g centrifugation step, yields a further enrichment of protein in the pellet – bands that are not seen in Lane 2. This is particularly true in the case of the three OA samples, though the other pathologies also display this enhanced enrichment. As before, a redistribution of albumin (~63kDa) from the pellet (Lane 3) to the SN (Lane 4) is clearly seen. An interesting observation is the absence of a band (~150kDa) in the PSA 200,000g CHAPS SN (Lane 6) that is present in the other six gels.

Overall there is a noticeable enrichment of soluble protein in the 18,000g (Lane 4) and 200,000g (Lane 6) CHAPS SN, relative to the corresponding crude SN fractions (Lanes 2 and 7) confirming that soluble or loosely-associated protein was removed from the crude pellet fraction following CHAPS treatment.

In order to establish the presence of exosome markers, samples representing different pathologies (OA, RA, PSA and Gout) were analysed by WB employing anti-Tsg101 and anti-CD63 as known exosomal markers (Table 2). These images are shown in Figures 3.17 and 3.18 respectively.

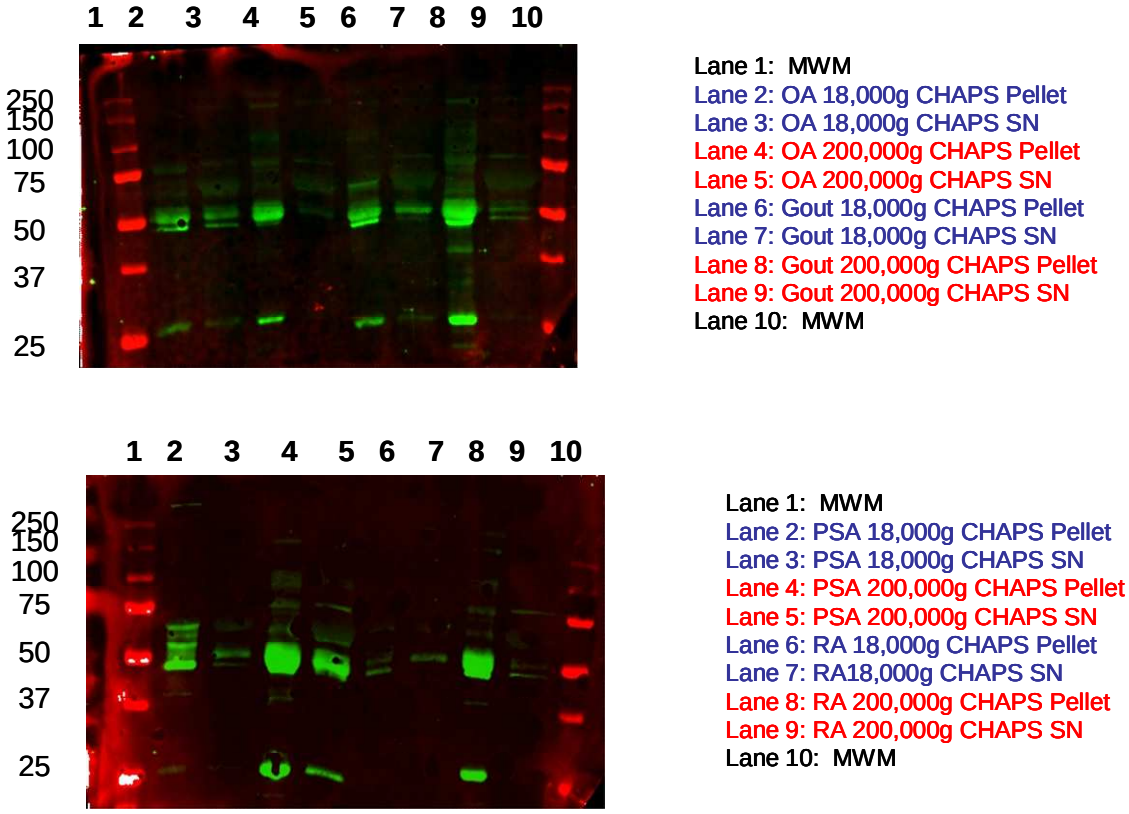

Figure 3.17: *Establishing the distribution of exosomes among differentially centrifuged fractions of four different arthritic pathologies, by incubation with the exosomal marker Tsg101 (18,000g (Blue) and 200,000g (Red))*

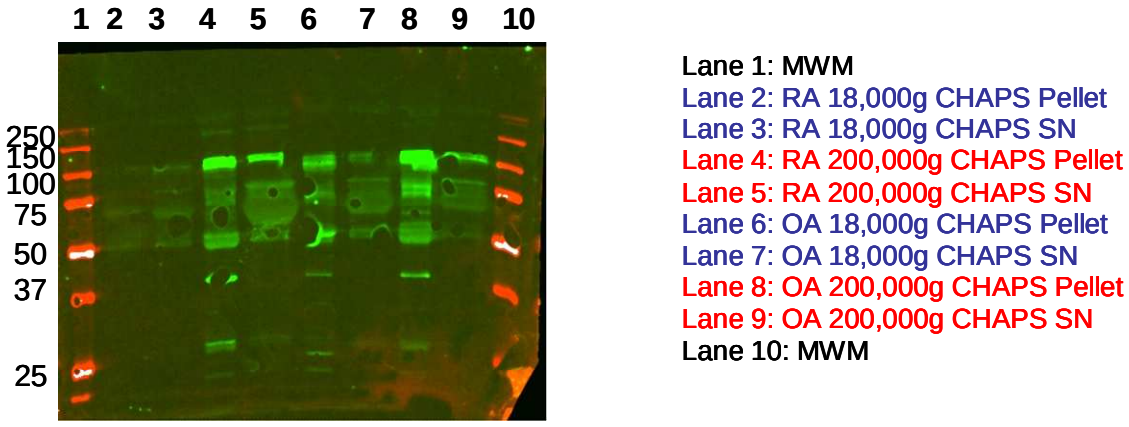

Figure 3.18: *Establishing the distribution of exosomes among differentially centrifuged fractions of one OA and one RA patient sample, by incubation with the exosomal marker CD63 (18,000g (Blue) and 200,000g (Red) pellets)*

In Figures 3.17 and 3.18, it is shown that exosomes are present in each patient sample. Further, though they are present in 18,000g pellet (Lanes 2 and 6), exosomes are particularly enriched in pellet 200,000g (Lanes 4 and 8). Finally, as seen in lanes 5 and 9 for both CD63 and Tsg101, the recovery of exosomes in the pellet is not complete, as there are still exosome markers present in the 200,000g CHAPS SN. Due to the low abundance of exosomal markers in the 18,000g pellet, relative to the 200,000g pellet, it was decided, in the interest of time available, to pursue a study of the latter and leave the study of the former to future research.

To evaluate the redistribution of soluble proteins following CHAPS treatment, a WB was carried out incubating with anti-albumin. The aim here is to confirm the transfer of albumin from the pellet to the SN following CHAPS treatment that was previously discussed in relation to a Coomassie-stained gel.

In addition, in order to establish if there are potential immuncomplexes present, incubation with anti-IgM was carried out. Knowing that IgM can exist either as a pentamer of ~900kDa, or as a monomer, a 6-10% gradient gel was prepared (rather than the usual 6-18% gradient as outlined in the material and methods section of this chapter) in order to enhance resolution. These are shown in Figure 3.19.

Inspection of the WB in Figure 3.19 (left) confirms that post CHAPS treatment, there is almost a complete relocation of albumin from the 200,000g CHAPS pellet (Lanes 4 and 8) to the 200,000g SN (Lanes 5 and 9). There is still albumin present in the pellet however, and this could be due to either incomplete removal from the vesicle surface or this protein is also a component of the inner vesicle cargo.

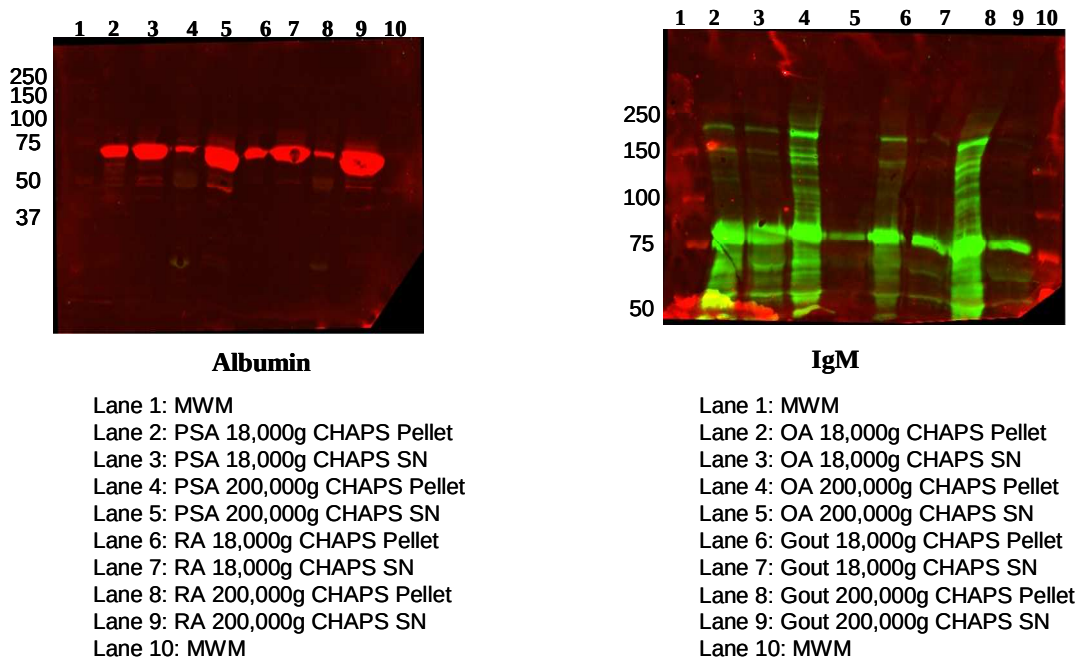

Figure 3.19: *WB analysis with anti-albumin to confirm transfer of soluble or loosely associated protein from the pellet to the SN following CHAPS treatment (left). WB image displaying incubation with anti-IgM aimed at confirming the possible existence of ICs (right).*

Examination of the WB image on the right in Figure 3.19 (IgM) shows a strong band in each fraction at ~ 75kDa which could be the mu chain of IgM. Incubation with anti-IgM shows that IgM is strongly associated with the 200,000g pellet (Lanes 4 & 8) with relatively little remaining in the 200,000g CHAPS SN (Lanes 5 & 9). There is also IgM enriched in both the 18,000g pellet and 18,000g SN. Further, the 18,000g pellet, 18,000g SN and 200,000g pellet fractions have high molecular weight bands that are absent in the 200,000g SN. The signal for these higher molecular weight species is most intense in the 200,000g pellet. At this point it is only possible to speculate that these may be dimers of IgM present due to incomplete disulphide bond cleavage. This speculation is based upon the fact that the more intense high molecular weight bands are approximately double the weight of mu chain at ~75kDa. The presence of IgM mu chain was confirmed by MS analysis. In addition, the immunoglobulin J chain was also shown to be present by MS. MS data will be discussed later in this section. This confirmation that IgM is MV-associated and the possibility that ICs could be present, leads to the hypothesis that

removal of these species may unearth and enrich other less abundant proteins in the MV proteome.

3.2.1.4 Removal of Immunoglobulins employing Protein A chromatography in order to maximize MV enrichment by elimination of interference from immunoglobulins

As ICs are likely to be most abundant in RA, a pooled-patient, HAase-treated RA sample was analysed employing Protein A chromatography. ICs are formed when rheumatoid factor reacts with the crystallisable fragment (Fc fragment) of IgG. Rheumatoid factor is one of three subclasses i.e. IgM, IgA and IgG auto-antibodies, with IgM the predominating species in arthritis [63]. Protein A binds with high affinity to human IgG and moderate affinity to IgM, IgA and IgE. It does not bind human IgD. Unbound proteins were eluted from the column with PBS while the targeted, bound immunoglobulins were eluted from the column with 0.1M glycine (pH2.3). An SDS-PAGE gel without CHAPS treatment of the differentially centrifuged fractions was prepared for (i) whole SF (blue), (ii) the non-bound (immunoglobulin-free) fraction (purple) and (iii) the bound, immunoglobulin fraction (green). This can be seen in Figure 3.20.

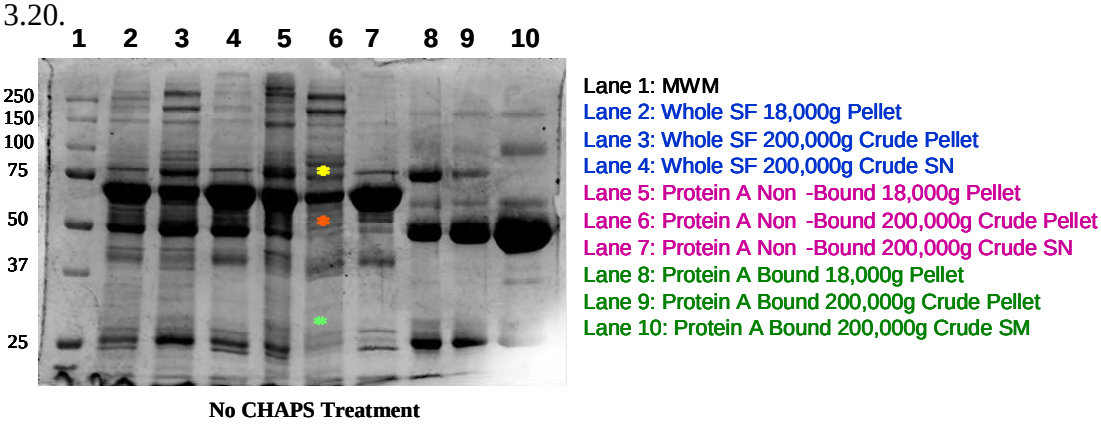

Figure 3.20: *Coomassie-stained gel showing the removal of immunoglobulins by Protein A chromatography before CHAPS treatment. To aid discussion, the bands of interest are represented by asterisks (IgM (yellow), IgG heavy chain (red) and immunoglobulin light chains (green).*

Lanes 2-4 in Figure 3.20 show the IgM mu chain (~75kDa), IgG gamma chain (~57kDa) and IgG light chain (~25kDa) are present in all three fractions of whole synovial fluid. There appears to be an enrichment of these species in the 200,000g pellet (Lane 3) relative to the other two fractions in Lanes 2 & 4. Following Protein A affinity chromatography, there is a clear redistribution of these immunoglobulins. For example, there is enrichment of the 75kDa species in both the non-bound 18,000g (Lane 5) and in the bound 18,000g (Lane 8) pellets. At the same time, there is low band intensity for this molecule in the non-bound 200,000g pellet (yellow asterisks Lane 6) relative to that in whole SF (Lane 3). This same reduction in band intensity also applies to both the 57kDa and 25kDa moieties (red and green asterisks respectively). There are however, still bands present at these molecular weights in the 200,000g non-bound pellet (Lane 6), though without analysis by WB, it is not possible to say if these moieties are immunoglobulins entrapped within or bound to the MV, or else other species that possess the same molecular weight as the species which were removed by Protein A chromatography.

What is clear though is that in the bound fractions (Lanes 8, 9, and 10), these bands intensities are much stronger than those in whole SF (Lanes 2, and 4) suggesting a significant removal of these proteins following Protein A affinity chromatography. Another interesting observation is the large enrichment of what may be IgM in the lower speed 18,000g pellet (Lane 8) relative to the 200,000g fractions (Lanes 9 & 10). On the other hand, IgG is redistributed across all three fractions in the bound sample, though slightly more so in the SN (Lane 10).

A study was then carried out to establish the effect of this immunoglobulin removal/reduction on further protein enrichment in the 200,000g pellet following CHAPS treatment. Pre- and post-CHAPS treated 200,000g pellets were analysed and a Coomassie stained gel is shown in Figure 3.21.

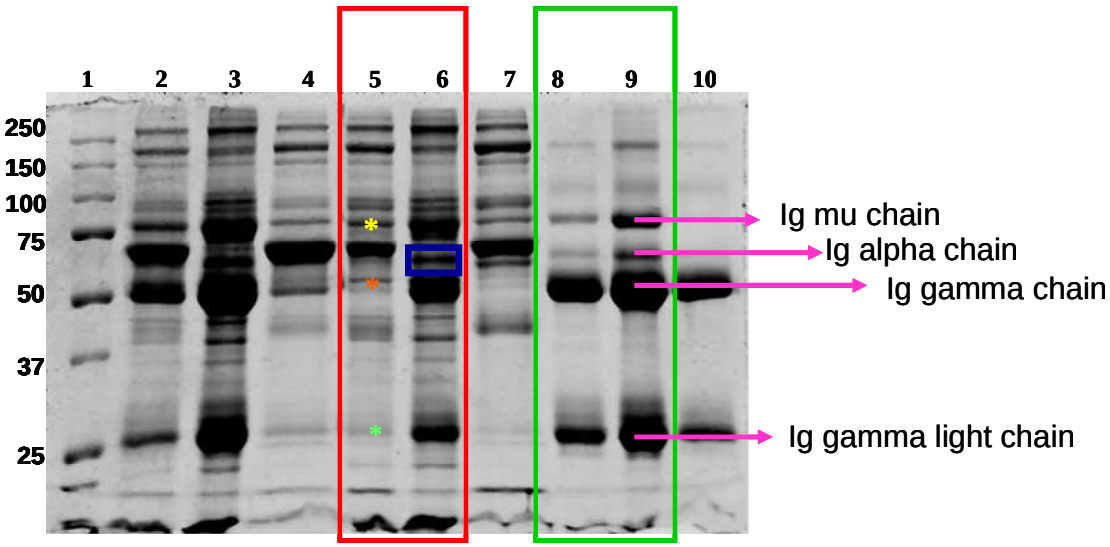

Lane 1: MWM
Lane 2: Whole SF 200,000g Crude Pellet
Lane 3: Whole SF 200,000g CHAPS Pellet
Lane 4: Whole SF 200,000g CHAPS SN
Lane 5: Protein A NonBound 200,000g Crude Pellet
Lane 6: Protein A NonBound 200,000g CHAPS Pellet
Lane 7: Protein A NonBound 200,000g CHAPS SN
Lane 8: Protein A Bound 200,000g Crude Pellet
Lane 9: Protein A Bound 200,000g CHAPS Pellet
Lane 10: Protein A Bound 200,000g CHAPS SN

Figure 3.21: *Coomassie-stained gel illustrating a comparison between crude and CHAPS-treated 200,000g pellets for whole SF (lanes 2-4), non-bound (lanes 5-7) and bound (lanes 8-10) fractions following Protein A affinity chromatography. Different immunoglobulin isotypes are indicated with a pink arrow.*

It was observed that in all three samples (whole SF, Protein A non-bound & Protein A bound), there is further enrichment of protein following CHAPS treatment i.e. comparing lanes 2 & 3, lanes 5 & 6 and lanes 8 & 9. Removal of loosely associated species with CHAPS, and loading the same amount of protein, leads to an enrichment of protein in the 200,000g CHAPS pellet. Bands (based on molecular weight) for each immunoglobulin isoform in the bound fractions (Lanes 8, 9 and 10) are labeled with a pink arrow. These can serve as a positive control.

Lanes 5 and 6 (within the red box) are worth discussing. These are the 200,000g non-bound pellets (the targeted proteome), pre- and post-CHAPS treatment respectively. As mentioned, there is considerable enrichment of protein post-CHAPS treatment as seen by stronger band intensities in Lane 6 relative to Lane 5. However, as seen here this enrichment also includes both IgM (yellow asterisks) and IgG (red and green asterisks). Knowing that Protein A affinity chromatography targeted these species, why are these species still associated with the vesicle proteome? It can only be concluded that IgM and IgG are either entrapped within the MV, strongly bound to the surface, or both present on the surface and within the vesicle. An alternative explanation could be the formation of immune complexes which may not be dissociated by CHAPS. At this point it is not possible to definitively say what the case is. Lanes 8 and 9 within the green box are also worthy of comment. It is the case that post-CHAPS treatment (Lane 9) there is a sizable increase in band intensity in IgM and IgG. Without CHAPS treatment, these species would have remained associated with the pellet and so prevent enrichment of other proteins. Therefore, Protein A affinity chromatography is an important step in any sample preparation protocol. Further, removal of albumin following CHAPS treatment led to an increase in band intensity of the protein in the blue box in Lane 6. On the basis the molecular weight (~ 60kDa), this may be IgA.

Finally, a WB with anti-Tsg101 of these samples was performed to establish the distribution of exosomes across the fractions. This is shown in Figure 3.22.

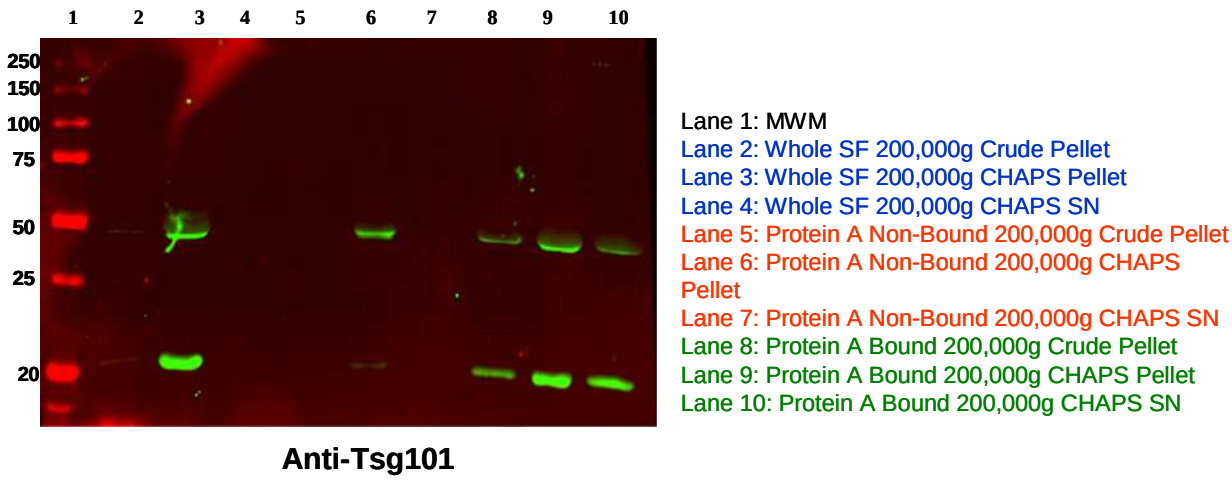

Figure 3.22: *WB with anti-Tsg101 of all fractions pre- and post-CHAPS treatment.*

As noted before, there is an enrichment of the Tsg101 exosomal marker (~46kDa) in the 200,000g CHAPS pellet Lane 3, 6 and 9. Surprisingly, there is also Tsg101 exosomal marker present in all three bound fractions (Lane 8, 9 and 10). A hypothesis for this phenomenon will be offered in the discussion section.

This concludes the customisation of a MV isolation protocol for SF. The entire workflow for this is displayed in Figure 3.23.

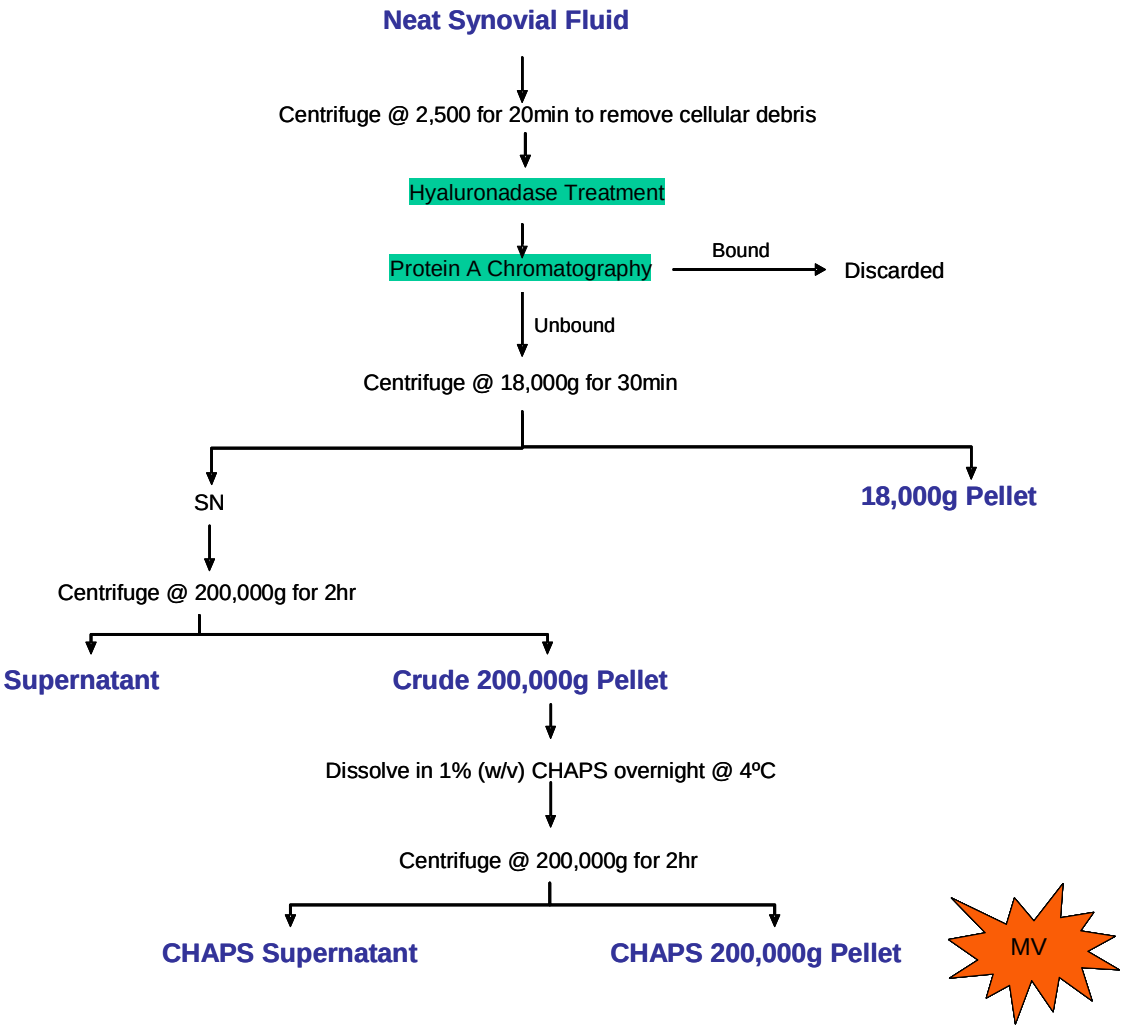

Figure 3.23: *Customised workflow developed for isolating MV from whole synovial fluid. Additional steps added to the standard differential centrifugation method (Figure 3.8) include treatment with HAase to release potentially entrapped vesicles, removal of potential ICs to aid protein enrichment in the targeted 200,000g pellet and finally CHAPS treatment to maximize protein enrichment through the removal of loosely associated proteins from the vesicle surface.*

3.2.2 Confirmation of the presence of MV in SF by electro-microscopy (EM)

Figure 3.24 is a display of MVs isolated from OA SF with increasing magnification.

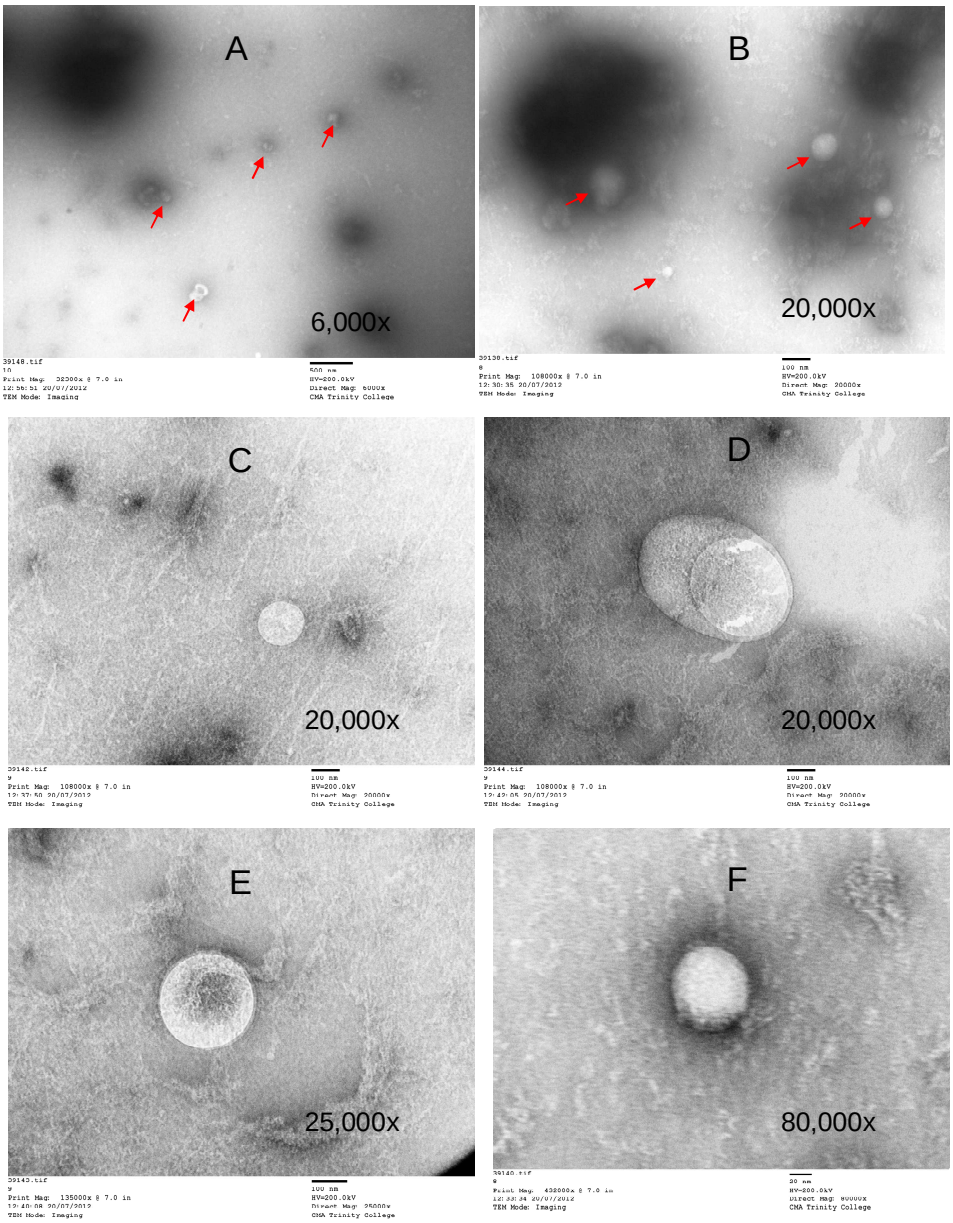

Figure 3.24: *Electronmicrographs displaying MVs isolated from OA SF. The figure shows different fields with increasing magnification. A 6,000x; B,C and D 20,000x; E 25,000x and F 80,000x. In the lower magnifications, MVs are indicated with red arrows.*

From Figure 3.24 it can be seen that MVs of various sizes are associated with SF following the method developed in Figure 3.23. Using the scale under each micrograph in conjunction with Figure 3.2, the vesicles in A and B fall within the size range of exosomes (50-100nm), ectosomes (50-200nm) and apoptotic vessels (50-500nm). The vesicles in micrographs C, D and E on the other hand, are certainly outside the exosome range. The vesicle(s) in D is - relative to exosomes - very large. This is most probably a micro-particle(s). However, F certainly has the dimensions of an exosome. As mentioned before, vesicles cannot be identified on the basis on physical parameters, so attempting to classify them on this basis is purely speculative. They suffice to show that MVs have been isolated and that the population is most certainly a heterogeneous assortment. That exosomes are present has already been verified through WB analysis with exosomal markers.

To conclude, it has been demonstrated by electro-microscopy and WB that following the application of a newly-developed, SF-customised MV-isolation protocol, a heterogeneous population of vesicle-types was obtained. The next objective is to characterise the proteome of these vesicles employing mass spectrometry (MS).

3.2.3 Protein characterisation of synovial fluid, CHAPS-treated 200,000g MVs, employing "off-gel" and "in-gel" approaches

Four OA patient samples were pooled and the previously developed MV-isolation protocol was employed (Figure 3.23). It was believed that a pooled sample would be more representative of the pathology in addition improving the MV yield for proteomic characterization. The 200,000g CHAPS pellet was prepared as in Figure 3.23 for MS analysis by the two methods detailed in the materials and methods section in this chapter and outlined here in Figure 3.25.

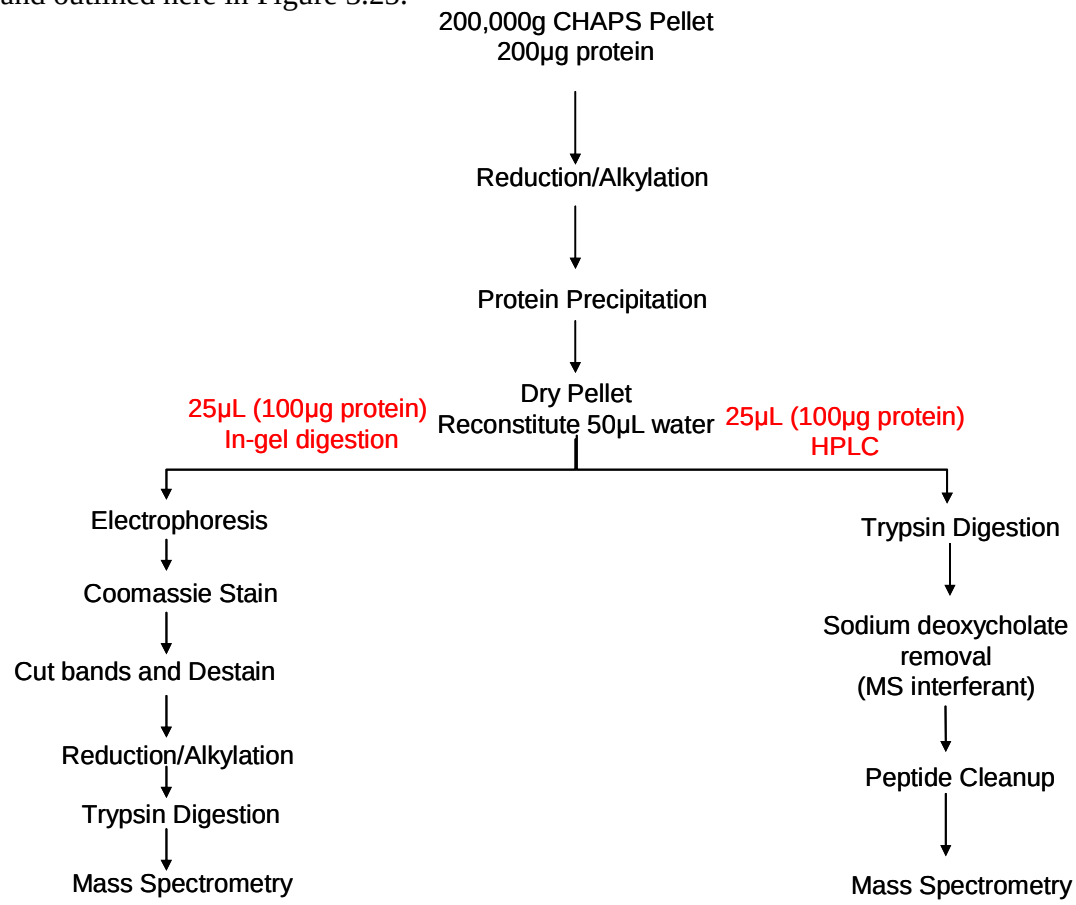

Figure 3.25: *Workflow of sample processing for MS analysis. Two different routes are employed – In-gel digestion (left) and the "shotgun" approach (right)*

Three modes of analysis were used i.e. 5-hour RP-HPLC, SCX-RP-HPLC and in-gel trypsin digestion. The raw data for each of these modes of analysis (arranged in order of decreasing number of peptide hits), is shown in appendices 1, 2 and 3 respectively. An on-line comparison tool was employed to aid analysis of the raw data. The list of

accession numbers for each dataset was entered and a comparison diagram generated. This Venn diagram is shown in Figure 3.26.

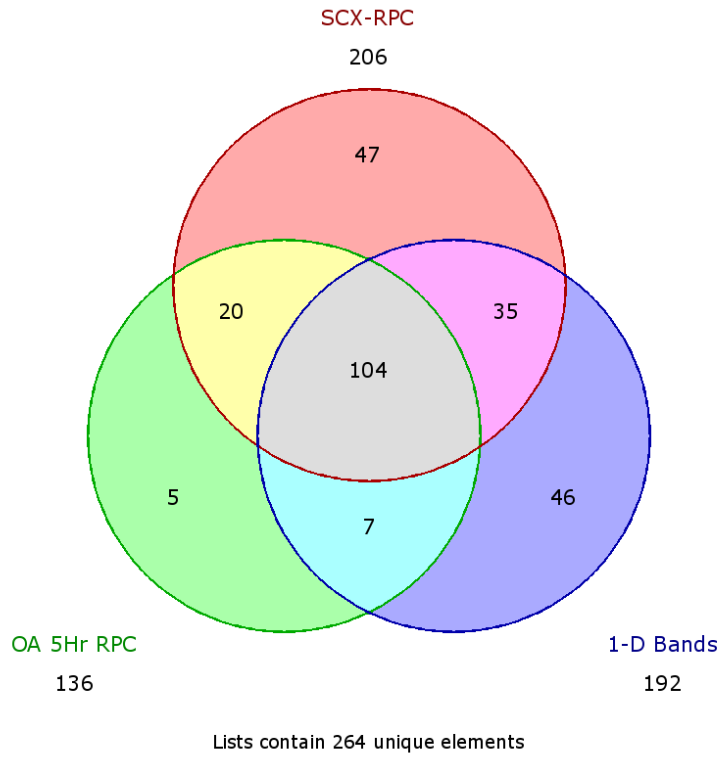

Figure 3.26: *Venn diagram comparing each protein list that was generated follow MS analysis using three different methods – 5-hour reverse-phase HPLC(green), SCX-reverse-phase HPLC(pink) and in-gel digestion of bands generated employing SDS-PAGE (blue)*

Analysis of the data yielded a total of 264 unique proteins associated with the 200,000g CHAPS-treated pellet.

Table 3.7 list all the proteins identified by MS. There is an additional column indicating which method(s) characterised each protein.

Reference	P (pro)	Score	Coverage	MW	Accession	Peptide	Method
Alpha-2-antiplasmin	7.83E-07	20.16	4.90	54531.2	P08697	2	1
Complement factor H-related protein 3	3.65E-13	20.19	7.90	37298.8	Q02985	2	1
Histidine-rich glycoprotein	1.23E-09	60.23	15.80	59540.9	P04196	6	1
Ig kappa chain V-II region RPMI 6410	4.11E-14	20.23	29.30	14697.4	P06310	2	1
Phospholipid transfer protein	3.49E-08	30.16	8.50	54704.7	P55058	3	1
Protein S100-A9	4.06E-09	20.19	26.30	13233.5	P06702	2	1
Aggrecan core protein	4.63E-07	30.18	1.30	250037.6	P16112	3	2
Angiotensinogen	5.21E-08	20.20	5.20	53120.6	P01019	2	2
Annexin A2	3.02E-05	20.16	6.20	38579.8	P07355	2	2
Apolipoprotein A-IV	1.63E-09	20.21	7.30	45371.5	P06727	2	2
Apolipoprotein D	3.00E-06	20.15	11.60	21261.8	P05090	2	2
Catalase	5.72E-07	20.18	4.60	59718.9	P04040	2	2
Chitinase-3-like protein 1	1.67E-08	20.19	6.30	42598.4	P36222	2	2
Coagulation factor XIII A chain	1.10E-08	20.17	3.70	83214.7	P00488	2	2
Complement C1s subcomponent	2.76E-08	50.16	10.30	76634.9	P09871	5	2
Coronin-1A	2.10E-06	20.15	6.90	50993.9	P31146	2	2
EGF-containing fibulin-like ECM protein 1	4.82E-09	50.16	12.20	54604.3	Q12805	5	2
Extracellular matrix protein 1	2.93E-07	20.15	5.00	60635.4	Q16610	2	2
Fibulin-1	3.79E-06	20.14	3.00	77162.4	P23142	2	2
Fructose-bisphosphate aldolase A	7.89E-08	40.22	18.70	39395.3	P04075	4	2
Hyaluronan-binding protein 2	1.65E-05	20.14	3.60	62630.5	Q14520	2	2
Ig delta chain C region	2.96E-09	20.19	6.80	42227.3	P01880	2	2
Ig heavy chain V-II region ARH-77	4.88E-10	20.22	17.10	16218.1	P06331	2	2
Ig heavy chain V-III region GAL	1.80E-06	30.21	17.20	12722.2	P01781	3	2
Ig heavy chain V-III region NIE	7.02E-08	18.16	19.30	13234.0	P01770	2	2
Ig kappa chain V-I region Wes	7.88E-14	28.26	16.70	11600.7	P01611	3	2
Kallistatin	1.66E-	50.17	13.30	48511.2	P29622	5	2

	07						
Lactotransferrin	1.09E-09	30.16	6.60	78132.0	P02788	3	2
L-lactate dehydrogenase A chain	1.61E-06	20.14	6.60	36665.4	P00338	2	2
Mannose-binding protein C	6.92E-08	30.21	15.30	26127.0	P11226	3	2
Plasma serine protease inhibitor	5.28E-07	40.16	11.10	45645.8	P05154	4	2
Polymeric immunoglobulin receptor	1.17E-06	30.19	5.80	83231.7	P01833	3	2
POTE ankyrin domain family member I	1.80E-06	20.24	2.00	121204.4	P0CG38	2	2
POTE ankyrin domain family member J	1.80E-06	20.24	2.00	117314.7	P0CG39	2	2
Procollagen C-endopeptidase enhancer 1	5.70E-11	40.21	13.60	47942.0	Q15113	4	2
Prolow-density lipoprotein receptor-related protein 1	6.30E-05	30.15	0.70	504274.2	Q07954	3	2
Proteasome subunit beta type-1	2.39E-09	20.16	9.50	26472.4	P20618	2	2
Putative annexin A2-like protein	3.02E-05	20.16	6.20	38634.8	A6NMY6	2	2
Putative heat shock 70 kDa protein 7	7.49E-04	18.12	6.00	40219.6	P48741	2	2
Putative macrophage-stimulating protein MSTP9	1.09E-07	20.17	2.90	79642.3	Q2TV78	2	2
Resistin	4.72E-09	20.17	24.10	11411.5	Q9HD89	2	2
Serine protease HTRA1	1.06E-05	20.14	4.80	51254.7	Q92743	2	2
Stromelysin-1	4.59E-07	60.19	12.60	53943.4	P08254	6	2
Tenascin	7.64E-07	20.20	1.00	240697.7	P24821	2	2
Transforming growth factor-beta-induced protein ig-h3	5.23E-05	20.14	4.10	74634.1	Q15582	2	2
Transthyretin	8.33E-09	20.23	23.80	15877.1	P02766	2	2
Vimentin	4.63E-07	20.17	5.20	53619.2	P08670	2	2
Vitamin D-binding protein	5.13E-13	30.21	9.10	52929.1	P02774	3	2
Aconitate hydratase, mitochondrial 25	1.55E-09	20.25	5.50	85372.0	Q99798	2	3
ATP synthase subunit beta, mitochondrial	3.30E-13	70.30	21.70	56524.7	P06576	7	3
Beta-enolase	5.81E-13	40.25	17.30	46902.3	P13929	4	3
Citrate synthase, mitochondrial	7.30E-10	20.18	6.90	51679.6	O75390	2	3
Collagen alpha-2(I) chain	5.65E-05	40.21	4.00	129235.8	P08123	4	3

Creatine kinase M-type	2.21E-10	20.26	8.10	43073.9	P06732	2	3
Dermcidin	5.80E-06	20.16	20.00	11276.8	P81605	2	3
Elongation factor 1-alpha 1	8.00E-10	20.25	8.40	50109.2	P68104	2	3
Ferritin light chain	1.23E-12	30.25	22.90	20007.1	P02792	3	3
General transcription factor IIF subunit 1	3.13E-04	20.14	3.30	58205.1	P35269	2	3
Glial fibrillary acidic protein	3.83E-09	18.20	4.20	49849.7	P14136	2	3
Histone H2B type 1-B	2.40E-11	38.22	11.90	13941.6	P33778	4	3
Histone H2B type 1-C/E/F/G/I	2.40E-11	38.22	11.90	13897.6	P62807	4	3
Histone H2B type 1-D	2.40E-11	38.22	11.90	13927.6	P58876	4	3
Histone H2B type 1-H	2.40E-11	38.22	11.90	13883.5	Q93079	4	3
Histone H2B type 1-J	2.40E-11	38.22	11.90	13895.6	P06899	4	3
Histone H2B type 1-K	2.40E-11	38.22	11.90	13881.6	O60814	4	3
Histone H2B type 1-L	2.40E-11	38.22	11.90	13943.6	Q99880	4	3
Histone H2B type 1-M	2.40E-11	38.22	11.90	13980.6	Q99879	4	3
Histone H2B type 1-N	2.40E-11	38.22	11.90	13913.6	Q99877	4	3
Histone H2B type 1-O	2.40E-11	38.22	11.90	13897.6	P23527	4	3
Histone H2B type 2-E	2.40E-11	38.22	11.90	13911.6	Q16778	4	3
Histone H2B type 2-F	2.40E-11	38.22	11.90	13911.6	Q5QNW6	4	3
Histone H2B type 3-B	2.40E-11	38.22	11.90	13899.5	Q8N257	4	3
Histone H2B type F-S	2.40E-11	38.22	11.90	13935.6	P57053	4	3
Ig heavy chain V-I region HG3	5.63E-07	20.22	22.20	12937.3	P01743	2	3
Ig lambda chain V-I region HA	2.64E-05	20.19	18.80	11888.9	P01700	2	3
Keratin, type II cytoskeletal 7	3.83E-09	18.20	3.80	51354.4	P08729	2	3
Keratin, type II cytoskeletal 72	3.33E-05	20.16	1.80	55842.5	Q14CN4	2	3
Keratin, type II cytoskeletal 8	3.83E-09	28.20	5.60	53671.2	P05787	3	3
Myosin light chain 3	8.86E-12	30.24	13.80	21917.9	P08590	3	3
Myosin regulatory light chain 2, ventricular/cardiac muscle isoform	1.54E-08	20.22	9.00	18777.4	P10916	2	3

Myosin-1	2.16E-05	16.20	1.40	223005.5	P12882	2	3
Myosin-2	2.16E-05	18.20	1.40	222905.1	Q9UKX2	2	3
Myosin-4	2.16E-05	16.20	1.40	222931.4	Q9Y623	2	3
Myosin-6	1.87E-13	58.27	5.00	223594.8	P13533	6	3
Myosin-7	1.55E-14	60.42	4.90	222957.8	P12883	6	3
Myosin-8	2.16E-05	18.20	1.40	222623.5	P13535	2	3
Plasminogen-related protein B	6.05E-07	20.16	18.80	10963.5	Q02325	2	3
Proteasome subunit alpha type-2	3.68E-11	20.21	17.10	25882.3	P25787	2	3
Proteasome subunit beta type-3	1.02E-09	20.25	15.60	22933.5	P49720	2	3
Putative elongation factor 1-alpha-like 3	8.00E-10	20.25	8.40	50153.2	Q5VTE0	2	3
Tropomyosin alpha-1 chain	8.62E-07	20.23	10.20	32688.7	P09493	2	3
Troponin C, slow skeletal and cardiac muscles	3.88E-09	20.22	18.00	18390.5	P63316	2	3
Apolipoprotein B-100	9.26E-11	450.28	12.20	515283.6	P04114	45	1 & 2
Apolipoprotein E	1.93E-10	60.22	23.00	36131.8	P02649	6	1 & 2
Carboxypeptidase N catalytic chain	8.46E-08	20.25	11.10	52253.4	P15169	2	1 & 2
Carboxypeptidase N subunit 2	3.59E-09	20.22	6.20	60518.2	P22792	2	1 & 2
Cartilage oligomeric matrix protein	3.13E-12	70.24	13.60	82807.7	P49747	7	1 & 2
Collagen alpha-1(VI) chain	1.80E-10	30.25	4.70	108462.0	P12109	3	1 & 2
Collagen alpha-3(VI) chain	3.59E-11	150.20	5.40	343454.2	P12111	15	1 & 2
Complement C2	1.04E-10	80.21	12.90	83214.4	P06681	8	1 & 2
Hemopexin	1.93E-12	30.22	11.50	51643.3	P02790	3	1 & 2
Inter-alpha-trypsin inhibitor heavy chain H1	1.05E-09	90.22	15.10	101325.8	P19827	9	1 & 2
Inter-alpha-trypsin inhibitor heavy chain H2	3.78E-09	80.23	12.60	106396.8	P19823	8	1 & 2
Inter-alpha-trypsin inhibitor heavy chain H4	6.62E-08	80.21	10.40	103293.2	Q14624	8	1 & 2
Myeloperoxidase	3.35E-08	70.18	10.50	83815.0	P05164	7	1 & 2
Myosin-9	3.34E-09	30.22	2.10	226390.6	P35579	3	1 & 2
N-acetylmuramoyl-L-alanine amidase	1.43E-09	30.21	8.00	62178.0	Q96PD5	3	1 & 2

Plasma kallikrein	7.34E-10	80.20	16.00	71322.8	P03952	8	1 & 2
Pyruvate kinase isozymes M1/M2	3.29E-06	50.17	11.90	57900.2	P14618	5	1 & 2
Thrombospondin-4	6.64E-09	60.23	10.70	105801.8	P35443	6	1 & 2
Ig kappa chain V-I region DEE	3.55E-14	36.31	16.70	11653.8	P01597	4	1,2 & 3
Alpha-1-antichymotrypsin	6.77E-14	40.26	13.70	47620.6	P01011	4	1,2 & 3
Alpha-1-antitrypsin	1.77E-10	40.22	13.20	46707.1	P01009	4	1,2 & 3
Alpha-2-macroglobulin	1.00E-30	630.29	49.60	163187.4	P01023	63	1,2 & 3
Alpha-enolase	5.81E-13	18.25	10.10	47139.4	P06733	2	1,2 & 3
Apolipoprotein A-I	4.46E-10	50.20	22.10	30758.9	P02647	5	1,2 & 3
Beta-2-glycoprotein 1	1.16E-10	50.26	23.80	38272.7	P02749	5	1,2 & 3
C4b-binding protein alpha chain	1.22E-14	250.35	50.30	66989.4	P04003	25	1,2 & 3
C4b-binding protein beta chain	2.60E-09	30.16	17.10	28338.5	P20851	3	1,2 & 3
Carboxypeptidase B2	8.61E-09	20.22	13.00	48393.5	Q96IY4	2	1,2 & 3
Cartilage acidic protein 1	1.91E-11	100.24	19.10	71375.9	Q9NQ79	10	1,2 & 3
CD5 antigen-like	2.22E-15	110.32	42.90	38063.0	O43866	11	1,2 & 3
Ceruloplasmin	2.00E-14	160.28	23.00	122127.6	P00450	16	1,2 & 3
Clusterin	1.20E-12	100.25	18.90	52461.1	P10909	10	1,2 & 3
Collagen alpha-2(VI) chain	1.09E-06	50.16	5.10	108511.9	P12110	5	1,2 & 3
Complement C1q subcomponent subunit B	6.12E-10	50.32	23.70	26704.5	P02746	5	1,2 & 3
Complement C1q subcomponent subunit C	6.66E-15	50.31	25.30	25757.1	P02747	5	1,2 & 3
Complement C1r subcomponent	6.35E-11	70.25	16.20	80066.8	P00736	7	1,2 & 3
Complement C3	1.00E-30	940.41	59.20	187029.3	P01024	95	1,2 & 3
Complement C4-A	5.55E-16	580.38	39.70	192649.5	P0C0L4	58	1,2 & 3
Complement C4-B	1.00E-30	580.37	39.70	192671.6	P0C0L5	58	1,2 & 3
Complement C5	7.77E-16	280.25	17.80	188185.3	P01031	28	1,2 & 3
Complement component C6	1.11E-14	80.26	13.00	104717.9	P13671	8	1,2 & 3
Complement component C7	1.33E-15	160.23	33.90	93457.3	P10643	16	1,2 & 3

Complement component C8 alpha chain	3.00E-14	120.41	27.90	65121.0	P07357	12	1,2 & 3
Complement component C8 beta chain	1.98E-12	110.28	25.20	67003.5	P07358	11	1,2 & 3
Complement component C9	1.95E-14	110.27	20.00	63132.8	P02748	11	1,2 & 3
Complement factor B	8.24E-13	110.21	21.60	85478.6	P00751	11	1,2 & 3
Complement factor H	9.99E-15	420.34	46.50	139004.4	P08603	42	1,2 & 3
Complement factor H-related protein 1	2.84E-10	70.25	27.60	37626.0	Q03591	7	1,2 & 3
Complement factor H-related protein 2	9.79E-10	50.20	20.70	30630.6	P36980	5	1,2 & 3
Complement factor I	1.44E-11	60.15	15.10	65706.7	P05156	6	1,2 & 3
Fibrinogen alpha chain	1.11E-15	190.31	21.80	94914.3	P02671	19	1,2 & 3
Fibrinogen beta chain	1.00E-30	338.43	57.40	55892.2	P02675	34	1,2 & 3
Fibrinogen gamma chain	2.11E-14	240.29	59.60	51478.9	P02679	24	1,2 & 3
Fibronectin	4.44E-15	640.34	39.20	262457.6	P02751	64	1,2 & 3
Ficolin-3	2.82E-10	40.28	16.10	32882.0	O75636	4	1,2 & 3
Galectin-3-binding protein	2.98E-10	50.20	16.20	65289.4	Q08380	5	1,2 & 3
Gelsolin	1.70E-11	80.23	17.50	85644.3	P06396	8	1,2 & 3
Haptoglobin	4.12E-10	130.26	26.40	45176.6	P00738	13	1,2 & 3
Haptoglobin-related protein	1.10E-09	60.20	25.00	39004.7	P00739	6	1,2 & 3
Ig alpha-1 chain C region	5.55E-15	100.27	36.80	37630.7	P01876	10	1,2 & 3
Ig alpha-2 chain C region	5.55E-15	70.26	23.20	36503.0	P01877	7	1,2 & 3
Ig gamma-1 chain C region	8.44E-09	50.23	18.80	36083.2	P01857	5	1,2 & 3
Ig gamma-2 chain C region	1.44E-08	30.17	8.90	35877.8	P01859	3	1,2 & 3
Ig gamma-3 chain C region	1.11E-15	100.29	44.00	41260.4	P01860	10	1,2 & 3
Ig gamma-4 chain C region	1.44E-08	30.17	8.90	35917.9	P01861	3	1,2 & 3
Ig heavy chain V-III region BRO	2.44E-14	20.33	25.00	13218.4	P01766	2	1,2 & 3
Ig heavy chain V-III region VH26	1.90E-08	30.19	18.80	12574.2	P01764	3	1,2 & 3
Ig heavy chain V-III region WEA	3.03E-08	38.21	36.00	12248.5	P01763	4	1,2 & 3
Ig kappa chain C region	1.00E-30	60.33	82.10	11601.7	P01834	6	1,2 & 3
Ig kappa chain V-I region AG	1.35E-	36.31	16.70	11984.9	P01593	4	1,2 & 3

	12						
Ig kappa chain V-I region AU	1.35E-12	36.31	16.70	11931.8	P01594	4	1,2 & 3
Ig kappa chain V-I region EU	2.71E-12	38.25	26.90	11780.8	P01598	4	1,2 & 3
Ig kappa chain V-I region Gal	1.35E-12	36.31	16.70	11806.9	P01599	4	1,2 & 3
Ig kappa chain V-I region Hau	1.35E-12	36.31	16.70	11663.7	P01600	4	1,2 & 3
Ig kappa chain V-I region Ni	1.43E-07	36.18	30.40	12238.0	P01613	4	1,2 & 3
Ig kappa chain V-I region Rei	1.35E-12	36.31	16.70	11894.9	P01607	4	1,2 & 3
Ig kappa chain V-I region Roy	1.35E-12	36.31	16.70	11774.8	P01608	4	1,2 & 3
Ig kappa chain V-I region Scw	1.35E-12	36.31	16.70	11756.8	P01609	4	1,2 & 3
Ig kappa chain V-I region WAT	3.40E-12	26.27	16.70	11729.8	P80362	3	1,2 & 3
Ig kappa chain V-I region WEA	3.40E-12	26.27	16.70	11832.8	P01610	3	1,2 & 3
Ig kappa chain V-III region GOL	1.22E-11	20.24	22.90	11823.0	P04206	2	1,2 & 3
Ig kappa chain V-III region HAH	1.22E-11	30.24	31.80	14064.1	P18135	3	1,2 & 3
Ig kappa chain V-III region HIC	1.22E-11	30.24	31.80	14080.1	P18136	3	1,2 & 3
Ig kappa chain V-III region WOL	2.30E-12	30.20	39.40	11738.9	P01623	3	1,2 & 3
Ig lambda-1 chain C regions	1.45E-12	40.31	55.70	11340.6	P0CG04	4	1,2 & 3
Ig lambda-2 chain C regions	1.45E-12	40.31	55.70	11286.6	P0CG05	4	1,2 & 3
Ig lambda-3 chain C regions	1.45E-12	40.31	55.70	11230.5	P0CG06	4	1,2 & 3
Ig lambda-6 chain C region	3.00E-14	30.25	46.20	11269.5	P0CF74	3	1,2 & 3
Ig mu chain C region	1.67E-14	170.36	38.10	49275.6	P01871	17	1,2 & 3
Ig mu heavy chain disease protein	1.67E-14	110.36	29.40	43030.3	P04220	11	1,2 & 3
Immunoglobulin J chain	8.13E-10	40.22	32.10	18087.0	P01591	4	1,2 & 3
Immunoglobulin lambda-like polypeptide 5	1.29E-11	40.25	32.20	23048.6	B9A064	4	1,2 & 3
Keratin, type I cytoskeletal 10	4.59E-11	170.25	31.30	58791.6	P13645	17	1,2 & 3
Keratin, type I cytoskeletal 14	2.91E-09	110.22	24.60	51529.4	P02533	11	1,2 & 3
Keratin, type I cytoskeletal 16	6.33E-12	130.29	34.00	51236.3	P08779	13	1,2 & 3
Keratin, type I cytoskeletal 9	1.00E-30	188.39	46.20	62026.7	P35527	19	1,2 & 3
Keratin, type II cytoskeletal 2 epidermal	6.66E-14	190.26	37.60	65393.2	P35908	19	1,2 & 3

Keratin, type II cytoskeletal 5	1.97E-09	110.24	16.80	62340.0	P13647	11	1,2 & 3
Keratin, type II cytoskeletal 6A	2.67E-06	20.15	4.10	60008.3	P02538	2	1,2 & 3
Keratin, type II cytoskeletal 6B	1.97E-09	210.24	36.90	60030.3	P04259	21	1,2 & 3
Keratin, type II cytoskeletal 6C	5.37E-11	220.24	39.90	59988.4	P48668	22	1,2 & 3
Keratin, type II cytoskeletal 75	6.33E-08	70.24	10.70	59524.1	O95678	7	1,2 & 3
Keratin, type II cytoskeletal 79	6.33E-08	40.24	7.10	57800.2	Q5XKE5	4	1,2 & 3
Neutrophil defensin 1	4.25E-06	20.15	19.10	10194.2	P59665	2	1,2 & 3
Neutrophil defensin 3	4.25E-06	20.15	19.10	10238.2	P59666	2	1,2 & 3
Pigment epithelium-derived factor	7.01E-12	90.22	21.80	46283.4	P36955	9	1,2 & 3
Plasma protease C1 inhibitor	7.70E-09	50.20	11.60	55119.5	P05155	5	1,2 & 3
Plasminogen	9.99E-16	280.30	44.30	90510.2	P00747	28	1,2 & 3
Pregnancy zone protein	9.92E-10	100.23	8.00	163759.1	P20742	10	1,2 & 3
Protein S100-A8	8.54E-08	40.19	39.80	10827.7	P05109	4	1,2 & 3
Proteoglycan 4	2.50E-13	90.26	7.70	150983.2	Q92954	9	1,2 & 3
Prothrombin	1.11E-16	220.27	53.50	69992.2	P00734	22	1,2 & 3
Serotransferrin	1.04E-11	240.27	37.00	77013.7	P02787	24	1,2 & 3
Serum albumin	1.00E-30	430.33	68.10	69321.6	P02768	43	1,2 & 3
Serum amyloid P-component	4.36E-10	50.22	23.80	25371.1	P02743	5	1,2 & 3
Serum paraoxonase/arylesterase 1	1.04E-10	40.17	18.90	39706.3	P27169	4	1,2 & 3
Vitamin K-dependent protein S	5.57E-11	80.25	12.60	75074.1	P07225	8	1,2 & 3
Vitronectin	7.22E-15	70.28	15.10	54271.2	P04004	7	1,2 & 3
Complement C1q subcomponent subunit A	1.14E-07	20.12	13.10	26000.2	P02745	2	1 & 3
Ig heavy chain V-III region TIL	4.12E-13	20.22	26.10	12348.1	P01765	2	1 & 3
Ig kappa chain V-II region TEW	4.79E-10	20.27	32.70	12308.2	P01617	2	1 & 3
Ig lambda-7 chain C region	1.45E-12	30.31	41.50	11295.6	A0M8Q6	3	1 & 3
Lysozyme C	1.29E-12	40.24	39.90	16526.3	P61626	4	1 & 3
Properdin	6.80E-06	30.24	8.50	51242.0	P27918	3	1 & 3
Keratin, type I cytoskeletal	1.86E-	20.16	3.90	50536.0	Q7Z3Y7	2	2 & 3

28	06						
Actin, alpha cardiac muscle 1	1.80E-06	40.24	11.10	41991.9	P68032	4	2 & 3
Actin, alpha skeletal muscle	1.80E-06	40.24	11.10	42023.9	P68133	4	2 & 3
Actin, aortic smooth muscle	1.11E-15	80.30	23.60	41981.8	P62736	8	2 & 3
Actin, cytoplasmic 1	1.80E-06	40.24	11.20	41709.7	P60709	4	2 & 3
Actin, cytoplasmic 2	1.00E-30	30.36	14.90	41765.8	P63261	3	2 & 3
Actin, gamma-enteric smooth muscle	1.11E-15	80.30	23.70	41849.8	P63267	8	2 & 3
Coagulation factor XI	1.36E-09	40.16	6.90	70063.6	P03951	4	2 & 3
Hemoglobin subunit alpha	8.51E-09	30.26	39.40	15247.9	P69905	3	2 & 3
Hemoglobin subunit beta	1.39E-05	30.19	21.80	15988.3	P68871	3	2 & 3
Hepatocyte growth factor activator	8.50E-08	30.16	6.00	70636.2	Q04756	3	2 & 3
Histone H4	8.05E-07	40.19	38.80	11360.4	P62805	4	2 & 3
Ig kappa chain V-I region CAR	2.71E-12	28.25	16.80	11696.3	P01596	3	2 & 3
Ig kappa chain V-I region Lay	2.34E-06	18.17	8.30	11826.8	P01605	2	2 & 3
Ig kappa chain V-III region CLL	1.59E-09	28.18	19.40	14266.2	P04207	3	2 & 3
Ig kappa chain V-III region NG9 (Fragment)	3.05E-07	46.17	41.00	10722.3	P01621	5	2 & 3
Ig kappa chain V-IV region (Fragment)	8.45E-08	30.20	24.80	13371.6	P06312	3	2 & 3
Ig kappa chain V-IV region B17	3.00E-06	20.17	13.40	14956.5	P06314	2	2 & 3
Ig kappa chain V-IV region JI	4.86E-08	30.19	22.60	14623.3	P06313	3	2 & 3
Ig kappa chain V-IV region Len	1.29E-09	50.22	42.10	12632.2	P01625	5	2 & 3
Ig kappa chain V-IV region STH (Fragment)	4.86E-08	20.19	19.30	12052.9	P83593	2	2 & 3
Ig lambda chain V-III region LOI	1.55E-08	20.20	21.60	11927.8	P80748	2	2 & 3
Keratin, type I cytoskeletal 13	4.33E-08	40.20	7.40	49557.4	P13646	4	2 & 3
Keratin, type I cytoskeletal 15	4.33E-08	40.20	7.00	49181.1	P19012	4	2 & 3
Keratin, type I cytoskeletal 17	3.56E-09	50.16	10.20	48076.1	Q04695	5	2 & 3
Keratin, type I cytoskeletal 19	1.09E-05	20.20	4.50	44079.2	P08727	2	2 & 3
Keratin, type I cytoskeletal 20	2.34E-05	26.16	4.00	48457.0	P35900	3	2 & 3
Keratin, type I cytoskeletal 25	1.86E-06	20.16	4.00	49287.4	Q7Z3Z0	2	2 & 3

Keratin, type I cytoskeletal 27	5.77E-06	20.17	3.90	49791.6	Q7Z3Y8	2	2 & 3
Keratin, type II cytoskeletal 2 oral	5.98E-06	30.19	4.50	65800.1	Q01546	3	2 & 3
Keratin, type II cytoskeletal 3	1.66E-06	30.16	4.60	64377.6	P12035	3	2 & 3
Keratin, type II cytoskeletal 4	6.49E-08	18.19	3.70	57249.9	P19013	2	2 & 3
Macrophage receptor MARCO	2.28E-04	20.14	5.20	52625.4	Q9UEW3	2	2 & 3
Malate dehydrogenase, mitochondrial	6.11E-06	30.18	10.90	35480.7	P40926	3	2 & 3
Plasma serine protease inhibitor	5.28E-07	40.16	11.10	45645.8	P05154	4	2 & 3
POTE ankyrin domain family member E	1.37E-11	20.23	2.40	121285.6	Q6S8J3	2	2 & 3
POTE ankyrin domain family member F	1.80E-06	20.24	2.00	121366.6	A5A3E0	2	2 & 3

Table 3.7: *Proteome of a pooled OA patient sample (n=4). This table is a condensed summary of appendices 1, 2 and 3. Also included (in the right hand column) is an indication of the method(s) that identified each particular protein – 1=5Hr RP-HPLC, 2=SCX/RP-HPLC, 3=In-gel digestion.*

A total of 104 proteins are common to all three methods of analysis. Of these, 17% are complement-related, while 34% belong to the immunoglobulin family. Surprisingly, the highly abundant proteins albumin and α-2-macroglobulin are included in this sub-group. It was expected that CHAPS treatment would remove these soluble species. It may be that they are members of the vesicle cargo. However, a very interesting protein, S100-A8, which will be discussed later, is also common to all three modes of analysis. This protein was cited as being unique to RA in the literature.

From Figure 3.26 it is revealed that SCX-RP-HPLC characterized the highest number of proteins (206) with in-gel digestion (192) next and finally the 5-hour RP-HPLC with 136 proteins.

Examination of Figure 3.26 reveals SCX-RP-HPLC and in-gel digestion yielded almost equal numbers of *unique* proteins (47 and 46 respectively), while the 5-hour RP-HPLC uncovered around 10 times less. This also supports the trend in the literature towards a

combination or coupling of orthogonal methodologies as a proteomic strategy [64]. Table 3.4 reveals that all histone (with the exception of histone H4) and myosin subtypes are exclusively unique to the in-gel trypsin digestion method. This maybe be due to protein enrichment in a particular band, while in the methods employing HPLC shotgun approach, these proteins may be masked by other more abundant proteins e.g. complement C3, fibronectin, alpha-2-macroglobulin, which are detected simultaneously.

Comparing any two methodologies in Figure 3.26 highlights that all actin associated with MV proteome, is a result of SCX-RP-HPLC and/or "in gel" digestion. No actin was found by employing RP-HPLC only. In addition, the commonality between SCX-RP-HPLC and in-gel digestion (35 proteins – mainly immunoglobulin fragments and skeletal proteins) is greater than the other two pairs (20 and 7). However, it is interesting to note that the important cartilage ECM protein, cartilage oligomeric matrix protein (COMP), which is widely cited as a putative OA marker (to be discussed later) was not detected by MS analysis of the gel bands, where as both shotgun approaches identified this protein. These findings highlight an important point. To attempt a proteomic profiling of any biofluid, it may be prudent to employ a variety of techniques and assess the list of proteins generated from each method. Reliance on any one single method may result in the loss of some potentially useful information.

Proteins were then classified with an on-line bioinformatics tool, known as Panther [65]. The goal of Panther is to sub-divide proteins into families and sub-families and therefore, classify proteins by function. Position-specific amino acids are used to determine if certain segments of a protein are conserved (e.g. hydrophobicity), and this leads to information on protein function. Thomas *et al*.[65] state that families can overlap so proteins may be members of multiple families. For example, an immunoglobulin variable region (Ig-V) appears in nine families while myosins appear in the largest number of families. Of the 264 proteins found, 50 were not recognized by the database. These are listed in Appendix A. Of these, 82% are immunoglobulin fragments. Two interesting proteins not classified by Panther are heat shock protein 70 (HSP70) which is a known exosome-associated protein (Figure 3.6) and dermcidin.

The Panther database classified 214 (264-50) proteins under four headings;

(i) Cellular Components

(ii) Protein Molecular Function

(iii) Biological Process

(iv) Protein Class

These complete protein classification lists are displayed in Appendices B, C, D, & E respectively.

3.2.3.1 Cellular Components

Three sub-groups make up this classification and these are shown in Figure 3.27.

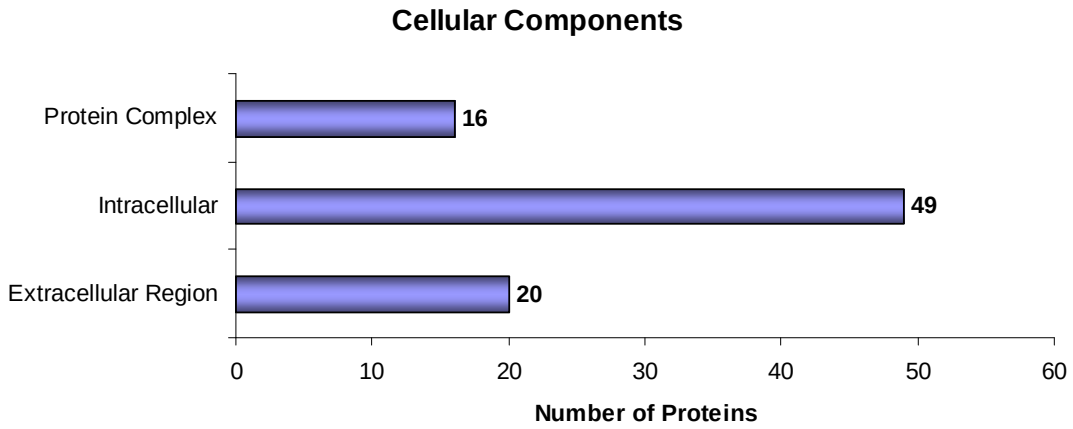

Figure 3.27: *Panther "Cellular Components" sub-classification.*

In addition to an expected intracellular and extracellular division, a protein complex sub-group is present. This is interesting in light of the recent work by György *et al.* [14] who issued a note of caution relating to the presence of immune complexes co-existing with isolated MVs. Proteins in this group include IgA, IgD, IgG and IgM. At this point it is not possible to state whether these are (i) in the form of immune complexes or (ii) vesicle-associated i.e. engulfed or trans-membrane species. Intracellular species are almost exclusively skeletal and motor proteins. Included in the extracellular region are some collagen species and COMP. As mentioned above, of the 264 proteins found, 50 were not classified by Panther. This means 214 were recognized. However, it is surprising that only 85 proteins are included in this sub-classification, leaving 129 not classified by location.

3.2.3.2 Protein Molecular Function

A complete list of each sub-group is shown in Appendix C. Figure 3.28 is a summary of this list in bar chart form.

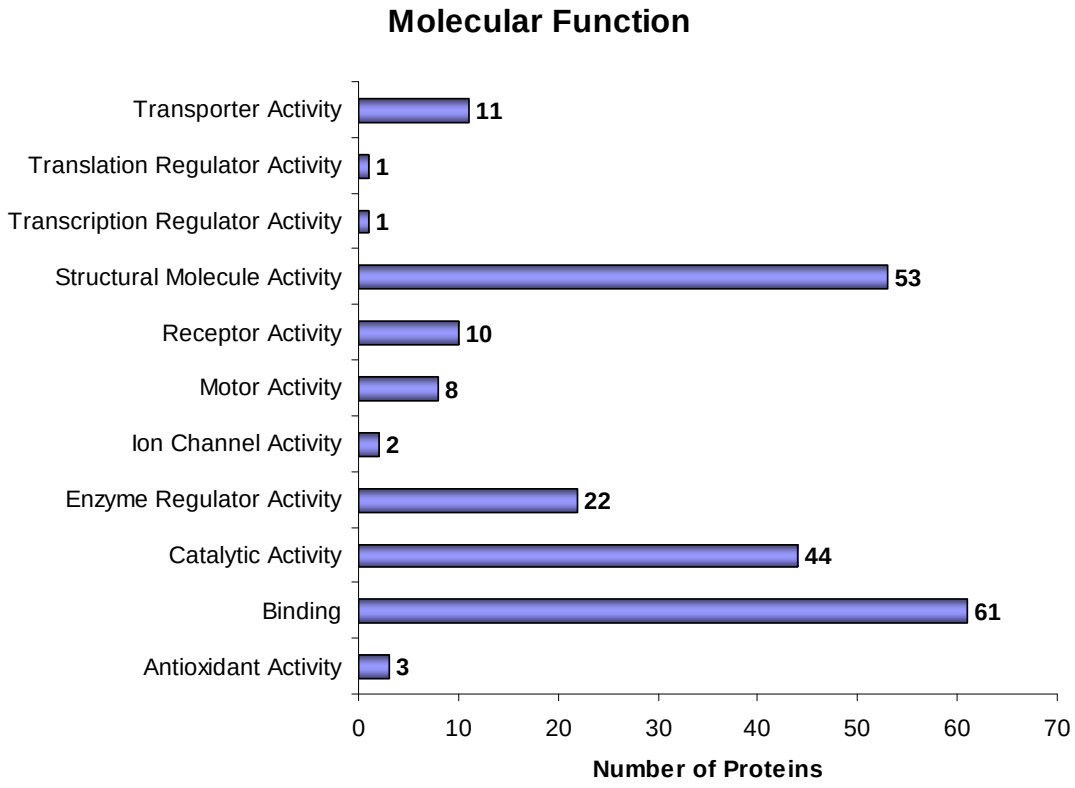

Figure 3.28: *Panther "Molecular Function" sub-classification of 214 uniquely identified proteins*

Three major molecular function sub-groups emerge from Figure 3.28, i.e. binding, catalytic activity and structural molecule activity. The binding sub-group includes antigen binding species such as immunoglobulins, fibrinogen, α-2-macroglobulin, COMP, complement components, cartilage acidic protein and the actin-scavaging protein, gelsolin. Serine-type peptidases represent a large proportion of molecules classified under catalytic activity e.g. MMP3 and serine protease Htra1. Type I and type II keratins were particularly represented in the sub-group, structural molecule activity. However, keratin is a well-known MS contaminant that comes from skin and dust. Care

was taken when preparing samples for MS. One interesting keratin species that was found was type I keratin 17 which was referred to as "*exosomal cytokeratin 17*" by Welton *et al.* [66]

3.2.3.3 Biological Process

A complete list of each sub-group is shown in Appendix D and a summary bar-chart is shown in Figure 3.29.

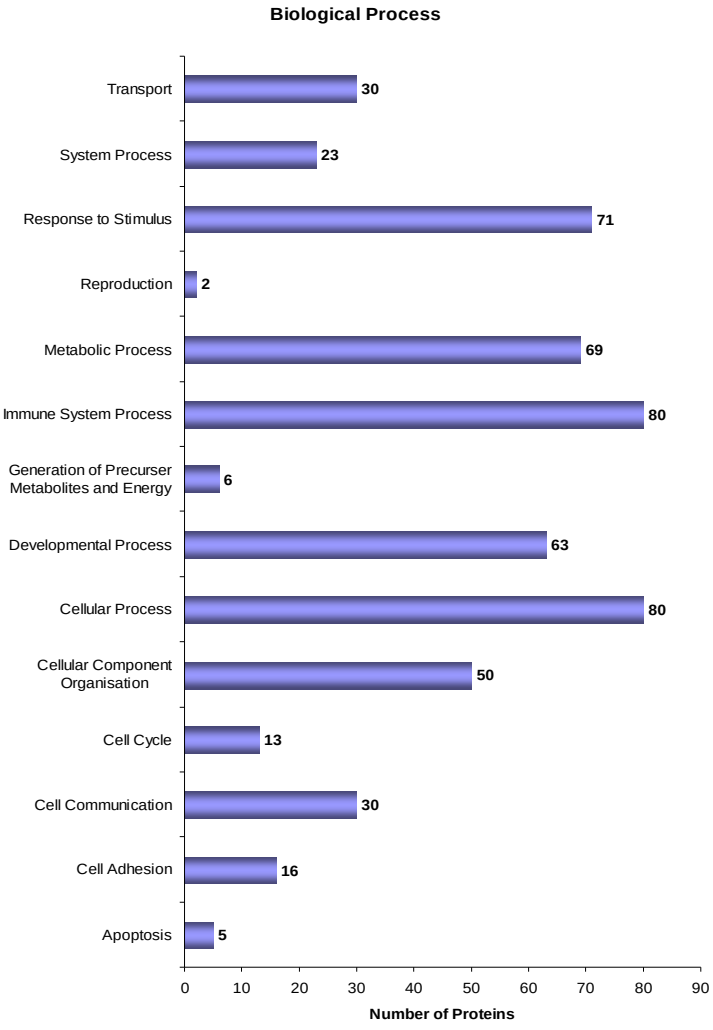

Figure 3.29: *Panther "Biological Process" sub-classification of 214 uniquely identified proteins*

Five proteins were classified as associated with apoptosis. Based on the information in Table 3.2 and a study by [67], histones are protein markers of apoptotic bodies, so it was surprising that even though histones (H2B and H4) are present in the 200,000g pellet proteome, Panther did not classify these species as apoptotic-related.

Some proteins involved in the cell adhesion subgroup include vitronectin, collagen α-3(VI) chain, collagen α-2(VI) chain, aggrecan core protein 2 (binds avidly to hyaluronic acid and resists cartilage compression), low-density lipoprotein receptor-related protein 1 intracellular domain (α-2 Macroglobulin and apolipoprotein E receptors). Another interesting MV-associated protein in this sub-group is transforming growth factor-beta-induced protein ig-h3, which, according to the UniProtKB database binds to type I, II, and IV collagens. This adhesion protein is also thought to play an important role in cell-collagen interactions. In cartilage, it may be involved in endochondral bone formation. As mentioned above, four classes of immunoglobulin are vesicle-associated and it was hypothesised that they are entrapped within the vesicle or else associated with the outer membrane (particularly IgM and IgD [68]). This hypothesis may have some merit due to the presence of IgGFc-binding protein. As protein A only binds to the Fc region of the molecule, IgGFc-binding protein may be already bound to IgG and may help explain why this immunoglobulin remains vesicle-associated. Shed vesicles/ectosomes may be the likely vesicle-type that has membrane-bound IgG.

In the cell communication sub-group interesting inflammation-inducing proteins include the calgranulins, protein S100-A8 and S100-A9. These will be discussed later. Also present are galectin-3-binding protein and CD5 antigen-like (IgM-associated peptide) - both involved in macrophage activation - and macrophage receptor MARCO. Procollagen C-endopeptidase enhancer 1 is cell surface receptor that, according to UniProtKB, may have a metalloproteinase inhibitory activity.

The cell cycle, cellular component organisation and cellular process sub-groups are largely composed of actin, keratin and myosin.

Species that are involved in activation of the immune system form a large proportion of this sub-classification e.g. immunoglobulins and components of the complement cascade. Components belonging to each of the three complement cascade pathways, are included i.e. classical pathway (C1q, C1r andC1s), lectin pathway (mannose binding lectin) and alternative pathway (complement factor B and properdin).

3.2.3.4 Protein Class

Classification of the MV proteome based on protein class or protein function is displayed in Figure 3.30.

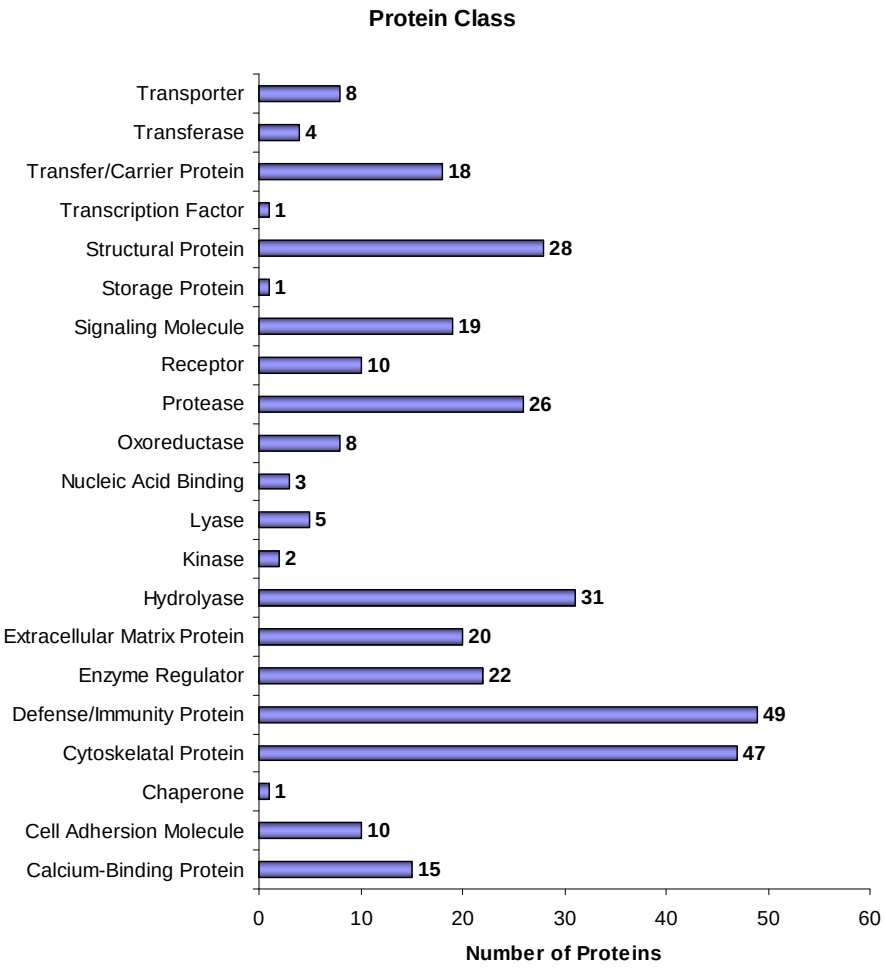

Figure 3.30: *Panther classification of MV proteome according to "Protein Class" or protein function*

As with the preceding classifications, cytoskelatal and immune system proteins form the largest subgroups. Proteases and protease inhibitors are also represented. Transporter proteins include apolipoproteins, ceruloplasmin and the transmembrane ion transporter, ATP synthase subunit β.

3.2.4 Selected protein analysis by Western Blot (WB) – a confirmatory study

It is important to ascertain the validity of some proteins identified by MS by confirming their presence by other techniques. In order to confirm the data obtained by MS, some proteins were selected for analysis by an orthogonal mode of analysis i.e. incubation with polyclonal antibodies and detection employing WB. It is also important to establish the presence of proteins that were not detected by MS, but which may be present and masked by more abundant species. Finally, the absence of a protein by MS analysis should be confirmed by WB.

Exosomal markers e.g. Tsg101 and CD63, were not detected by MS in our study. However, both proteins were detected by WB analysis (Figures 3.9, 3.17 and 3.22 for Tsg101) and (Figures 3.14 and 3.18 for CD63). This echoes the observation made by Welton *et al.* [66] There, due to a minimum of two peptides required for positive identification "cut-off", these species were not included as part of the proteome of exosomes derived from bladder cancer cells, but their presence was confirmed by WB.

Both IgM and albumin were identified by MS and their presence in MVs was confirmed by WM in Figure 3.19. The exosomal protein β-actin, which was shown to be present in Figure 3.14, was not identified by MS analysis (thought six other actin species were identified).

Apolipoprotein A-I was found as part of the proteome of OA MVs when analysed by MS. It presence was confirmed by WB (Figure 3.31, at ~25kDa)

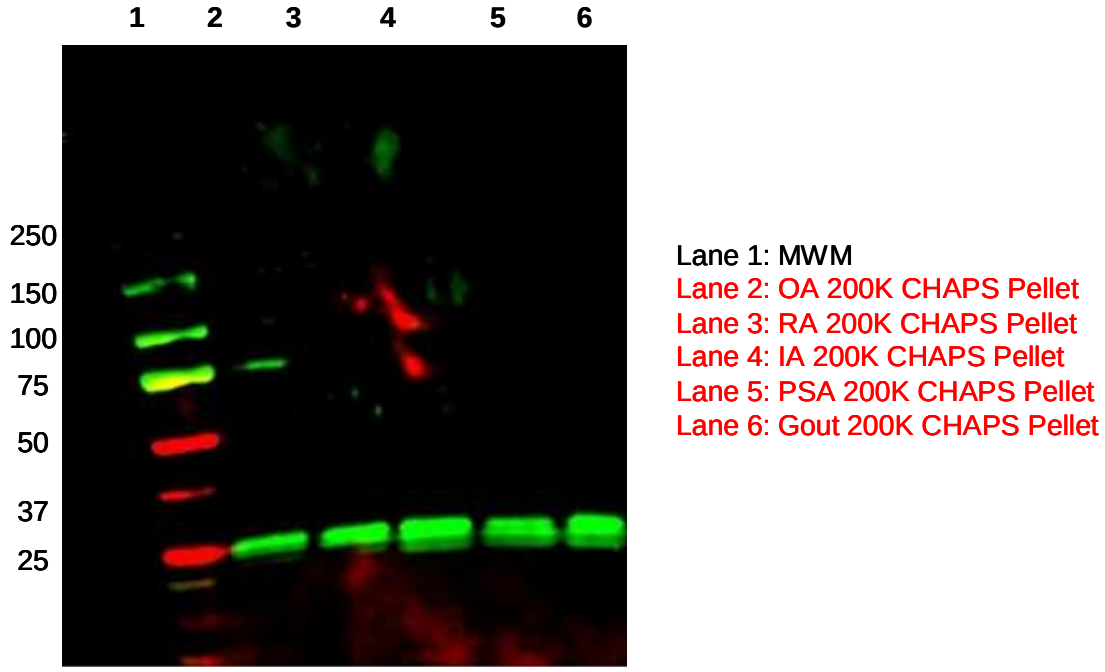

Figure 3.31: *WB analysis of the 200,000g CHAPS pellet for five different patient pathologies following incubation with anti-apolipoprotein A-I*

Orosomucoid (α_1-acid glycoprotein) is one of the most abundant plasma proteins, accounting for about 1% of all plasma proteins and is expressed in hepatocytes and secreted into the plasma under stressful conditions such as tissue injury, infection, and inflammation [69]. It is known to be involved in three biological functions: immunomodulatory function, barrier function, and carrier function. Therefore, it came as a surprise that this versatile species was not included in the list of proteins returned following MS analysis. It was decided to confirm its absence by WB analysis. The WB of the 200,000g CHAPS pellet is displayed in Figure 3.32.

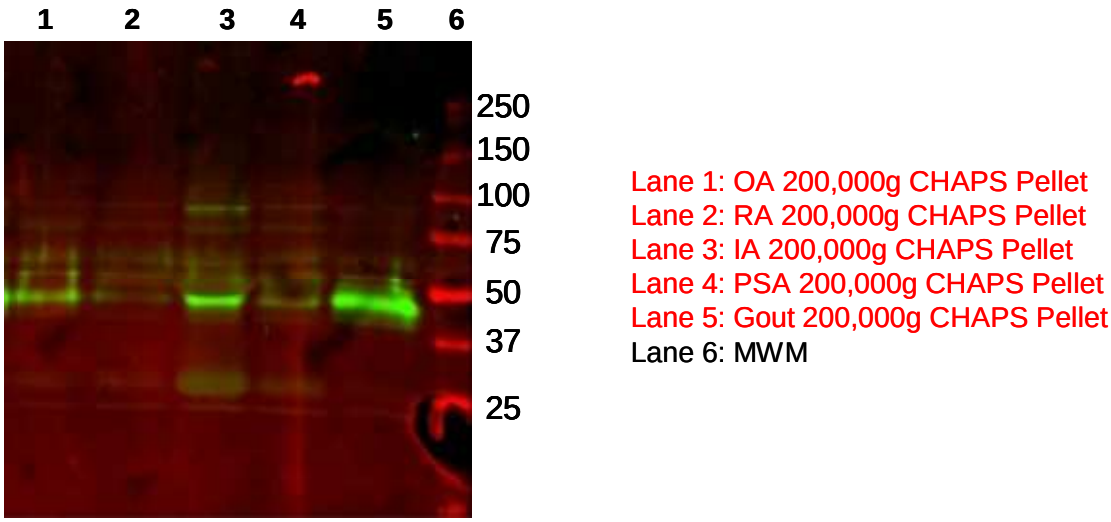

Figure 3.32: *Incubation of 200,000g CHAPS pellet fractions with anti-orosomucoid and detection by WB*

In Figure 3.32 it shown that with the exception of gout (Lane 5) and IA (Lane 3), there is practically no orosomucoid present at 44kDa, the molecular weight of this protein [70]. It is completely absent in the RA sample and a low amount is present in the OA sample. This explains why this species was not detected by MS. The peptides for this protein are most likely masked by the most abundant species which are present e.g. complement factors, α-2-macroglobulin, fibronectin etc.

So far, (with the exception of IgM), confirmatory studies were carried out on monomeric proteins. Two further analyses were carried out to include polymeric moieties. These were the high abundant protein α-2-macroglobulin (63 peptide hits and 50% coverage) and the low abundant IgD (2 peptide hits and 6.8% coverage).

α-2-macroglobulin (α-2-M) is a 720kDa homotetrameric glycoprotein (each monomer ~ 180kDa) that can cleave into a dimer of dimers under very mild denaturating conditions [71]. WB analysis under both reducing and non-reducing conditions was performed. This is displayed in Figure 3.33.

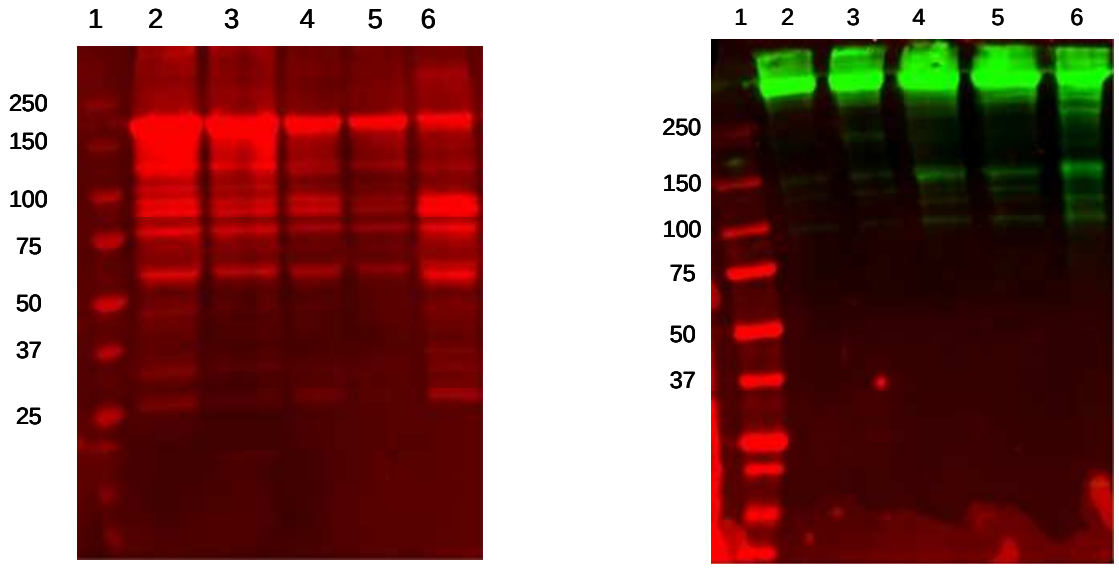

Lane 1: MWM
Lane 2: OA 200,000g CHAPS Pellet
Lane 3: RA 200,000g CHAPS Pellet
Lane 4: IA 200,000g CHAPS Pellet
Lane 5: PSA 20000g CHAPS Pellet
Lane 6: Gout 200,000g CHAPS Pellet

Figure 3.33: *Incubation of 200,000g CHAPS pellet fractions with α-2-macroglobulin under non-reducing conditions (left) and reducing conditions (right)*

Under reducing conditions (Figure 3.33, left), fragmentation took place due to the reduction of its 13 disulphide bridges. There was no such fragmentation under non-reducing conditions (Figure 3.33, right). Here there was a single band at a molecular weight > 250kDa and may be the dimer structure (~ 360kDa). The fragmentation may be explained by proteases activity whereby the α-2-M monomer molecules were cleaved along their amino acid backbones. The entire structure remained intact due to the linkage of the disulphide bridges which held the cleaved fragments together. However, under

reducing conditions these disulphide bridges were broken and the entire molecular edifice collapsed and fragmented at the points along the chain where cleavage occurred.

From appendix 1 (i.e. raw MS data), it can be seen that IgD was identified with SCX-RP-HPLC only, with two peptide matches and a protein coverage of 6.8%. Therefore, to establish the presence of this antibody, analysis by SDS-PAGE under both non-reducing and reducing conditions was performed followed by WB. The WB images are shown in Figure 3.34.

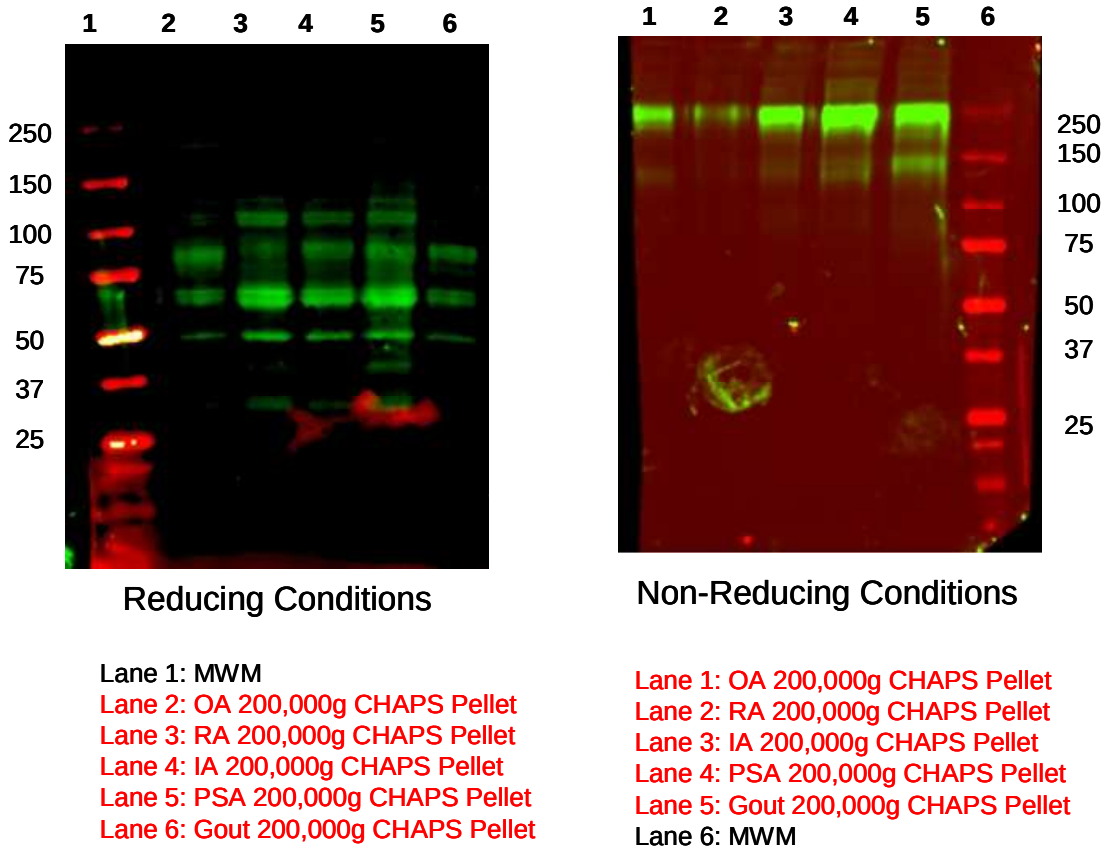

Figure 3.34: *Incubation of 200,000g CHAPS pellet with anti-IgD under non-reducing condition (left) and under reducing conditions (right)*

Under reducing conditions (Figure 3.34, left), it is the case that IgD is present in the 200,000g CHAPS pellet. Repeating the experiment under non-reducing conditions

(Figure 3.34, right) confirmed that the whole IgD protein is present in all five pathologies. As immunoglobulins were removed using Protein A chromatography prior to differential centrifugation, the likely source of IgD is either direct binding to the vesicle membrane or/and engulfed within the vesicle. There is an interesting point to note here. IgD has a molecular weight of 185kDa. However, in this analysis it was noted that the molecular weight of the entire molecule is ~250kDa. What could explain this discrepancy? Vladutiu *et al*. [68] studied the properties, measurement and the clinical relevance of IgD and advanced that there are two forms of IgD – membrane-bound and secreted. They explain that both forms are antigenetically similar; they differ in their proteolysis by plasmin. Moreover, the δ chains of each type possess different molecular weights, with the membrane-bound species having a higher weight than the secreted form. Therefore, it is possible that the species if IgD present in MV, is membrane bound.

All these protein-confirmation studies are important for definitively establishing the presence/absence of proteins listed/not listed on algorithm-generated MS data. Of course it is neither possible nor practical to complete an exhaustive confirmation study. However, for proteins identified as potentially interesting, it would be wise to establish their status employing an orthogonal method e.g. by analysis with antibodies.

3.2.5 Determination if proteases are associated with SF MVs employing zymography

Appendix E displays the Panther classification "Protein Class". Included in this list is the sub-heading "Proteases". A zymography experiment was carried out in order to confirm if there are proteases associated with MVs. Other groups have already characterized the protease activity in whole SF [72-75] [76, 77], but to my knowledge no study has been performed to establish if MVs may harbour proteases. Figure 3.35 shows the proteinase activity of various fractions across four patient pathologies.

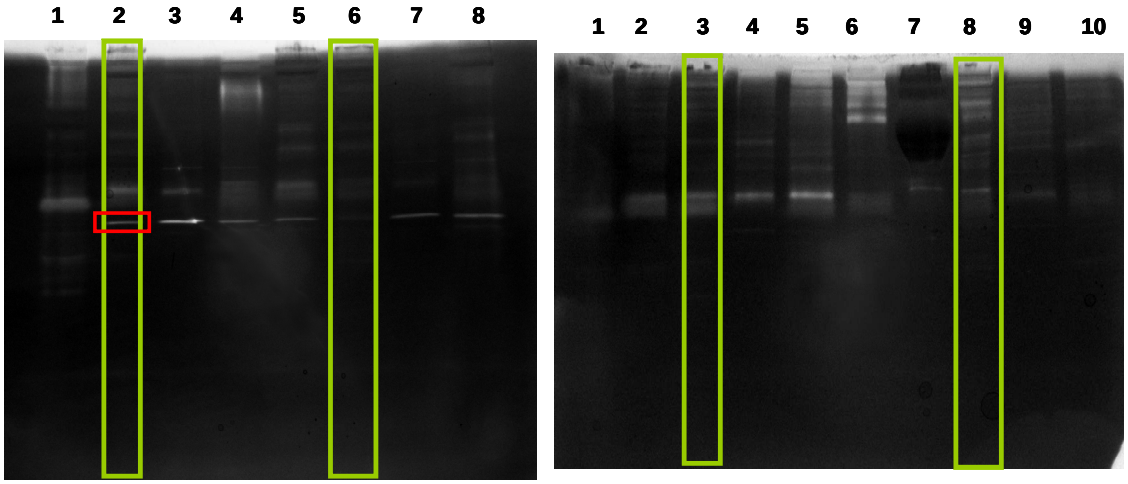

Figure 3.35: *Proteases activity of various differentially centrifuged fractions across four patient pathologies. The substrate was gelatin. Light bands indicate protease activity. The lanes highlighted in a yellow box are the targeted 200,000g CHAPS pellet for each pathology.*

Protease activity is spread across all fractions. In the OA sample (Red) there are differences between the 18,000g and 200,000g CHAPS pellets with the 18,000g pellet (Lane 1) having a wider molecular weight range of proteases. In the RA sample (blue)

there is a striking similarity between the 200,000g Crude and 200,000g CHAPS pellets (Lanes 5 and 6) – the difference being one of intensity - with the CHAPS pellet having a lower overall intensity. This may indicate that these particular proteases are mainly membrane associated, which on treatment with CHAPS, move to the SN. There is also further enrichment of proteases in the CHAPS SN relative to the crude SN (lanes 7 and 8). In the IA sample (green), there is a clear enrichment of protease activity in the 200,000g CHAPS pellet (lane 3) and the 200,000g CHAPS SN (Lane 5) relative to the crude fractions (Lanes 2 and 4 respectively). Finally in the PSA patient (purple), there is clear enrichment of proteases in the 200,000g CHAPS pellet (Lane 8) relative to all the other fractions. This could be interpreted as an indication that for this sample the proteases are engulfed with the vesicle or else so strongly bound to the vesicle membrane that CHAPS treatment does not remove them.

Of interest though is a comparison between the 200,000g CHAPS pellets. These are highlighted in yellow boxes. The RA sample exhibits the least protease activity, possibly due to amount of protein loaded. High molecular weight proteases are most strongly expressed in the PSA sample. Close inspection shows that the RA and IA samples have similar band patterns, though they differ in intensity. The OA sample has a band (highlighted in a red box) that is either absent from or more intensely expressed relative to, the other three pathologies.

3.2.6 Determination of hyaluronidase (HAase) activity employing zymography with a hyaluronic acid (HA) substrate

As mentioned in the literature review for this project (Chapter 1), HA is the component of synovial fluid that imparts viscosity and gives the joint fluid an “egg-like” appearance and consistency. It is known that the size of the HA molecule decreases while its actual abundance increases with age and with the onset of arthritic diseases. This decrease in size is attributed to degradation and is thought to involve the action of hyaluronidases or free radicals. Girish *et al.* [78] explain that HAase-mediated degradation of HA increases the permeability of connective tissues and decreases the viscosity of body fluids and is

also involved in bacterial pathogenesis, the spread of toxins and venoms, acrosomal reaction/ovum fertilization, and cancer progression. Tranchepain *et al*. [79] demonstrated that (HA) has different biological functions according to its molar mass with short HA fragments being involved in the inflammation processes whereas native, full-length HA is not.

In order to establish if there is endogenous HAase activity in SF, a zymography experiment was carried out employing HA as a substrate. As bovine HAase was used in the sample preparation in order to maximize the yield of MVs, it is important to establish that this does not produce "false-positive" bands and that any bands that may be present are due to HAase endogenous to SF. Therefore, 1mg/mL bovine HAase was used as a control in this study. Figure 3.36 is a display of the images acquired following the experiment.

The lane enclosed within the blue box is bovine HAase control. It can be seen that there is no HAase activity in this lane. Therefore, the original sample treatment with HAase does not interfere with the analysis here. The reason for this is a matter of pH. Originally, newly acquired SF samples were treated with bovine HAase at physiological pH i.e. ~ pH 7. However, in this experiment the gels were incubated at pH 3.5 as per the protocol by Miura *et al*.[54].

The lanes enclosed by a yellow box are the targeted 200,000g CHAPS pellet that contains exosomes and other MVs. Examination of these reveals that there is no HAase activity (or very little in the case of the PSA patient sample). This suggests that there are no HA proteases associated with MVs following CHAPS treatment.

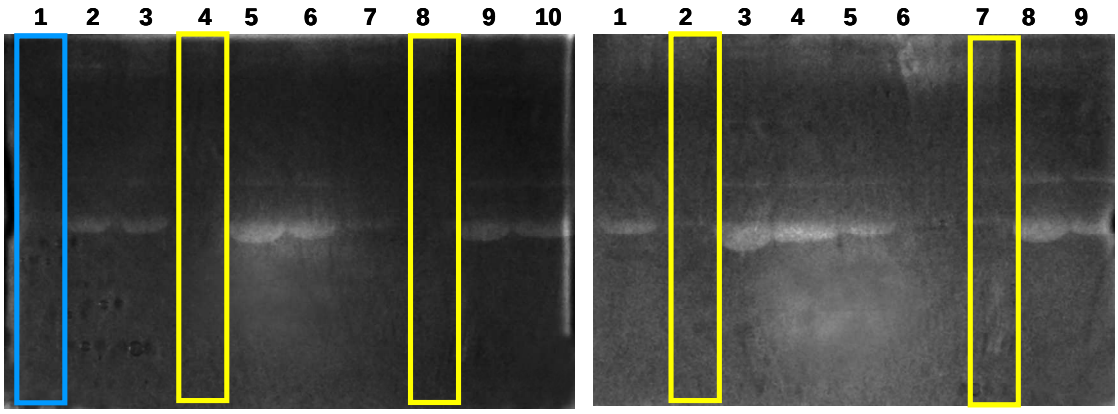

Lane 1: 1mg/mL Bovine Testes Hyaluronadase (Control)
Lane 2: OA 18,000g Crude Pellet
Lane 3: OA 200,000g Crude Pellet
Lane 4: OA 200,000g CHAPS Pellet
Lane 5: OA 200,000g Crude SN
Lane 6: OA 200.000g CHAPS SN
Lane 7: RA 200,000g Crude Pellet
Lane 8: RA 200,000g CHAPS Pellet
Lane 9: RA 200,000g Crude SN
Lane 10: RA 200,000CHAPS Pellet

Lane 1: IA 200,000g Crude Pellet
Lane 2: IA 200,000g CHAPS Pellet
Lane 3: IA 200,000g Crude SN
Lane 4: IA 200,000g CHAPS SN
Lane 5: PSA 18,000g Crude Pellet
Lane 6: PSA 200,000g Crude Pellet
Lane 7: PSA 200,000g CHAPS Pellet
Lane 8: PSA 200,000g Crude SN
Lane 9: PSA 200,000g CHAPS SN

Figure 3.36: *HAase activity of various differentially centrifuged fractions across four patient pathologies. The substrate was hyaluronic acid. Light bands indicate protease activity. The lanes highlighted in a yellow box are the targeted 200,000g CHAPS pellet. The lane highlighted in blue is the bovine HAase control. Boxes are included to aid discussion.*

In the OA and IA samples there is HAase activity in the crude 200,000g pellet, which is completely removed post CHAPS-treatment. The bands showing this activity reappear in the CHAPS 200,000g SN (Lane 6 for the OA sample and Lane 4 for the IA sample). Therefore any HA proteases that are present are likely to be associated with the MV membrane.

When the SN fractions are examined, it may be seen that there is definite HAase activity. The evidence for this activity is for the most part in the form of clear bands at two separate molecular weights in the middle of the gels. Also, close examination of the imaged also show hints of activity at high molecular weights at the top of the gels.

3.4 Discussion

Throughout this report the generic term microvesicle (MV) was intentionally used in order to emphasise that a heterogeneous assortment of microparticles is more likely to be present, rather than a homogeneous population of exosomes or any other vesicle class. Table 3.2 suggested that no physical characteristic e.g. centrifugation speed, size and shape, can be employed in order to secure a homogeneous population of any one vesicle type. A vesicle "signature species" was deemed a better aid to classification. Exosomes were never-the-less present in SF as shown by incubation with established exosomal markers e.g. CD63 and Tsg101. MS analysis found another exosome-associated protein - heat shock protein 70 (HSP70) (see Tables 3.3, 3.4 and Figure 3.6). Table 3.2 also lists the main protein markers for each of the other vesicle types while Table 3.8 shows the top ten proteins found in exosomes.

	Protein	Found in MV in this study	Method of detection
1	Heat shock protein 8	No	
2	CD63 antigen	Yes	WB
3	Actin, β	Yes	WB
4	Glyceraldehyde-3-phosphate dehydrogenase	No	
5	Enolase 1, α	Yes	MS
6	Heat shock protein 90, α (cytosolic), class A member 1	No	
7	CD9 antigen	No	
8	CD81 antigen	No	
9	Tyrosine 3-monooxygenase/tryptophan 5-monooxygenase activation protein, zeta polypeptide	No	
10	Pyruvate kinase, muscle	Yes	MS

Table 3.8: *List of the top ten proteins found in most exosomes. Data adapted from Mathivanan et al.* [61]*. Included is an indication if any of these species were found in the 200,000g CHAPS pellet in this project. Also included is the method of detection that was used to characterise any proteins that were found to be associated with MVs.*

However, some element of uncertainty still remained. For example, in Table 3.2 the biological signature of apoptotic bodies is the presence of histones, which Thery *et al.*[80] suggested are not present in exosomes. They believe that during the exosome purification step, a slight contamination with apoptotic blebs at the top of the sucrose cushion

occurred. Histone molecules H2B and H4 were found to be present in MVs in the current study.

A number of members from the apolipoprotein family were identified following MS analysis e.g. Apolipoprotein A-I, Apolipoprotein A-IV, Apolipoprotein B-100, Apolipoprotein D, Apolipoprotein E and clusterin [Apolipoprotein J or SP40SP40 (protects cells against cytolysis by complement)]. Apolipoprotein A-I (apo A-I) is the main protein associated with high density lipoproteins (HDL), in addition to apo C, apo E, apo D and apo J [81]. HDLs have a density 1.063-1.210g/mL[16] while that of exosomes lies in the range 1.13-1.19g/mL. Therefore, the possibility HDLs were present in both the 200,000g pellet and the corresponding SN was realised. This was confirmed by western blot (Figure 3.31), where similar band intensities in the 200,000g CHAPS pellet of each pathology were observed. HDLs therefore, represent another possible "contaminant" in any exosome isolation protocol and subsequent characterisation. The role of apolipoproteins and HDLs in the immune system will be discussed later.

In a recent study aimed at isolating exosomes and assessing the yield purity, Bobrie *et al.*[82], employing electron microscopy and SDS-PAGE/WB, concluded *"sucrose gradients are not resolutive enough to separate vesicles with small differences in densities, which use different intracellular machineries for their secretion"*. Therefore, definitive MV classification remains uncertain, and a suggestion to exercise caution when laying claim to the isolation of a homogeneous population of any particular MV type, is proposed. Any isolation protocol based on physical characteristics may result in varying s of MV heterogeneity.

One of the aims of this project was to customise a protocol for isolating MVs from whole SF. During method development, it was discovered that sample treatment with hyaluronidase (HAase) was necessary in order to increase the MV yield. For example, it was appreciated that in purifying MVs from urine, the Tamm-Horsfall protein adversely affected the yield of MV recovery, due to polymerisation and subsequent vesicle entrapment [47]. Therefore, sample treatment with dithiothreitol (DTT) was employed as a critical step in urine vesicle preparation. In the case of SF, it was hypothesised that

hyaluronic acid (HA) would influence the MV yield. This hypothesis was realised on finding a paper in the literature stating that HA possesses a CD44 receptor [83]. This is particularly relevant in light of the fact that all exosomes contain CD44 [66] on the surface membrane as confirmed by the exosome-specific ExoCarta database (http://exocarta.org/gene_summary?gene_id=960). This project demonstrated HA does trap MV (Figures 3.11 & 3.14) and so adversely impacts on the yield on MV obtained, which in turn, may affect the proteomic characterisation of such vesicles due to reduced sensitivity. It was therefore concluded, that treatment of SF samples with HAase prior to differential centrifugation, was desirable in order to maximise vesicle yield.

Another important step towards optimal MV protein enrichment, was removal of loosely associated/soluble proteins or weak protein-protein interactions with 1% (w/v) CHAPS followed by a further 200,000g ultracentrifugation step. It was not established if these species were "contaminants" or if they had a specific interaction with the vesicle. Sodium deoxycholate and SDS are well known detergents. However, SDS is incompatible with down-stream MS analysis. Sodium deoxycholate, on the other hand can be removed by acid precipitation prior to MS analysis. However, this detergent has been used previously to successfully solubilise membrane-bound proteins prior to trypsin digestion [56, 57, 84]. Therefore, this would most likely solubilise the membrane surrounding MVs. CHAPS, by contrast, was known to be able to break protein-protein interactions [60, 85] without being able to disrupt strong protein-protein interactions, such as those found in tetraspanin-membrane interactions [86]. Musante *et al*. [48] employed 1% (w/v) CHAPS to remove loosely bound proteins from MVs isolated from urine. That soluble/loosely bound proteins are removed from MVs, was demonstrated in Figure 3.13, where there is a redistribution of protein from the original 200,000g pellet to the SN following CHAPS treatment. Here for example, the bulk of albumin moved from the pellet to the SN, though both MS and WB analysis indicated that albumin was still vesicle-associated despite CHAPS treatment. This was believed to indicate that albumin was a constituent of the inner vesicle cargo, or else strongly associated with the vesicle membrane. The integrity of the MV was preserved following CHAPS treatment as shown by the presence of exosomal markers Tsg101 (Figures 3.17 and 3.22) and CD63 (Figure 3.18) in the

200,000g CHAPS pellet fraction. If the vesicle was compromised by CHAPS, then all the Tsg101 and CD63 would have been moved to the corresponding SN. However, the overarching merit of CHAPS treatment was an enrichment of the lower abundant vesicle-associated proteome that was previously masked by high-abundant soluble proteins.

To offset any interference of immuncomplexes which can potentially co-precipitate with the targeted 200,000g pellet, immunoglobulin removal took place employing Protein A affinity chromatography (Figure 3.20). Further protein enhancement was achieved through the use of Protein A chromatography, followed by CHAPS treatment (Figure 3.21). This step not only enhanced the band intensities of some proteins, but led to the discovery of bands previously masked by high abundant proteins.

The customisation of a MV-harvesting protocol for SF resulted in the workflow displayed in Figure 3.23.

Mass spectrometry was then employed in order to identify proteins associated with the isolated 200,000g CHAPS pellet.

In this project, MVs isolated from a four-patient-pooled sample was sent for analysis by MS. A multi-dimensional approach employing three methods was applied i.e. (i) 5 hour gradient elution RP-HPLC, (ii) SCX/RP-HPLC and (iii) SDS-PAGE followed by in-gel digestion of individual bands. The aim here was to identify as many proteins as possible. The first two methods involved trypsinisation in solution followed by two different modes of chromatography, while the third approach consisted of a gel separation followed by digestion with trypsin. A comparison of the three methods in terms of the number of individual proteins returned was made and displayed in Figure 3.26. There, it was shown that there are proteins unique to each particular mode of analysis, proteins common to any two methods and finally a subset common to all three modes. For the 5-hour gradient elution RP-HPLC, 4% of the proteins are unique to that method, while for SCX/RP-HPLC and the in-gel techniques the percentage of unique proteins are 23% and 24% respectively. That there are proteins unique to each method is testament to the fact

that the method employed will influence the output in terms of proteins identified. Therefore, for a thorough, comprehensive shotgun proteomic study, it may be prudent to adopt an experimental design that utilises a suite of orthogonal techniques. A study of the literature makes it clear that there is no "one method catches all" approach in proteomics. An example of this is in the simultaneous analysis of soluble and membrane-bound/transmembrane proteins, with the former possessing a high degree of hydrophilic moieties while the latter are known to be characterised with hydrophobic domains. Of the proteins unique to the relatively simple 5-hour RP-HPLC, none of them (according to UniProt) are membrane-associated.

Gilmore *et al.* [87] reviewed the proteomic toolbox available to the researcher wishing to characterise membrane proteins. All methods discussed were based on the principle of coupling orthogonal techniques, two of which were SCX/RP-HPLC and in-gel digestion.

The bioinformatic tool Panther, was then used to classify the resulting list of proteins. It was noted with some surprise that 19% of proteins characterised by MS were not identified by Panther, while 40% of those that were identified, could not be classified by location. From Appendix A it can be seen that Panther also included the sub-family "Protein Complex" which was exclusively composed of members of the immunoglobulin family. This came a surprise result in light of the fact that the MV isolation protocol included an immunoglobulin-removal step i.e. Protein A chromatography. Further, the experiment was carried out under non-saturating conditions, where the binding capacity of the beads was not exceeded (see Materials and Methods 3.1.15). A sizable proportion of the total OA MV proteome in this project (Table 3.7) was composed of members of the immunoglobulin family i.e. IgA, IgD, IgG and IgM. The presence of IgM (Figure 3.19) and IgD (Figure 3.34) was also confirmed by WB. Therefore a discussion of these species and their possible role within the targeted 200,000g CHAPS pellet deserves attention.

In the introduction to this chapter a precaution urged by György *et al.* [14] was noted. This concerned the possible co-precipitation of immune complexes (ICs) with MV since both species share many of the same biophysical properties (size, light scattering and

sedimentation centrifuge speed). They expressed concern that any MV purification method will be compromised by the presence of ICs.

A recent post-György study carried out by Neilson *et al.*[88] into plasma microparticles in systemic lupus erythematosus (SLE) set out with the aim of *"evaluating the putative role of MPs in SLE as circulating antigenic targets and carriers of ICs"*. It is important to note that they used the term *"microparticles"* throughout, which they said are shed from cells constitutively or during activation or during apoptosis. Therefore, analogous with the current project, there is likely to be a heterogeneous host of vesicle types present. They found that cell-derived MVs carried increased cargos of IgG, IgM and also C1q and that IgG containing MVs were associated with auto-antibodies and compliment activation. They listed three possible consequences for this, namely; (i) autoantigen-presenting MVs may be highly autoimmunogenic, (ii) bound immunoglobulins invite the classical complement cascade to occur and (iii) MVs traffic ICs to other cells and deposit them there (they gave an example of trafficking ICs to endothelial cells in kidney glomeruli). The group also found that patients with active disease had the highest levels of IgG, IgM and C1q and concluded that the compliment system is activated by cell derived MVs carrying ICs in SLE. A possible role for MVs in off-setting compliment-associated damage to chondrocytes will be discussed later. Draeger *et al*. [89] found that on activation, an influx of extracellular Ca^{2+} by the cell is sensed and interpreted as a danger signal. They believed that the cell responds to this with the formation shedding vesicles or underwent blebbing. These processes serve to eject dangerous moieties that have become attached to the membrane.

However, it also needs to be acknowledged that MV (in light of Nielson's work) could be involved in trafficking ICs *to* the chondrocytes and off-loading their cargo there.

Pisetsky [90] offers an insightful commentary on the study carried out by Nielsen. This editorial point out that while Nielsen did not specify *how* auto-antibodies appear on vesicles, a correlation with the presence of nuclear proteins and the presence of antibodies was observed, suggesting a display of nuclear autoantigens by MVs arising during apoptosis. As noted above and in Table 3.2, the presence of histones is indicative

of apoptotic blebbing and Pisetsky notes *"These considerations put the bleb at centre stage during the generation of self antigens that drive autoimmunity"*. In addition to histone H2B and histone H4, two other nucleus-associated proteins were found in the 200,000g CHAPS pellet i.e. general transcription factor IIF and elongation factor 1α (Appendix C). By definition, for these nuclear species to be antigenic and form ICs, they must be accessible to the antibody. Therefore, these proteins may also be present on the surface of MVs and hence acquire a role as auto-antigens. However, Pisetsky pointed out that particles/vesicles originating from apoptotic cells have undergone membrane permeability changes and so their membranes are likely to be sufficiently porous to allow an in-flow of antibodies along with other proteins. Therefore immunoglobulins may be a constituent of the vesicle inner cargo.

In the discussion on immunoglobulins thus far, two models for the presence of these species on/in MVs were outlined i.e. (i) IC formation on the vesicle surface and (ii) an in-flux of antibodies into the vesicle through the membrane. A third possibility exists. The presence of IgGFc-binding protein in the 200,000g CHAPS pellet was confirmed by MS (Table 3.7). In this model, IgG binds directly to the receptor leaving the Fab region exposed to the ECM and bind to a target antigen.

In the results section it was shown that protein A chromatography is a necessary step for the removal of soluble and loosely associated immunoglobulins leading to a subsequent enrichment in the MV yield and an increase in the band intensities of less abundant proteins. Changes in band intensities were discussed at that point. However, this study culminated in a surprise finding. Following incubation with anti-Tsg101 (Figure 3.22), it was seen that exosomes were present in each of the bound fractions (Lanes 8, 9 &10). How can exosomes bind to protein A (an immunoglobulin, Fc-region binding protein)? A possible answer to this question is found in the above discussion. IgG or IgM possibly binds to an auto-antigen exposed on the exosome surface. In turn, the Fc region of the antibody becomes bound to the stationary protein A. This finding expands on the work of others which was already discussed here. Throughout this discussion it was highlighted that other research groups discovered auto-antigens to be associated with

MVs such as apoptotic blebs and ectosomes/shedding vesicles. The result here suggests that exosomes (products of the endocytic pathway) possibly present auto-antigens on their membrane surface and this is why total recovery of exosomes in the targeted unbound fraction was not achieved.

Finally, recent research by Ramirez-Alvarado *et al*. [91] into differences in immunoglobulin light chain species in urinary exosomes yielded a very interesting result. The group found that particular high molecular weight, SDS-resistant light-chain species were present on the surface of exosomes of light chain amyloidosis patients. They suggested that as only patients suffering from amyloidosis possessed this feature, this would warrant further investigation as a marker for this pathology. In light of this study, it is also conceivable that these immunoglobulin fragments are also present on the surface of SF exosomes. As with the above-mentioned research, the significance of this in terms of arthritic pathologies may be the subject of interesting future research.

A search of PubMed for papers relating to synovial fluid MVs reveals that there is no proteomic characterisation study performed on MVs isolated from whole SF. A number of SF proteomic studies appear in the literature. Four recent, representative proteomic studies relating to SF and OA were found. They are;

1. Analysis of SF exosomes for citrullinated proteins [18]
2. Differential profiling of whole SF from RA and OA patients [92]
3. Differential profiling of whole SF from healthy and OA patients [93]
4. Analysis of articular cartilage vesicles (ACVs) from normal and OA cartilage [94]

One interesting study into a specific sub-proteome of SF MVs was carried out by Skriner *et .al*. [18] in 2006. The subject of this research was to establish an association of citrullinated proteins with exosomes among RA, OA and reactive arthritis patients. No control SF was analysed. Citrullination is an enzyme-catalysed conversion of arginine residues to citrulline by peptidyl arginine deiminase. Previously, Van Venrooij at al. [95] argued that citrullination may be a modification that could create a novel epitope or uncover a previously "hidden" epitope in a protein. This modification could thus create

an auto-antigen and so induce a primary and specific immune response. Skriner *et al.* [18] extended this work to exosomal analysis of citrullinated proteins in RA, OA and reactive arthritis patients. They list a number of proteins and indicate those that are citrullinated. This list is shown in Table 3.9.

Protein	Citrullination
Fibronectin/IgG immune complex	No
$_2$-macroglobulin	No
Fibrinogen fragment D	Yes
Fibrinogen β-chain precurser	Yes
Fibrinogen β-chain	Yes
IgG1 γ-chain C region	No
Unidentified protein	Yes
Fibrin -chain N-terminal fragment	Yes
Spa (CD5 antigen-like protein)	Yes

Table 3.9: *A list of proteins generated by Skriner et al.[18] found in exosomes of OA, RA and reactive arthritis patients. The authors indicate those that were found to be citrullinated. Though each pathology possessed these species, only RA patients produced auto-antibodies.*

The authors found the same proteins present in all three pathologies (one protein was unidentified). However, auto-antibodies to these citrullinated proteins were present in the RA cohort only. With the exception of Spa, the other species were soluble proteins.

To the best of my knowledge, this current project is the only research carried out with the aim to characterise the proteome of SF MVs. Therefore, the characterisation of this sub-proteome in this project is novel. Other research groups identified the proteome of whole SF and some of these will now be discussed and compared with proteins found to be associated with MV. The purpose of this comparison is to compare a whole biofluid proteome with that of a sub-proteome of the same biofluid to ascertain if there are species present in the latter that were absent in the former, possibly due to masking by high abundant soluble proteins.

Recently, Mateos *et al.* [92] carried out a differential proteomic study of whole SF from OA and RA patients. Prior to analysis, the top 20 must abundant proteins were removed by immuno-depletion in order to enrich the lower-abundant, potentially more interesting

proteins and a total of 136 proteins were identified. This was followed by a relative quantification between OA and RA by spectral counting analysis, in order to compile a list of pathology-specific proteins. The authors stress that "*extreme ratios do not necessarily indicate that a given protein is absent in one of the conditions, only that the concentration in SF of such proteins is below the detection limit of the followed technique*". A summary of these findings is shown in Table 3.10. Also included is a yes/no indication of whether a specific protein was found to be vesicle-associated in the current project.

The authors listed 18 proteins that were relatively more abundant in RA. Of these, 12 were not found in the OA pooled sample, while the remaining six were found in both pathologies, with a higher expression in RA. However, five of the 12 proteins not present in OA SF were found in the proteome of OA MVs. They included: complement C4 gamma chain, pregnancy zone protein, transforming growth factor-beta-induced protein ig-h3, histone 4 and Protein S100-A8. Four of the seven proteins not found in the OA MV proteome - azurocidin, neutrophil gelatinase-associated lipocalin, neutrophil defensin 2 and leucocyte elastase inhibitor – are according to the authors, of neutrophil origin. They stated that neutrophil enzymatic activities were closely related to the persistence of inflammation, cartilage damage and progression of joint disease. Though neutrophil defensin 2 was not found to be associated with MVs, neutrophil defensin 1 and neutrophil defensin 3 were. The UniProtKB database cited defensin 2 as a cleaved species from defensin 1. Therefore a sub-population of MV found in the current study is likely to be of neuclophilic origin, confirming an association of OA with inflammation.

Protein Name	Unique to RA [a]	Present in OA microvesicles [b]
Azurocidin	Yes	No
Complement C4 gamma chain	Yes	Yes
Apolipoprotein B-48	Yes	No
27 kDa interstitial collagenase	Yes	No
Leucocyte elastase inhibitor	Yes	No
Pregnancy zone protein	Yes	Yes
Transforming growth factor-beta-induced protein ig-h3	Yes	Yes
Histone H4	Yes	Yes
Neutrophil gelatinase-associated lipocalin	Yes	No
Neutrophil defensin 2	Yes	No
Protein S100-A8	Yes	Yes
Plastin 2	Yes	No
Complement component C8 gamma chain	No	Yes
Proteoglycan 4 C-terminal part	No	Yes
Apolipoprotein E	No	Yes
Stromelysin-1	No	Yes
Ficolin-3	No	Yes
Complement component C8 gamma chain	No	Yes

Protein Name	Unique to OA [c]	Present in OA microvesicles [b]
Aggrecan core protein 2	Yes	Yes
Cartilage oligomeric matrix protein (COMP)	Yes	Yes
Complement factor D	Yes	No
Tetranectin	Yes	Yes
Inter-alpha-trypsin inhibitor heavy chain H1	No	Yes
Gelsolin	No	Yes
Plasma protease C1 inhibitor	No	Yes
35kDa inter-alpha-trypsin inhibitor heavy chain H4	No	Yes
Alpha-2-antiplasmin	No	Yes
Cartilage acidic protein1	No	Yes
Fibronectin	No	Yes
Pigment epithelium-derived factor	No	Yes
Low molecular weight growth-promoting factor	No	No
Histidine-rich glycoprotein	No	Yes
Thrombin heavy chain	No	Yes
Cjitinase-3-like protein 1	No	Yes
Alpha-1B-glycoprotein	No	No

Table 3.10: *A list of differentially expressed proteins between pooled OA and RA samples compiled by Mateos et al.*[92] *The top table lists differentially expressed proteins in RA synovial fluid, while the bottom table displays proteins relatively enriched in the OA pooled sample. Also shown is an indication of whether these species were found in SF micro-vesicles*
a *adapted from Table 1* [92] ***b*** *proteome of MV in this study* ***c*** *taken from Table 2* [92]

Examination of the four proteins cited by Mateos *et al*. [92] as being unique to OA (lower half of Table 3.10), shows that three of them are also found in the MV sub-proteome i.e. aggrecan core protein 2, COMP (to be discussed below), and tetranectin. Complement factor D was not found to be vesicle-associated. Further, low molecular weight growth-promoting factor and alpha-1B-glycoprotein were absent in OA MV. Finally, as was the case in the current project, the authors sought verification of their proteomic data by an orthogonal study employing incubation with antibodies and analysis by WB. They confirmed that some proteins that were previously thought to be RA-exclusive, were actually present in OA samples e.g. 27kDa interstitial collagenase (MMP-1) and transforming growth factor-beta-induced protein ig-h3. This highlights a limitation to any shotgun strategy, which is the possibility of masking low abundant peptides by those from high abundant proteins or proteins that undergo extensive fragmentation. As this current research study represents a specific sub-proteome, it follows that proteins previously deemed absent in whole SF, may actually be present and associated with MVs. Therefore, experimental design and specific proteome targeting will have a bearing on the final outcome in any proteomic study.

The above study by Mateos was a differential proteomic study whose aim was to identify proteins that differ between OA and RA in whole synovial fluid. Gobezie *at al*.[93] also performed a differential study in whole SF, only this study examined the proteome differences between SF from 20 healthy subjects and 39 patients with OA. They reported 135 unique proteins, from which 15 were found to be unregulated in the OA patient cohort, while three down-regulated relative to the control group. Table 3.11 summarises this group's findings. Also included is confirmation whether these proteins were found to be associated with MV in this project.

Protein Name	Upregulated/Down-regulated relative to control group	Present in OA MV
Cystatin A (stefin A)	Down	No
Aggrecan 1 (Chondroitin sulfate proteoglycan core protein 1)	Down	Yes
Dermcidin	Down	Yes
Albumin	Up	Yes
α_1-Microglobulin/bikunin precurser	Up	No
Fibrinogen, α chain	Up	Yes
Fibrinogen, γ chain	Up	Yes
α_2-Macroglobulin	Up	Yes
Apolipoprotein E	Up	Yes
Apolipoprotein H (β_2-glycoprotein I)	Up	Yes
Complement component 3	Up	Yes
Ceruloplasmin	Up	Yes
Haptoglobin	Up	Yes
Orosomucoid 1 (Alpha-1-acid glycoprotein 1)	Up	Yes
Vitamin D binding protein	Up	Yes
Complement component 4B	Up	Yes
Apolipoprotein A-1	Up	Yes
Retinol-binding protein 4	Up	No

Table 3.11: *Eighteen proteins which Gobeize et al.[93] found to be significantly differentially expressed across control and OA groups. Also shown is an indication of whether these same species were found to be present in OA synovial fluid MVs.*

All of these proteins, with the exception of cystatin A, α1-microglobulin and retinol-binding protein 4 were found within the MV proteome in this project. Cystatin A (a cysteine protease inhibitor) was found to be down-regulated in OA SF relative to the control group, suggesting that cysteine proteases may play a significant role in OA pathogenesis. The authors expressed surprise in finding that although serine protease inhibitors were present in both OA and healthy SF, there was not a significant difference in these species between control and OA samples. Serine protease inhibitors were also found to be associated with OA synovial fluid MVs in this project. Table 3.12 compares the serine protease inhibitors found by Gobezie's group with those found to be associated with OA MVs (as classified by Panther) in this project. They classified eight serine protease inhibitors in their study of whole synovial fluid. The authors speculate that the abundance and large number of these inhibitors is consistent with their importance in joint function. They cite examples of processes within the joint regulated by these

species, and include, regulation of MMPs, aggrecanase, plasmin, tissue mitogens (initiate cell division), angiogenesis (growth of new blood vessels) activity, inhibition of inflammatory leukocyte proteases e.g. neutrophil elastase and finally, regulation of fibroblast mitogen binding to extracellular matrix. Of the eight protease inhibitors found, five were found to be associated with MVs in this study.

Serine Protease Inhibitors	
Microvesicle-associated	**Whole Synovial Fluid**
Alpha-1-antichymotrypsin	Alpha-1-antichymotrypsin
Alpha-1-antitrypsin	Alpha-1-antitrypsin
Pigment epithelium-derived factor	Pigment epithelium-derived factor
Plasma protease C1 inhibitor	Plasma protease C1 inhibitor
Pregnancy zone protein	Pregnancy zone protein
Alpha-2-antiplasmin	Kinninogen
Alpha-2-macroglobulin	C1q (with C1s & C1r)
Angiotensin-3	AT III
Inter-alpha-trypsin inhibitor heavy chain H1	
Inter-alpha-trypsin inhibitor heavy chain H2	
Kallistatin	
35 kDa inter-alpha-trypsin inhibitor heavy chain H4	
Plasma serine protease inhibitor	
Plasmin light chain B	

Table 3.12: *Comparison of serine protease inhibitors found to be associated with MV (left column) and those found in whole SF (right column) by Gobeize et al.* [93]. *Common species are displayed in red, while differences are in black. Classification of proteins in microvesicles was achieved by the Panther Classification System.*

It was urged by the authors that continued focus on the contribution of both classes of protease inhibitors to OA pathogenesis should continue. The study by Mateos (discussed above) made no mention of cystatin A. Bearing in mind that they analysed RA and OA samples i.e. pathologic samples, a tentative conclusion may be drawn, that decreasing levels of cystatin A could be an interesting OA biomarker. This would merit further study.

As stated above, there is a relative paucity of studies on MVs in synovial fluid in the literature by comparison with plasma or urine. One interesting study however, was that carried out by Rosenthal *et al.* [94]. This research consisted of a proteomic analysis of

articular cartilage vesicles (ACV) isolated from normal and OA cartilage. These vesicles fall into the same size category as exosomes but are said by the authors to possess a different cargo composition and function. The proteome was characterised and listed. A comparison was made between both proteomes i.e. ACVs (151 unique proteins) and synovial fluid MVs (263 unique proteins). This comparative analysis is shown in Figure 3.37

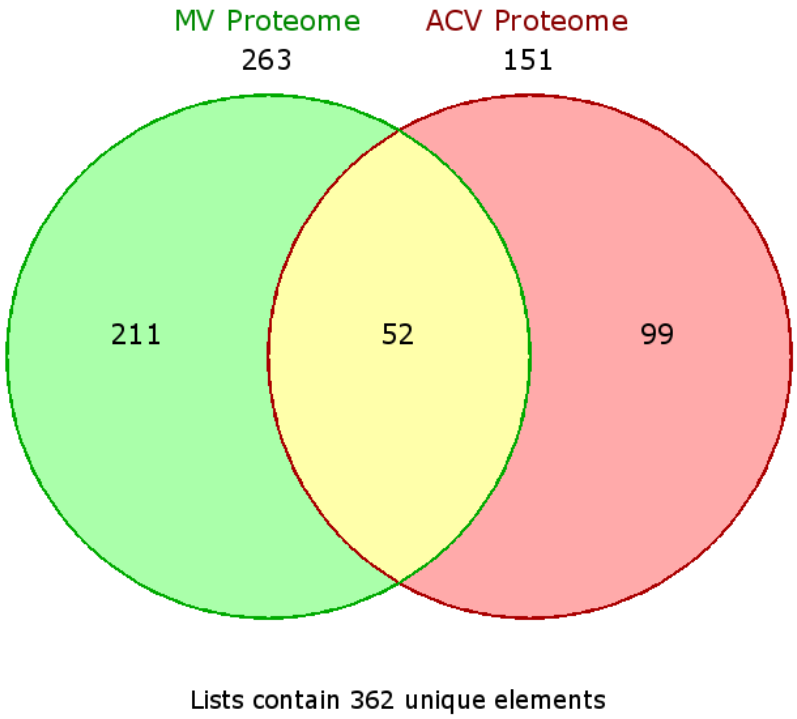

Figure 3.37: *A comparative analysis between the proteomic profiles of articular cartilage vesicles (red) generated by Rosenthal et al.* [94] *and synovial fluid MV generated in the present study (green). The number of proteins common to both sets of data is in yellow.*

Proteins common to both data sets are displayed in Table 3.13. In terms of proteins unique to each particular proteome, 80% (211 proteins) of MV proteins and 66% (99 proteins) of ACV proteins are unique. The total number of proteins associated with SF MV was 1.7 times that associated with ACVs. This was likely due to the fact that MVs originate from multiple sources i.e. cartilage, lymphocytes, synovium etc., while those associated with ACVs came from a specific tissue i.e. cartilage. It must be borne in mind throughout the discussion that follows, that the ACVs may be a *subset* of SF MVs.

Proteins common to the proteome of ACVs and OA synovial fluid MVs	
P68032	Actin, alpha cardiac muscle 1
P68133	Actin, alpha skeletal muscle
P62736	Actin, aortic smooth muscle
P60709	Actin, cytoplasmic 1
P63261	Actin, cytoplasmic 2
P63267	Actin, gamma-enteric smooth muscle
P16112	Aggrecan core protein
P01009	Alpha-1-antitrypsin
P01023	Alpha-2-macroglobulin
P06733	Alpha-enolase
P07355	Annexin A2
P02647	Apolipoprotein A-I
P06727	Apolipoprotein A-IV
P05090	Apolipoprotein D
P02649	Apolipoprotein E
P13929	Beta-enolase
P49747	Cartilage oligomeric matrix protein
P10909	Clusterin
P00488	Coagulation factor XIII A chain
P12109	Collagen alpha-1(VI) chain
P12110	Collagen alpha-2(VI) chain
P12111	Collagen alpha-3(VI) chain
P01031	Complement C5
P13671	Complement component C6
P07357	Complement component C8 alpha chain
P68104	Elongation factor 1-alpha 1
P02671	Fibrinogen alpha chain
P02751	Fibronectin
P06396	Gelsolin
O60814	Histone H2B type 1-K
P62805	Histone H4
P01876	Ig alpha-1 chain C region
P01877	Ig alpha-2 chain C region
P01857	Ig gamma-1 chain C region
P01859	Ig gamma-2 chain C region
P01860	Ig gamma-3 chain C region
P01861	Ig gamma-4 chain C region
P01834	Ig kappa chain C region
P01871	Ig mu chain C region
P04220	Ig mu heavy chain disease protein
P04264	Keratin, type II cytoskeletal 1
P00338	L-lactate dehydrogenase A chain
P61626	Lysozyme C
P06702	Protein S100-A9
Q92954	Proteoglycan 4 (Lubricin)
P14618	Pyruvate kinase isozymes M1/M2
Q92743	Serine protease HTRA1
P02743	Serum amyloid P-component
P24821	Tenascin
P35443	Thrombospondin-4
Q15582	Transforming growth factor-beta-induced protein ig-h3
P04004	Vitronectin

Table 3.13: *List of proteins common the proteome of ACVs and OA synovial fluid MVs*

It was expected that some commonality was shared by the two proteomes, which include, cytoskelatal (e.g. actin, keratin, elongation factor 1-alpha 1), extracellular matrix (collagen, lubricin, COMP, aggrecan) and cell adhesion (clusterin) proteins. The author noted that while inflammatory components probably originate from SF, chondrocytes are capable of synthesising components of the classical complement pathway e.g. C1, C2 and C4 and concluded that *"the presence of complements and immunoglobulins in OA AVCs warrants further consideration"*. It may be hypothesised that the other complement components i.e. C5, C6 and C8 and all the other inflammatory-related species (Table 3.13) come from SF to the cartilage either as soluble proteins or possibly packaged in MVs. Nauta *et al.* [96] described the role of MVs in inflammation through activation of the complement cascade. The recognition unit of the classical complement pathway, C1q, binds to MVs released from apoptotic cells. Gasser *et al.* [97] also found C1q on the surface of ectosomes/shedding vesicles. In turn, C1q activates the complement pathway by binding to C3 and C4 on the MV surface. Distler *et al.*[40] interpreted this as a trigger to inflammation while Gasser *et al.*[97] hypothesised that the binding of C1q to the cell surface triggers the release of ectosomes, which they suggested is important for the prevention of the compliment cascade on the cell surface, thus inhibiting the development of autoimmunity. Further, the likely source of these species was the local synovial tissue cells and the complement cascade was implicated in the innate immunologic defence of the avascular cartilage and also had a role in the patho-physiology of *both* OA and RA [93]. A host of complement components were found to be associated with MVs in OA synovial fluid in the current project. Further discussion on complement components will take place in relation to COMP (below).

Rosenthal *et al.* [94] then listed all those proteins that were found (i) in OA ACVs only, (ii) in normal ACVs only, (iii) up-regulated in OA and finally, (iv) down-regulated in OA. This list is produced in Table 3.14, and as before, a column was added indicating if each protein was found in synovial fluid OA MVs.

	Differentially Expressed ACV Proteome	Present in OA MV
	OA Only	
P02671	Fibrinogen alpha chain	Yes
P02649	Apolipoprotein E	Yes
P01857	Ig gamma-1 chain C region	Yes
P01031	Complement C5	Yes
P60174	Triosephosphate isomerase	No
P01834	Ig kappa chain C region	Yes
P21589	5'-nucleotidase	No
P00738	Haptoglobin	Yes
P06727	Apolipoprotein A-IV	Yes
	Normal Only	
Q9UKU9	Angiopoietin-related protein 2	No
P68104	Elongation factor 1-alpha 1	Yes
Q14055	Collagen a2(IX) chain	No
Q16674	Melanoma-derived growth regulatory protein	No
P13611	Versican core protein	No
P57053	Histone H2B type F-S	Yes
	Up-regulated in OA	
P02768	Serum albumin	Yes
Q15582	Transforming growth factor-beta-induced protein ig-h3	Yes
O43854	Intgrin-binding protein	No
P02743	Serum amyloid P-component	Yes
P04004	Vitronectin	Yes
Q92743	Serine protease HTRA1	Yes
P12111	Collagen alpha-3(VI) chain	Yes
P12109	Collagen alpha-1(VI) chain	Yes
P12110	Collagen alpha-2(VI) chain	Yes
	Down-regulated in OA	
P10915	Proteoglycan link protein	No
Q08431	Lactadherin	No
P02458	Collagen a1(II) chain	No
P10909	Clusterin	Yes
P26038	Moesin	No
P21810	Biglycan	No
P51888	Prolargin	No
O75339	Cartilage intermediate-layer protein 1	No
P16112	Aggrecan core protein	Yes
O15335	Chondroadherin	No
Q92954	Proteoglycan 4 (Lubricin)	Yes
Q8IUL8	Cartilage intermediate-layer protein 2	No
O60687	Sushi repeat-containing protein SRPX2	No
P49747	Cartilage oligomeric matrix protein	Yes
P02751	Fibronectin	Yes
P35443	Thrombospondin-4	Yes
P35241	Radixin	No
O15232	Matrilin 3	No
P29992	Guanine nucleotide-binding protein a11 subunit	No
P15311	Ezrin	No
P07996	Thrombospondin-1	No
P98160	Perlecan	No

Table 3.14: *Comparison of the proteome of ACVs derived from normal and OA cartilage as performed by Rosenthal et al.* [94] *Also included is whether each protein was found to be associated with OA MV.*

In the ***OA only*** category, nine proteins were listed as significantly increased in OA ACVs. Many of these were markers of inflammation i.e. fibrinogen, complement, immunoglobulins and lipoproteins. Of these nine moieties, two were not found in the MV proteome i.e. Triosephosphate isomerise and 5'-nucleotidase.

In the ***Normal only*** category, six proteins were down-regulated in OA cartilage relative to normal cartilage. With the exception of histone 2B and elongation factor 1, none of the remaining four species were found in MVs from OA patients. One of these was angiopoietin-related protein which is a member of the tumour necrosis factor α family and was said to be related to the development of connective tissue and cartilage [98]. Another interesting protein absent in OA MVs was versican. Research by Matsumoto *et al.* [99] revealed that versican is a large chondroitin sulfate proteoglycan of the extracellular matrix mainly present on the surface of developing cartilage. Interestingly, an inverse relationship exists between levels of versican and aggrecan – as the expression of one is increased, the other decreases. Neither of these proteins was present in the afore-mentioned studies on whole SF. That these proteins are not found in ACVs or SF MVs lead one to speculate that their expression was either arrested or greatly reduced in OA.

The third category - ***Up-regulated in OA***- was comprised of nine proteins. Eight of these were found to be associated with OA vesicles. Integrin-binding protein DEL-1 was the single protein not found in MVs and the authors claim its role in ACVs and in cartilage is not known. Transforming growth factor-beta-induced protein ig-h3 (TGFBIp) was found to be both ACV- and MV-associated. According to UniProtKB this protein binds to type I, II, and IV collagens and may play an important role in cell-collagen interactions. In cartilage, it may be involved in endochondral bone formation. This protein was also listed in Table 3.10 above as being found in RA SF only, though the authors later confirmed its presence in OA by WB [92]. As its name implies, TGFBIp is a result of transforming growth factor-beta protein (TGF-β) which Rosenthal [94] believed supports the idea of the putative role for the latter in OA. However, Nam *et al.* [100] found this protein to be also induced by IL-1β and TNF-α in fibroblast-like synoviocytes in RA

patients. It may be that those MVs which contained TGFBIp isolated in this project originated from synoviocytes, or may actually be ACVs that are present in the SF as mentioned above or indeed be present in exosomes released by activated chondrocytes. TGFBIp was found to be associated with chondrocyte-collagen interactions [101]. These interactions were recently elucidated by Zhang *et al.* [102] in their study of the pericellular matrix (PCM) - a thin layer of extracellular matrix that immediately surrounds the chondrocyte where chondrocytes and extracellular matrix exchange signals. They concluded that TGFBIp is *"located pericellularly but its distribution is beyond the PCM……The distribution pattern of TGFBIp indicates that it is not a restrict PCM component"*. This conclusion may be explained by the proposition that TGFBIp was now MV and/or ACV cargo and departed the PCM micro-environment. Of interest though, TGF-β itself (a precursor to TGFBIp) was not found to be associated with ACVs or SF MVs, though this protein has an important role in cartilage homeostasis[103]. Interesting questions presented themselves here in relation to TGFBIp. Which species are precursors to this PCM protein that was found in OA MVs? Was it TGF-β in the cartilage or cytokines (IL-1β & TNF-α) from synoviocytes? In MVs isolated from OA whole SF, it probable that both scenarios were the case. As this protein is involved in cell-collagen interactions via integrins as the sole cell surface receptors [104], it maybe that activation of chondrocytes may induce TGFBIp endocytosis followed by trafficking through the cell via the endosomal pathway, and finally released into the ECM in exosomes. It could be speculated that this may be a precursor stage to subsequent collagen type VI degradation. Another possibility is that as TGFBIp can undergo both covalent and non-covalent interactions with collagen type VI [105] and hence, these two species were present in MVs bound to each other. Finally, as mentioned in the introduction to this chapter, exosomes are also known to be antigen-presenting entities. It is possible that if TGFBIp is associated with exosomes it may fulfil this role, especially in light of the work published by Cao *et al.* [106] which detailed an immune regulatory role for this protein through stimulation of macrophage endocytosis.

Zhang's group [102] also noted fragmentation of collagen type VI in the PCM when the cartilage was treated with Il-1β and TNF-α and interestingly, mechanical compression.

Three collagen type VI fragments (collagen α1(VI) chain, collagen α2(VI) chain and collagen α3(VI) chain) were also present in ACVs under the heading "Up-regulated in OA" in Table 3.14 and the same three fragments were found associated with SF MVs in the current project (Table 3.7). Disruption of collagen type VI in the PCM is believed to destabilise chondrocyte phenotype [107]. This may be very relevant in the early pathogenesis of OA. Polur *et al.* [108] suggested that biomechanical stress may initiate a disruption of the pericellular matrix through serine protease HtrA1.

Serine protease HtrA1 (High-Temperature Requirement A serine peptidase 1), is a 51.3kDa species that was also found in microvesicles in OA synovial fluid in this project and also up-regulated in OA ACVs by Rosenthal [94]. It is known to be associated with a variety of targets, including extracellular matrix proteins such as fibronectin and within the context of arthritis it was concluded that it contributes to cartilage catabolism and degradation [109]. Elevated synovial HtrA1 levels were detected in fluids obtained from RA and OA patients, with synovial fibroblasts identified as a major source of this protein, and the study confirmed that fibronectin was the major target of this protease. Interestingly, fibronectin was also detected in microvesicles in this project despite the assertion that this protein is solely associated with RA exosomal fractions [18]. Treatment of synovial fibroblasts with HtrA1 or HtrA1-generated fibronectin fragments, in turn resulted in the specific induction of MMP1 and MMP3 expression, suggesting that HtrA1 contributes to the destruction of extracellular matrix through both direct and indirect mechanisms [109]. It is worth noting that MMP3 (stromelysin-1) was found associated with synovial fluid MV in this project, though MMP1 was not. In order to establish the extent of protease activity in MVs, a zymography experiment was carried out (Figure 3.35) which demonstrated that gelatinases are associated with SF MVs. This is the first study to identify protease activity in SF MVs. However, without WB analysis it is not possible to definitively identify these species, though other studies [72, 74-77, 110] have identified proteases in whole SF. No MMPs were found in ACVs. Tsuchiya *et al.* [111] examined HtrA1 expression pattern during bone and cartilage development and in articular cartilage affected by experimental arthritis. They found that HtrA1 digests other major components of cartilage, such as aggrecan, decorin, fibromodulin, and soluble type II

collagen, and concluded that HtrA1 may promote degeneration of cartilage by digesting cartilage matrix. Examples of matrix proteins found to be associated with SF MVs include, fibrinogen, COMP, fibronectin and collagen type VI. Polur *et al.* [108] found that pericellular type VI collagen was absent in chondrocytes expressing HtrA1 and that the expression of HtrA1 was associated with the expression of discoidin domain receptor 2 (DDR2) in the chondrocytes. The activation of DDR 2 in turn led to binding with its ligand, namely type II collagen. They argued that these results indicated that HtrA1 may disrupt the pericellular matrix network, resulting in alteration of chondrocyte metabolisms which eventually led to OA. Xu *et al.* [112] recently supported this theory and reminded us that type II collagen is not present in the pericellular matrix, so there is unlikely to be direct contact between chondrocytes and type II collagen in healthy cartilage. The group concluded that damage to the pericellular matrix induced by HtrA1 occurs in the early development of OA and this led to aberrant interactions between chondrocytes and type II collagen. MVs from the OA-pooled patient sample in the current study, contains three isoforms of collagen type VI (collagen α1(VI) chain, collagen α2(VI) chain and collagen α3(VI) chain) along with HtrRA1 and TGFBIp. Further study of MV isolated from a larger cohort of OA patient samples and control SF would be required to verify if these species are unique to OA MVs. Markers of PCM destruction in MV could have useful early-stage OA diagnostic value. This can be appreciated as important given that once the collagen type II structure is severely degraded, the chondrocyte is unable to undertake repair steps [113] .

As mentioned above, MMP3 (~54kDa) was also found to be associated with synovial fluid microvesicles. Figure 3.35 was the result of a zymography study, which is an extremely sensitive technique (10pg of a gelatinase may be detected [114]), and it demonstrated that a host of gelatinases were present in/on MVs and the corresponding supernatants. The list of proteins generated by MS included MMP3. The stromelysins MMP3 and MMP10, digest ECM components such as collagen IV and fibronectin [115], with MMP3 having a higher proteolytic efficiency higher than that of MMP10 [116]. Indeed MMP3 is the most strongly expressed MMP in OA cartilage, but its expression decreases in late OA [73]. Though MMP3 is incapable of cleaving collagen type II (the

major structural protein in cartilage) [72], it does play an important role in cartilage degradation either by direct cleavage of proteoglycans from the cartilage matrix, or indirectly by activation of other members of the MMP family (namely MMP1, MMP9 & MMP13). This indirect activation of other members of the MMP family (notably MMP9), by MMP3 in OA and RA, was studied by Dreier *et al.* [117]. They noted that MMP-9 was secreted as a stable, inactive zymogen (pro-MMP9) and was subsequently proteolytically converted to the active form. Importantly, macrophages extensively expressed and secreted pro-MMP-9 whereas chondrocytes failed to produce this enzyme. Of interest though, is the fact that MMP3 production was triggered by chondrocytes from OA, but not normal joints. This study led the authors to conclude that, "*articular chondrocytes are not innocent bystanders in joint diseases"*. Recognising that MMP3 is associated with MV cargo, it is interesting to speculate that this species may transit from the chondrocyte to the pro-MMP9 producing cells via microvesicles. Somehow disrupting this vesicle trafficking may go towards inhibiting the activation of destructive proteases, particularly MMP9 and MMP13. A question worth asking is; why not explore MMP3 inhibition? In that way MMP1, MMP9 and MMP13 may remain in the inactive, zymogen form. The literature appears to have mixed views on this. Some studies with MMP3 and MMP9 knock-out mice demonstrated protection against cartilage loss and aggrecan cleavage [118] [119], while others [120, 121] found the converse to be true. It is worth bearing in mind that these are animal models and that the onset of arthritis was artificially produced and instant. In humans, OA has a heterogeneous assortment of causes and develops over time. Therefore, the development and progression of the disease may be quite different in humans relative to that in artificially-induced OA murine models.

Sinz *et al.* [122] conducted a 2-DE comparative proteomic study of synovial fluid and plasma from patients suffering from RA, reactive arthritis, and OA, which identified two spots unique to the SF of RA patients. These were not observed in the other two pathologies or in any of the plasma samples studied. MS identified these spots as calgranulin B (MRP14 or S100-A9) - a 13.2kDa species. The S100 proteins are also known as alarmins. The authors concluded that calgranulin B is a "*sensitive marker for the molecular characterisation of RA, as it can be detected quite easily in SF*". However,

this project would appears to counter that hypothesis, as this protein (identified as Protein S100-A9) was found associated with MVs in an OA SF sample. Calgranulin B is a calcium-binding protein, which is primarily expressed together with another calcium-binding protein, calgranulin A (MRP8 or S100-A8) [123] by circulating neutrophils and monocytes. Sinz *et al*. [122] acknowledged that they did not identify calgranulin A (S100-A8) in any of the pathologies (including RA) in their study, though S100-A8 was found associated with MVs in an OA patient sample in this project. One of the functions of the S100-A8/S100-A9 complex is to mediate leukocyte migration and adhesion to vascular endothelium [124]. A possible explanation for the presence of S100-A9 and S100-A8 in OA MVs is the fact that this fraction represents a highly concentrated sub-proteome. The difficulty experienced by Sinz to detect these moieties in other samples may simply be a matter of low abundance in OA, exasperated by the fact that their study characterised the proteome of whole synovial fluid. However, their research did identify calgranulin C (S100-A12) in RA patients, whereas this species was not identified to be associated with OA MVs. Therefore, experimental design and specifically targeted proteomes are a factor and an influence on the generated list of proteins. Other studies [125-127] showed that S100-A8 and S100-A9 may have a sustained role in cartilage degradation in inflammatory arthritis. However, while these proteins may have a role in initiating early cartilage degradation in OA by up-regulating MMPs and aggrecanases, their reduced expression in late stages of OA suggested they do not have an ongoing role in cartilage degradation. Therefore, these proteins could be important early OA markers and suppression of their expression may instigate a possible halt to the subsequent signalling cascade that leads to cartilage decay, thus closing down one of the many pathways implicated in this complex disease.

In their very recent review paper, Loeser et al. [128] made a very interesting point. They advise that as articular cartilage matrix proteins are degraded, fragments of these degraded proteins can feedback and stimulate further matrix destruction thus self-perpetuate the disease. They cited examples of protein fragments that can stimulate this feedback loop. These include fragments of fibronectin, collagen and small leucine-rich proteoglycans. Fibronectin and collagen fragments were said to stimulate the production

of inflammatory cytokines, chemokines and MMPs. A hypothesis that was proposed earlier, in which collagen VI fragments from the pericellular matrix may enter the endosomal pathway and re-enter the EMC in exosomes or become vesicle-associated in the ECM, may also have some credence here. MVs ferrying fragmented collagen VI cargo may be destined for uptake by neutrophils or macrophages, which results in the stimulation of an inflammatory response. As fibronectin is also associated with OA MVs, the same hypothesis may apply.

Another protein fragment that can induce an immunological response is Cartilage Oligomeric Matrix Protein (COMP/thrombospondin 5). From Table 3.14, Rosenthal listed this species under the heading ***Down-regulated in OA***. COMP is a 524kDa pentameric glycoprotein expressed primarily in cartilage, tendon, ligament and synovium [129]. From Figure 1.2 in the introduction chapter, it was shown that COMP is an ECM protein and is known to bind collagens type I, II and IX (fibrillogenesis), as well as fibronectin and aggrecan [130]. DiCesare *et al.* [131] performed a study of COMP metabolism in cartilage obtained from a cohort of healthy, OA and RA patients and their conclusions indicated that the degree of COMP fragmentation mirrored degenerative processes occurring in the matrix.

From the analysis of OA SF in this project, it was found that COMP is associated with MVs. However, further study will be required to elucidate the exact structure of this. Many questions immediately present themselves. Is the structure/fragmentation of COMP found in MVs uniform, or is there heterogeneous fragmentation? Is there any difference in the structure/fragmentation of COMP found to be associated with MVs and that found in whole SF? Indeed, why are some fragments associated with MVs while other fragments (possibly the major part) are in the exo-vesicular milieu? These are important questions, especially in light of the research performed by Gagarina *et al.*[132] This group showed for the first time that the *"carboxyl-terminal half"* of COMP played a critical role in chondrocyte survival. It accomplished this by the induction of members of the inhibitor of apoptosis (IAP) family of survival proteins, which were very effective at blocking the activation of caspase 3, and so effected inhibition of apoptosis. Their work suggested that during the process of cartilage breakdown, some fragments of COMP still

retain their anti-apoptotic function. They further hypothesised that these fragments may be bioactive; leading to a reduction in the level of apoptosis in OA cartilage, and finally, that COMP fragments may also affect tissues at sites removed from cartilage. All these theories lead to a suggestion that MVs could play a COMP- trafficking role here. This reverts back to establishing the nature of COMP associated with MVs and whole SF.

Wang *et a*l. [133] recently identified the complement cascade as a key factor in OA. They stated that cartilage ECM components released by or exposed in OA cartilage may trigger the complement cascade; "*dysregulation of gene expression in joint tissues may contribute to a local preponderance of complement effectors over inhibitors in osteoarthritis, permitting complement activation to proceed unchecked"*. A consequence of triggering this effect was the formation of membrane attack complex (MAC) on chondrocytes, which the authors stated either kills the cells or causes them to produce matrix-degrading enzymes, inflammatory mediators and other complement effectors. These species further propagate joint disease. This whole concept of protein fragmentation promoting the complement cascade was studied by Happonen *et al*. [134] in relation to COMP. Theirs was the first study to demonstrate that an extracellular protein has an active role in inflammation *in vivo*. They found that COMP fragments can activate the alternative complement pathway due to a direct interaction with properdin, while simultaneously inhibiting the classical and lectin pathways due to interaction with C1q (classical pathway) and mannose-binding lectin (lectin pathway) precursors. A simplified schematic diagram of the three known complement cascade pathways is displayed in Figure 3.38.

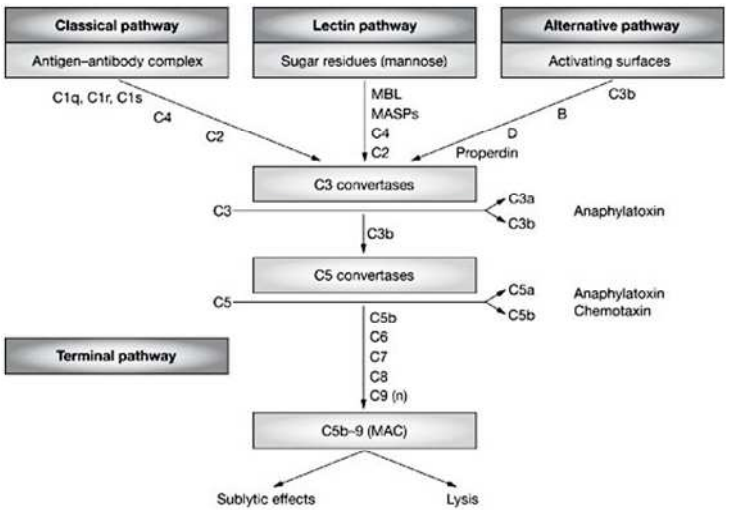

Figure 3.38: *A simplified schematic diagram of the three complement cascade pathways. Diagram taken from Cook et al.* [135]

With the exception of complement factor D, all complement components required for each of the three possible pathways in Figure 3.38 (including properdin) were found to be present in/on OA MVs. It may be worth considering the function of COMP and MVs in relation to the complement cascade. Is it possible that COMP fragments are exposed on the surface of MVs with the purpose of initiating the complement cascade there, rather than on the surface of chondrocytes and so preventing a sustained inflammatory response at the cartilage?

Hunter *et al.* [136] performed a longitudinal study on a number of markers of cartilage turnover in serum, to ascertain if they could serve as predictors of cartilage loss on magnetic resonance imaging (MRI). The authors concluded that, with the exception of COMP, none of the other markers was a statistically significant predictor of cartilage

loss. They claimed that a single measurement of increased COMP predicted subsequent cartilage loss, but added that the "*association was modest"*. Williams *et al.* [137] predicted that COMP will be useful as a biomarker of early-stage OA and urge serious research into the behavior of COMP, which may shed light on early pathogenic pathways and thus determining its clinical usefulness as a biomarker.

Having discussed the role of COMP fragmentation in relation to the complement cascade and the hypothesis that MVs may have a function in off-setting continued damage to the chondrocytes, another family of proteins with the same function (i.e. complement cascade regulation) was also found to be associated with SF MVs. These are the apolipoprotein family. The complement cascade is essentially a bacterial killing mechanism by means of rupturing the cell wall of the invading pathogen. From Figure 3.38 it can be seen that in the final stage of the complement assembly, C9 binds to the C5b-C8 unit. C9 then undergoes polymerisation ultimately forming a circular polymer, which then penetrates the lipid bilayer of the bacteria resulting in cell lysis. Hamilton *et al.* [138] studied the interaction of apoA-I and apoA-II with the membrane attack complex of complement. They found that apoproteins interacted with a site on the C9 polymerised complex which interferes with the assembly of the MAC and its subsequent ability to penetrate the cell wall. The authors interpreted this as a means to protect cells which were exposed to complement i.e. apoproteins act as complement inhibitors. Finally, they advanced that identification of the binding site for apoA-I or apoA-II on C9 is a potential target for complement inhibitory agents. In a recent review paper Norata *et al.* [81] discussed the current thinking around high density lipoproteins (HDL) in the immune system. This paper was extremely interesting in terms of relevance to the current project. At the beginning of this discussion it was advised exosomes and HDLs possess similar density values. Therefore, co-precipitation of HDLs with MVs is a possibility. The author claimed that HDL particles are enriched in complement pathway and complement regulatory proteins such as C3, C4a, C4b, C9 and vitronectin. All of these species were found in OA MVs. Therefore, it is possible that there are HDL particles in the 200,000g CHAPS pellet as apoA-I was found to be vesicle-associated (Figure 3.31). It was hypothesised that HDL could bind these proteins promoting their clearance and so

preventing over-activation of the complement system. In their conclusion the authors noted that HDLs are a reservoir for a number of biologically active substances that may impact the immune system. They expressed a need for understanding the role of HDLs as delivery agents of these biologically active substances to relevant targets in the immune system.

As mentioned above, HA is the component of synovial fluid that imparts viscosity and gives the joint fluid an "egg-like" appearance and consistency. It is known that the size of the HA molecule decreases while its actual abundance increases with age and with the onset of arthritic diseases. But what are the agents of HA fragmentation? This decrease in size is attributed to degradation and is thought to involve the action of hyaluronidases or free radicals. This project established for the first time, by employing zymography with a HA substrate, that there are hyaluronidases (HAase) associated with SF MV. Figure 3.36 demonstrates HAase activity by two different species. One band is very well expressed in the middle of the gel, while the other is present at a higher molecular weight, though the latter is less intense than the former. Interestingly, there does not appear to be HAase activity in the 200,000g pellet post-CHAPS treatment. This may be compared with the same sample pre-CHAPS treatment, suggesting that any HAase species present are associated with the vesicle surface. Is it possible to speculate on the identity of these proteases? Csoka *et al*. [139] identified six genes that code for HAases. They are HYAL-1, HYAL-2, HYAL-3, HYAL-4, PH-20/ SPAM 1 and HYALP-1. Hyal-1 is an acid-active HAase - a single polypeptide chain of 57-kDa (49 kDa with approximately 8 kDa of post-translational glycosylation). Hyal-2 is also an acid-active HAase which is present on the outer cell membrane. The authors stated that it has unusual substrate specificity, cleaving high-molecular-weight HA polymers to intermediate size fragments of approximately 20 kDa. Hyal-3 is believed to be important in stem cell regulation, while Hyal-4 is restricted to placenta and skeletal muscle. PH-20/ SPAM 1 is a testicular HAase which is important for egg fertilisation by sperm. HYALP-1 was termed a pseudogene and the authors don't list a protein that is expressed by this. It was then suggested that Hyal-2 and Hyal-1 are the major mammalian hyaluronidases in somatic tissues, and that they act in concert to degrade high molecular weight HA to a tetrasaccharide. As mentioned, 20

kDa HA fragments are generated by Hyal-2 digestion in an acidic environment at the cell surface. Bourguignon *et al.* [140] explain that it is the interaction of CD44, Sodium/hydrogen exchanger 1 and Hyal-2 that creates the acidic microenvironment necessary for the catabolism of HA. These fragments are first endocytosed, then transported intracellularly, and finally further digested by Hyal-1. Two β-exoglycosidases remove sugars from reducing termini of HA oligomers, and supplement hyaluronidases in their catabolism of HA. The process can be seen in Figure 3.39.

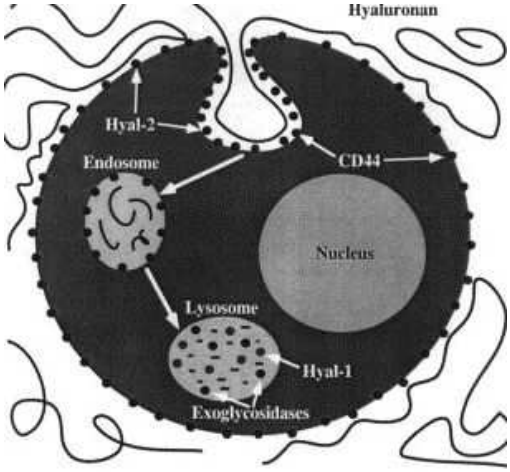

Figure 3.39: *Schematic diagram outlining the process of HA digestion by the concerted action of two HAases, Hyal-1 and Hyal-2. HA is first digested into 20kDa fragments at the cell surface by Hyal-2, followed by endocytosis to the lysosome for final digestion to the tetrasaccharide by Hyal-1. Exoglycosidases remove any sugars present in the fragments. Image taken from Csoka et al.* [139]

From the location descriptions of HYAL-3, HYAL-4, PH-20/SPAM 1 and HYALP above, it is reasonable to speculate that the clear bands in Figure 3.36 are manifestations of Hyal-1 and Hyal-2 activity. An alternative hypothesis may be that, as Hyal-1 appears to be located in the lysosome (Figure 3.39), both bands could be due to different Hyal-2 isoforms or indeed be Hyal-2 and a different protease. A positive identification would only be possible by incubation with the respective antibodies and analysis by WB.

At this point it may be instructive to put forth a potentially interesting hypothesis. In Figure 3.3 (reproduced here to aid the reader) it can be seen that during the endosomal pathway there comes a point whereby the cell encounters two alternate pathways – either target the MVB to the lysosome for cargo destruction, or fuse with the plasma membrane and shed its load in the form of exosomes. The point of alternate routes is highlighted with a red box. Theoretically, it may be possible for the endosome carrying the 20kDa HA fragments to avoid the lysosome pathway, hence avoiding further digestion by Hyal-1 to the tetrasaccharide. The MVB may then fuse with the plasma membrane and release these fragments within exosomes into the ECM milieu.

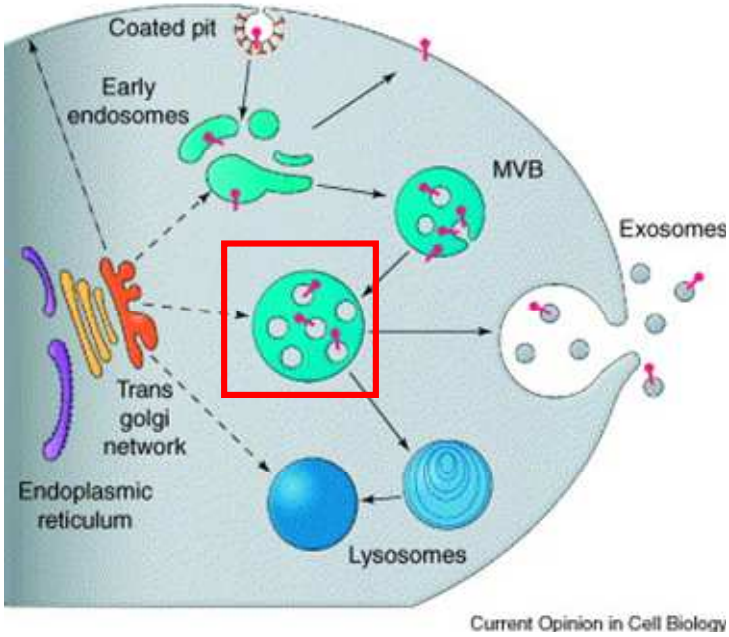

Figure 3.3: *A schematic diagram of the endosomal pathway. Proteins (in red) are endocytosed and enter the endosomal pathway with the formation of MVBs. At the point highlighted by a red box, there two destination routes possible, – destruction by fusion with the lysosome or exocytosis via fusion with the plasma membrane in the form of exosomes. Diagram is taken from Fevrier et al.* [26]

This hypothesis may have some merit in light of a paper published by Scanzello *et al.* [141]. Here it was suggested *"that initial responses to tissue injury may be triggered by endogenous danger signals - damage-associated molecular patters (DAMPS also called alarmins)"*. Some examples of DAMPS were cited e.g. HA and fibronectin fragments,

heat-shock proteins and members of the S100/calgranulin (discussed above) family. These species were said to bind to either toll-like receptors (TLRs) or the receptor for advanced glycation endproducts (RAGE). The authors advised that this process has been implicated in cartilage catabolism in OA and concluded that DAMP interaction with TLRs may stimulate the inflammatory response in synovium, bone and cartilage in an attempt to initiate repair.

An appropriate and informative diagram by Loeser *et al.* [128] indicating a host of possible factors involved in the OA process was published very recently. A number of species that were found to be associated with OA MVs and argued as being associated with OA in this project are shown in the diagram. Figure 3.40 is an amended copy of this diagram, highlighting any species that were discussed here (red arrows).

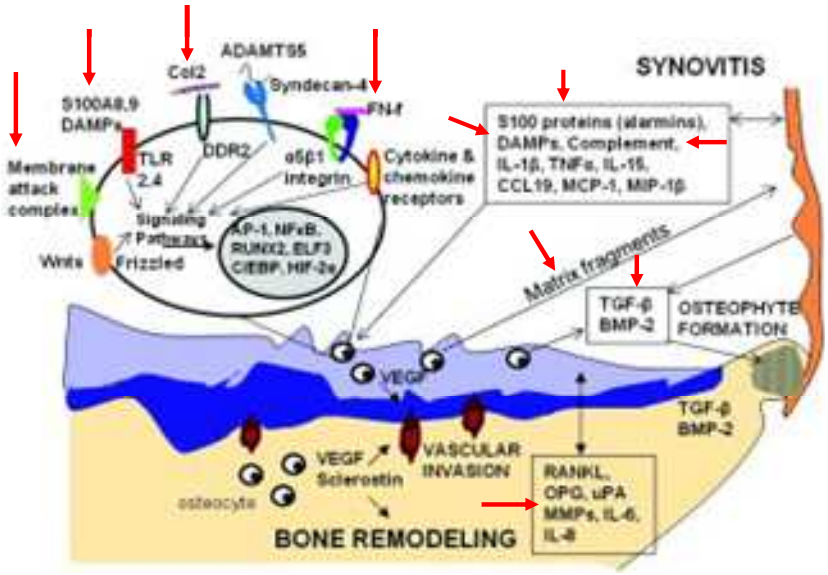

Figure 3.40: *Factors involved in the OA process. Those factors that were discussed above are indicated with red arrows. A number of proteins (S100-A8, S100-A9, DAMPS and complement components released from the synovium) can activate articular chondrocytes though the activation of cell surface receptors e.g. TLRs, membrane attack complex. Pericellular matrix destruction by HtrA-1 leads to the exposure of the DDR2 receptor to its ligand, type II collagen. Matrix fragments e.g. fibronectin and COMP can induce an inflammatory response. Transforming growth factor β stimulate osteophyte formation. Diagram taken from Loeser et al.* [128]

3.5 Conclusions

A novel workflow for isolating microvesicles (MVs) from synovial fluid was established. For optimal recovery of MVs, this necessitated prior treatment with hyaluronidase (to avoid vesicle entrapment by hyaluronic acid via a CD44 receptor), and protein A chromatography (to remove interfering immunoglobulins). This was followed by a differential centrifugation process which included treatment with 1% CHAPS (to remove loosely associated proteins from the vesicle surface.

A four-patient-pooled sample was prepared employing the newly developed method and the 200,000g CHAPS pellet was characterised by mass spectrometry employing three methods (RP-HPLC, SCX-RP-HPLC and in-gel digestion). The generated protein lists were classified by a bioinformatic tool (Panther). A number of confirmation studies were carried out on selected proteins using the western blot technique, aimed at supporting the MS data. Proteases activity associated with MVs was established employing zymography (including hyaluronidases).

In the discussion section, the intention was to postulate plausible explanations for the presence of a number of interesting proteins based on a thorough search and understanding of the literature, rather than a comparison of the number of proteins identified with other researchers. This approach tendered a number of possibilities for a role MVs might mirror the pathophysiological events in the genesis and development of OA. It is hoped that these hypotheses may spark interest in this topic and stimulate further research.

3.6 References

References

(1) Pap, E.; Pallinger, E.; Pasztoi, M.; Falus, A. Highlights of a new type of intercellular communication: microvesicle-based information transfer. *Inflammation Research* **2009**, *58*, 1-8.

(2) Majka, M.; Janowska-Wieczorek, A.; Ratajczak, J.; Ehrenman, K.; Pietrzkowski, Z.; Kowalska, M.; Gewirtz, A.; Emerson, S.; Ratajczak, M. Numerous growth factors, cytokines, and chemokines are secreted by human CD34(+) cells, myeloblasts, erythroblasts, and megakaryoblasts and regulate normal hematopoiesis in an autocrine/paracrine manner. *Blood* **2001**, *97*, 3075-3085.

(3) Rustom, A.; Saffrich, R.; Markovic, I.; Walther, P.; Gerdes, H. Nanotubular highways for intercellular organelle transport. *Science* **2004**, *303*, 1007-1010.

(4) Sherer, N. M.; Mothes, W. Cytonemes and tunneling nanotubules in cell-cell communication and viral pathogenesis. *Trends in cell Biology* **2008**, *18*, 414-420.

(5) Camussi, G.; Deregibus, M. C.; Bruno, S.; Cantaluppi, V.; Biancone, L. Exosomes/microvesicles as a mechanism of cell-to-cell communication. *Kidney International* **2010**, *78*, 838-848.

(6) Cocucci, E.; Racchetti, G.; Meldolesi, J. Shedding microvesicles: artefacts no more. *Trends in Cell Biology* **2009**, *19*, 43-51.

(7) Debroe, M.; Wieme, R.; Logghe, G.; Roels, F. Spontaneous Shedding of Plasma-Membrane Fragments by Human Cells Invivo and Invitro. *Clinica Chimica Acta* **1977**, *81*, 237-245.

(8) Simpson, R. J.; Jensen, S. S.; Lim, J. W. E. Proteomic profiling of exosomes: Current perspectives. *Proteomics* **2008**, *8*, 4083-4099.

(9) Sadallah, S.; Eken, C.; Schifferli, J. A. Ectosomes as modulators of inflammation and immunity. *Clinical and Experimental Immunology* **2011**, *163*, 26-32.

(10) Johnstone, R. M. Exosomes biological significance: A concise review. *Blood Cells Molecules and Diseases* **2006**, *36*, 315-321.

(11) Heijnen, H.; Schiel, A.; Fijnheer, R.; Geuze, H.; Sixma, J. Activated platelets release two types of membrane vesicles: Microvesicles by surface shedding and exosomes derived from exocytosis of multivesicular bodies and alpha-granules. *Blood* **1999**, *94*, 3791-3799.

(12) Thery, C.; Ostrowski, M.; Segura, E. Membrane vesicles as conveyors of immune responses. *Nature Reviews Immunology* **2009**, *9*, 581-593.

(13) Lee, T.; D'Asti, E.; Magnus, N.; Al-Nedawi, K.; Meehan, B.; Rak, J. Microvesicles as mediators of intercellular communication in cancer—the emerging science of cellular 'debris'. *Seminars in Immunopathology* **2011**, *33*, 455-467.

(14) Gyoergy, B.; Modos, K.; Pallinger, E.; Paloczi, K.; Pasztoi, M.; Misjak, P.; Deli, M. A.; Sipos, A.; Szalai, A.; Voszka, I.; Polgar, A.; Toth, K.; Csete, M.; Nagy, G.; Gay, S.; Falus, A.; Kittel, A.; Buzas, E. I. Detection and isolation of cell-derived microparticles are compromised by protein complexes resulting from shared biophysical parameters. *Blood* **2011**, *117*, E39-E48.

(15) Mayr, M.; Grainger, D.; Mayr, U.; Leroyer, A. S.; Leseche, G.; Sidibe, A.; Herbin, O.; Yin, X.; Gomes, A.; Madhu, B.; Griffiths, J. R.; Xu, Q.; Tedgui, A.; Boulanger, C. M. Proteomics, Metabolomics, and Immunomics on Microparticles Derived From Human Atherosclerotic Plaques RID F-2853-2010. *Circulation-Cardiovascular Genetics* **2009**, *2*, 379-U228.

(16) Tulenko, T.; Sumner, A. The physiology of lipoproteins. *Journal of Nuclear Cardiology* **2002**, *9*, 638-649.

(17) Ratajczak, J.; Wysoczynski, M.; Hayek, F.; Janowska-Wieczorek, A.; Ratajczak, M. Z. Membrane-derived microvesicles: important and underappreciated mediators of cell-to-cell communication. *Leukemia* **2006**, *20*, 1487-1495.

(18) Skriner, K.; Adolph, K.; Jungblut, P. R.; Burmester, G. R. Association of citrullinated proteins with synovial exosomes. *Arthritis & Rheumatism* **2006**, *54*, 3814.

(19) Schorey, J. S.; Bhatnagar, S. Exosome function: From tumor immunology to pathogen biology. *Traffic* **2008**, *9*, 871-881.

(20) Futter, C.; Pearse, A.; Hewlett, L.; Hopkins, C. Multivesicular endosomes containing internalized EGF-EGF receptor complexes mature and then fuse directly with lysosomes. *Journal of Cell Biology* **1996**, *132*, 1011-1023.

(21) Sorkin, A.; von Zastrow, M. Endocytosis and signalling: intertwining molecular networks. *Nature Reviews Molecular Cell Biology* **2009**, *10*, 609-622.

(22) Johnstone, R.; Adam, M.; Hammond, J.; Orr, L.; Turbide, C. Vesicle Formation during Reticulocyte Maturation - Association of Plasma-Membrane Activities with Released Vesicles (Exosomes) Rid A-4524-2008. *Journal of Biological Chemistry* **1987**, *262*, 9412-9420.

(23) Harding, C.; Heuser, J.; Stahl, P. Receptor-Mediated Endocytosis of Transferrin and Recycling of the Transferrin Receptor in Rat Reticulocytes. *Journal of Cell Biology* **1983**, *97*, 329-339.

(24) Pan, B. T.; Teng, K.; Wu, C.; Adam, M.; Johnstone, R. M. Electron-Microscopic Evidence for Externalization of the Transferrin Receptor in Vesicular Form in Sheep Reticulocytes. *Journal of Cell Biology* **1985**, *101*, 942-948.

(25) Thery, C.; Zitvogel, L.; Amigorena, S. Exosomes: Composition, biogenesis and function. *Nature Reviews Immunology* **2002**, *2*, 569-579.

(26) Fevrier, B.; Raposo, G. Exosomes: endosomal-derived vesicles shipping extracellular messages. *Current Opinion in Cell Biology* **2004**, *16*, 415-421.

(27) Piper, R.; Katzmann, D. Biogenesis and function of multivesicular bodies. *Annual Review of Cell and Developmental Biology* **2007**, *23*, 519-547.

(28) Katzmann, D.; Sarkar, S.; Chu, T.; Audhya, A.; Emr, S. Multivesicular body sorting: Ubiquitin ligase Rsp5 is required for the modification and sorting of carboxypeptidase S. *Molecular Biology of the Cell* **2004**, *15*, 468-480.

(29) van Niel, G.; Wubbolts, R.; ten Broeke, T.; Buschow, S. I.; Ossendorp, F. A.; Melief, C. J.; Raposo, G.; van Balkom, B. W.; Stoorvogel, W. Dendritic cells regulate exposure of MHC class II at their plasma membrane by oligoubiquitination. *Immunity* **2006**, *25*, 885-894.

(30) de Gassart, A.; Geminard, C.; Fevrier, B.; Raposo, G.; Vidal, M. Lipid raft-associated protein sorting in exosomes. *Blood* **2003**, *102*, 4336-4344.

(31) Theos, A.; Truschel, S.; Tenza, D.; Hurbain, I.; Harper, D.; Berson, J.; Thomas, P.; Raposo, G.; Marks, M. A lumenal domain-dependent pathway for sorting to intralumenal vesicles of multivesicular endosomes involved in organelle morphogenesis. *Developmental Cell* **2006**, *10*, 343-354.

(32) Hurley, J. H.; Boura, E.; Carlson, L.; Rozycki, B. Membrane Budding. *Cell* **2010**, *143*, 875-887.

(33) Hurley, J. H.; Hanson, P. I. Membrane budding and scission by the ESCRT machinery: it's all in the neck. *Nat. Rev. Mol. Cell Biol.* **2010**, *11*, 556-566.

(34) Wollert, T.; Hurley, J. H. Molecular mechanism of multivesicular body biogenesis by ESCRT complexes. *Nature* **2010**, *464*, 864-U73.

(35) Matsuo, H.; Chevallier, J.; Mayran, N.; Le Blanc, I.; Ferguson, C.; Faure, J.; Blanc, N.; Matile, S.; Dubochet, J.; Sadoul, R.; Parton, R.; Vilbois, F.; Gruenberg, J. Role

of LBPA and Alix in multivesicular liposome formation and endosome organization. *Science* **2004**, *303*, 531-534.

(36) Raposo, G.; Marks, M. S. Melanosomes-dark organelles enlighten endosomal membrane transport. *Nature Reviews Molecular Cell Biology* **2007**, *8*, 786-797.

(37) Trajkovic, K.; Hsu, C.; Chiantia, S.; Rajendran, L.; Wenzel, D.; Wieland, F.; Schwille, P.; Bruegger, B.; Simons, M. Ceramide triggers budding of exosome vesicles into multivesicular Endosomes RID A-4546-2010 RID A-4983-2010. *Science* **2008**, *319*, 1244-1247.

(38) Stein, J.; Luzio, J. Ectocytosis Caused by Sublytic Autologous Complement Attack on Human Neutrophils - the Sorting of Endogenous Plasma-Membrane Proteins and Lipids into Shed Vesicles. *Biochemical Journal* **1991**, *274*, 381-386.

(39) Wolf, P. Nature and Significance of Platelet Products in Human Plasma. *British Journal of Haematology* **1967**, *13*, 269-&.

(40) Distler, J.; Pisetsky, D.; Huber, L.; Kalden, J.; Gay, S.; Distler, O. Microparticles as regulators of inflammation - Novel players of cellular crosstalk in the rheumatic diseases. *Arthritis and Rheumatism* **2005**, *52*, 3337-3348.

(41) E.M. Bevers, P. Comfurius, D.W.C Dekkers, R.F.A Zwaal Lipid translocation across the plasma membrane of mammalian cells. *Biochimica Et Biophysica Acta-Molecular and Cell Biology of Lipids* **1999**, *1439*, 317-330.

(42) Hugel, B.; Carmen, M.; Martinez, M.; Kunzelmann, C.; Freyssinet, J. Membrane microparticles: Two sides of the coin. *Physiology* **2005**, *20*, 22-27.

(43) Keller, S.; Sanderson, M. P.; Stoeck, A.; Altevogt, P. Exosomes: From biogenesis and secretion to biological function. *Immunology letters* **2006**, *107*, 102-108.

(44) del Conde, I.; Shrimpton, C.; Thiagarajan, P.; Lopez, J. Tissue-factor-bearing microvesicles arise from lipid rafts and fuse with activated platelets to initiate coagulation. *Blood* **2005**, *106*, 1604-1611.

(45) Hendrix, A.; Westbroek, W.; Bracke, M.; De Wever, O. An Ex(o)citing Machinery for Invasive Tumor Growth. *Cancer Research* **2010**, *70*, 9533-9537.

(46) Taylor, D. D.; Gercel-Taylor, C. Exosomes/microvesicles: mediators of cancer-associated immunosuppressive microenvironments. *Seminars in Immunopathology* **2011**, *33*, 441-454.

(47) Gonzales P.A., Zhou H.,Pisitkun T., Wang N.S., Star R.A., Knepper M.A., Yeun P.S.T. In *Isolation and Purification of Exosomes in Urine;* A.J. Rai, Ed.; The

Urinary Proteome; Methods and Protocols, Methods in Molecular Biology; Springer Science+Business Media: 2010; Vol. 641, pp 89.

(48) Musante, L.; Saraswat, M.; Duriez, E.; Byrne, B.; Ravida, A.; Domon, B.; Holthofer, H. Biochemical and Physical Characterisation of Urinary Nanovesicles following CHAPS Treatment. *Plos One* **2012**, *7*, e37279.

(49) Looze, C.; Yui, D.; Leung, L.; Ingham, M.; Kaler, M.; Yao, X.; Wu, W.; Shen, R.; Daniels, M.; Levine, S. Proteomic profiling of human plasma exosomes identifies PPAR gamma as an exosome-associated protein. *Biochemical and biophysical research communications* **2009**, *378*, 433-438.

(50) Boilard, E.; Nigrovic, P. A.; Larabee, K.; Watts, G. F. M.; Coblyn, J. S.; Weinblatt, M. E.; Massarotti, E. M.; Remold-O'Donnell, E.; Farndale, R. W.; Ware, J.; Lee, D. M. Platelets Amplify Inflammation in Arthritis via Collagen-Dependent Microparticle Production. *Science* **2010**, *327*, 580-583.

(51) Candiano, G.; Bruschi, M.; Musante, L.; Santucci, L.; Ghiggeri, G.; Carnemolla, B.; Orecchia, P.; Zardi, L.; Righetti, P. Blue silver: A very sensitive colloidal Coomassie G-250 staining for proteome analysis. *Electrophoresis* **2004**, *25*, 1327-1333.

(52) Kruger, N. In *The Protein Protocols Handbook;* Walker, J., Ed.; Humana Press: 2009; .

(53) Towbin, H.; Staehelin, T.; Gordon, J. Electrophoretic Transfer of Proteins from Polyacrylamide Gels to Nitrocellulose Sheets - Procedure and some Applications. *Proceedings of the National Academy of Sciences of the United States of America* **1979**, *76*, 4350-4354.

(54) Miura, R.; Yamagata, S.; Miura, Y.; Harada, T.; Yamagata, T. Analysis of Glycosaminoglycan-Degrading Enzymes by Substrate Gel-Electrophoresis (Zymography). *Analytical Biochemistry* **1995**, *225*, 333-340.

(55) Wessel, D.; Flugge, U. A Method for the Quantitative Recovery of Protein in Dilute-Solution in the Presence of Detergents and Lipids. *Analytical Biochemistry* **1984**, *138*, 141-143.

(56) Lin, Y.; Zhou, J.; Bi, D.; Chen, P.; Wang, X.; Liang, S. Sodium-deoxycholate-assisted tryptic digestion and identification of proteolytically resistant proteins. *Analytical Biochemistry* **2008**, *377*, 259-266.

(57) Lin, Y.; Liu, Y.; Li, J.; Zhao, Y.; He, Q.; Han, W.; Chen, P.; Wang, X.; Liang, S. Evaluation and optimization of removal of an acid-insoluble surfactant for shotgun analysis of membrane proteome. *Electrophoresis* **2010**, *31*, 2705-2713.

(58) Mi, H.; Dong, Q.; Muruganujan, A.; Gaudet, P.; Lewis, S.; Thomas, P. D. PANTHER version 7: improved phylogenetic trees, orthologs and collaboration with the Gene Ontology Consortium. *Nucleic acids research* **2010**, *38*, D204-D210.

(59) Schmidt, O.; Teis, D. The ESCRT machinery. *Current Biology* **2012**, *22*, R116-R120.

(60) Hjelmeland L.M. A Non-Denaturing Zwitterionic Detergent for Membrane Biochemistry - Design and Synthesis. *Proceedings of the National Academy of Sciences of the United States of America-Biological Sciences* **1980**, *77*, 6368-6370.

(61) Mathivanan, S.; Simpson, R. J. ExoCarta: A compendium of exosomal proteins and RNA RID D-2045-2009. *Proteomics* **2009**, *9*, 4997-5000.

(62) Ageberg, M.; Lindmark, A. Characterisation of the biosynthesis and processing of the neutrophil granule membrane protein CD63 in myeloid cells. *Clinical and Llaboratory Hematology* **2003**, *25*, 297-306.

(63) Moore, E. In *Autoimmune Diseases and their Environmental Triggers;* McFarland & Co Inc: Jefferson; NC/US, 2002; .

(64) Dugo,P.Cacciola,F.Kumm,T.Dugo,G.Mondello,L. Comprehensive multidimensional liquid chromatography: Theory and applications. *Journal of Chromatography A* **2008**, *1184*, 353-368.

(65) Thomas, P.; Campbell, M.; Kejariwal, A.; Mi, H.; Karlak, B.; Daverman, R.; Diemer, K.; Muruganujan, A.; Narechania, A. PANTHER: A library of protein families and subfamilies indexed by function. *Genome Research* **2003**, *13*, 2129-2141.

(66) Welton, J. L.; Khanna, S.; Giles, P. J.; Brennan, P.; Brewis, I. A.; Staffurth, J.; Mason, M. D.; Clayton, A. Proteomics Analysis of Bladder Cancer Exosomes. *Molecular & Cellular Proteomics* **2010**, *9*, 1324-1338.

(67) Fullgrabe, J.; Hajji, N.; Joseph, B. Cracking the death code: apoptosis-related histone modifications. *Cell death and differentiation* **2010**, *17*, 1238-1243.

(68) Vladutiu, A. Immunoglobulin D: Properties, measurement, and clinical relevance. *Clinical and Diagnostic Laboratory Immunology* **2000**, *7*, 131-140.

(69) Lee, Y.; Choi, J.; Hwang, I.; Lee, J.; Lee, J.; Kim, A.; Huh, J.; Koh, Y.; Koh, G.; Son, H.; Masuzaki, H.; Hotta, K.; Alfadda, A.; Kim, J. Adipocytokine Orosomucoid Integrates Inflammatory and Metabolic Signals to Preserve Energy Homeostasis by Resolving Immoderate Inflammation. *Journal of Biological Chemistry* **2010**, *285*, 22174-22185.

(70) Garcia-Munoz, A.; Rodriguez, J.; Bologna-Molina, R.; Cazares-Raga, F.; Hernandez-Hernandez, F.; Farfan-Morales, J.; Tnujillo, J.; Liceaga-Escalera, C.; Mendoza-hernandez, G. The orosoumcoid 1 protein (alpha 1 acid glycoprotein) is overexpressed in odontogenic myxoma. *Proteome Science* **2012**, *10*, 49.

(71) Barrett, A.; Brown, M.; Sayers, C. Electrophoretically Slow and Fast Forms of the Alpha-2-Macroglobulin Molecule. *Biochemical Journal* **1979**, *181*, 401-418.

(72) Fuchs, S.; Skwara, A.; Bloch, M.; Dankbar, B. Differential induction and regulation of matrix metalloproteinases in osteoarthritic tissue and fluid synovial fibroblasts. *Osteoarthritis and Cartilage* **2004**, *12*, 409-418.

(73) Troeberg, L.; Nagase, H. Proteases involved in cartilage matrix degradation in osteoarthritis. *Biochimica Et Biophysica Acta-Proteins and Proteomics* **2012**, *1824*, 133-145.

(74) Marini, S.; Francesco Fasciglione, G.; Monteleone, G.; Maiotti, M.; Tarantino, U.; Coletta, M. A correlation between knee cartilage degradation observed by arthroscopy and synovial proteinases activities. *Clinical Biochemistry* **2003**, *36*, 295-304.

(75) Tchetverikov, I.; Lohmander, L. S.; Verzijl, N.; Huizinga, T. W. J.; TeKoppele, J. M.; Hanemaaijer, R.; DeGroot, J. MMP protein and activity levels in synovial fluid from patients with joint injury, inflammatory arthritis, and osteoarthritis. *Annals of the Rheumatic Diseases* **2005**, *64*, 694-698.

(76) Maiotti, M.; Monteleone, G.; Tarantino, U.; Fasciglione, G.; Marini, S.; Coletta, M. Correlation between osteoarthritic cartilage damage and levels of proteinases and proteinase inhibitors in synovial fluid from the knee joint. *Arthroscopy* **2000**, *16*, 522-526.

(77) Makowski, G.; Ramsby, M. Zymographic analysis of latent and activated forms of matrix metalloproteinase-2 and -9 in synovial fluid: correlation to polymorphonuclear leukocyte infiltration and in response to infection. *Clinica Chimica Acta* **2003**, *329*, 77-81.

(78) Girish, K. S.; Kemparaju, K. The magic glue hyaluronan and its eraser hyaluronidase: A biological overview. *Life Sciences* **2007**, *80*, 1921-1943.

(79) Tranchepain, F.; Deschrevel, B.; Courel, M.; Levasseur, N.; Le Cerf, D.; Loutelier-Bourhis, C.; Vincent, J. A complete set of hyaluronan fragments obtained from hydrolysis catalyzed by hyaluronidase: Application to studies of hyaluronan mass distribution by simple HPLC devices. *Analytical Biochemistry* **2006**, *348*, 232-242.

(80) Thery, C.; Boussac, M.; Veron, P.; Ricciardi-Castagnoli, P.; Raposo, G.; Garin, J.; Amigorena, S. Proteomic analysis of dendritic cell-derived exosomes: A secreted

subcellular compartment distinct from apoptotic vesicles. *Journal of Immunology* **2001**, *166*, 7309-7318.

(81) Norata, G.; Pirillo, A.; Ammirati, E.; Catapano, A. Emerging role of high density lipoproteins as a player in the immune system. *Atherosclerosis* **2012**, *220*, 11-21.

(82) Bobrie, A.; Colombo, M.; Krumeich, S.; Raposo, G.; Thery, C. Diverse subpopulations of vesicles secreted by different intracellular mechanisms are present in exosome preparations obtained by differential ultracentrifugation. *Journal of Extracellular Vesicles* **2012**, *1*.

(83) Jamison, F. W. I.; Foster, T. J.; Barker, J. A.; Hills, R. D. J.; Guvench, O. Mechanism of Binding Site Conformational Switching in the CD44-Hyaluronan Protein-Carbohydrate Binding Interaction. *Journal of Molecular Biology* **2011**, *406*, 631-647.

(84) Proc, J.; Kuzyk, M.; Hardie, D.; Yang, J.; Smith, D.; Jackson, A.; Parker, C.; Borchers, C. A Quantitative Study of the Effects of Chaotropic Agents, Surfactants, and Solvents on the Digestion Efficiency of Human Plasma Proteins by Trypsin. *Journal of Proteome Research* **2010**, *9*, 5422-5437.

(85) Labeta M.O.; Fernandez N.; Festenstein H. Solubilization Effect of Nonidet P-40, Triton X-100 and Chaps in the Detection of Mhc-Like Glycoproteins. *Journal of Immunological Methods* **1988**, *112*, 133-138.

(86) Levy, S.; Shoham, T. Protein-protein interactions in the tetraspanin web. *Physiology* **2005**, *20*, 218-224.

(87) Gilmore, J.; Washburn, M. Advances in shotgun proteomics and the analysis of membrane proteomes. *Journal of Proteomics* **2010**, *73*, 2078-2091.

(88) Nielsen, C.; Ostergaard, O.; Stener, L.; Iversen, L.; Truedsson, L.; Gullstrand, B.; Jacobsen, S.; Heegaard, N. Increased IgG on Cell-Derived Plasma Microparticles in Systemic Lupus Erythematosus Is Associated With Autoantibodies and Complement Activation. *Arthritis and Rheumatism* **2012**, *64*, 1227-1236.

(89) Draeger, A.; Monastyrskaya, K.; Babiychuk, E. Plasma membrane repair and cellular damage control: The annexin survival kit. *Biochemical pharmacology* **2011**, *81*, 703-712.

(90) Pisetsky, D. Microparticles as Autoantigens: Making Immune Complexes Big. *Arthritis and Rheumatism* **2012**, *64*, 958-961.

(91) Ramirez-Alvarado, M.; Ward, C.; Huang, B.; Gong, X.; Hogan, M.; Madden, B.; Charlesworth, M. C.; Leung, N. Differences in Immunoglobulin Light Chain

Species Found in Urinary Exosomes in Light Chain Amyloidosis (AL). *Plos One* **2012**, *7*, e38061.

(92) Mateos, J.; Lourido, L.; Fernandez-Puente, P.; Calamia, V.; Fernandez-Lopez, C.; Oreiro, N.; Ruiz-Romero, C.; Blanco, F. J. Differential protein profiling of synovial fluid from rheumatoid arthritis and osteoarthritis patients using LC-MALDI TOF/TOF. *Journal of Proteomics* **2012**, *75*, 2869-2878.

(93) Gobezie, R.; Kho, A.; K., B.; Thornhill, T.; Chase, M.; Millett, P.; Lee, D. High abundance synovial fluid proteome: distinct profiles in health and osteoarthritis. *Arthritis Research & Therapy* **2007**, *9*, R36.

(94) Rosenthal, A. K.; Gohr, C. M.; Ninomiya, J.; Wakim, B. T. Proteomic analysis of articular cartilage vesicles from normal and osteoarthritic cartilage. *Arthritis & Rheumatism* **2011**, *63*, 401-411.

(95) van Venrooij, W.; Pruijn, G. Citrullination: a small change for a protein with great consequences for rheumatoid arthritis. *Arthritis Research* **2000**, *2*, 249-251.

(96) Nauta, A.; Trouw, L.; Daha, M.; Tijsma, O.; Nieuwland, R.; Schwaeble, W.; Gingras, A.; Mantovani, A.; Hack, E.; Roos, A. Direct binding of C1q to apoptotic cells and cell blebs induces complement activation. *European Journal of Immunology* **2002**, *32*, 1726-1736.

(97) Gasser, O.; Schifferli, J. Activated polymorphonuclear neutrophils disseminate anti-inflammatory microparticles by ectocytosis. *Blood* **2004**, *104*, 2543-2548.

(98) Lai, D.; Tu, Y.; Hsieh, Y.; Hsu, W.; Lee, C.; Cheng, W.; Hsieh, F.; Li, H. Angiopoietin-like protein 1 expression is related to intermuscular connective tissue and cartilage development. *Developmental Dynamics* **2007**, *236*, 2643-2652.

(99) Matsumoto, K.; Kamiya, N.; Suwan, K.; Atsumi, F.; Shimizu, K.; Shinomura, T.; Yamada, Y.; Kimata, K.; Watanabe, H. Identification and characterization of versican/PG-M aggregates in cartilage. *Journal of Biological Chemistry* **2006**, *281*, 18257-18263.

(100) Nam, E.; Sa, K.; You, D.; Cho, J.; Seo, J.; Han, S.; Park, J.; Kim, S.; Kyung, H.; Kim, I.; Kang, Y. Up-regulated transforming growth factor beta-inducible gene h3 in rheumatoid arthritis mediates adhesion and migration of synoviocytes through alpha v beta 3 integrin - Regulation by cytokines. *Arthritis and Rheumatism* **2006**, *54*, 2734-2744.

(101) Hashimoto, S.; Ochs, R.; Rosen, F.; Quach, J.; McCabe, G.; Solan, J.; Seegmiller, J.; Terkeltaub, R.; Lotz, M. Chondrocyte-derived apoptotic bodies and calcification of articular cartilage. *Proceedings of the National Academy of Sciences of the United States of America* **1998**, *95*, 3094-3099.

(102) Zhang, Z.; Jin, W.; Beckett, J.; Otto, T.; Moed, B. A proteomic approach for identification and localization of the pericellular components of chondrocytes. *Histochemistry and Cell Biology* **2011**, *136*, 153-162.

(103) Davidson, E.; van der Kraan, P.; van den Berg, W. TGF-beta and osteoarthritis. *Osteoarthritis and Cartilage* **2007**, *15*, 597-604.

(104) Thapa, N.; Lee, B.; Kim, I. TGFBIp/beta ig-h3 protein: A versatile matrix molecule induced by TGF-beta. *International Journal of Biochemistry & Cell Biology* **2007**, *39*, 2183-2194.

(105) Hanssen, E.; Reinboth, B.; Gibson, M. Covalent and non-covalent interactions of beta ig-h3 with collagen VI - beta ig-h3 is covalently attached to the amino-terminal region of collagen VI in tissue microfibrils. *Journal of Biological Chemistry* **2003**, *278*, 24334-24341.

(106) Cao, W.; Tan, P.; Lee, C.; Zhang, H.; Lu, J. A transforming growth factor-beta-induced protein stimulates endocytosis and is up-regulated in immature dendritic cells. *Blood* **2006**, *107*, 2777-2785.

(107) Murray, D.; Bush, P.; Brenkel, I.; Hall, A. Abnormal Human Chondrocyte Morphology Is Related to Increased Levels of Cell-Associated IL-1 beta and Disruption to Pericellular Collagen Type VI. *Journal of Orthopaedic Research* **2010**, *28*, 1507-1514.

(108) Polur, I.; Lee, P.; Servais, J.; Xu, L.; Li, Y. Role of HTRA1, a serine protease, in the progression of articular cartilage degeneration. *Histology and histopathology* **2010**, *25*, 599-608.

(109) Grau, S.; Richards, P.; Kerr, B.; Hughes, C.; Caterson, B.; Williams, A.; Junker, U.; Jones, S.; Clausen, T.; Ehrmann, M. The role of human HtrA1 in arthritic disease. *Journal of Biological Chemistry* **2006**, *281*, 6124-6129.

(110) Gupta, K.; Shukla, M.; Cowland, J.; Malemud, C.; Haqqi, T. Neutrophil gelatinase-associated lipocalin is expressed in osteoarthritis and forms a complex with matrix metalloproteinase 9. *Arthritis and Rheumatism* **2007**, *56*, 3326-3335.

(111) Tsuchiya, A.; Yano, M.; Tocharus, J.; Kojima, H.; Fukumoto, M.; Kawaichi, M.; Oka, C. Expression of mouse HtrA1 serine protease in normal bone and cartilage and its upregulation in joint cartilage damaged by experimental arthritis. *Bone* **2005**, *37*, 323-336.

(112) Xu, L.; Servais, J.; Polur, I.; Kim, D.; Lee, P. L.; Chung, K.; Li, Y. Attenuation of Osteoarthritis Progression by Reduction of Discoidin Domain Receptor 2 in Mice. *Arthritis and Rheumatism* **2010**, *62*, 2736-2744.

(113) Goldring, M.; Goldring, S. Osteoarthritis. *Journal of Cellular Physiology* **2007**, *213*, 626-634.

(114) Kleiner, D.; Stetlerstevenson, W. Quantitative Zymography - Detection of Picogram Quantities of Gelatinases. *Analytical Biochemistry* **1994**, *218*, 325-329.

(115) Snoek-van Beurden, P.; Von den Hoff, J. Zymographic techniques for the analysis of matrix metalloproteinases and their inhibitors. *BioTechniques* **2005**, *38*, 73-83.

(116) Visse, R.; Nagase, H. Matrix metalloproteinases and tissue inhibitors of metalloproteinases - Structure, function, and biochemistry. *Circulation Research* **2003**, *92*, 827-839.

(117) Dreier, R.; Grassel, S.; Fuchs, S.; Schaumburger, J.; Bruckner, P. Pro-MMP-9 is a specific macrophage product and is activated by osteoarthritic chondrocytes via MMP-3 or a MT1-MMP/MMP-13 cascade. *Experimental cell research* **2004**, *297*, 303-312.

(118) van Meurs, J.; van Lent, P.; Stoop, R.; Holthuysen, A.; Singer, I.; Bayne, E.; Mudgett, J.; Poole, R.; Billinghurst, C.; van der Kraan, P.; Buma, P.; van den Berg, W. Cleavage of aggrecan at the ASN(341)-PHE342 site coincides with the initiation of collagen damage in murine antigen-induced arthritis - A pivotal role for stromelysin 1 in matrix metalloproteinase activity. *Arthritis and Rheumatism* **1999**, *42*, 2074-2084.

(119) Heilpern, A. J.; Wertheim, W.; He, J.; Perides, G.; Bronson, R. T.; Hu, L. T. Matrix Metalloproteinase 9 Plays a Key Role in Lyme Arthritis but Not in Dissemination of Borrelia burgdorferi. *Infection and immunity* **2009**, *77*, 2643-2649.

(120) Clements, K.; Price, J.; Chambers, M.; Visco, D.; Poole, A.; Mason, R. Gene deletion of either interleukin-1 beta, interleukin-1 beta-converting enzyme, inducible nitric oxide synthase, or stromelysin 1 accelerates the development of knee osteoarthritis in mice after surgical transection of the medial collateral ligament and partial medial meniscectomy. *Arthritis and Rheumatism* **2003**, *48*, 3452-3463.

(121) Glasson, S. S. In vivo Osteoarthritis target validation utilizing genetically-modified mice. *Current Drug Targets* **2007**, *8*, 367-376.

(122) Sinz, A.; Bantscheff, M.; Mikkat, S.; Ringel, B.; Drynda, S.; Kekow, J.; Thiesen, H.; Glocker, M. O. Mass spectrometric proteome analyses of synovial fluids and plasmas from patients suffering from rheumatoid arthritis and comparison to reactive arthritis or osteoarthritis. *Electrophoresis* **2002**, *23*, 3445-3456.

(123) Hessian P.A.; Edgewood J.; Hogg N. Mrp-8 and Mrp-14, 2 Abundant Ca-2+-Binding Proteins of Neutrophils and Monocytes. *Journal of Leukocyte Biology* **1993**, *53*, 197-204.

(124) Liao, H.; Wu, J.; Kuhn, E.; Chin, W.; Chang, B.; Jones, M. D.; O'Neil, S.; Clauser, K. R.; Karl, J.; Hasler, F.; Roubenoff, R.; Zolg, W.; Guild, B. C. Use of mass spectrometry to identify protein biomarkers of disease severity in the synovial fluid and serum of patients with rheumatoid arthritis. *Arthritis & Rheumatism* **2004**, *50*, 3792-3803.

(125) Wilson, R.; Whitelock, J. M.; Bateman, J. F. Proteomics makes progress in cartilage and arthritis research. *Matrix Biology* **2009**, *28*, 121-128.

(126) van Lent, P. L. E. M.; Grevers, L.; Blom, A. B.; Sloetjes, A.; Mort, J. S.; Vogl, T.; Nacken, W.; van den Berg, W. B.; Roth, J. Myeloid-related proteins S100A8/S100A9 regulate joint inflammation and cartilage destruction during antigen-induced arthritis. *Annals of the Rheumatic Diseases* **2008**, *67*, 1750-1758.

(127) Zreiqat, H.; Belluoccio, D.; Smith, M.; Wilson, R.; Rowley, L.; Jones, K.; Ramaswamy, Y.; Vogl, T.; Roth, J.; Bateman, J.; Little, C. S100A8 and S100A9 in experimental osteoarthritis. *Arthritis Research & Therapy* **2010**, *12*, R16.

(128) Loeser, R.; Goldring, S.; Scanzello, C.; Goldring, M. Osteoarthritis: A disease of the joint as an organ. *Arthritis and Rheumatism* **2012**, *64*, 1697-1707.

(129) Adams, J. Thrombospondins: Multifunctional regulators of cell interactions. *Annual Review of Cell and Developmental Biology* **2001**, *17*, 25-51.

(130) Chen, F. H.; Herndon, M. E.; Patel, N.; Hecht, J. T.; Tuan, R. S.; Lawler, J. Interaction of cartilage oligomeric matrix protein/thrombospondin 5 with aggrecan. *Journal of Biological Chemistry* **2007**, *282*, 24591-24598.

(131) DiCesare, P.; Carlson, C.; Stolerman, E.; Hauser, N.; Tulli, H.; Paulsson, M. Increased degradation and altered tissue distribution of cartilage oligomeric matrix protein in human rheumatoid and osteoarthritic cartilage. *Journal of Orthopaedic Research* **1996**, *14*, 946-955.

(132) Gagarina, V.; Carlberg, A. L.; Pereira-Mouries, L.; Hall, D. J. Cartilage Oligomeric Matrix Protein Protects Cells against Death by Elevating Members of the IAP Family of Survival Proteins. *Journal of Biological Chemistry* **2008**, *283*, 648-659.

(133) Wang, Q.; Rozelle, A.; Lepus, C.; Scanzello, C.; Song, J.; Larsen, D.; Crish, J.; Bebek, G.; Ritter, S.; Lindstrom, T.; Hwang, I.; Wong, H.; Punzi, L.; Encarnacion, A.; Shamloo, M.; Goodman, S.; Wyss-Coray, T.; Goldring, S.; Banda, N.; Thurman, J.; Gobezie, R.; Crow, M.; Holers, V.; Lee, D.; Robinson, W.

Identification of a central role for complement in osteoarthritis. *Nature medicine* **2011**, *17*, 1674-U196.

(134) Happonen, K.; Saxne, T.; Aspberg, A.; Morgelin, M.; Heinegard, D.; Blom, A. Regulation of Complement by Cartilage Oligomeric Matrix Protein Allows for a Novel Molecular Diagnostic Principle in Rheumatoid Arthritis. *Arthritis and Rheumatism* **2010**, *62*, 3574-3583.

(135) Cook, T.; Botto, M. Mechanisms of Disease: the complement system and the pathogenesis of systemic lupus erythematosus. *Nature Clinical Practice Rheumatology* **2006**, *2*, 330.

(136) Hunter D.J., Li J., LaValley M., Bauer D.C. Nevitt M., De groot J., Poole R., Eyre D., Guermazi A., Gale D., Felson D.T. Cartilage markers and their association with cartilage loss on magnetic resonance imaging in knee osteoarthritis: the Boston Osteoarthritis Knee Study. *Arthritis Research & Therapy* **2007**, *9*, 108.

(137) Williams, F.; Spector, T. Biomarkers in osteoarthritis. *Arthritis Research & Therapy* **2008**, *10*, 101.

(138) Hamilton, K.; Zhao, J.; Sims, P. Interaction between Apolipoprotein-A-i and Apolipoprotein-A-Ii and the Membrane Attack Complex of Complement - Affinity of the Apoproteins for Polymeric-C9. *Journal of Biological Chemistry* **1993**, *268*, 3632-3638.

(139) Csoka, A.; Frost, G.; Stern, R. The six hyaluronidase-like genes in the human and mouse genomes. *Matrix Biology* **2001**, *20*, 499-508.

(140) Bourguignon, L.; Singleton, P.; Diedrich, F.; Stern, R.; Gilad, E. CD44 interaction with Na+-H+ exchanger (NHE1) creates acidic microenvironments leading to hyaluronidase-2 and cathepsin B activation and breast tumor cell invasion. *Journal of Biological Chemistry* **2004**, *279*, 26991-27007.

(141) Scanzello, C.; Plaas, A.; Crow, M. Innate immune system activation in osteoarthritis: is osteoarthritis a chronic wound? *Current Opinion in Rheumatology* **2008**, *20*, 565-572.

Chapter 4

Characterisation of differentially expressed glycoproteins in synovial fluid between the various arthritic pathologies employing lectin affinity chromatography and mass spectrometry

4.0 Introduction

4.0.1 Glycobiology

The term glycobiology or glycoscience is generally reserved for the study of sugar functionality in living organisms. The function of carbohydrates in the context of energy metabolism in cells, fall outside the scope of what is generally termed glycobiology. Specifically, it is usually defined as the study of the role of covalently bound sugars to biomolecules (e.g. proteins and lipids) in the form of mono-, oligo- or polysaccharides [1]. These glycosylated moieties are termed glycoconjugates in general, and glycoproteins and glycolipids in particular. Thus glycobiology is the science of glycoconjugates [2]. Sugar decorated proteins or lipids are referred to as glycans. These glycans are hetero-oligomers and are structurally more diverse than the homo-polymeric storage carbohydrates e.g. glycogen and amylase.

4.0.2 Glycan Composition – monosaccharides are the building blocks of glycosylation

Glycans are mainly composed of hexoses – monosaccharides with the general formula $C_6H_{12}O_6$. Four of the six carbon atoms in a hexose are chiral centres since C_2, C_3, C_4 and C_5 are bonded to four chemically distinct groups. As there are four chiral centres, each of which has two isoforms, there are therefore 16 hexose stereoisomers. The prefixes D- and L- are used to distinguish between a pair of stereoisomers. For example, D-glucose and L-glucose are stereoisomers. The D- and L- forms differ in the orientation of the –OH group at C_5. The most common monosaccharides found in human glycan structures are shown in Figure 1. Also included are the three letter abbreviations for each sugar.

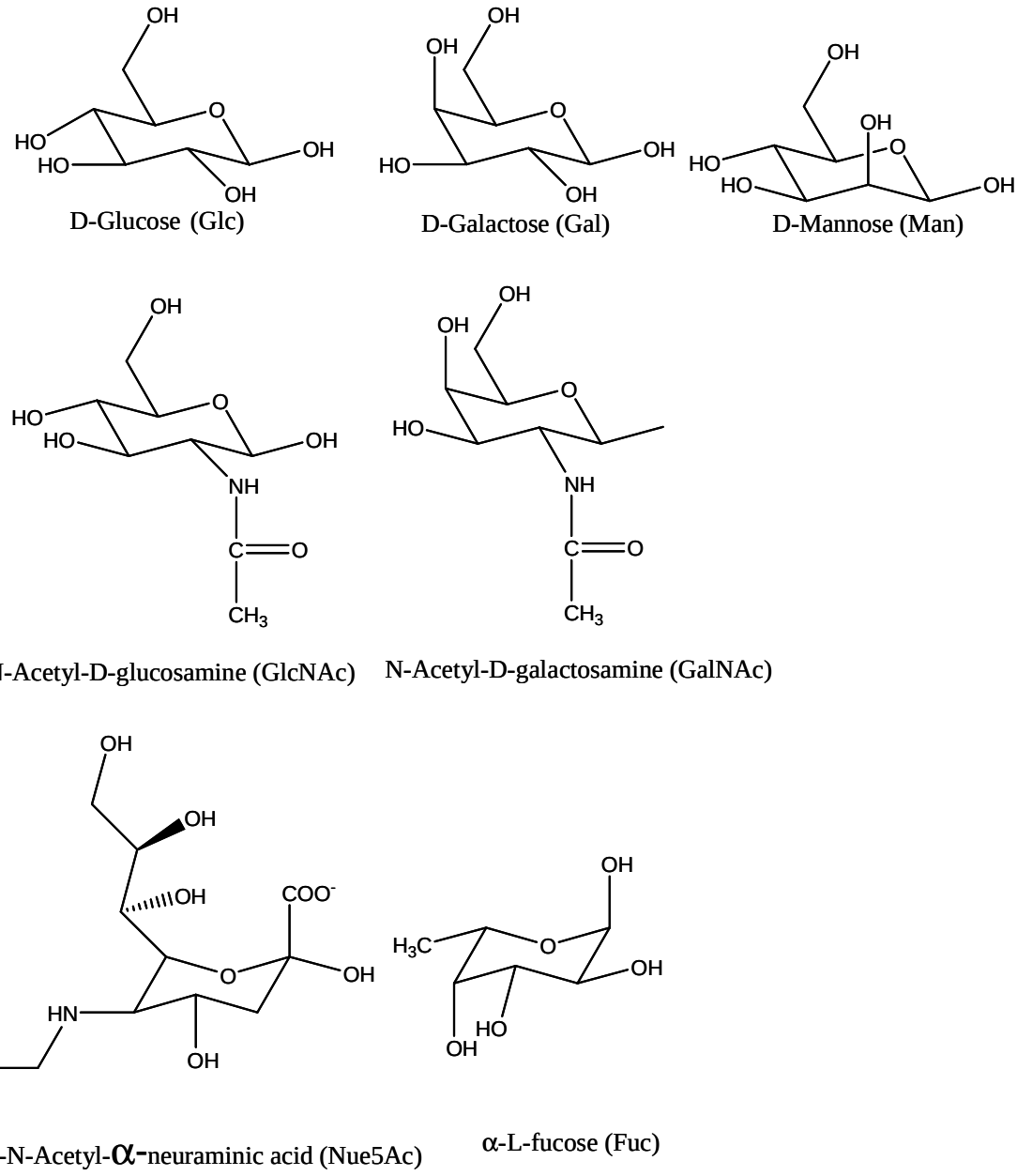

Figure 4.1: *Structure of common monosaccharides found in mammalian glycoconjugates.*

Epimerisation is the term given to a change in the stereochemical configuration of a single carbon atom in a sugar. From Figure 4.11, it can be seen that D-glucose and D-galactose are epimers as are D-glucose and D-mannose. Substitution of the C_2-OH group of glucose or galactose with an acetylated amino group yields N-acetyl-D-glucosamine

and N-acetyl-galactosamine respectively. Fucose is structurally related to galactose whereby the C_6 -OH group of Gal is replaced with a $–CH_3$ group. C_1 is referred to as the anomeric carbon and two configurations or anomers are known by the labels α and β. The α anomer is distinguished by possessing an axial –OH group on the anomeric carbon, while in the β anomer, the –OH group is in the equatorial position.

Monosaccharides can react with each other to form di-, oligo- and polysaccharides. The bond between any two monosaccharides is referred to as a glycosidic linkage. Formation of the glycosidic linkage occurs following a condensation reaction between two monosaccharides with the concomitant elimination of a water molecule. For example, the formation of lactose - a disaccharide composed of galactose and glucose – is shown in Figure 4.2.

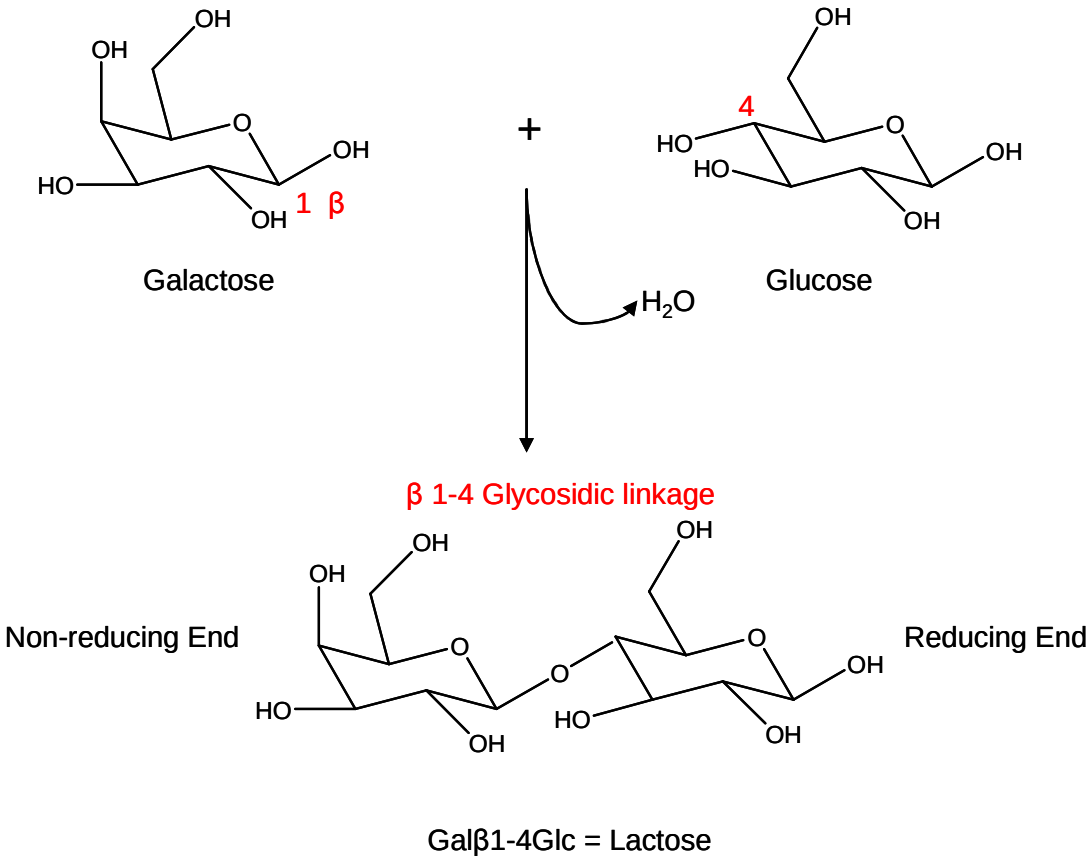

Figure 4.2: *Formation of a glycosidic linkage between galactose and glucose monosaccharides to form a lactose disaccharide molecule.*

The synthesis of a di-, oligo- and polysaccharides through glycosidic linkages requires an input of energy [1]. In general, glycosyl-transferase catalyses a transfer of one

monosaccharide -in the form of a nucleotide sugar donor- to another monosaccharide acceptor molecule. Each transferase is specific for a particular glycosidic linkage between any two specific monosaccharides. The hydrolysis of glycosidic bonds also requires specific enzymes known as glycosidases. Each glycosidase catalyses cleavage of a specific link between specific sugars.

4.0.3 Major classes of glycoconjugates

In broad terms, there are two main groups of glycoconjugates: those attached to lipids (glycolipids) and those attached to proteins (glycoproteins). The analysis of glycolipids is beyond the scope of this project and so will receive no further attention. Glycoproteins are generally sub-divided into two classes; *N*-linked and *O*-linked glycans. The *N* and *O* refer to the species of atom on the amino acid residue of the protein, to which the glycan is attached. Thus an *N*-linked glycan is covalently bonded to a nitrogen atom in the amino acid side chain, while for an *O*-linked glycan the bonding site is to an amino acid oxygen atom. The synthesis of both *N*- and *O*-linked species is initiated in the lumen of the endoplasmic reticulum (ER) and further processed in the Golgi apparatus of the cell. Ultimately, many types of glycoprotein are found at the extracellular surface of the plasma membrane or secreted into biological fluids and the extracellular matrix that surround cells.

4.0.3.1 N-linked glycosylation

In this class of glycoprotein, the carbohydrate structures are attached to the amide nitrogen atom of an asparagine (Asn) side chain. More specifically, a specific amino acid sequence is generally required for *N*-glycosylation. These sequences are usually either –*Asn-Xaa-Ser*- or –*Asn-Xaa-Thr*- where Xaa is any amino acid residue except proline. In animal cells the monosaccharide attached to the Asn residue is almost always N-acetyl-D-glucosamine (GlcNAc). *N*-linked glycan synthesis is believed to be divided into three stages: (1) formation of a dolichol (Dol) lipid-linked precursor oligosaccharide in the

cytosol of the ER; (2) complete transfer of this 14-saccharide core oligosaccharide unit to a nascent, unfolded polypeptide in the lumen of the ER; and (3) processing the transferred oligosaccharide i.e. trimming some of the original sugars and completion of terminal glycosylation in the Golgi body. An overall schematic diagram depicting the entire *N*-glycosylation biosynthesis process is shown in Figure 4.3.

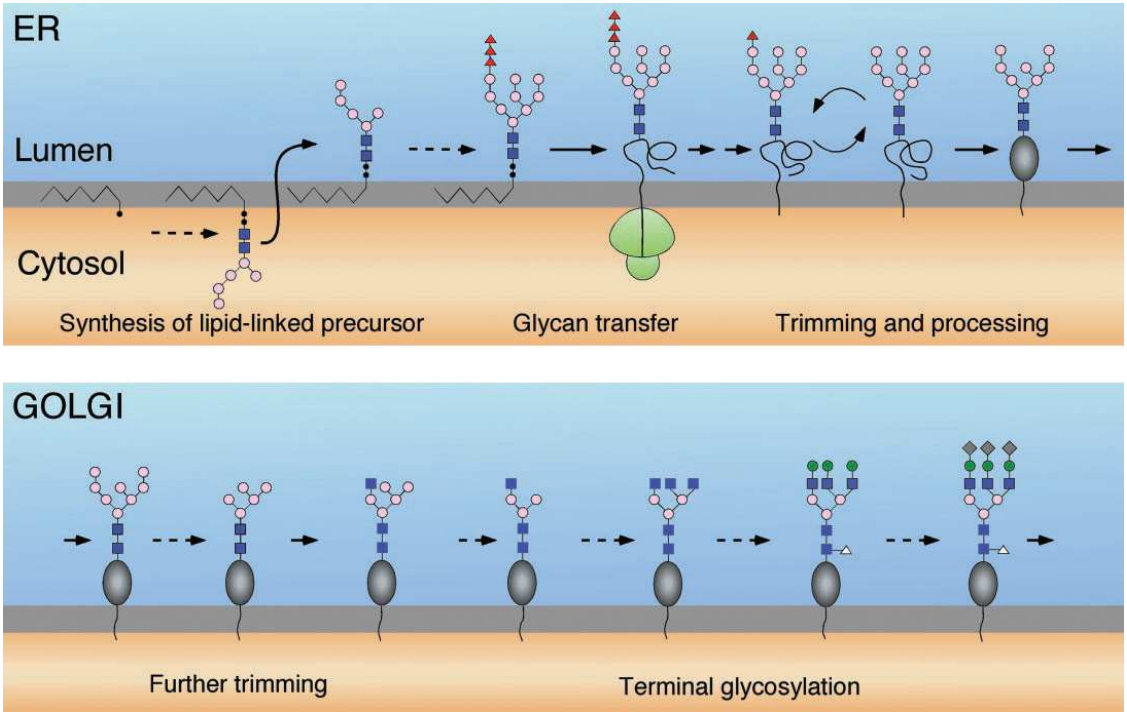

Figure 4.3 *Sequence of stages leading to the biosynthesis of N-linked glycans. Synthesis begins in the cytosol surface of the ER. Following a flip across the ER membrane, individual monosaccharides are attached one at a time. Transfer of the sugar structure to the nascent protein takes place by means of a catalytic reaction with oligosaccharyltransferase. The entire edifice then transfers to the Golgi body, where further trimming and processing takes place. Diagram taken from Helenius et al.*[3]

Biosynthesis of the precursor dolichol-linked oligosaccharide is achieved by the sequential addition of monosaccharides catalysed by specific glycosidases. The final precursor has a total of two GlcNAc residues, nine mannose residues (Man) and three glucose residues (Glc) i.e. Dol-$(GlcNAc)_2$ $(Man)_9(Glc)_3$. The structure of complete precursor can be seen in Figure 4.4.

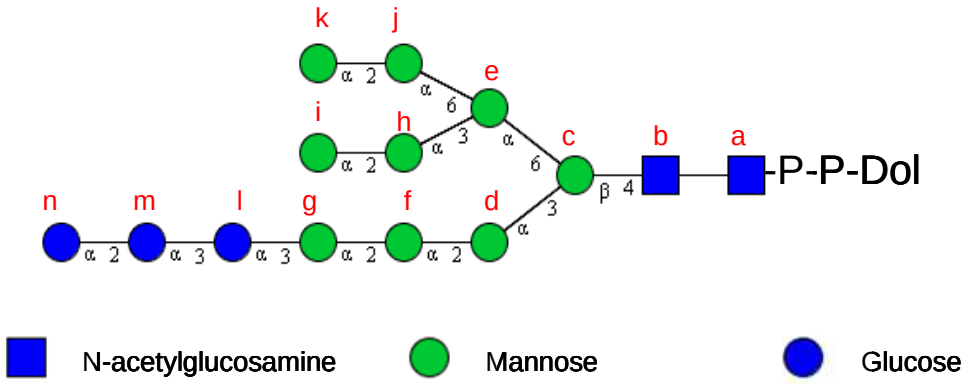

Figure 4.4: *The dolichol- oligosaccharide core structure. The letters in red indicate the order of addition of the monosaccharide units* [4] .

The entire core glycan sequence is then transferred to the newly-formed polypeptide as it emerges from the ribosome in the cytosol of the ER. This is achieved through use of the enzyme, oligosaccharyltransferase and it is this enzyme that recognises the –Asn-Xaa-Ser/Thr- sequence. The next stage is the removal of the glucose residues. This is important for the protein folding stage. The precise detail as to how this comes about is not yet clear [5]; i.e. whether all three glucose residues are removed at once and then one put back later or, just two are removed initially remains uncertain. However, one glucose residue is required for the next step – the attachment of the molecular chaperone, calnexin. Calnexin is a lectin that is crucial for aiding the folding of the linear polypeptide in the cytosol of the E.

Glycans are usually classed as having high mannose, complex, hybrid or truncated structures. The degree of heterogeneity is not only determined by the individual sugar residues, but by the number of antenna and/or polylactoseamine extensions. Glycans can be bi-, tri-, tetra- or more rarely, penta-antennary. Figure 4.5 displays the various structures that *N*-glycans may adapt.

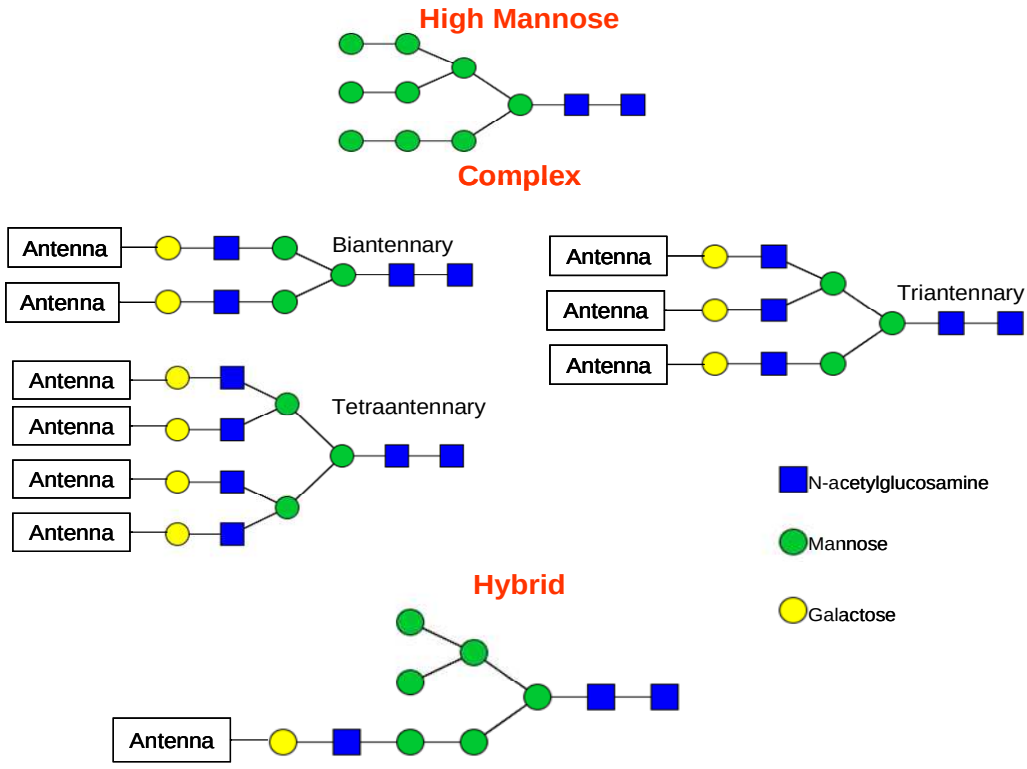

Figure 4.5: *The various structure types possible in N-linked glycosylation.*

Polylactoseamine extensions are composed of number of (Galβ1-4GlcNAcβ1-)$_n$ disaccharide units within one of the antenna. Fucosylation of the GlcNAc residue directly attached to the Asn residue or on the antennae is another modification possibility [3]. Despite the structural composition of each antenna, all *N*-linked glycans may be capped with an N-acetylneuraminic acid- galactose (NeuAc-Gal) disaccharide. The sialic acid, NeuAc residue is either α2-3 or α2-6 to the galactose. A summary of the various potential modifications that can occur are shown in Figure 4.6.

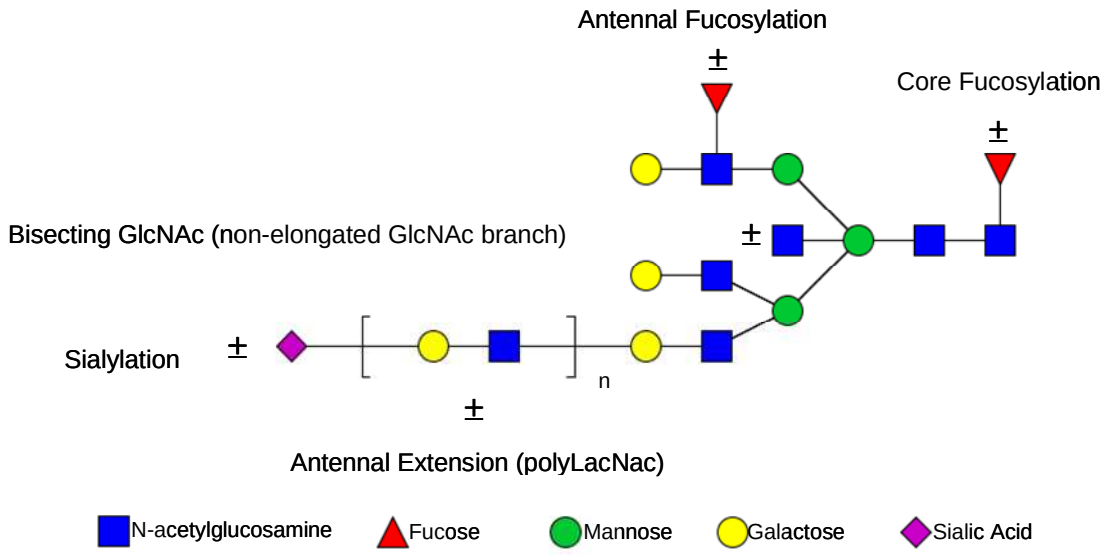

Figure 4.6: *A summary of the various potential modifications that N-glycans may adopt which leads to heterogeneities in structure and composition*

4.0.3.2 O-linked glycosylation

O-linked glycans are synthesised following an initial attachment of a GalNAc monosaccharide to either a Ser or Thr amino acid residue. The point of attachment to the Ser/Thr amino acid is the oxygen atom in the side chain. Following attachment of the GalNAc residue to Ser/Thr, a Galβ1-3 attachment to the GalNac forms what is termed a core-1 *O*-linked glycan. This is either disialyated to complete the core-1 structure or further extended to produce a core-2 *O*-linked glycan. Core-1 and -2 structures may be seen in Figure 4.7.

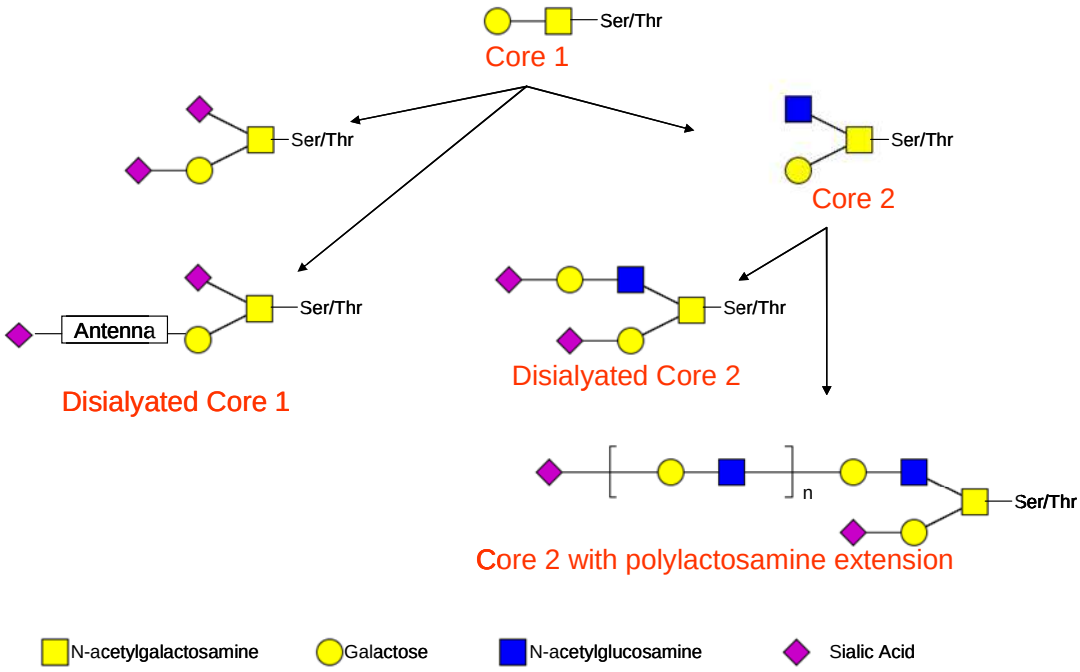

Figure 4.7: *Core 1 and 2 structures attached to Ser and Thr side chains through a GalNAc sugar residue.*

Unlike *N*-glycosylation, there is no preformed core structure that is formed before the final glycan structure is established. Further, *O*-glycosylation is prominent in regions containing high levels of proline and alanine. A further difference between *O*- and *N*-linked glycosylation is that *O*-linked glycans are considered post-translational modifications that take place in the Golgi apparatus [3].

There are two groups of glycoproteins in particular that are dominated by a large number of *O*-linked sugars. These are mucins and proteoglycans. In mucins, sialylation of the core 1 structures imparts regions of negative charge on the glycans. This charge in turn has the capacity to bind large amounts of water, which in turn, aids retention of water for cells lying close to the outside environment. In addition to water retention, mucins serve as lubrication and help protect the organism from invasion by microorganisms. Finally,

cross linking between the glycans through di-sulphide bonds allows for the formation of gels.

Proteoglycans also have the ability to bind water, but their primary function is to provide structure rather than lubrication. Another notable difference between mucins and proteoglycans is that the *O*-linked glycans on mucins are small, whereas those attached to proteoglycans may contain approximately 100 residues each. These long structures possess an underlying repeating disaccharide unit and are known as glycosaminoglycans (GAGs). Examples of these GAGs are hyaluronic acid, chondroitin sulphate, dermatan sulphate, heparin sulphate and keratin sulphate. Aggrecan is one the major proteoglycans of cartilage. Here, chondroitin sulphate is *O*-linked to a polypeptide filament, while keratin sulphate is *N*-linked [6]. These in turn are linked in their hundreds to a central filament of hyaluronic acid.

It is generally acknowledged that understanding the structure-function relationship for glycans is much more difficult than for any other class of biopolymer [1]. This is a consequence of the high degree of heterogeneity that glycosylation can entail by virtue of, for example, potential multiple branching, a diversity of linkages, fucosylation of the outer arm and various types and differing extents of terminal sialylation [7 8 9]. There are more than 30 sialic acid structural types that may have significance in recognition processes [2]. Though proteins possess a range of biological roles e.g. signalling, transportation, enzymatic, channelling etc., their structure-function relationship is better understood. Each protein is generally synthesised by translation of an mRNA template and the subsequent function results from the precise nature of the three-dimensional structure after folding. By contrast, for glycan assembly, monosaccharides are attached one-at-a-time through a series of individual enzymatic reactions, without a template mechanism. This permits the possibility of a heterogeneous glycan composition. For example, analysis of DSPAα1 (a thrombolytic agent present in vampire bats) revealed around thirty glycoforms present at a single *N*-linked site [10]. Another example of a high degree of heterogeneity can be found in IgG [11]. This molecule is one of the least glycosylated in our system (2.8% sugar coverage), and yet a single glycosylation site was found to possess 36 different glycoforms. Though glycan structures are not encoded

directly in the DNA sequences, they are encoded indirectly by the transcription and translation of genes that generate glycolsyltransferases [5]. These enzymes control the synthesis of the glycans that attach to the protein. Experiments with knockout mice in which certain glycolsyltransferases are eliminated, show that although the individual cell remains viable, complete elimination of any of these enzymes is fatal to the organism as a whole.

4.0.4 Lectins

Lectins are defined as *'proteins or glycoproteins of nonimmune origin derived from plants, animals, or microorganisms that have specificity for terminal or subterminal carbohydrate residues'* [12]. Another feature of lectins is that they have no enzyme activity. They are multivalent as two or more sugar binding sites are required for cross-linking or agglutination of cells to occur [13]. The nominal or preferred sugar specificity of lectins is ascertained by the simple monosaccharides that inhibits their effect. However, that said, lectin-binding inhibition by a simple monosaccharide is an over-simplification and binding involves three monosaccharides with a particular three dimensional spatial arrangement. Hydrophobic and electrostatic interactions also aid binding.

Lectins isolated from plants and animals are used in the study of glycans [14] [15]. Sometimes more than one lectin with different binding specificities may be obtained from a single source and these are termed isolectins. Examples of isolectins used in this project include MAL I and MAL II which are isolated from *Maackia amurensis* seeds.

Mislovičová *et al.* [13] and Gremenier *et al.* [16] published a two-part joint review on *"Lectinomics"* and in particular the relevance of plant lectins in biomedicine. In these extensive and comprehensive reviews, there are tables detailing a large number of studies relating to protein glycosylation changes, the particular lectins used in the screening process, the diseases concerned and finally the methods of analysis employed. Figure 4.8 summarises the applications that lectins have found in biomedical diagnostics.

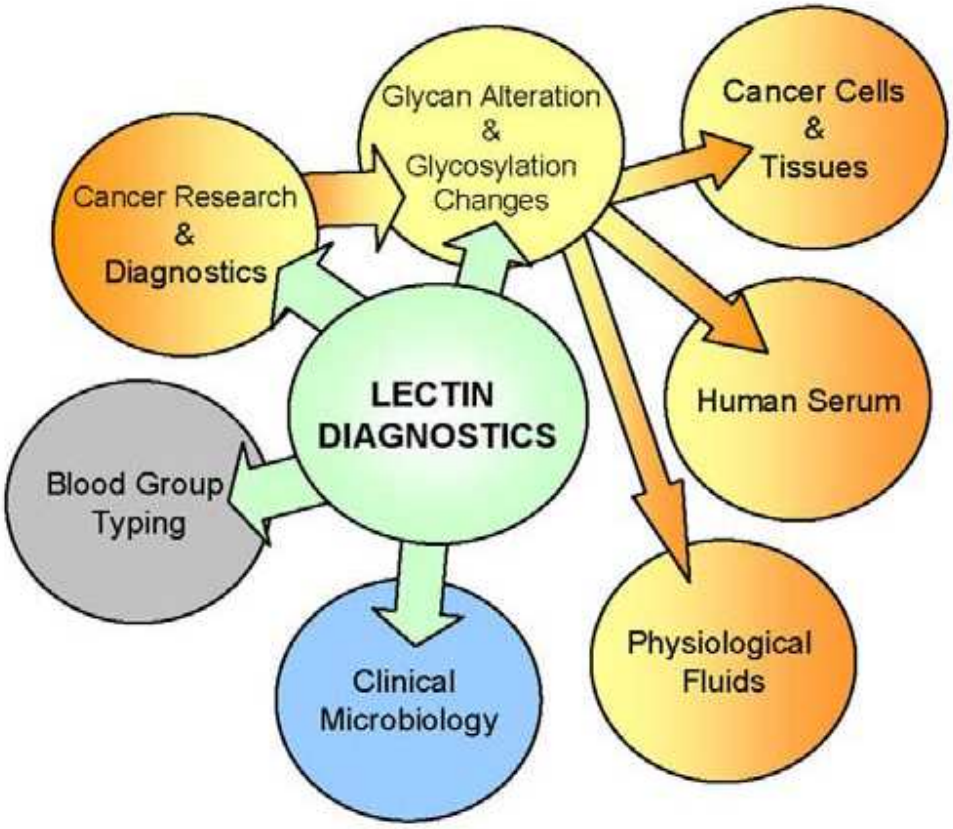

Figure 4.8: *A schematic diagram displaying the many applications of lectins in clinical diagnostics. Diagram taken from Mislovicova et al.* [13]

4.0.5 The role of glycans

Glycans have a variety of roles and functions, comparable to the multiple and diverse role of proteins. Glycoproteins are found on the surface of our entire cellular network, in the extracellular matrix (ECM) and in various biofluids [17]. Also, the cell surfaces of bacterial and viral pathogens are decorated with glycoconjugates [11]. A summary of the functions of glycans can be seen in Figure 4.9.

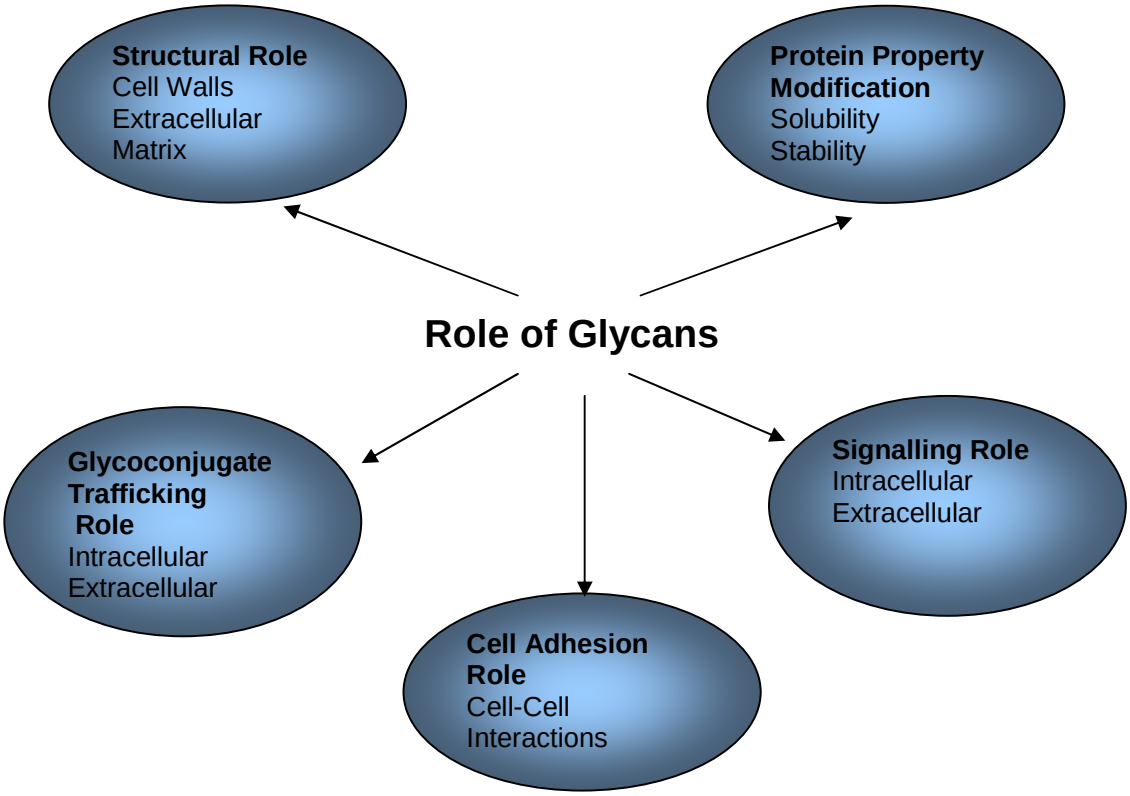

Figure 4.9: *A schematic summary of the biological functions of glycans*

The composition of the bacterial cell wall is an example of a structural role attributed to carbohydrates. The cell wall is composed of a macromolecular network called peptidoglycan which imparts a rigidity not found in eukaryotes. This consists of a repeating N-acetylglucosamine/N-acetlymuramic disaccharide unit linked in rows of 10 to 65 sugars to form a polysaccharide. Adjacent polysaccharides are attached to each other by polypeptide bridges. In mammals, bone sialoprotein (BSP) is an example of a glycoprotein which functions as a structural entity [18]. BSP has a mass of 65 – 75,000Da, half of which is attributed to carbohydrate attachments. It accumulates in areas of bone, dentin and cartilage and is also considered very important as a cell adhesion molecule and is also known to be involved in mineralising tissue.

As monosaccharides are polar entities, attachment of sugars to a protein can modify its properties e.g. solubility and stability. Modifications in solubility, for example, may occur due to differences in the number monosaccharide units which possess polar –OH, sulphate and sialic acid groups, each to a varying degree. Other protein modifications that occur due to glycosylation include altered folding, secretion, targeting and greater resistance to protease lysis [19]. Helenius *et al.* [3] state that when glycosylation is inhibited, the most commonly observed effects is the generation of misfolded aggregated proteins that fail to attain a functional state. It was noted that the dependence of correct folding on glycosylation ranges from proteins that are completely dependent on glycosylation, through partial dependence to no dependence at all. Though a protein conformation may exhibit no dependence on any particular individual carbohydrate structure, multiple site modifications can compromise folding. An example of enhanced stability was demonstrated by studies of the β-sheet core in the PMP-C protease inhibitor [20]. Here, a single fucose residue attached to threonine at position nine (Thr-9), imparted greater stability to the entire structure relative to the stability of the glycan after the fucose was removed. Protection from protein degradation was demonstrated in another study by Raju *et al.* [21]. This study proved that glycosylation of the crystallisable fragment (Fc) domain in IgG offered resistance to proteolysis by the enzyme, papain.

In order for glycans to mediate as trafficking, adhesion or signalling entities, the sugar epitope must selectively bind with sugar receptors e.g. lectins, collectins, adhesion molecules and anti-carbohydrate antibodies [11]. Cells of the immune system that participate in inflammatory responses (i.e. T-cells, neutrophils, macrophages and endothelial cells) are also known to synthesise glycoproteins that play a key role in the attachment of endothelial cells to L-selectin during the attachment of lymphocytes [22]. Here, glycosylation-dependent cell adhesion molecule 1 (GlyCAM 1), a mucin-like, sialylated and sulphated endothelial glycoprotein, acts as an adhesive ligand for L-selectin by presenting one or more *O*-linked carbohydrates to the lectin domain of this cell surface selectin which is present on the surface of leukocytes. This process aids the "rolling" effect of leucocytes (e.g. neutrophils) along the epithelial cells prior to entry into the tissue. Mammalian lectins are known to mediate control of the immune system

through recognition of cell surface glycoproteins [23]. For example, in the innate immune system, lectins such as the macrophage mannose receptor (a mannose binding lectin), bind to microbial carbohydrates. The ability of the human body to convert high mannose *N*-glycans to complex *N*-glycans is thought to offer protection against self-recognition by the innate immune system and so prevent inflammation and autoimmune disease [24, 25].
Some glycoproteins on the cell surface act as receptors for cytokines, growth factors or apoptosis factors. Indeed, glycosylation is often a requirement for the expression of these receptors [26]. In this study it was found that the presence of two large, *N*-linked glycans bound to Fas (a cell surface receptor involved in the induction of apoptosis) is required before the attachment of Fas-ligand can take place.

4.0.6 Glycosylation in various diseases including arthritic pathologies

It is now believed that glycans are directly involved in almost every biological process and play a significant part in most human diseases [27]. The multifunctional importance of glycoconjugates range from developmental biology, immune response (both innate and adaptive), homing of pathogens to their host tissues, cell division processes, cancer cells' ability to 'camouflage' in order to avoid detection by the immune system, injury and inflammation and prion diseases [2].
Bones *et al*. [28] discovered alterations in the glycosylation of four highly abundant serum glycoproteins (IgG, haptoglobin, transferrin, and alpha 1-acid glycoprotein) which they claim may offer potential as biomarkers for stomach cancer. Alterations in the glycosylation of these four proteins isolated from the pathologically staged cancer serum using either UPLC-fluoresence or two-dimensional electrophoresis were investigated as possible markers for stomach cancer progression. They observed an increase in sialylation on haptoglobin, transferrin, and alpha 1-acid glycoprotein in the cancerous state. Increased levels of core fucosylated biantennary glycans and decreased levels of monogalactosylated core fucosylated biantennary glycans were present on IgG with increasing disease progression.

Studies have been carried out on the lectin derived from *Helix pomatica* (HPA) in relation to cancer metastasizes. HPA recognises terminal GalNAc and to a lesser extent GlcNAc and Gal residues. Brooks *et al.* [29] proposed that HPA recognises a glycoprotein that is associated with metastasis (to auxiliary lymph nodes and elsewhere) and poor prognosis in breast cancer. 80% of breast cancers stained strongly for the binding of HPA and 20% were completely negative. The positively stained cancers tend to be aggressive and undergo metastasis to other sites whereas the negative cases tend not to spread and have a much more favourable prognosis. They conclude that HPA binding to paraffin sections of primary tumour could aid difficult treatment decisions by providing an additional assessment of staging and likely long-term patient prognosis. This study was further developed more recently by Welinder *et al.* [30]. Here the authors state that the aberrant glycosylation modification on protein function remains unknown. The major HPA binding proteins in serum were found to be IgA1, complement factor C3, von Willebrand factor (vWF), alpha-2-macroglobulin and IgM. However, the study also found that blood group phenotypes can have a major impact on any conclusions when analysing HPA lectin binding.

Smith *et al.* [31] studied the glycosylation of α-1-acid glycoprotein (a 41kDa plasma glycoprotein of hepatic origin) in the sera and synovial fluid of a rheumatoid arthritis patient employing the lectin concanavilin A (ConA) affinity chromatography. The study indicated that there maybe localised production of α-1-acid glycoprotein in the joint based on glycosylation differences between serum and synovial fluid. It was found that serum α-1-acid glycoprotein was largely composed of fucosylated tri- and tetra-antennary oligosaccharide chains while synovial fluid contained mainly bi-antennary chains that were fucosylated to a less extent. They also noted that this glycosylation heterogeneity also resulted in a difference in α-1-acid glycoprotein function - serum but not synovial fluid α-1-acid glycoprotein was able to inhibit binding to the cell adhesion molecule through expression of antigen sialyl Lewis X.

Sialylation and fucosylation of synovial and plasma fibronectins in relation to the progression and activity of rheumatoid arthritis has been studied by Przybysz *et al.* [32] employing lectin-ELISA. They established three distinct phases in the disease namely, early, established and late. The study showed that synovial fibronectin sialylation and

fucosylation was significantly increased in patients with established and late-phase RA, relative to those with early-phase RA. However, sialylation showed a slight decrease in the late-phase group relative to the established group. Fucosylation remained at almost the same level in the late group relative to the established group. It was noted that the expression of α1-6-linked fucose was found to correlate to disease activity. It is worth pointing out that there was no control group in the study of synovial fluid. The glycosylation of fibronectin in plasma on the other hand displayed different dynamic alterations. In the early RA group the reactivity of the lectins with fibronectin was similar to that of a control group. Fucosylation and sialylation increased significantly in the established group. Surprisingly, the reactivity in the late RA group decreased to a level similar to that of the normal group. The authors concluded that lower expressions of terminal sugars in synovial fibronectin were mainly associated with the early degenerative processes of RA and that the higher expression of terminal sugars in fibronectin could be associated with repair and adaptation processes. Kratz *et al*. [33]screened the terminal monosaccharides of synovial immunoglobulins IgA, IgG and IgM for the early detection of RA employing lectin-immunoblotting. In these studies the relative amounts of terminal monosaccharides in the synovial fluid of two RA groups (early and late) were compared to a control plasma sample by means of lectin-immunoblotting employing seven lectins. Their results showed differences between early and advanced RA stages in the terminal sugar profile of synovial IgG and IgA, but not IgM. A galactose-deficient glycotype with exposed GlaNAc appeared exclusively in the IgG 33.1kDa fragment of the early RA sample. However, in the intact form of both immunoglobulins, this glycotype was present in both groups, although to a greater extent in the late RA group. Sialyl and fucosyl moieties of intact IgG and IgA were notably lower in the early RA group relative to the late group.

It is acknowledged that, although the study of glycans and glycomics is not as advanced as proteomics and genomics in terms of understanding biologic processes, advances are being made over recent years to close this gap. A complete understanding of the causation of any disease will depend on the elucidation of all post-translational

modifications, but most especially glycosylation, which is the most abundant and most heterogeneous modification.

4.0.8 Aim of Project

From the introduction above, it may be appreciated that glycoconjugates are extremely important in all aspects of our system. Over a half of all known proteins are glycosylated [34].

With the development of experimental techniques, up- or down-regulation of a particular glycoconjugate and/or changes to the glycan structure and/or changes in the activity levels of enzymes which are responsible for particular glycan synthesis, have been studied and correlated to disease.

The objective of this study is to characterise differentially expressed glycoproteins in OA relative to other joint pathologies. This will be achieved in three stages:

1. Screen SF samples from patients diagnosed with different arthritic pathologies employing a panel of lectins. Determine which lectins exhibit differential glycosylation patterns and select these for further study.
2. Perform lectin affinity chromatography (LAC) employing the most promising lectins. The bound fractions will then be analysed by gel electrophoresis and differentially expressed bands noted.
3. Bands of interest will be excised and characterised by MS.
4. With the identity of the glycoprotein(s) now known, it may be possible to obtain antibodies and then assess the up- or down-regulation of this species in various pathologies.

4.1 Materials & Methods

4.1.0 Reagents

Absolute Ethanol (reagent, >99.5%), Acetic Acid (reagent, >99.7%), Acrylamide (for molecular biology, >99%), Ammonium Sulphate (for molecular biology, >99.0%), Ammonium persulphate (APS) ((for molecular biology, >98%), β-mercaptoethanol ((for molecular biology, >98%), Bovine Serum Albumin (BSA) (lyophilised powder, >96%), Calcium Chloride (anhydrous, >96%), Coomassie Brilliant Blue G-250, Ethylenediaminetetraacetic Acid (EDTA) (BioUltra, anhydrous,>99%), Glycerol (for molecular biology, >99%), Glycine (for electrophoresis, >99%), HEPES (99.5%), Manganese Chloride (reagent, >98%), Methanol (LC/MS Ultra) , α-methyl mannoside, Phosphoric Acid (Bioreagent, 85%), Ponceau Stain, Sodium Chloride (for molecular biology, >98%), Sodium Dodecyl Sulphate (SDS) (for molecular biology, >98.5%), Tetramethylethylenediamine (TEMED) (BioReagent, 99%), Tris-HCl, Tris pH 6.8, Tris pH 8.8, Tween-20 were obtained from Sigma-Aldrich (Ireland)

All biotinylated lectins and Agarose *Lens culinaris* Agglutinin (LCA) were obtained from Vector Laboratories (Peterborough, UK) and are listed in Table 4.1.

Lectin	Common Abbreviation	Preferred Sugar Specificity
Sambucus nigra	SNA	NeuNAcα2-6Gal; GalNAc **1, 3**
Maackia amurensis I	MAL I	NeuNAcα2-3Gal; Galβ1-4GlcNAc **1, 3**
Maackia amurensis II	MAL II	NeuNAcα2-3Gal **1, 3**
Lens culinaris	LCA	Fucα1-6GlcNAc; a-Man; a-Glc **2, 3**
Pisum sativum	PSA	Fucα1-6GlcNAc; a-Man **2, 3**
Ulex europaeus I	UEA-I	Fucα1-2LacNAc; a-Fuc **1, 3**
Ricinus communis	RCA120	β-Gal **2**
Phaseolus vulgaris	PHA(L)	3 or 4-antennary complex type **3**
Phaseolus vulgaris	PHA(E)	2 or 3-antennary complex type **3**
Canavalia ensiforms	ConA	a-Man; a-Glc **2,3**
Triticum vulgaris	WGA	Terminal N-acetylglucosamine or chitobiose; NeuNAc **2**
Triticum vulgaris	succinylated WGA	Terminal N-acetylglucosamine or chitobiose **2**
Arachis hypogea	PNA	Galβ1-3GalNAc **3**
Artocarpus integrifolia	Jacalin	Galβ1-3GalNAc-Thr/Ser also mono- or disialyted forms of this structure **2**
Griffonia simplicifolia	GSI	α-GalNAc **2**
Dolichos biflorus	DBA	α-GalNAc **2, 3**
Glycine max	SBA	Terminal a- or β-linked GalNA; Gal **3**
Sophora japonica	SJA	β-GalNAc; β-Gal **2**

Sugar Abbreviations		
Fuc	L-Fucose	
Gal	D-Galactose	
GalNAc	N-Acetylgalactosamine	
Glc	D-Glucose	
GlcNAc	N-Acetylglucosamine	
Man	Mannose	
NeuAc	N-Acetylneuraminic acid	(sialic acid)
Other Abbreviations		
Thr	Threonine	
Ser	Serine	

Table 4.1: *A list of plant lectins employed in the screening of synovial fluid of patients with a variety of arthritic diseases. Also included is the binding specificity for each lectin which were obtained from 1. Kratz et al.* [33] *2. Mislovicova et al.* [13] *3. Kumada et al.*[35]

Odyssey blocking buffer and molecular weight standards were obtained from LI-COR Biosciences (Lincoln, New England, USA)

4.1.1 Equipment

Solid-phase extraction columns obtained from Waters

Nitrocellulose, with a membrane pore size of 0.22mm filter paper and filter paper were purchased from Whatman (Springfield, United Kingdom)

Odyssey Infrared Laser Scanner (manufactured by LI-COR Biosciences, Lincoln, NE, USA)

Electrophoretic chamber, Western blot transfer chamber and power supply by BioRad (UK).

Stuart mini see-saw rocker (Staffordshire,UK)

Invitrogen iBlot dry gel transfer apparatus and Invitrogen iBlot gel transfer stacks, nitrocellulose (regular) were purchased from Invitrogen (Dublin, Ireland)

4.1.2 Synovial fluid sample preparation

As in section 3.1.4

4.1.3 Protein assay

As in section 3.1.7

4.1.4 Sample preparation for electrophoresis

As in section 3.1.8

4.1.5 Gel electrophoresis

As in section 3.1.9

The lectin screening study was carried out using 4 – 20% commercial pre-cast gels (1mm) with a HEPES buffer (12.1g Tris, 23.8g HEPES, 1.0g SDS to 1L final volume, pH 8.0).

4.1.6 Coomassie Staining

As in section 3.1.10

4.1.7 Transfer to nitrocellulose membrane

As in section 3.1.11

The lectin screening study was carried out employing the dry gel transfer method.

4.1.8 Lectin Incubation

Following the membrane blocking stage, the membrane was washed with PBST (PBS + 0.1% (v/v) Tween 20). Lectins were diluted 1:2,000 in Odyssey blocking buffer/PBST 1:1. Incubation of the membrane with the lectin took place for 1 hour at room temperature. Excess lectin was removed employing a series of 6 x 5mins washes with PBST. Next, the membrane was incubated in streptavidin (1:10,000) in PBST for 1 hour in the dark. Finally, washing 6 x 5mins with PBST took place before imaging with the Odyssey scanner.

4.1.9 Lectin affinity chromatography

500µL of *Lens culinaris* Agglutinin (LCA) agarose beads were added to the disposable column. The column was conditioned by washing with 25mL buffer (10mM HEPES, pH7.5, 0.15M NaCl, 0.1mM Ca^{2+}, 0.01mM Mn^{2+}) as per the manufacturer's instructions. Dilute 500µL SF to 1mL with buffer and add to beads. Mix end-over-end overnight. The non-bound fraction was eluted and the column washed with a further 10mL buffer. The bound (targeted) proteins were removed with 0.5M α-methyl mannoside + 1mM EDTA) as per the manufacturer's datasheet. Removal of elution buffer was performed by dialysis against water. The bound fraction was dried under vacuum and 20µLx1 reducing sample buffer was added. Electrophoresis was carried out followed by Coomassie staining.

4.1.10 Mass spectrometry using LC–MS/MS

All mass spectrometry analysis was carried out by the National Institute of Cellular (NICB) Biotechnology with whom collaboration was obtained. The following protocol was supplied by NICB.

Nano LC–MS/MS analysis was carried out using an Ultimate 3000 nanoLC system (Dionex) coupled to a hybrid linear ion trap/Orbitrap mass spectrometer (LTQ Orbitrap XL; Thermo Fisher Scientific). Five microlitres of digest were loaded onto a C18 trap column (C18 PepMap, 300μm ID × 5mm, 5μm particle size, 100 Å pore size; Dionex) and desalted for 10 min using a flow rate of 25μL/min in 0.1% (v/v) TFA. The trap column was then switched online with the analytical column (PepMap C18, 75μm ID × 250 mm, 3μm particle and 100 Å pore size; (Dionex)) and peptides were eluted with the following binary gradients of solvent A and B: 0–25% solvent B in 120 min and 25–50% solvent B in a further 60 min, where solvent A consisted of 2% (v/v) acetonitrile (ACN) and 0.1% (v/v) formic acid in water and solvent B consisted of 80% (v/v) ACN and 0.08% (v/v) formic acid in water. Column flow rate was set to 350nL/min.

Data were acquired with Xcalibur software, version 2.0.7 (Thermo Fisher Scientific). The mass spectrometer was operated in data-dependent mode and externally calibrated. Survey MS scans were acquired in the Orbitrap in the 400–1800 m/z range with the resolution set to a value of 60,000 at m/z 400. Lock mass was set at 445.120025 u (protonated $(Si(CH_3)_2O)_6$). Up to seven of the most intense ions (1+, 2+ and 3+) per scan were CID fragmented in the linear ion trap. A dynamic exclusion window was applied within 40 s. All tandem mass spectra were collected using normalised collision energy of 35%, an isolation window of 3 m/z, and one microscan.

Proteins were identified using BioWorks 3.2 from Thermo Fisher Scientific using the HUPO criteria with XC scores of 1.8, 2.2, 3.75 for single, double and triple charged ions. A peptide probability score of 0.05 was also used. The database used was Human UniProt-SwissProt downloaded January 2012. Carboxymethylation of Cysteine was set as fixed and oxidation of methionine as a variable modification. Two missed cleavages were allowed. The mass tolerance for precursor ions was 20ppm and the mass tolerance for fragment ions was 0.5Da.

4.2 Results

4.2.1 Patient sample screening with a panel of plant lectins

Samples taken from a number of patients suffering representing a variety of arthritic diseases were screened with a number of biotinylated plant lectins. As this is a pilot study and OA is the most prevalent form of arthritis and the pathology of interest in this project, four separate patient samples were analysed while one pooled (four different patients) samples from each of the other arthritic diseases were compared. All lectins employed were shown seen in Table 4.1. Also included in the table is the binding specificity for each lectin. The choice of these lectins was made based on availability, specificity for a broad range of sugars and glycosylation types i.e. *N*-linked and *O*-linked species, complex versus non-complex (Figure 4.4) and finally to establish differences between the same sugars in different binding arrangements e.g. three different fucose-binding lectins were included (LCA, PSA and UEA-1) because fucose possesses different binding options (Table 4.1).

4.2.2 Profiling of SF proteome

Employing the Bradford protein assay, 10µg of protein were loaded into each lane. The gel was then stained in colloidal Coomassie solution overnight (Figure 4.10).

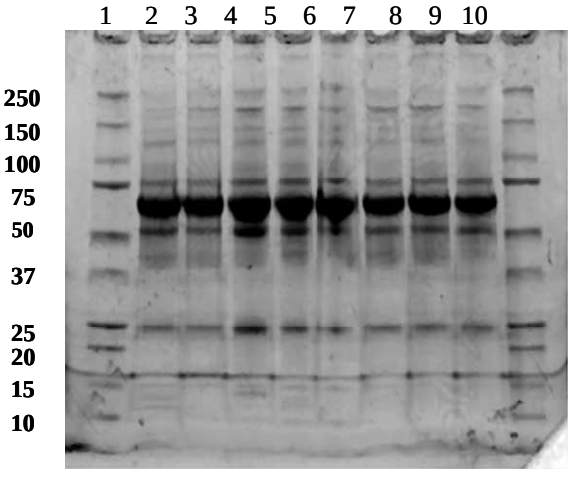

Figure 4.10: *Coomassie stained gel of various patient samples*

In terms of band patterns there is practically no difference between the five pathology types and within the same type i.e. OA. No important naked-eye differences in terms of band intensities were apparent so a qualitative differential study by lectin blot was undertaken with these well balanced (in terms of protein amount) samples. It was hypothesised that there may be glycosylation changes that are disease-specific

4.2.3 SF sample screening with a panel of lectins

The panel of lectins displayed in Table 1.1 were then used to probe for differentially expressed glycoproteins in the same SF samples as in Figure 4.10. Western blot images of each lectin are displayed in Figures 4.11- 4.18 along with details of the nominal binding specificity for each lectin. The grouping of lectins in each figure was made based on similar sugar-binding specificities.

Lectin	Common Abbreviation	Preferred Sugar Specificity
Sambucus nigra	SNA	NeuNAcα2-6Gal; GalNAc
Maackia amurensis I	MAL I	NeuNAcα2-3Gal; Galβ1-4GlcNAc
Maackia amurensis II	MAL II	NeuNAcα2-3Gal

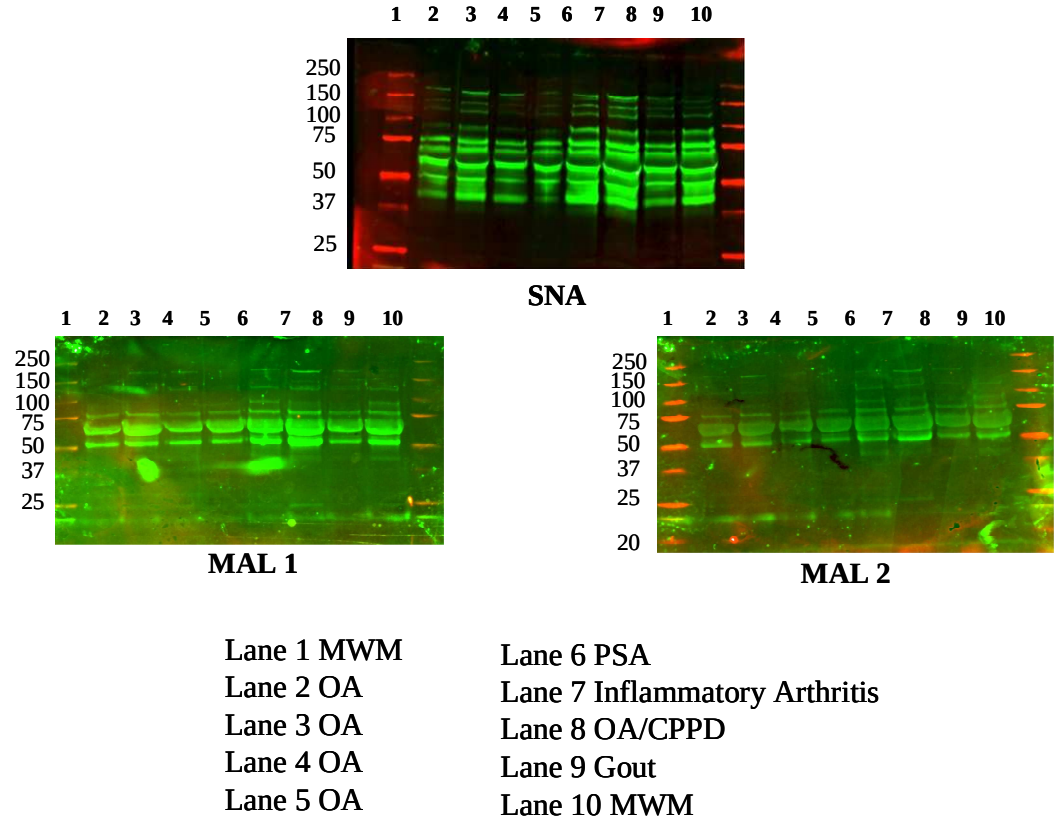

Figure 4.11: *WB images of whole SF samples incubated with sialic acid-binding lectins SNA, MAL 1 and MAL 2.*

These three lectins are mainly sialic acid-binding proteins though SNA and MAL differ in terms of the sialic acid-galactose stereochemistry. Each OA sample (Lanes 2-5 in each blot) possesses the same band pattern, though the sample in Lane 3 in the SNA blot has higher intensity bands in the 100-200kDa range. For each lectin, there is an increase in the intensity of the ~90kDa band in the PSA, IA and gout samples (Lanes 6, 7 & 9) relative to the OA samples. SNA exhibits more clearly defined bands and coverage over a broader molecular weight range than the MAL family, suggesting NeuNAc2-6Gal bonding is more prevalent than NeuNAc2-3Gal bonding. MAL 1 and MAL 2 are similar in terms of bands present, though the band intensities of the former are increased relative

to the latter suggesting that a NeuNAc2-3Galβ1-4GlcNAc binding site may afford stronger affinity for the lectin than that without the GlcNAc monosaccharide. This supports the statement about three monosaccharide binding sites made in section 4.0.4. Inter-patient differences with any one specific lectin are of intensity rather than bands unique to any particular disease type, possibly suggesting differences in protein amount or degree of glycosylation.

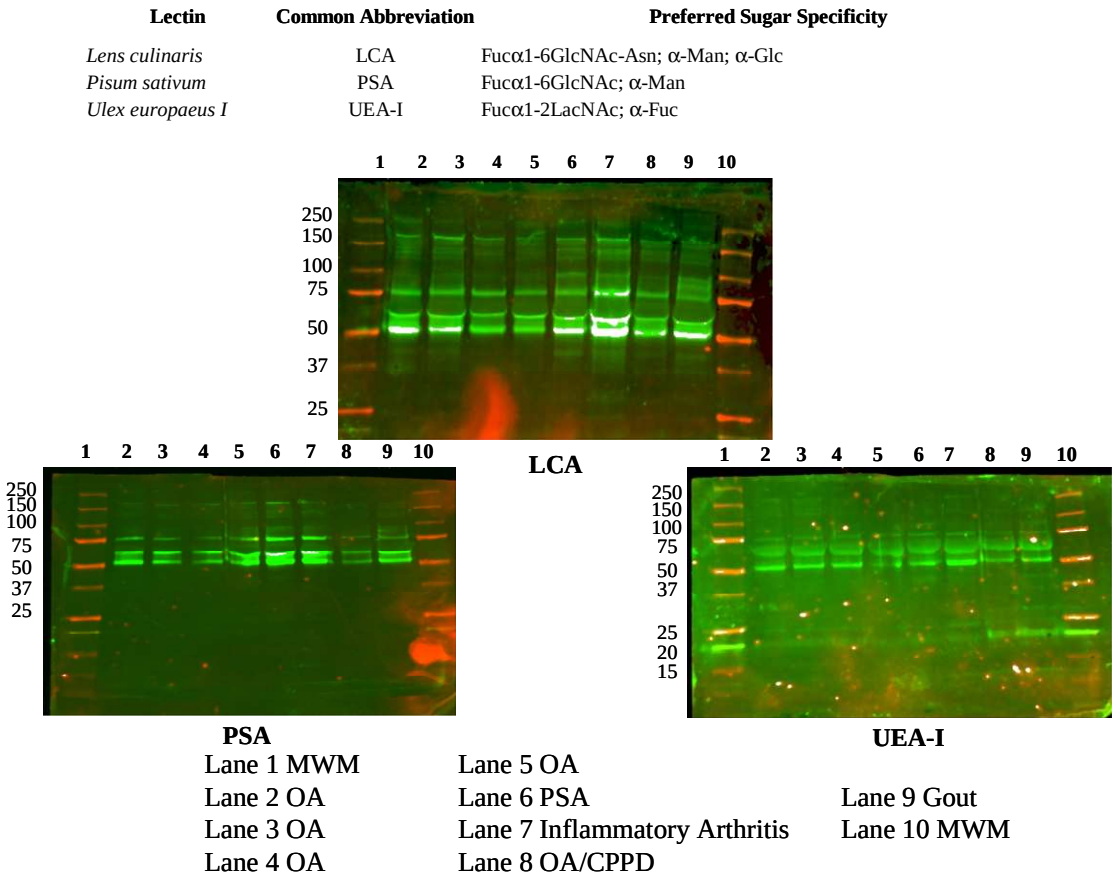

Figure 4.12: *WB images of whole SF samples incubated with lectins LCA, PSA and UEA.*

LCA, PSA and UEA-1 share commonality in that they bind fucose, with LCA and PSA specific for *N*-linked glycans, while UEA-1 binds to *O*-linked glycans [35]. From Table 4.1 above, it can be seen that LCA and PSA are remarkably similar in terms of binding specificity (fucose and mannose) with LCA having additional affinity for α-Glc. However, though the fucose-binding capabilities of both are identical in terms of

monosaccharide-binding orientation, LCA possesses preferential binding to core fucose (i.e. fucose attached to GlcNAc, which in turn is attached to the asparagine amino acid residue) while PSA binds fucose without this locational restriction. UEA-I on the other hand binds to Fucα1-2LacNAc rather than Fucα1-6GlcNAc and this lectin is fucose-specific.

PSA and UEA did not display any glycosylation changes – either in terms of band differences or intensity differences- between disease types. Both also exhibited bands within the same molecular weight range, with the strongest bands down to 50kDa. When the two blots are compared there is identical banding in the 50-75kDa region. However, in the 75-100kDa region, rather more interesting differences were manifest. The OA and OA/CPPD samples (Lanes 2-5 inclusive and Lane 8) are identical in terms of band patterns. However, extra banding is found in the PSA, inflammatory arthritis (IA) and gout samples when incubated with LCA. PSA and IA each feature an extra band at ~ 90kDa, while gout also had this band in addition to a unique band at ~80kDa. With reference to Table 4.1, additional affinity by LCA for α-glucose may account for this observation. Alternatively, the case may be that the location-specific fucose-binding character of LCA may account for this. It may be that LCA interacts with the asparagine amino acid residue or indeed another amino acid on the protein chain. Brooks *et al*. [36] deemed this possible by stating that when the binding site of the lectin combines with the sugar, it does so in a particular spatial arrangement and "*sometimes even part of the protein or lipid to which the oligosaccharide is attached"*. UEA-1 did not exhibit any inter-patient differences, suggesting that there are no fucosylation differences between patient pathologies in any *O*-linked glycoproteins that may be present in whole SF. In light of this analysis LCA was considered a good candidate lectin for further study. The additional bands in PSA, IA and gout relative to OA for this lectin may be due to additional glycoprotein species or else changes in the glycosylation decoration of a commonly expressed glycoprotein present in each pathology. It is not possible at this stage to speculate on the nature of these bands. Are they glycoproteins specific to PSA, IA and gout, or are they ubiquitous glycoproteins which are absent in OA? An enlarged

image of the LCA WB can be seen in Figure 4.13 with differentially expressed bands highlighted.

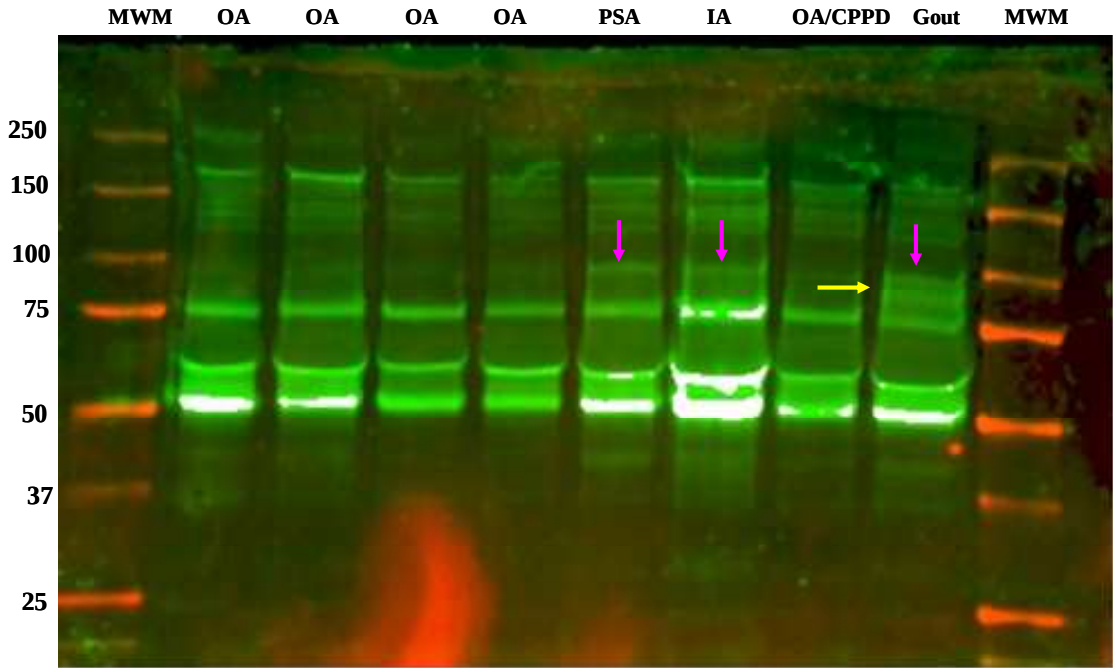

Figure 4.13: *Enlarged image of WB showing whole SF from patients with different arthritic pathologies incubated with the lectin LCA. This is the same image that was shown in Figure 4.11. Differentially expressed bands are highlighted with an arrow.*

PHA-E and PHA-L bind to complex or branched glycans that terminate with a galactose residue. RCA-120 also binds to terminal galactose glycans. The WB analysis for these lectins is shown in Figure 4.14

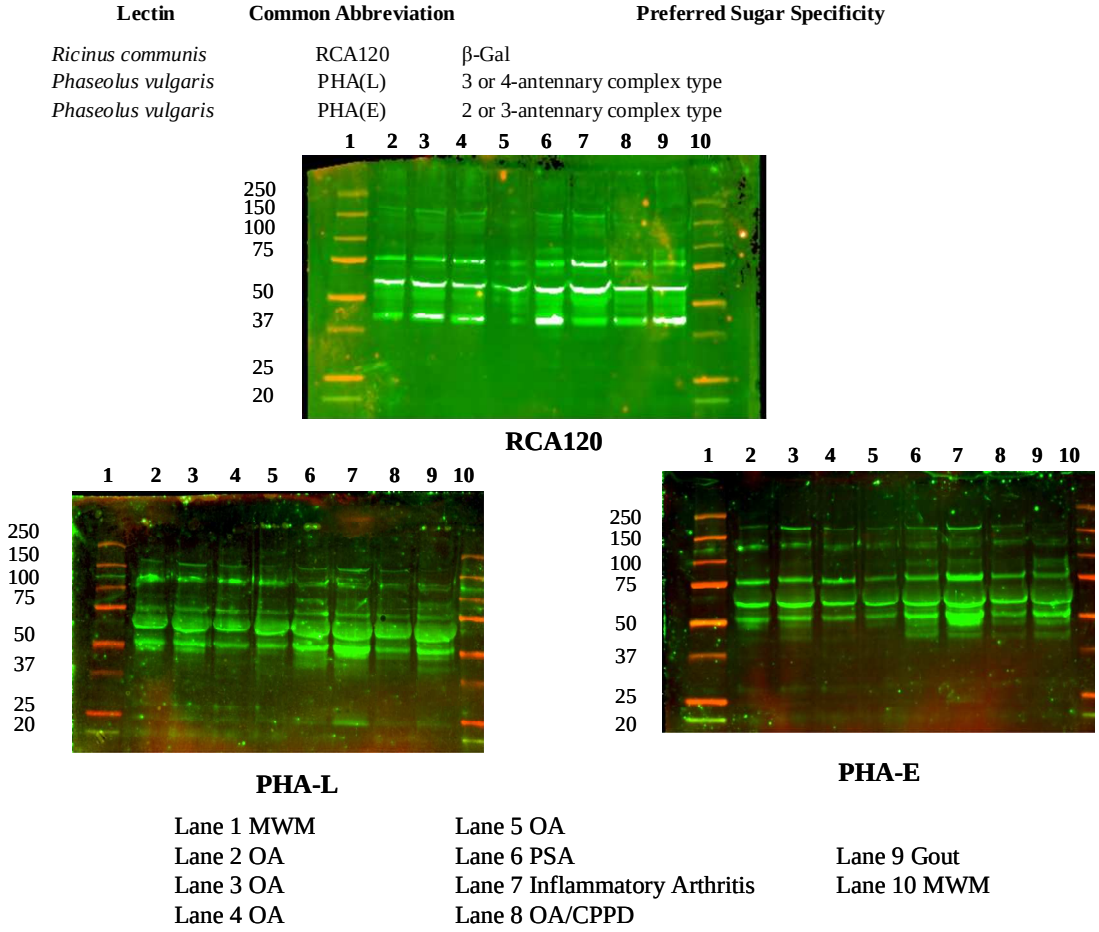

Figure 4.14: *WB images of whole SF samples incubated with terminal galactose-binding lectins RCA-120, PHA(L) and PHA(E).*

Close examination of Figure 4.14 reveals a very intense band in the IA sample (Lane 7) at ~50kDa in both blots. This band is present in all the other pathologies, though the intensity is somewhat less intense. Therefore, a glycan species with this molecular weight possesses a higher degree of complex glycosylation in IA relative to the other arthritic pathologies.

With the galactose-binding lectin RCA120 there are no differential glycosylation differences, though the OA patient sample in lane 5 appears to exhibit overall reduced glycosylation relative to the other OA patients.

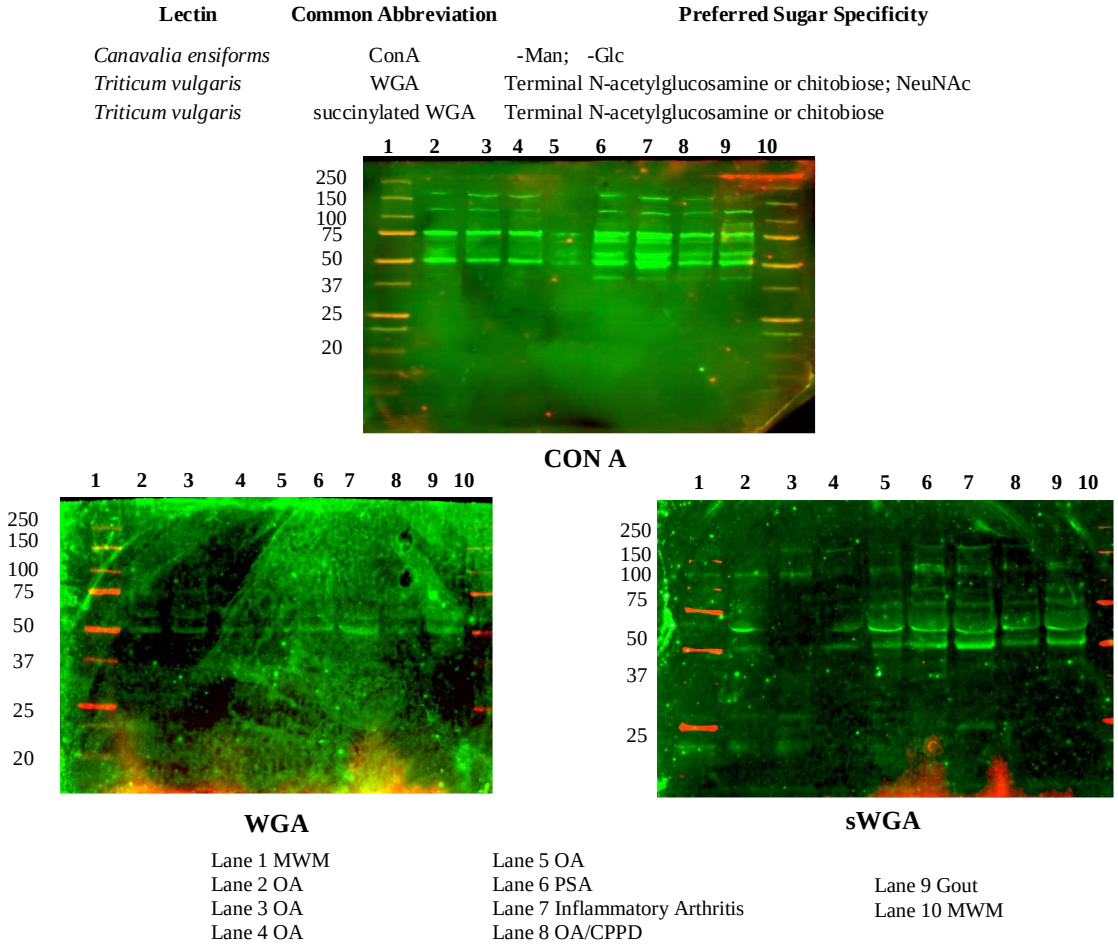

Figure 4.15: *WB images of whole SF samples incubated with the lectins ConA, WGA and succinylated WGA.*

As the WB image of WGA in Figure 4.15 displayed a high background noise, no glycosylation differences between the various arthritic pathologies could be ascertained. This background noise was consistently found to be a feature with this particular lectin over repeated experiments. Succinylated WGA on the other hand did not exhibit this limitation. Succinylation is a protein post-translational modification in which a –CO-$(CH_2)_2$-CO- group is attached to the amino acid, lysine. The charge on lysine changes

from +1 to -1 and this is believed to change the structure and function of the protein, possibly because of an alteration in electrostatic interactions. The differences in the 50-75kDa molecular range for lanes 2, 3 and 4 were believed to be artifacts associated with the experiment. Therefore, it was concluded that differences in terminal GlcNAc or chitobiose (a dimer of β1-4 linked GlcNAc units) were not a feature that could distinguish disease types. On the other hand ConA was deemed interesting as glycosylation differences were evident between patient pathologies. What is also noteworthy is that ConA and LCA share sugar-binding specificities (Table 4.1). In order to aid discussion the ConA WB is enlarged and displayed in Figure 4.16.

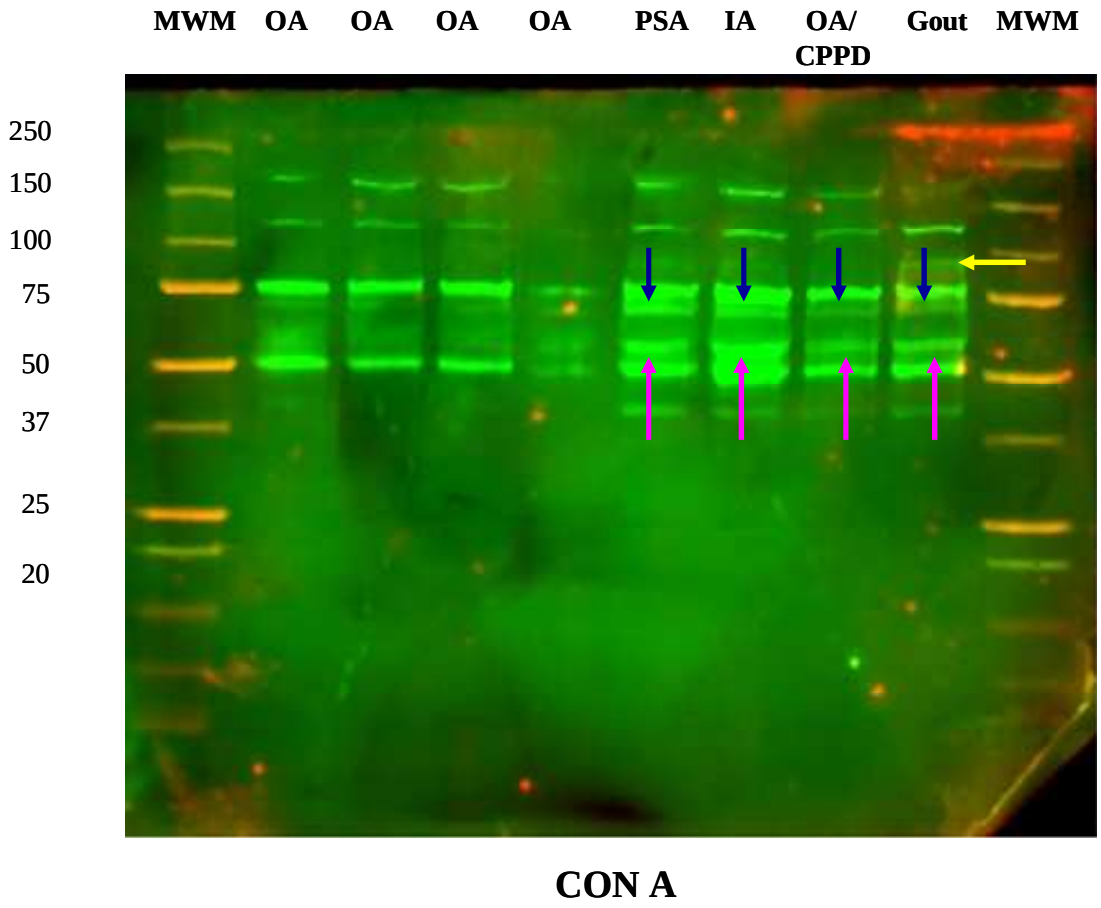

Figure 4.16: *Enlarged image of WB showing whole SF from patients with different arthritic pathologies incubated with the lectin ConA. This is the same image that was shown in Figure 4.14. Differentially expressed bands are highlighted by arrows.*

As with LCA ConA exhibited interesting differences between OA and the other pathologies i.e. PSA, IA and gout. In particular, there were double bands present in the latter that are absent in OA and these are highlighted with coloured arrows (pink and blue) in the figure. At this point it is not possible to ascertain if these are differences due to extra glycoproteins or differences in glycosylation of the same glycoprotein or even differences in amount of each protein. An extra band (~ 80kDa) in the gout sample was evident in both Figure 4.13 (yellow arrow) and Figure 4.16 (yellow arrow). The commonality between LCA and ConA is that both of these lectins bind to α-mannose and α-glucose monosaccharides. It was therefore concluded that there may be a glycoprotein at ~ 80kDa that is unique to gout, though only a larger patient cohort could establish this claim. The differences in glycosylation revealed by LCA and ConA were not the same however. In LCA differences were found to occur in the 75-100kDa range, while those found in ConA were manifest in the 50-75kDa interval. Therefore, these highlighted bands could not be the same species. As mentioned above, it is not possible to establish the nature of these bands, i.e. whether they represent different glycans or the same protein with different glycosylation attachments. Another point worthy of note concerns the OA/CPPD sample (Lane 8). As indicated with the blue arrow in Figure 4.16, this patient possess the same glycosylation difference as PSA, IA and gout, and is absent in OA. This may be an inflammatory-related species attributed to CPPD where the build up of calcium crystals in the joint may have triggered an inflammatory response.

PNA and jacalin both specifically bind to *O*-glycans [37]. The WBs following incubation with these lectins is displayed as Figure 4.17. The PNA and jacalin glycosylation patterns are very similar especially in the high molecular weight region, where the signal appeared as a smear. A possible source of these high molecular weight species might be proteoglycans (polymers consisting of repeating disaccharide units). As mentioned in the introduction to this chapter, chondroitin sulphate (a glycosaminoglycan) is *O*-linked to aggrecan and constitutes a major component in cartilage [6]. This species may bind to PNA and jacalin and so account for the species detected at a molecular weight >250kDa. The fact that the band appeared as a smear could be accounted for by polymers of different lengths bound to the lectins. With jacalin there is a differentially expressed

glycoprotein at ~90kDa in the PSA, IA and gout samples that is not represented in the OA patients. In addition, these bands are not present in the PNA WB and may be explained by the fact that these species may be end-capped with sialic acid. From Table 4.1, it is known that jacalin also recognises a sialic acid residue, while PNA does not. Examination of the SNA blot in Figure 4.10 reveals a band at approximately 90kDa. As before, it was noticed that the OA patient sample in lane 5 is very different in the jacalin blot relative to that of PNA. This difference was already encountered with ConA and RCA120 and it was established that none of these three lectins share the same binding specificities. The fact that this occurred in the same patient sample with three different lectins, analysed on three different days, leads one to suspect that this feature is not one of incorrect sample loading and is instead a genuine feature of the SF from this particular individual.

Lectin	Common Abbreviation	Preferred Sugar Specificity
Arachis hypogea	PNA	Galβ1-3GalNAc
Artocarpus integrifolia	Jacalin	Galβ1-3GalNAc-Thr/Ser; also mono- or disialyted forms of this structure

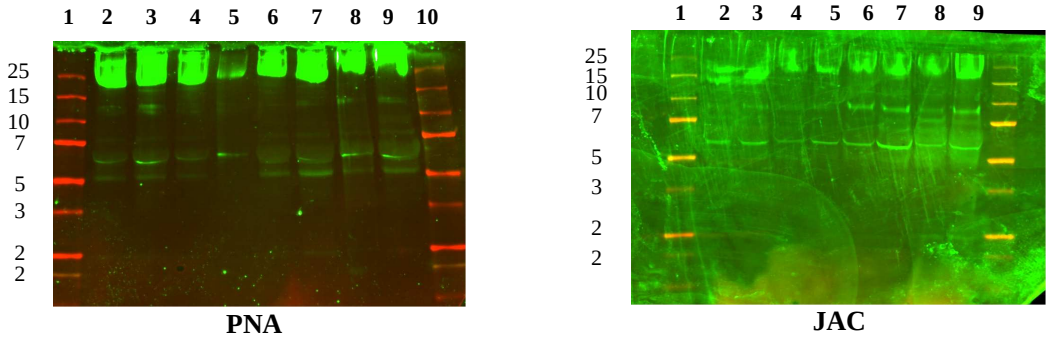

Lane 1
MWM
Lane 2 OA
Lane 3 OA

Lane 5 OA
Lane 6 PSA
Lane 7 Inflammatory
Arthritis

Lane 9 Gout
Lane 10

Figure 4.17: *WB images of whole SF samples incubated with the lectins PN and, Jacalin.*

Incubation with the mainly GalNAc-binding lectins GSI, DBA, SBA and SJA (Figure 4.18), did not highlight glycosylation changes between patient samples. However, with

SBA there was a clear difference in the intensities of some bands e.g. at ~ 200kDa there were increased band intensities for one OA patient (Lane 4), the OA/CPPD patient (Lane 8) and the gout sample (Lane 9).

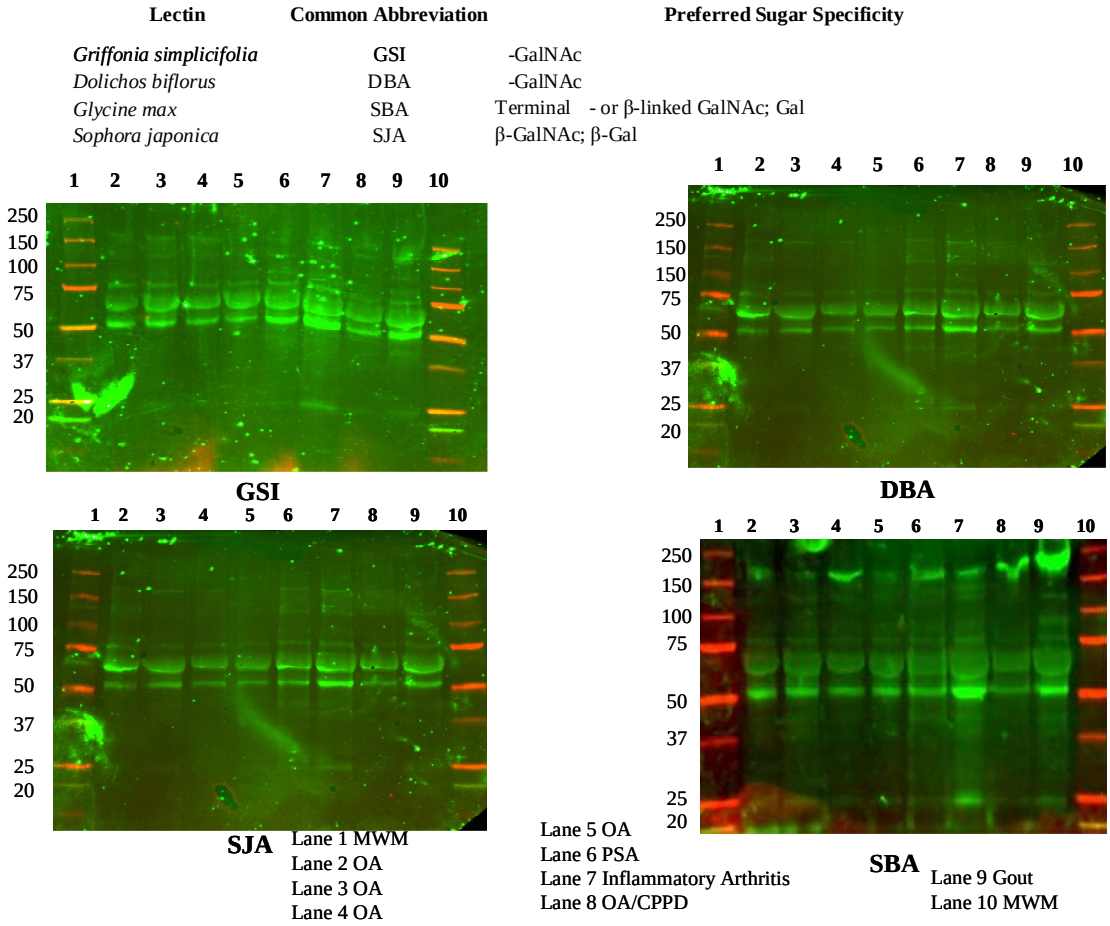

Figure 4.18: *WB images of whole SF samples incubated with the GalNAc-binding lectins GSI, DBA, SJA and SBA.*

Of the 18 lectins employed in the screening process, three (LCA, ConA and jaclin) featured potentially interesting glycosylation differences between OA and other arthritic pathologies (PSA, IA and gout) i.e. bands present in that latter that are absent in the former. It may be the case that these specific glycoproteins are indicative of a specific

pathology, as in for example, the band highlighted in yellow in gout (Figures 4.13 & 4.16). This is absent in all other pathologies. Another hypothesis is that the other "extra" bands in PSA, IA and gout are endogenous to SF, but are down-regulated in OA or the glycosylation is significantly altered in OA.

It was then decided to explore this hypothesis further by employing lectin-affinity chromatography to further elucidate any glycan changes – either in terms of protein changes and/or glycosylation changes – with a new cohort of patient samples using LCA.

As mentioned previously and indicated in Table 4.1, LCA and ConA are very similar in terms of their sugar-binding specificities. Both bind α-Man and α-Glc. ConA binds non-specifically to glucose and mannose [38]. LCA however, also has a preferred specificity for a Fucα1-6GlcNAc motif at the core oligosaccharide (Figure 4.6), and the presence of this feature markedly enhances the affinity of this lectin.

Sobiesiak [39] studied the glycosylation of human serum transferrin with LCA and ConA and concluded that both can be used as diagnostic tools of the acute phase response, although variants produced using LCA were much more apparent. Ferens-Sieczkowska *et al.* [40] studied fucosylation in SF and found that the density of fucosylated epitopes differs significantly in particular glycoproteins. As LCA has a binding specificity for core fucosylation in addition to mannose and glucose, it was believed that employing lectin-affinity chromatography experiment with LCA in the stationary phase could be interesting. As mentioned in section 4.0.7 above, fucosylation of fibronectin was found to be related to RA disease activity, while increased fucosylation of IgG heavy chains distinguished between acute and remission phases of juvenile chronic arthritis [41].

4.2.4 Analysis of whole SF employing lectin-affinity chromatography with LCA as the stationary phase

Lectin-affinity chromatography was carried out as outlined in 4.1.9 and a Coomassie stained gel was prepared for each fraction (whole SF, unbound and bound). This is shown in Figure 4.19.

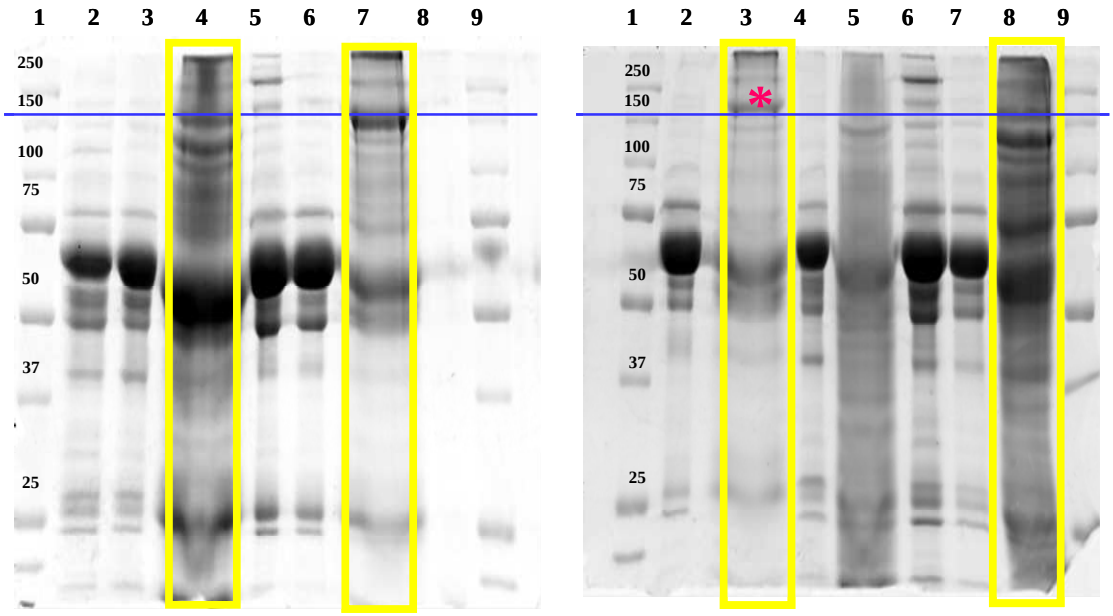

Figure 4.19: *Coomassie-stained gel of all fractions following lectin affinity chromatography with LCA lectin. The targeted bound fractions are highlighted with a yellow box. The blue line is serves as a reference to aid a comparison between the two gels A and B.*

Gel A (Lane 8) is a LCA positive control to ensure that none of the bands in the samples are due to the lectin itself. LCA is a 49kDa protein composed of four subunits – two ~ 17kDa and two ~ 8kDa [37]. That the samples were dissolved in sample buffer containing under reducing conditions and then boiled ensured that the lectin dissociated into its

component subunits. From Figure 4.18, it may be seen that there are no bands due to LCA. As LCA is composed of four subunits (two of 17kDa and two of 8kDa), under reducing conditions these subunits would have exited the bottom of the gel. The lanes highlighted with a yellow box are the targeted, LCA-bound fractions i.e. those glycoproteins that bind to LCA. Comparing the bound fractions in the Coomassie-stained gels in Figure 4.19 with the WB of LCA in Figure 4.13, it may be expected that both should reveal identical banding patterns. However, this is not the case. This is readily explained by consideration of the conditions under which each experiment was performed.

The initial lectin screening process was carried out under reducing conditions i.e. the glycoproteins were treated with β-mercaptoethanol and boiled prior to incubation with the lectins. By contrast in the lectin affinity chromatography study, all glycoproteins were in their native condition when captured by the stationary LCA. This is important (as already outlined in the introduction to this chapter) considering lectin binding depends on the stereochemistry of the glycan-binding region. Sample conditions (i.e. reducing versus non-reducing) greatly influence the conformational structure of proteins and therefore the lectin binding region environment. Further, in lectin affinity chromatography, divalent cations (Ca^{2+} and Mn^{2+}) were required to ensure successful lectin-glycan binding. It was not possible to employ these cations in the lectin screening process as incubation with the phosphate buffer would result in the formation of insoluble phosphate salts which precipitate on the surface of the membrane during incubation of the lectin. This increases the background noise in both channels (emission wavelengths λ=700nm and λ=800nm). Also, the commonly used tris buffer could not be used either as this would render image acquisition with the Odyssey scanner difficult due to high background noise.

A band in the OA sample (Gel B, Lane 3) was found to have a band that was either absent from or at a slightly higher molecular weight relative to the other pathologies and this is indicated in Figure 4.18 with a red asterisk. For example, this band is completely absent in the gout sample (Gel B, Lane 5) and at a higher molecular weight than comparable bands in IA, PSA and RA. This is demonstrated by using a reference visual

aid (blue line). It may be the case that this is a glycoprotein unique to OA, or a species common to each pathology but possessing a different glycosylation signature in OA. Indeed, the perceived difference may not exist. It was not possible to speculate which is the case without further investigation.

The corresponding whole SF and unbound fractions from each of the pathologies do not seem to exhibit notable differences. Other studies in the literature (see introduction) have already characterized the proteome of whole SF and therefore, it is outside the scope of this project to explore these fractions any further.

The band marked with a red asterisk was excised for characterisation by MS. In addition, bands on the blue line from the other patient samples were also cut out for characterisation and comparison. As the gout sample did not possess a band at this molecular weigh, no band from this sample was sent for MS analysis.

A full list of proteins identified for each band is displayed in Appendix F. The list was studied and a screening process was adopted in order to remove unlikely redundant candidates. For example, all contaminating keratin species (possibly due to skin, hair etc.) were removed, all non-glycosylated proteins were removed (e.g. albumin) and finally as the excised band is ~150kDa, all species less than 80kDa were ignored. This modified list of proteins is given in Table 4.2.

Inflammatory Arthritis

Reference	P (pro)	Score	Coverage	MW	Accession	Peptide (Hits)
Scan(s)	P (pep)	XC	DeltaCn	Sp	RSp	Ions
Alpha-2-macroglobulin	1.00E-30	1148.35	67.60	163187.4	308153640	115
Ceruloplasmin	7.77E-15	350.33	38.30	122127.6	116117	35
Attractin	1.48E-12	150.25	12.50	158431.7	13431311	15
Fibronectin	4.17E-12	140.23	8.30	262457.6	300669710	14
Pregnancy zone protein	3.34E-12	150.28	6.70	163759.1	281185515	15
Lactotransferrin	4.79E-09	30.21	5.40	78132.0	85700158	3
Complement factor H	3.98E-07	30.18	2.80	139004.4	158517847	3
Complement C4-B	2.27E-10	30.23	2.10	192671.6	81175167	3
Complement C4-A	2.27E-10	30.23	2.10	192649.5	81175238	3
Apolipoprotein B-100	6.06E-06	20.14	0.50	515283.6	300669605	2

Psoriatic Arthritis (PSA)

Reference	P (pro)	Score	Coverage	MW	Accession	Peptide
Scan(s)	P (pep)	XC	DeltaCn	Sp	RSp	Ions
Alpha-2-macroglobulin	4.44E-16	1648.36	79.00	163187.4	308153640	165
Ceruloplasmin	9.99E-15	310.38	43.50	122127.6	116117	31
Attractin	1.11E-15	230.31	17.70	158431.7	13431311	23
Pregnancy zone protein	1.48E-12	220.29	13.00	163759.1	281185515	22
Fibronectin	5.53E-13	160.26	9.30	262457.6	300669710	16
Hornerin	3.54E-09	30.21	5.20	282225.7	45476906	3
Complement factor H	3.24E-05	30.15	3.10	139004.4	158517847	3
Apolipoprotein B-100	5.32E-09	30.19	0.80	515283.6	300669605	3

Osteoarthritis

Reference	P (pro)	Score	Coverage	MW	Accession	Peptide
Scan(s)	P (pep)	XC	DeltaCn	Sp	RSp	Ions
Alpha-2-macroglobulin	1.00E-30	1408.36	72.90	163187.4	308153640	141
Ceruloplasmin	8.88E-15	170.35	25.60	122127.6	116117	17
Attractin	3.79E-11	230.27	18.00	158431.7	13431311	23
Pregnancy zone protein	5.01E-12	190.27	10.70	163759.1	281185515	19
Fibronectin	3.17E-11	80.27	4.70	262457.6	300669710	8

Rheumatoid Arthritis

Reference	P (pro)	Sf	Score	Coverage	MW	Accession
Scan(s)	P (pep)	Sf	XC	DeltaCn	Sp	RSp
Alpha-2-macroglobulin	1.00E-30	119.01	1338.36	72.60	163187.4	308153640
Ceruloplasmin	4.44E-16	38.42	420.38	47.50	122127.6	116117
Fibronectin	2.22E-16	57.13	622.34	36.80	262457.6	300669710
Pregnancy zone protein	2.11E-14	27.16	300.31	22.50	163759.1	281185515
Complement factor H	5.21E-10	10.59	120.27	13.00	139004.4	158517847
Attractin	3.77E-07	10.75	130.26	11.30	158431.7	13431311
Fibrinogen alpha chain	4.14E-06	1.78	20.18	2.90	94914.3	1706799
Apolipoprotein B-100	4.75E-11	2.32	30.24	0.80	515283.6	300669605

Table 4.2: *Modified list of proteins identified following excision of ~150kDa band from SDS-PAGE gel in Figure 4.18. The bands were taken from the bound fraction after analysis of whole SF by lectin affinity chromatography employing LCA lectin. This list is a subset of that given in Appendix 9 following a screening process to remove unlikely candidates.*

From Table 4.2 it can be seen that, on the basis of total protein coverage and the number of peptide hits, a strong degree of confidence may be had in identifying alpha-2-macroglobulin (α-2-M) as the major species present in all the bands excised at ~150kDa. It was therefore decided to pursue a study of the glycosylation of this protein with a larger cohort of patient samples. Incubation with both anti-α-2-M and LCA, and then measuring the intensity of for each species at ~ 150kDa, would yield a ratio of intensities. These ratios would then be compared in order to ascertain if there are changes in the protein moiety or the sugar attachments. Other potentially interesting species present are ceruloplasmin, attractin and pregnancy zone protein. UniProt describe the latter as a relative to α-2-M and indeed the functionality description given for both species is identical. Knowing its known role as a proteinase inhibitor and a regulator of cytokine and growth factor activities (by binding and inhibiting these signaling molecules from interacting with their cell-surface receptors) [42], α-2-M offered an interesting line of study. Confirmation as to whether there is a change in the protein entity and/or the glycosylation decoration (these changes may be manifest by changes in molecular weight) of the protein was the aim of the next phase of the experiment. For this, a larger cohort of patient samples was gathered and analysed by SDS-PAGE (under reducing conditions) followed by incubation with LCA (λ_{em}800nm) and anti-α-2-M (λ_{em}700nm). The samples set consisted of; 8 OA samples, 5 RA samples; 2 IA samples; 2 CPPD samples; 4 PSA samples and finally 2 Gout samples. The band intensity ratio (LCA: anti-α-2-M) was calculated for each sample using the Odyssey scanner. The result of this study can be seen in Figure 4.20.

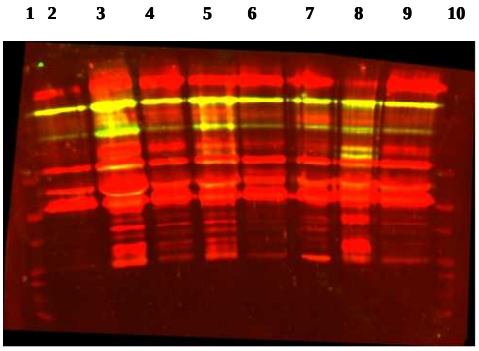

α-2-M and LCA

		LCA (Red)	α-2-M (Green)	Ratio LCA:α-2-M
Lane 1	MWM			
Lane 2	OA	23.08	50.63	0.46
Lane 3	OA	51.15	196.77	0.26
Lane 4	OA	25.68	57.85	0.44
Lane 5	OA	38.42	150.63	0.26
Lane 6	OA	22.09	53.38	0.41
Lane 7	OA	14.96	41.07	0.36
Lane 8	OA	16.05	57.98	0.28
Lane 9	OA	30.61	46.10	0.66
Lane 10	MWM			

A

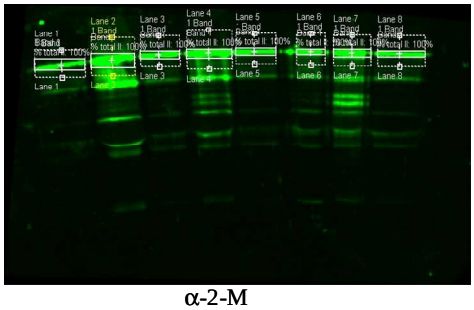

α-2-M

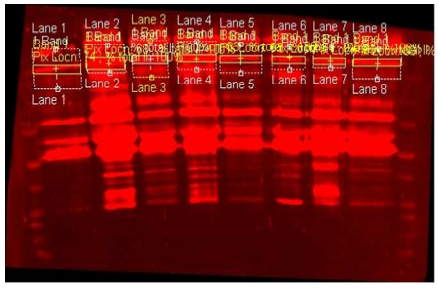

LCA

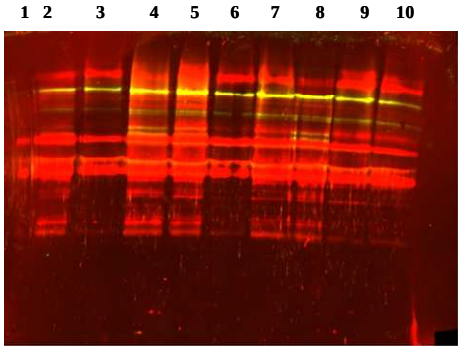

α-2-M and LCA

		LCA (Red)	α-2-M (Green)	Ratio LCA:α-2-M
Lane 1	MWM			
Lane 2	RA	7	11.07	0.63
Lane 3	RA	5.63	11.75	0.48
Lane 4	RA	13.16	27.14	0.48
Lane 5	RA	18.97	30.51	0.62
Lane 6	RA	10.18	18.84	0.54
Lane 7	IA	15.4	28.64	0.54
Lane 8	IA	13.89	30.34	0.46
Lane 9	CPPD	10.11	22.17	0.46
Lane 10	CPPD	5.06	11.41	0.44

B

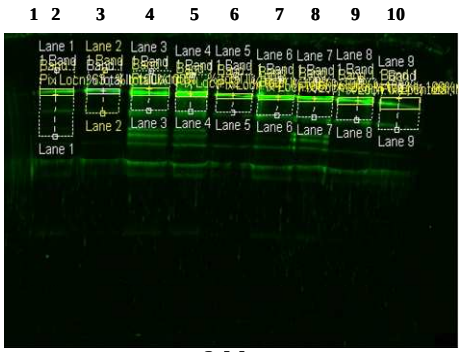

α-2-M

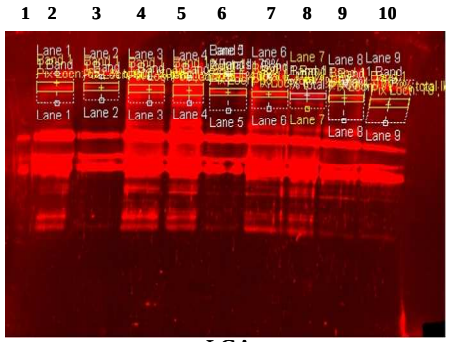

LCA

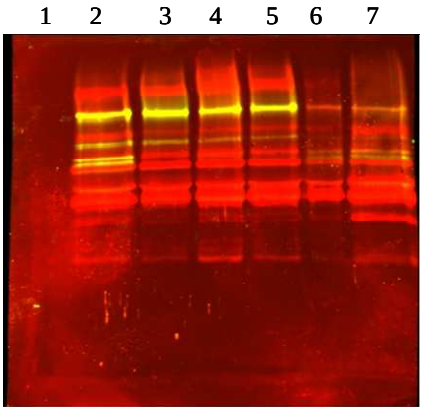

α-2-M and LCA

		LCA (Red)	α-2-M (Green)	Ratio LCA:α-2-M
Lane 1	MWM			
Lane 2	PSA	36.62	59.99	0.61
Lane 3	PSA	28.29	61.38	0.46
Lane 4	PSA	19.12	41.01	0.47
Lane 5	PSA	20.04	35.85	0.56
Lane 6	Gout	6.12	3.42	1.79
Lane 7	Gout	6.13	6.52	0.94

C

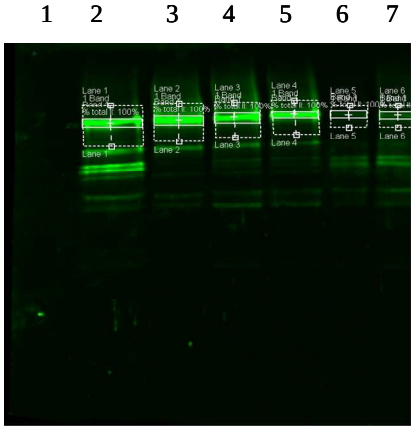

α-2-M

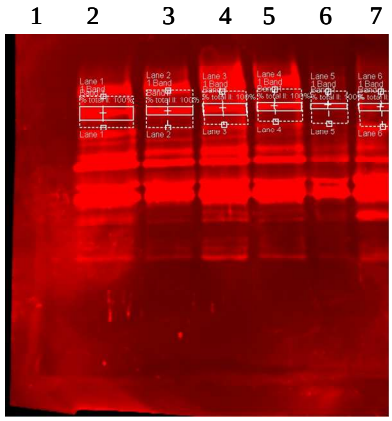

LCA

Figure 4.20: *WB image sets (**A, B,** and **C**) of various arthritic patient pathologies incubated with anti-α-2-Macroglobulin (λ_{em}800) and LCA lectin (λ_{em}700). Also included is the image which displays both channels simultaneously. Regions in which both red and green channels overlap, show up as yellow. A table showing the band intensities of monomeric α-2-M in both the red and green channels is displayed with each image set. The final column is ratio of LCA intensity to α-2-M intensity.*

Comparison of the whole synovial fluid WB image for LCA in Figure 4.13 with those in Figure 4.20 highlights remarkable difference in terms of band patterns. Though there are differences in terms of individual patients, the principal reason for this phenomenon could be due to differences in methodology. In the initial lectin screening process, electrophoresis was performed using commercial pre-cast gradient gels with a HEPES buffer, while in the study performed in Figure 4.20, electrophoresis was carried out employing home-made gradient gels with a tris-glycine buffer system. A further

difference between the two studies concerned the mode of protein transfer from gel to membrane. In the lectin screening experiment the "dry" method was adopted while in the study of α-2-M the "wet" method was used. An important distinction between these modes of transfer concerned the amount of heat generated. With the "dry" method the amount of heat was appreciable while with the "wet" method transfer took place under ice. It may be appreciated by comparing the WBs that the latter method generated much more information and better resolved bands than the former. Thus the choice of method employed, greatly influences the experimental result.

The mean and standard deviation LCA:α-2-M intensity ratios representing each of the pathologies were calculated and a histogram was produced. This is shown in Figure 4.21.

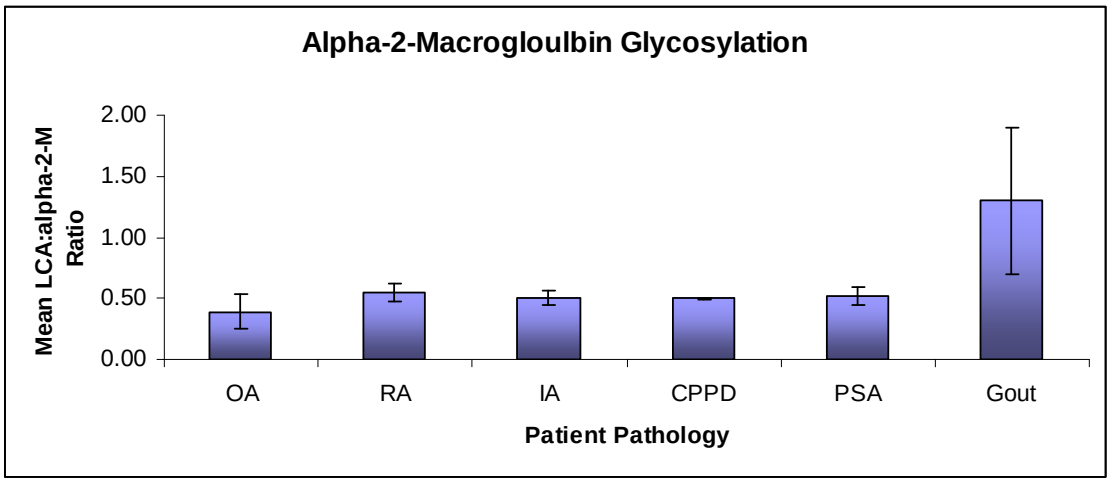

Figure 4.21: *Histogram displaying the mean and standard deviation of LCA:α-2-M intensity ratios obtained from the raw data in Figure 4.20.*

Figure 4.21 suggests that there some slight differences in the LCA:α-2-M intensity ratios between the various arthritic pathologies with this larger cohort of samples. The peak for gout may be somewhat misleading as it is based on two patient samples with a very large standard deviation. OA (n=8) has a slightly lower ratio relative to the other pathologies. However, a larger sample size for each of the pathologies would be required in order to acquire meaningful statistical information and conclude a valid inference.

4.2.5 The analysis of the glycosylation of α-2-M in SF MV

However, at this point it was decided to engage in a further study of α-2-M glycosylation, only this time in relation to MVs. That continued interest in this protein was maintained, is in part due to a publication [43] that was found citing α-2-M as a substrate for ADAMTS-4 and ADAMTS-5 (putative OA markers) and thereby inhibiting their activity. Mass spectrometry found α-2-M to be associated with MV and this was confirmed by WB (Figure 3.33). The current work is aimed at establishing if any differences exists between soluble α-2-M and vesicle-associated α-2-M in terms of glycosylation and/or protein band patterns. The approach taken was to analyse all differentially centrifuged fractions of several patient samples with LCA and anti-α-2-M, and ascertain if any notable differences are evident. The WB images of the pellet fractions (i.e. 18,000g crude and 200,000g CHAPS) are displayed in Figure 4.22, while the SN fraction (i.e. 200,000g crude and 200,000g CHAPS) are shown in Figure 4.23.

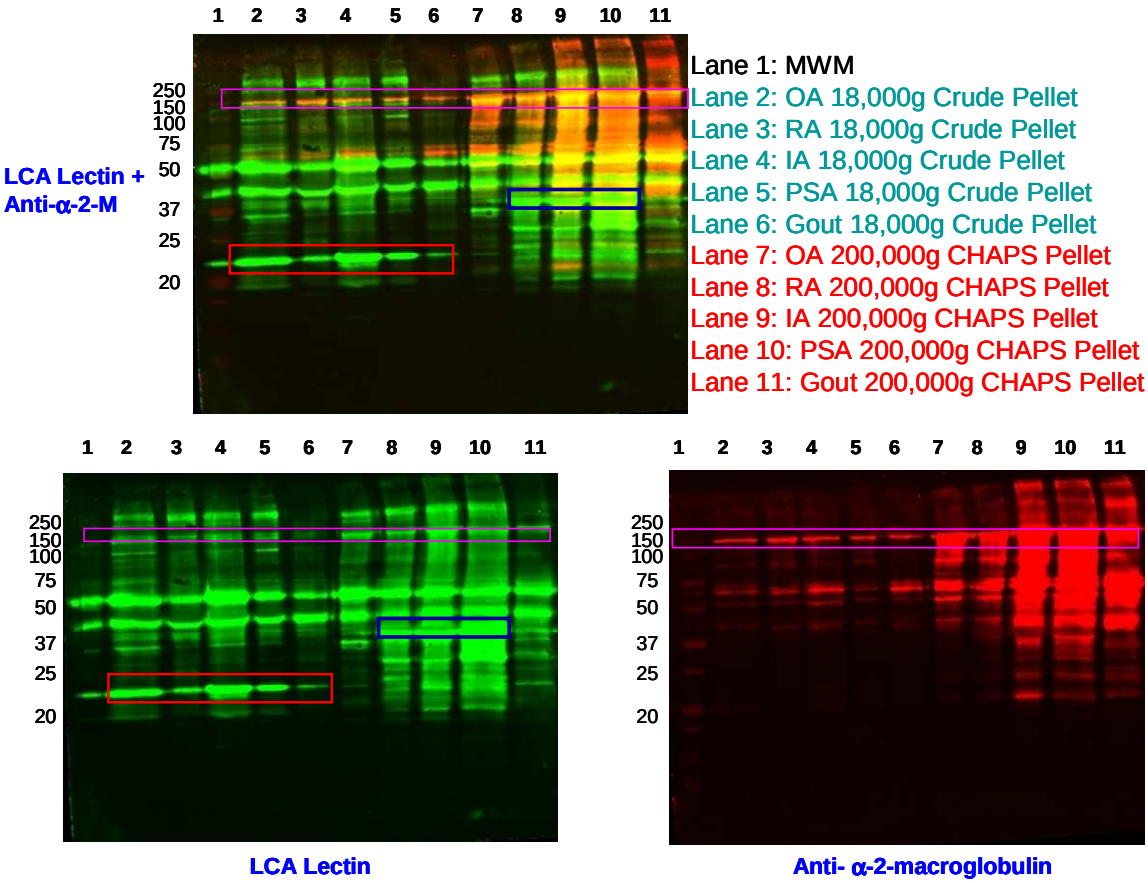

Figure 4.22: *WB images of the **pellet** fractions resulting from the differential centrifugation process developed to isolate MV from SF. Incubation with LCA lectin was carried out in the λ_{em}800nm (lower left), incubation with anti-α-2-M was in the λ_{em}700nm (lower right). The upper blot is a compound image of both LCA and anti-α-2-M. The orange/yellow bands are where there is an overlap of both images. The bands enclosed within the coloured boxes are discussion aids*

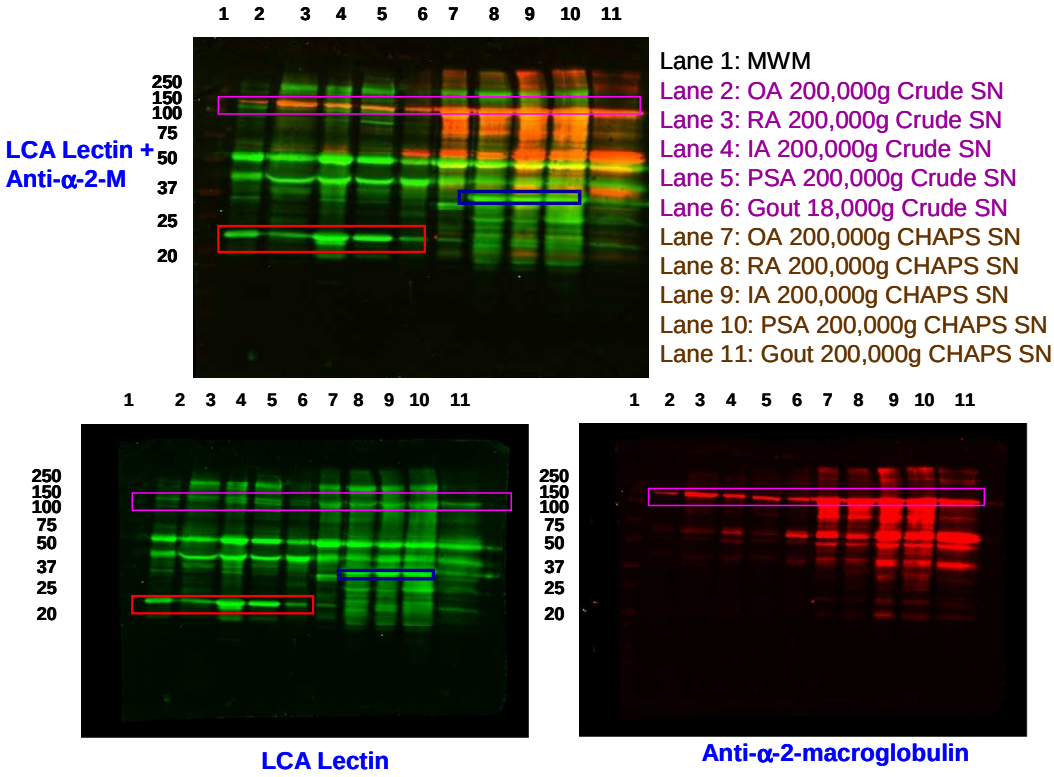

Figure 4.23: *WB images of the **SN** fractions resulting from the differential centrifugation process developed to isolate MV from SF. Incubation with LCA lectin was carried out in the λ_{em}800nm (lower left), incubation with anti-α-2-M was in the λ_{em}700nm (lower right). The upper blot is a compound image of both LCA and anti-α-2-M. The orange/yellow bands are where there is an overlap of both images. The bands enclosed within the coloured boxes are discussion aids.*

In Figure 4.22 there is a striking difference in the band patterns between the 18,000g crude and 200,000g CHAPS pellets. Relative to the 18,000g pellet (Lanes 2-6), there is extensive fragmentation of α-2-M in the 200,000g pellets (Lanes 7-11) of all patient samples (red channel). All samples in both 18,000g and 200,000g pellets indicate that the monomeric form of α-2-M is present at ~ 180kDa (highlighted with a purple box). Hypothetical reasons for this fragmentation unique to the 200,000g CHAPS pellet will be explored in the discussion section.

This same fragmentation of α-2-M is mirrored in the SN fractions (Figure 4.23, red channel). Here it may be seen that the 200,000g CHAPS SN possesses the same fragmentation as the 200,000g CHAPS pellet, while this feature is absent in the 200,000g crude SN. In light of the discussion in the previous chapter, this is not a surprise. There,

a discussion was had concerning the likelihood of MVs remaining in the 200,000g CHAPS SN i.e. a 100% recovery of MVs in the pellet fraction does not occur. But why is fragmentation of α-2-M not evident in the crude SN (Figure 4.23, λ_{em}700nm, Lanes 2-6) bearing in mind that both the crude and CHAPS fractions are analysed under reducing conditions? Here it needs to be appreciated that the crude SN represents the entire SF proteome minus the isolated MV proteome, whereas the CHAPS SN is a combination of proteins from any entrapped MVs plus proteins removed by CHAPS from the 200,000g CHAPS pellet surface. Comparing Figures 4.22 and 4.23 with Figure 4.19 it can be seen that the crude SN is an almost whole SF proteome, whereas the CHAPS SN represents a unique sub-proteome i.e. the band profile between the crude SN and whole SF is very similar. Thus this study uncovered for the first time that the nature of α-2-M fragmentation in the 200,000g CHAPS pellet is a characteristic feature not evident in whole SF and may indicate that other proteins may exhibit such alterations. This would warrant further study in the future.

In addition to α-2-M fragmentation, there are also noted differences in glycoproteins between various fractions. For example, both the 200,000g CHAPS pellets and CHAPS SN lack the strong band intensities that are present in the 18,000g pellet and 200,000g crude SN at ~23kDa (enclosed in a red box in both Figure 4.22 and 4.23, λ_{em}800nm). There are also differences between pathologies within the same fraction. The bands enclosed in the blue boxes at ~37kDa (Lanes 8, 9 and 10) in each figure are more strongly represented in RA, IA and PSA, than in OA or gout. This may be a difference in glycosylation rather than a protein difference.

As noted, the study that was performed on the MV sub-proteome revealed interesting differences that were masked in the analysis of whole SF. It may be the case that future screening of MVs rather than whole SF with the same 18 lectins that were used in this project would be interesting and worthwhile.

4.3 Discussion

The role which protein glycosylation plays in the human body was previously discussed in the introduction and a summary is outlined in Figure 4.9. There, diverse functionalities were mentioned e.g. modifications in protein solubility and stability, alterations in protein folding, mediators for targeting and receptor recognition, resistance to protein lysis and prevention to inflammation and autoimmune disease.

A panel of plant lectins with a diverse range of sugar specificities was employed to probe any glycan differences between OA and other arthritic pathologies. It was hypothesised that differentially expressed bands would signify the presence/absence of glycans and/or changes to glycosylation between disease states. Lectins that exhibited disease marker potential would then be used in lectin-affinity chromatography to further aid in characterising potentially interesting glycoproteins.

Sialic acid-binding lectins i.e. SNA, MAL I and MAL II (Figure 4.11) yielded interesting intensity differences between OA and the other disease states. Previously, Przybysz *et al*. [32] used the same three lectins to probe fibronectin in order to classify the different stages of RA (early, middle or late-stage) and concluded that the degree of sialylation increased with disease duration. Though RA was not one of the pathologies explored in this stage of the project, there is stronger band intensity at ~90kDa for SNA and MAL I in IA, PSA and gout relative to OA.

The same author also found that the expression of α1-6-linked fucose in fibronectin was found to be related to disease activity. Again, three lectins were used in fucosylation analysis by the authors of which only one (UEA) was common to the three lectins in this project (which were LCA, PSA and UEA-1, Figure 4.12. Of the three fucose-specific lectins used, LCA was found to show the most interesting band differences between disease types (Figure 4.13). However, the choice of conditions under which the experiment was performed greatly influenced the result. In Figure 4.13 the entire glycan population was denaturated prior to lectin incubation while in Figure 4.20 the converse was the case where all glycoproteins were in their native conformation at the time of

lectin binding. Alterations in the binding site were believed to be the primary reason for the marked differences in band profiles in denaturing versus non-denaturing conditions.

ConA and jacalin also featured differential band patterns between patient pathologies. However, due to additional affinity for core fucose and encouraged by other studies in the literature [32, 33, 40] , LCA was the candidate lectin for further analysis employing lectin-affinity chromatography.

Following lectin affinity chromatography it was found that one band, at a molecular weight just above 150kDa, was unique to OA. Other pathologies had bands in the same region, but at a lower molecular weight. It was hypothesised that this was either a glycan unique to OA or else a protein(s) that is common to all pathologies, though possessing a different glycosylation signature in OA. MS analysis indentified a number potential candidates this band and based on the number of peptide hits, the protein coverage and the closeness of the molecular weight to the monomeric form of α-2-M, this was the protein that received priority for further study.

A larger cohort of patient samples was obtained and the whole SF of each was analysed by SDS-PAGE followed by incubation with both anti-α-2-M and LCA lectin. However, when the ratio of the intensity of the lectin to the intensity of α-2-M was compared for each sample, no significant difference presented itself between different patient pathologies. Gout and OA appeared to exhibit a different ratio, but a larger patient cohort would be required to confirm this result before anything definitive can be hypothesised. It was recognised that this study was on a patient sample set of *whole* SF, and not on an LCA-separated sub-set. However, the principal aim of this particular study was to be able to establish biomarker differences in whole SF after having first identified that marker using more extensive methodologies. The next logical step would have been to repeat the lectin-affinity experiment with this larger cohort of samples, but a potentially more interesting side-study of α-2-M presented itself following a further literature research into this protein.

α-2-M is a 720kDa homotetrameric species and is the third most abundant glycoprotein in human plasma [44]. The tetramer structure itself is composed of two 370kDa disulphide-linked homodimers. This protein has eight *N*-linked glycosylation sites and 13 disulphide bridges (11 of which are intra-chain and two are inter-chain) to form the final tertiary structure [45, 46]. From the UniProt database α-2-M is able to inhibit all four classes of proteinases (serine, aspartic, cysteine and MMPs) by a unique "trapping" mechanism. Each α-2-M monomer possesses a "bait region" (a short stretch of amino acids beginning at Pro^{667} and ending at Thr^{705})[43] and it is this region which is susceptible to proteolytic cleavage. When cleaved by an enzyme, α-2-M undergoes a conformational change which "traps" the proteinase. This resulting change in α-2-M morphology, results in the inhibition of protease activity through the prevention of substrate access by means of steric hindrance. It may be possible that α-2-M itself may become a substrate for the entrapped enzyme. As proteases were confirmed to be associated with MVs by MS and zymography (chapter 3), this theory is a distinct possibility. This would offer a plausible explanation for the observed fragmentation especially in light of a recent paper by Paiva *et al.* [44] who found that covalently-linked proteinases to the bait region converted *"the native or electrophoretically slow S-α2M into the electrophoretically fast form or F-α2M"*. The terms "fast" and "slow" may relate to the relative sizes of α-2-M fragments or indeed any induced changes in charge. Extensive fragmentation of α-2-M experienced in the 200,000g CHAPS pellet suggested the activated form of this inhibitor was en route to some as yet, unknown destination.

A very interesting study by Tortorella *et al.* [43] into cleavage of α-2-M by ADAMTS-4 and ADAMTS-5 found that these species cleave α-2-M at a specific and unique amino acid residue in the bait region i.e. Met^{690}. Moreover, they found that this cleavage produces a 98kDa α-2-M fragment plus *"higher molecular weight fragments representing an SDS-stable complex between α-2-M and ADAMTS-4"*. Figures 4.22 and 4.23 clearly show intense bands in the 100kDa region for the 200,000g CHAPS pellet and SN for each patient sample. This was also found in the anti-α-2-M WB under reducing conditions in Figure 3.33 in the previous chapter. Bands in this regions are absent in the 18,000g pellet and 200,000g crude SN. This result leads to the hypothesis that cleaved

α-2-M residues are solely vesicle associated. Further, the authors identified α-2-M fragments containing the N-terminal ^{691}GRGHAR and C-terminal YESDVM^{690} generated by cleavage of the α-2-M subunit by both ADAMTS species, as potential markers of aggrecanase activity, which in turn by means of aggrecan degradation, reduces the ability of cartilage to resist compressive forces. The authors regret that they were unable to find these neoepitopes in OA synovial fluid and they conclude, *"That we were unable to detect the α-2-M:ADAMTS-4/-5 complex in OA synovial fluid suggests the complex is rapidly cleared through the vascular and lymph systems. It is well known that conformational change of α-2-M leads to exposure of recognition sites that bind receptors such as lipoprotein receptor-related protein on a variety of cells, including macrophages, resulting in clearance"*. The afore-mentioned receptor, also known as alpha-2-macroglobulin receptor (UniProt), was one of the species characterized by MS in the OA 200,000g CHAPS pellet (Table 3.7, Q07954). One of the functionalities listed by the UniProt database for this receptor is the clearance of activated α-2-M. Based on the results of the current project displayed in Figures 4.22 and 4.23 and above discussion, also in light of the above quotation by Tortorella *et al.* [43], there is sufficient evidence to hypothesise that proteinase-activated α-2-M, is associated with MVs and ferried thus out of the joint cavity.

An earlier study by Wu *et al.* [47] focused on the effects of oxidation on α-2-M in terms of proteinase-inhibitory function. They concluded that α-2-M from RA SF is significantly more oxidized than that in OA SF, hence the proportion of α-2-M capable of inhibiting proteases is reduced in RA relative to OA. However, they did state that the degree of oxidation correlates with the number of bands in WB, and it was concluded that oxidation correlates with α-2-M susceptibility to proteolytic degradation. Applying this criterion to the current study was the case that the IA, PSA and gout 200,000g CHAPS pellet samples exhibited greater fragmentation (Figure 4.22, λ_{em}700nm) than OA and RA suggesting that the former samples have been subject to a greater degree of α-2-M oxidation. Comparing Figure 4.22 of this thesis with Figure 5 in Wu's paper revealed that there are many bands in common. This evidence indirectly implies that an oxidation event could be the origin of the fragmentation detected by WB. Another interesting insight offered

by the group concerned the association of α-2-M with the regulation of the pro-inflammatory cytokine, TNF-α. Here it was found that increased oxidation of α-2-M resulted in increased binding to TNF-α and the authors attributed this phenomenon to the fact that oxidised α-2-M has impaired tissue clearance through the already mentioned lipoprotein receptor-related protein. Consequently, oxidised α-2-M may remain in the inflammatory fluid for a great period of time and so inhibit TNF-α . Thus, it may be possible MVs bearing activated α-2-M via the lipoprotein receptor-related protein, could in principle, aid in trafficking harmful TNF-α out of the joint. Finally, the authors recognised an apparent contradiction in their results. They ask how proteinases are able to function given that some proteinase inhibitory activity is present in all of the SF samples that they studied. They offer three possible solutions to this question;

1. Concentrations of oxidants and proteinases may rise and fall transiently. During *"each oxidative burst"* the amount of these species released overwhelms the protective effects of α-2-M. The result is inflammation which in turn increases the vascular permeability allowing a replenishment of functional α-2-M which completes the inactivation of proteinases.
2. Large proteinases with molecular weights > 90kDa and lysine-specific proteinases that cannot be inhibited by α-2-M are released into SF to mediate α-2-M proteolysis.
3. Proteinases and oxidants are released in *"sequestered pockets"* such that α-2-M localized within these pockets is for the most part oxidised and proteolysed.

The authors hypothesised that the first explanation, based on their results, was the more likely. Not surprisingly, the third option is the one that fits with the result obtained in this project. Again, Figures 4.22 and 4.23 indicate that proteolysed α-2-M is strongly associated with MVs, the *"sequestered pockets"* referred to by Wu *et al.* [47]. Another protein that was identified by MS in the previous chapter was myeloperoxidase. This protein produces hypochlorous acid (HOCl) which is a powerful protein oxidizing agent [48] and may lead to α-2-M oxidation which in turn leads to greater susceptibility to proteases activity. From the previous chapter proteases were found to be vesicle-associated by MS and zymography. It may be that oxidation of α-2-M by HOCl is

indirectly responsible for the fragmentation in MVs. In reality, the possibility of all three proposals being the case exists.

A very interesting link between the previous chapter of this thesis and the current chapter is a study carried out by Luan *et al.* [49]. The link to the previous chapter lies in the fact that they found that ADAMTS-7 and -12 were induced from the cartilage and synovium of arthritic patients, which then bound to and degraded COMP. The molecular mass of the COMP fragments produced by either ADAMTS-7 or -12 were stated to be similar to those observed in OA patients. The connection to the present chapter is their conclusion that both ADAMTS-7 and ADAMTS-12 were able to cleave α-2-M, giving rise to 180- and 105-kDa cleavage products, respectively. Furthermore, they found that α-2-M inhibited both ADAMTS-7- and ADAMTS-12-mediated COMP degradation in a concentration (or dose)-dependent manner. Figures 4.22 and 4.23 clearly show bands at these molecular weights in the 200,000g CHAPS pellets. The authors stated that "*α-2-M represents the first endogenous inhibitor of ADAMTS-7 and ADAMTS-12*".

4.4 Conclusion

The initial aim of this study was to ascertain if there were differences in glycosylation and/or glycoprotein moieties in whole SF between different arthritic patient pathologies, employing a panel of 18 available plant lectins. Two lectins (LCA and ConA) highlighted some potentially interesting differences between OA and the other diseases. LCA was selected for use in the employment of immunoaffinity chromatography. A band that appeared to be unique to OA was characterised by MS and a number of candidate proteins were identified. Based on protein coverage and the number of peptides identified, alpha-2-macroglobulin (α-2-M) was pursued for further study. A slightly larger cohort of patient samples was screened in order to establish if there was a change in glycosylation of α-2-M or that the α-2-M itself manifestly changed. This pilot experiment indicated that there maybe a slight decrease in the glycosylation of α-2-M in OA and an increase in this proteins glycosylation in gout, relative to the other pathologies. Only with a much larger sample set from each disease-type, can this preliminary finding be ascertained.

However, α-2-M became the object of further study - this time in MVs. It was found that α-2-M (under reducing conditions) present in vesicles displayed extensive fragmentation relative to that in whole SF. A hypothesis for this phenomenon was suggested, whereby MVs may be carriers of activated α-2-M i.e. α-2-M that trapped proteinases, thus rendering them inactive.

Wu *et al.* [47] stated that oxidised α-2-M has decreased ability to entrap proteases and hypochlorite is a potent α-2-M modifier *in vivo*. Further, hypochlorite oxidation is evident in RA but not OA. A recent study by Kahn *et al.* [50] also noted that hypochlorite significantly reduced the anti-proteolytic potential of α-2-M. Their study examined the role of nitrite as an anti-oxidant by removing hypochlorite.

In the next chapter it is proposed to establish if nitrite is present in MV.

4.5 References

References

(1) Taylor; ME.; Drickamer; KD. In *Introduction to Glycobiology;* Oxford University Press: New York, 2006; .

(2) Mechref, Y.; Novotny, M. V. Structural Investigations of Glycoconjugates at High Sensitivity. *Chemical reviews* **2002**, *102*, 321-370.

(3) Helenius, A.; Aebi, M. Intracellular Functions of N-Linked Glycans. *Science* **2001**, *291*, 2364-2369.

(4) Parodi, A. J. Role of N-oligosaccharide endoplasmic reticulum processing reactions in glycoprotein folding and degradation. *Biochemical Journal* **2000**, *348*, 1-13.

(5) Varki A., Cummings R. , Esko J., Freeze H. , Hart G. , Marth J. In *Essentials of Glycobiology;* Cold Spring Harbour Laboratory Press: New York, 1999; .

(6) Roughley PJ The structure and function of cartilage proteoglycans. *European Cells & Materials* **2006**, *12*, 92.

(7) Gabius, H. J. Cell surface glycans: The why and how of their functionality as biochemical signals in lectin-mediated information transfer. *Critical Reviews in Immunology* **2006**, *26*, 43-79.

(8) Guo, N. X.; Liu, Y.; Masuda, Y.; Kawagoe, M.; Ueno, Y.; Kameda, T.; Sugiyama, T. Repeated immunization induces the increase in fucose content on antigen-specific IgG N-linked oligosaccharides. *Clinical Biochemistry* **2005**, *38*, 149-153.

(9) Kaneko, Y.; Nimmerjahn, F.; Ravetch, J. V. Anti-inflammatory activity of immunoglobulin G resulting from Fc sialylation. *Science* **2006**, *313*, 670-673.

(10) Udiavar, S.; Apffel, A.; Chakel, J.; Swedberg, S.; Hancock, W. S.; Pungor, E. The use of multidimensional liquid-phase separations and mass spectrometry for the detailed characterization of posttranslational modifications in glycoproteins. *Analytical Chemistry* **1998**, *70*, 3572-3578.

(11) Alavi, A.; Axford, J. S. Sweet and sour: the impact of sugars on disease. *Rheumatology* **2008**, *47*, 760-770.

(12) Rhodes, J.; Milton, J., Eds.; In *Lectin Methods and Protocols;* Walker J.M., Ed.; Methods in Molecular Medicine; Humana Press Inc.: New Jersey, 1998; .

(13) Mislovicova, D.; Gemeiner, P.; Kozarova, A.; Kozar, T. Lectinomics I. Relevance of exogenous plant lectins in biomedical diagnostics. *Biologia* **2009**, *64*, 1-19.

(14) Mechref Y.; Novotny M.V. In *High-sensitivity analytical approaches to the anlysis of N-glycans;* R.D. Cummings, J.M. Pierce, Eds.; Handbook of Glycomics; Academic ress: London, 2009; pp 3.

(15) Lam, S.; Ng, T. Lectins: production and practical applications. *Applied Microbiology and Biotechnology* **2011**, *89*, 45.

(16) Gemeiner, P.; Mislovicova, D.; Tkac, J.; Svitel, J.; Patoprsty, V.; Hrabarova, E.; Kogan, G.; Kozar, T. Lectinomics II. A highway to biomedical/clinical diagnostics. *Biotechnology Advances* **2009**, *27*, 1-15.

(17) Matsuhashi, T.; Iwasaki, N.; Nakagawa, H.; Hato, M.; Kurogochi, M.; Majima, T.; Minami, A.; Nishimura, S. -. Alteration of N-glycans related to articular cartilage deterioration after anterior cruciate ligament transection in rabbits. *Osteoarthritis and Cartilage* **2008**, *16*, 772-778.

(18) Midura, R. J.; Hascall, V. C. Bone sialoprotein - A mucin in disguise? *Glycobiology* **1996**, *6*, 677-681.

(19) Wong, C. Protein Glycosylation: New Challenges and Opportunities. *The Journal of Organic Chemistry* **2005**, *70*, 4219-4225.

(20) Mer, G.; Hietter, H.; Lefevre, J. Stabilization of proteins by glycosylation examined by NMR analysis of a fucosylated proteinase inhibitor. *Nature Structural Biology* **1996**, *3*, 53.

(21) Raju, T. S.; Scallon, B. J. Glycosylation in the Fc domain of IgG increases resistance to proteolytic cleavage by papain. *Biochemical and Biophysical Research Communications* **2006**, *341*, 797-803.

(22) Dowbenko, D.; Kikuta, A.; Fennie, C.; Gillett, N.; Lasky, L. A. Glycosylation-Dependent Cell-Adhesion Molecule-1 (Glycam-1) Mucin is Expressed by Lactating Mammary-Gland Epithelial-Cells and is Present in Milk. *Journal of Clinical Investigation* **1993**, *92*, 952-960.

(23) Brockhausen, I. The role of galactosyltransferases in cell surface functions and in the immune system. *Drug News & Perspectives* **2006**, *19*, 401-409.

(24) Takahashi, K.; Ezekowitz, R. A. B. The role of the mannose-binding lectin in innate immunity. *Clinical Infectious Diseases* **2005**, *41*, S440-S444.

(25) Buzas, E. I.; Gyorgy, B.; Pasztoi, M.; Jelinek, I.; Falus, A.; Gabius, H. Carbohydrate recognition systems in autoimmunity. *Autoimmunity* **2006**, *39*, 691-704.

(26) Li, Y.; Yang, X.; Nguyen, A. H. T.; Brockhausen, I. Requirement of N-glycosylation for the secretion of recombinant extracellular domain of human Fas in HeLa cells. *International Journal of Biochemistry & Cell Biology* **2007**, *39*, 1625-1636.

(27) Hart, G. W.; Copeland, R. J. Glycomics Hits the Big Time. *Cell* **2010**, *143*, 672-676.

(28) Bones, J.; Mittermayr, S.; O'Donoghue, N.; Guttman, A.; Rudd, P. M. Ultra Performance Liquid Chromatographic Profiling of Serum N-Glycans for Fast and Efficient Identification of Cancer Associated Alterations in Glycosylation. *Analytical Chemistry* **2010**, *82*, 10208-10215.

(29) Brooks, S. A.; Leathem, A. J. C. Prediction of Lymph-Node Involvement in Breast-Cancer by Detection of Altered Glycosylation in the Primary Tumor. *Lancet* **1991**, *338*, 71-74.

(30) Welinder, C.; Jansson, B.; Fernoe, M.; Olsson, H.; Baldetorp, B. Expression of Helix pomatia Lectin Binding Glycoproteins in Women with Breast Cancer in Relationship to Their Mood Group Phenotypes. *Journal of Proteome Research* **2009**, *8*, 782-786.

(31) Smith, K. D.; Pollacchi, A.; Field, M.; Watson, J. The heterogeneity of the glycosylation of alpha-1-acid glycoprotein between the sera and synovial fluid in rheumatoid arthritis. *Biomedical Chromatography* **2002**, *16*, 261-266.

(32) Przybysz, M.; Maszczak, D.; Borysewicz, K.; Szechinski, J.; Katnik-Prastowska, I. Relative sialylation and fucosylation of synovial and plasma fibronectins in relation to the progression and activity of rheumatoid arthritis. *Glycoconjugate Journal* **2007**, *24*, 543-550.

(33) Kratz, E.; Borysewicz, K.; Katnik-Prastowska, I. Terminal monosaccharide screening of synovial immunoglobulins G and A for the early detection of rheumatoid arthritis. *Rheumatology International* **2010**, *30*, 1285-1292.

(34) Lauc, G. Sweet secret of the multicellular life. *Biochimica Et Biophysica Acta-General Subjects* **2006**, *1760*, 525-526.

(35) Kumada, Y.; Ohigeshi, Y.; Emori, Y.; Imamura, K.; Omura, Y. Improved lectin ELISA for glycosylation analysis of biomarkers using PS-tag-fused single-chain Fv. *Journal of Immunological Methods* **2012**, *385*, 15.

(36) Brooks, S. A.; Leathem, A. J. C.; Schumacher, U. In *Lectin Histochemistry;* BIOS Scientific Publishers Limited: Oxford, UK, 1997; .

(37) Vector Laboratories In *Catalogue 2012;* USA, 2012; .

(38) Raghav, S.; Gupta, B.; Agrawal, C.; Saroha, A.; Das, R.; Chaturvedi, V.; Das, H. Altered expression and glycosylation of plasma proteins in rheumatoid arthritis. *Glycoconjugate Journal* **2006**, *23*, 167-173.

(39) Sobiesiak, M. Reactivity of human serum transferrin with two mannose-binding lectins: LCA and ConA. *Central European Journal of Immunology* **2002**, *27*, 63.

(40) Ferens-Sieczkowska, M.; Kossowska, B.; Gancarz, R.; Dudzik, D.; Knas, M.; Popko, J.; Zwierz, K. Fucosylation in synovial fluid as a novel clinical marker for differentiating joint diseases - a preliminary study. *Clinical and Experimental Rheumatology* **2007**, *25*, 92-95.

(41) Flogel, M.; Lauc, G.; Gornik, I.; Macek, B. Fucosylation and galactosylation of IgG heavy chains differ between acute and remission phases of juvenile chronic arthritis. *Clinical Chemistry and Laboratory Medicine* **1998**, *36*, 99-102.

(42) Wu, S.; Patel, D.; Pizzo, S. Oxidized alpha(2)-macroglobulin (alpha(2)M) differentially regulates receptor binding by cytokines growth factors: Implications for tissue injury and repair mechanisms in inflammation. *Journal of Immunology* **1998**, *161*, 4356-4365.

(43) Tortorella, M.; Arner, E.; Hills, R.; Easton, A.; Korte-Sarfaty, J.; Fok, K.; Wittwer, A.; Liu, R.; Malfait, A. alpha(2)-Macroglobulin is a novel substrate for ADAMTS-4 and ADAMTS-5 and represents an endogenous inhibitor of these enzymes. *Journal of Biological Chemistry* **2004**, *279*, 17554-17561.

(44) Paiva, M. M.; Soeiro, M. N. C.; Barbosa, H. S.; Meirelles, M. N. L.; Delain, E.; Araujo-Jorge, T. C. Glycosylation patterns of human alpha2-macroglobulin: Analysis of lectin binding by electron microscopy. *Micron* **2010**, *41*, 666-673.

(45) Jensen, P.; SottrupJensen, L. Primary Structure of Human Alpha-2-Macroglobulin - Complete Disulfide Bridge Assignment and Localization of 2 Interchain Bridges in the Dimeric Proteinase Binding Unit. *Journal of Biological Chemistry* **1986**, *261*, 5863-5869.

(46) SottrupJensen, L.; Stepanik, T.; Kristensen, T.; Wierzbicki, D.; Jones, C.; Lonblad, P.; Magnusson, S.; Petersen, T. Primary Structure of Human Alpha-2-Macroglobulin .5. the Complete Structure. *Journal of Biological Chemistry* **1984**, *259*, 8318-8327.

(47) Wu, S.; Pizzo, S. alpha(2)-Macraglobulin from rheumatoid arthritis synovial fluid: Functional analysis defines a role for oxidation in inflammation. *Archives of Biochemistry and Biophysics* **2001**, *391*, 119-126.

(48) Klebanoff, S. Myeloperoxidase: friend and foe. *Journal of Leukocyte Biology* **2005**, *77*, 598-625.

(49) Luan, Y.; Kong, L.; Howell, D. R.; Ilalov, K.; Fajardo, M.; Bai, X. -.; Di Cesare, P. E.; Goldring, M. B.; Abramson, S. B.; Liu, C. -. Inhibition of ADAMTS-7 and ADAMTS-12 degradation of cartilage oligomeric matrix protein by alpha-2-macroglobulin. *Osteoarthritis and Cartilage* **2008**, *16*, 1413-1420.

(50) Khan, M.; Naqshbandi, A.; Zubair, H.; Ahsan, H.; Khan, S.; Khan, F. Nitrite, a Reactive Nitrogen Species, Protects Human Alpha-2-Macroglobulin from Halogenated Oxidant, HOCl. *Protein Journal* **2010**, *29*, 276-282.

Chapter 5

Determination of the presence of nitrite in synovial fluid microvesicles

5.0 Introduction

5.0.1 Nitric Oxide

Prior to the 1980's Nitric Oxide (NO) was believed to be a free radical gas that contributed to atmospheric pollution [1]. In 1980 however, Furchgott and Zawadzki published their landmark paper in Nature [2] describing the endothelium-derived relaxing factor (EDRF) which is released by the endothelium upon stimulation with acetylcholine. In 1987 Ignarro and co-workers [3] discovered that the identity of this EDRF was in fact NO. A year later Furchgott and Ignarro were awarded the Nobel Prize '*for their discoveries concerning nitric oxide as a signalling molecule in the cardiovascular system'*. The synthesis of NO by vascular endothelium is responsible for the vasodilation essential for the regulation of blood pressure. Today, NO is known to act as a mediator and a signalling molecule in both physiological and pathophysiological processes in the body. The critical functions of NO in the human body include (i) its role as a neurotransmitter in the central nervous system, (ii) its mediating roles in mechanisms that regulate various gastrointestinal, respiratory and genitourinary tract functions, (iii) the control of platelet aggregation, (iv) regulation of cardiac contractility and finally (v) its production in large quantities during host defence and immunologic reactions [1] .

5.0.2 Biosynthesis of NO

NO is synthesised by a family of enzymes termed nitric oxide synthases (NOS) which use the amino acid L-Arginine as a substrate [4]. There are three forms of NOS known to exist – neuronal (nNOS, NOS-I) [5], inducible (iNOS, NOS-II) [6] and endothelial (eNOS, NOS-III) [7]. Generally speaking nNOS and eNOS are thought to be constitutively expressed and expression depends on the concentration of intercellular free calcium and calmodulin. These enzymes produce picomolar to nanomolar concentrations of NO for short periods of time – *"NO puffs"* [8]. By contrast, iNOS is expressed in response to cytokines e.g. interleukin 1β (Il-1β), tumour necrosis factor-α (TNF-α), lipopolysaccharide (LPS) or γ-interferon (IFN-γ). It is produced by some cell types e.g. macrophages, neutrophils, hepatocytes, smooth muscle cells and importantly for the various arthritic diseases, chondrocytes. The iNOS isoform can generate higher quantities of NO (micromolar quantities) for a greater amount of time (up to 72 hours *in vitro*) [4]. While the overall NO synthesis pathway is quite complex and the end result can be simplified to:

$$\text{Arginine} + O_2 \xrightarrow{\text{NOS}} \text{Citrulline} + \text{NO}$$

A schematic diagram outlining NO production from NOS and L-arginine can be seen in Figure 5.1 [9]. The overall active NOS enzyme is a tetramer composed of a NOS dimer and two molecules of calmodulin. In addition, a number of cofactors are required for enzyme activation in order to effect NO production – flavin mononucleotide (FMN), flavin adenine dinucleotide (FAD), tetra hydrobiopterin (BH_4) and haem (Fe). The BH_4 cofactor is bound to the C-terminal reductase domain and is known to be critical for the overall dimerisation of iNOS. Indeed, in BH_4-deficient cells the iNOS is in a monomeric form and is proven to be inactive [10]. Ellis *et al.*[11] state that as much as 90% of circulating NO_2^- is derived from the L-arginine : NO pathway.

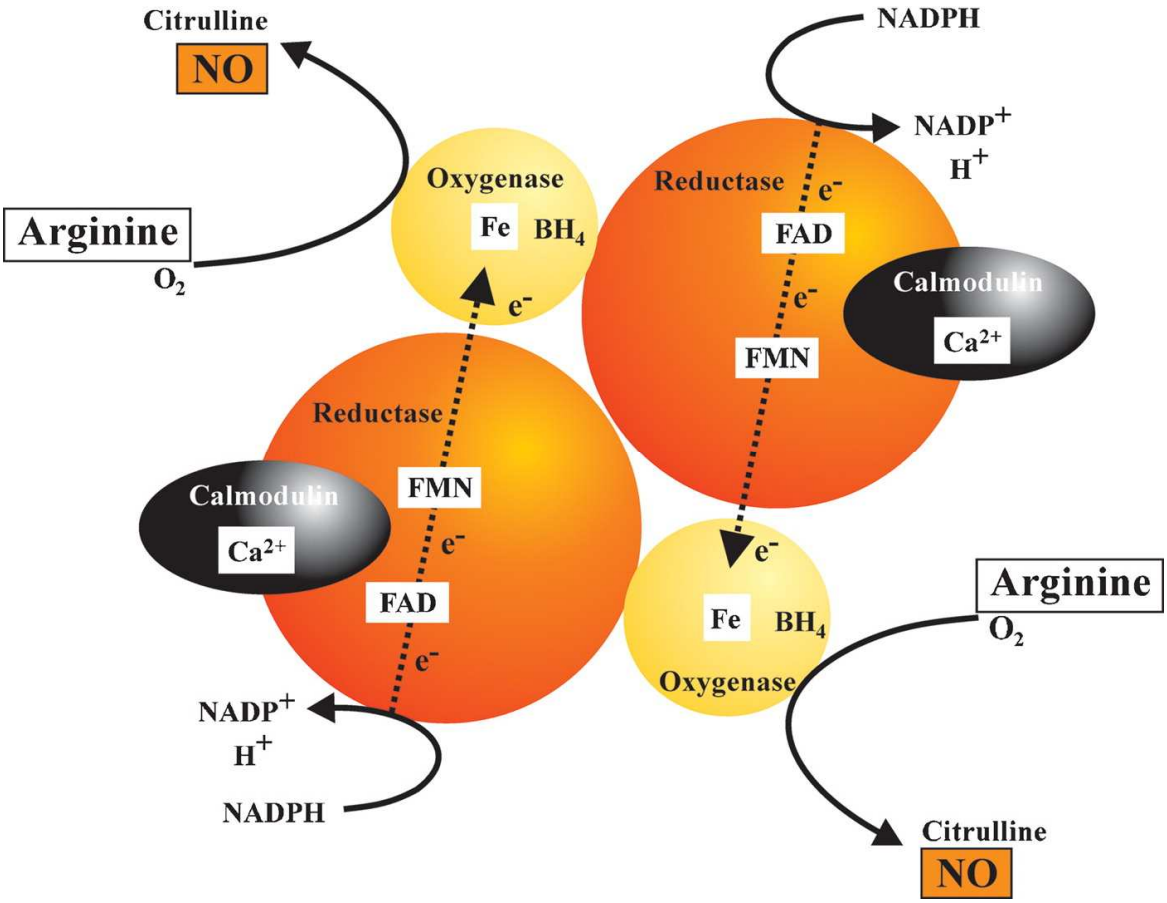

Figure 5.1: *Schematic diagram outlining the production of NO and citrulline from arginine and O_2 by means of a catalytic reaction with the Nitric Oxide Synthase (NOS) enzyme. Diagram taken from Vuolteenaho et al.* [9]

All three isoforms of NOS require calmodulin as a cofactor in order to facilitate the essential flow of electrons from the reductase domain to the oxygenase domain. However, in the eNOS and nNOS constitutive isoforms, calmodulin binding and activation is modulated by changes in [Ca^{2+}]. By contrast, in the iNOS isoform the calmodulin is so tightly bound that even at low [Ca^{2+}], the enzyme is active. Therefore, once the iNOS isoform is expressed, it can continue to synthesise NO until the substrate and or cofactors are depleted [12].

5.0.3 Biochemical reactions of NO

From the discussion above it recognised that NO acts as a signalling and mediator molecule in the human body e.g. in the cardiovascular system (maintains blood pressure), immune system and neurotransmission. The biological activity of NO is dependant on the micro-environmental conditions (e.g. pH and oxygen levels) at the site of production and also the quantity of NO produced. Concomitantly, the quantity produced depends on the particular NOS isomer involved in the synthesis. NO levels also determine whether a regulatory or proinflammatory/destructive role is produced [13].

NO is a free radical with a half life in the order of seconds [4]. It has a high affinity for and readily reacts with heme iron, sulfhdryl or thiol groups, superoxide anion $O_2^{\cdot -}$, and molecular oxygen. The decomposition products of NO in the presence of oxygen are NO_2^- and NO_3^-. The conversion of NO to NO_2^- is given by:

$$4NO^{\cdot} + O_2 + 2H_2O \rightarrow 4\,NO_2^- + 4H^+ \ldots\ldots\textbf{(i)}$$

However in blood, NO_2^- is oxidised to NO_3^- by the presence of oxyhaemoglobin. The overall reaction is:

$$4HbO_2 + 4NO_2^- + 4H^+ \rightarrow 4Hb^+ + 4NO_3^- + O_2 + 2H_2O \quad [14]\ldots\ldots\ldots\textbf{(ii)}$$

The biochemical effects of NO are in part governed by the concentration of NO in the micro-vicinity. At low concentrations (< 0.5μM) [15], the biological action of NO said to be direct i.e. NO itself mediates with various species. These interactions account for the normal regulatory effects of NO in the body. Examples of these effects include interactions with metals, metalloproteins and free radical scavenging. Some examples of interactions with metals and metalloproteins include binding of NO to the heme group of soluble guanylyl cyclise (involved in the relaxation of smooth muscle) [16], cytochrome P-450 and cyclooxygenase (COX). Direct scavenging of free radicals include superoxide, O_2^- (forming peroxynitrite, $ONOO^-$), hydroxyl radicals (forming nitrous acid, HNO_2) and lipid peroxides (which prevent lipid peroxidation) [15].

At higher concentrations of NO (> 0.5μM), the biological effects are said to be indirect. Instead, the effects of NO are mediated through reactive nitrogen species (RNS) [15]. One such RNS is formed by the auto oxidation of NO [17]:

$$2NO + O_2 \rightarrow 2NO_2 \ldots\ldots\ldots\ldots\ldots\text{(i)}$$
$$NO_2 + NO \rightarrow N_2O_3 \ldots\ldots\ldots\ldots\ldots\text{(ii)}$$
$$N_2O_3 + RS^- \rightarrow RSNO + NO_2^- \ldots\text{(iii)}$$

Dinitrogen trioxide is produced which is readily hydrolysed to NO_2^- and NO^+. The nitrosonium ion NO^+ interacts with cysteine and tyrosine residues of proteins and so changes the activity of the protein [18] . Some consequences of this include modification of several transcription factors, kinases involved in signaling cascades, ion channels and the activation of matrix metalloproteinases (MMPs) [19].

When NO and O_2^- (produced by mitochondria, macrophages and granulocytes) are present in equal amounts, $ONOO^-$ is produced. This is a highly reactive oxidant and nitrating agent. When produced in excess, it has been identified as a major factor of cellular toxicity [17]. In particular $ONOO^-$ is known to cause the mis-pairing and separating of DNA strands, oxidation and nitration of proteins [20], oxidation of lipids, the inhibition of mitochondrial respiration [21] and finally cellular death and apoptosis [22]. At neutral pH $ONOO^-$ rapidly decomposes to peroxynitrous acid (ONOOH). This is an unstable molecule and rapidly decomposes to NO_3^-. Both $ONOO^-$ and HONOOH are strong oxidizing agents and produce NO_2^-:

$$ONOO^- + 2H^+ + e^- \rightarrow NO_2^- (aq) + H_2O \ldots\ldots\textbf{(iv)}$$

Therefore it can be seen that NO_2^- and NO_3^- are also metabolites of $ONOO^-$.

5.0.4 NO synthesis: an alternative pathway

However the L-arginine/NOS pathway is not the sole pathway leading to the production of NO. An alternative theory for NO synthesis was recently published [15] . In hypoxic conditions, NO is produced by the reduction of NO_2^-. It was hypothesised that the reduction of NO_2^- may serve to prevent a drop in NO when oxygen levels fall and production from NOS becomes insufficient. The author therefore concluded that NO_2^- is not merely an oxygenised product of NO, but also has a significant biological role. In short, NO_2^- is not a metabolic end product of NOS activity, but must also be considered as a precursor of NO production under hypoxic conditions. In their recent review paper Vitturi *et al*.[23] acknowledged that the recent interest in NO_2^- biology stems from the realisation that the generation of NO from NO_2^- reduction can occur *"under conditions that span a range of oxygen tensions and pH observed over the pathophysiological spectrum"*. Ford [24] concurred and stated that the nitrite ion has received renewed attention and that much of mammalian biology of both NO and NO_2^- involves heme proteins. Feelish [15] however, cautions that *"without understanding the relative contribution of local versus systemic factors, knowing what the concentration of nitrite/nitrate is in synovial fluid or blood is of limited value"*. He believed this was relevant to the study of OA as oxygen availability in the joint is somewhat intermittent and usually significantly lower than other tissues. In addition, during inflammation the concentration of O_2 is further reduced. However it is interesting to note that in the same year as Feelisch's paper, Vuolteenaho *et al.* [9] stated that *"Increased concentrations of nitrite in synovial fluid from OA patients indicate local NO production in the joint"*. It would appear then that the clinical importance of NO_2^- levels in the joint remains to be elucidated.

5.0.5 The role of NO in the destruction of articular cartilage

It has been shown by a number of groups that iNOS is expressed by the chondrocyte and that the chondrocyte is the major source of NO in the joint [4, 9, 25, 26]. Other sources of iNOS are the synovium and infiltrating inflammatory cells e.g. neutrophils and

macrophages. Vuolteenaho *et al.* [9] list a number of cytokines and other factors which if unregulated, promote the synthesis of iNOS by the chondrocyte and by extension, the up-regulation of NO. These include Il-1, TNF-α, Il-17, IFN-γ, bacterial LPS, fibronectin fragment (FN-f), shear stress, endothelin-1 (ET-1) and finally, leptin in synergy with Il-1 or IFN-γ. A brief summary of the effects of excessive NO production on cartilage may be seen in Figure 5.2.

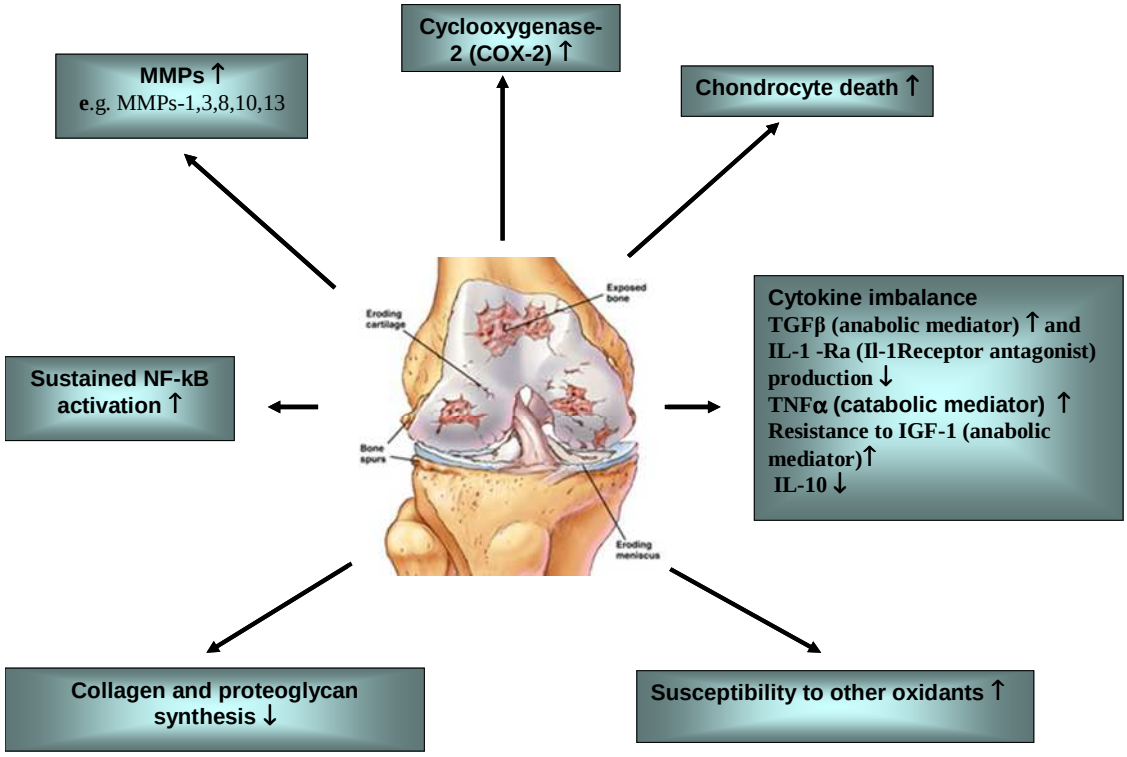

Figure 5.2: *Summary of the effects of excess NO on cartilage in the OA joint.*

As noted in the introduction, OA is a complex, multi-faceted and highly heterogeneous pathological condition. Therefore, it is not suggested that NO production, its metabolites and their potential effects on cartilage, are the sole contributors to the onset of OA. Rather, it may be one of many causes for this disease or indeed it may have little to contribute to the initial triggering of OA. Feelish [15] stated that we still do not know how NO functions, whether it is *"friend or foe"*, or even if *in vitro* studies mirror the *in vivo* hypoxic metabolism of the joint. He finally concludes "*Thus, the question as to whether*

NO is of benefit or detriment in OA remains open." More recently, Jedlickova [27] proposed a renewed interest in plasma levels of NO_2^- as a marker of endothelial function in relation to ageing. It was noted by the author that there are conflicting reports on NO levels with increasing age with some authors reporting decreasing levels with increasing age, while others have reported the converse. Ford [24] remarks that although NO_2^- was once thought to be physiologically deleterious by contributing to amine nitrosation, recent research suggests that endogenous NO_2^- may play a role in vasodilation under hypoxic conditions and in organ protection during incidents of ischemia. Indeed, Hines *et al.*[28] proclaimed that therapeutic uses of NO or NO_2^- are currently underway in several different laboratories to treat a variety of ischemic disorders.

5.0.6 Nitric Oxide in Microvesicles

Vitturi *et al.* [23] studied the biochemical schemes for NO production and their findings led them to ask the question - how could NO signalling activity escape savaging by ferrous heme? A number of hypothesis were explored, one of which is the possible compartmentalisation of NO_2^- reduction away from excess ferrous heme. In particular, the authors argue the production of N_2O_3 in equation (iii) above, might under physiological conditions; require special spatial localisation conditions in red blood cells. Relatively little is known about how nitrite reductase proteins and their ability to reduce NO_2^- to NO are regulated by availability of cofactors and substrates, the level of expression, post translational modification, or cellular/tissue localization. In a separate study [29] it was found that sub-cellular compartmentalization of distinct NO_2^- reducing activities have been reported in the liver. Figure 5.3 depicts a summary of the current perspectives on the regulation and function of NO_2^- as a mediator of NO signaling. Though this represents NO_2^- uptake into the cell, from the viewpoint of this project, what is interesting about this figure is the ability of NO_2^- to traverse bi-lipid membranes, whether by facilitated transport or passive diffusion. Either of these transport modes may offer a route for NO_2^- into MVs.

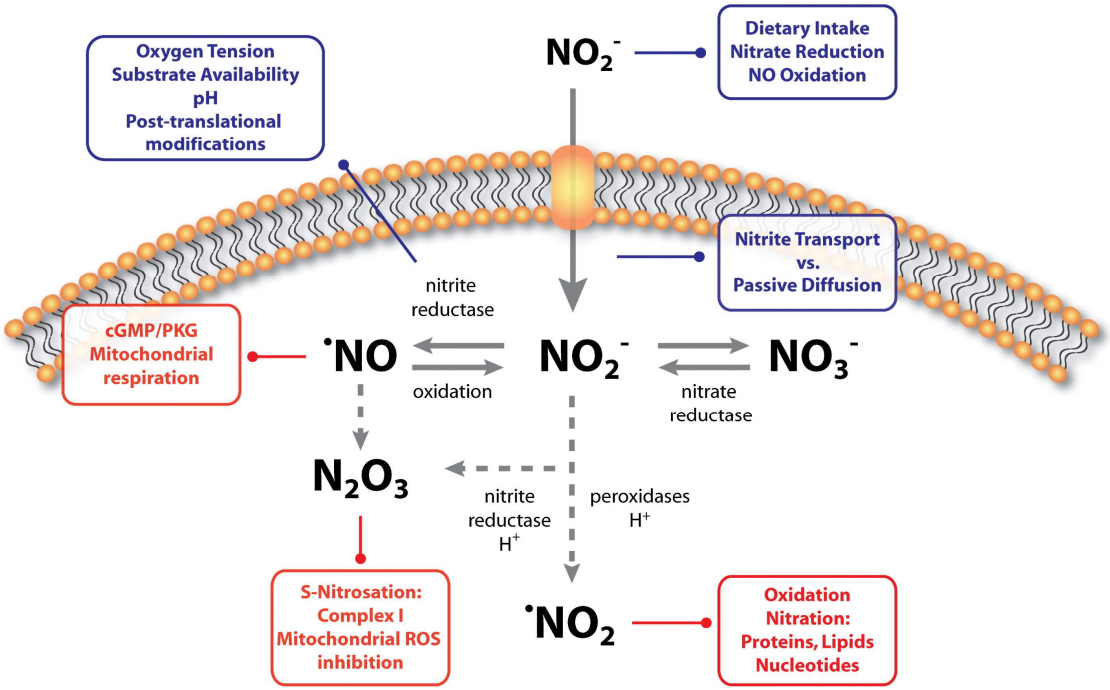

Figure 5.3: *Schematic diagram outlining current perspectives on the regulation and role of nitrite as a mediator of NO signaling. The blue boxes show known and potential mechanisms for nitrite transport and reduction to NO. The red boxes summarise known and potential targets for NO and other RNS. Diagram taken from Vitturi et al.* [23]

5.0.7 Aim of project

Due to the relatively recent resurge of interest in the biology of NO_2^-, and in particular, its probable role as a precursor to the formation of NO, the aim of this project is to ascertain if this anion is present in microvesicles which may offer a "safe" environment for reduction of NO_2^- to NO and subsequent delivery to a specific target, thus avoiding NO scavenging. As outlined above, the detection of NO_2^- in whole synovial fluid has been studied before, but no literature has been discovered pertaining to the presence of NO_2^- in microvesicles. This is important especially in light of Vitturi's [23] comment, *"The major challenges remain theoretical in trying to rationalize NO formation and bioactivity in the presence of ferrous heme……it is (NO_2^-) still biologically and therapeutically important, which could simply reflect the fact that activation of NO-dependant signaling pathways requires relatively low concentrations of this mediator"*. It is envisioned that

should NO_2^- prove to be present in MVs, it will be present in very low concentrations. Therefore a very sensitive and selective method of detection will be required. In order to investigate if NO_2^- is present inside MVs, it will be necessary to solublise the vesicle membrane. From a study of five different detergents Garner *et al.* [30] found β-octlyglucopyranoside (OG) to be the most effective and efficient membrane-dissolving agent. Therefore this is the detergent of choice for this project.

5.0.8 Methodologies for measurement of nitrite in biological matrices

The most commonly employed method for the analysis of NO_2^- is the Griess method [31]. This is a colorimetric method based on a two-step diazotisation reaction in which acidified NO_2^- produces a nitrosating agent which in turn reacts with sulfanilic acid to produce the diazonium ion. The second step in the assay is the coupling of the diazonium ion to N-(1-naphthyl)ethylene to form a chromophoric azo derivative. One mole of NO_2^- yields one mole of the azo dye. This method is used quite extensively in the literature. Though the Griess method is quick and simple, it does have limitations in terms of sensitivity when used to analyse biological samples. It is said that measuring NO_2^- below the μM threshold is not possible with this assay [32, 33]. Therefore, other methods have been developed to overcome this limitation.

Jobgen *et al.* [34] offer a very lucid and detailed critique of various HPLC modes of detection employed for the analysis of NO_2^-. From their paper it can be seen that fluorescence detection is an extremely sensitive method, with detection limits in the pM range. However, NO_2^- cannot be directly detected by fluorescence. Derivitisation with an appropriate reagent that yields a stable fluorescent compound is required. Fortunately, such a derivatising reagent is available and involves a one step reaction between NO_2^- and 2,3-diaminonaphthalene (DAN) to yield 2,3-naphthotriazole (NAT). The reaction is carried out in acidic conditions and proceeds to completion as seen in Figure 5.4.

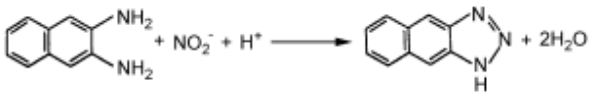

2,3-diaminonapthalene 2,3-naphthotraizole

Figure 5.4: *The reaction of nitrite with 2,3-diaminonapthalene (DAN) to form the fluorescent adduct 2,3-napthotraizole (NAT). The reaction takes place under acidic conditions.*

The NAT product was found to be stable for 24 hours [32]. The author also found that at an emission wavelength of 415nm and an excitation wavelength of 375nm, the NAT product-complex exhibits relatively high fluorescence intensity while the DAN reactant does not. This reaction offers high specificity for NO_2^-.

Therefore, analysis by HPLC employing fluorescence detection will be used to detect NO_2^- in synovial fluid microvesicles.

5.1 Materials and Methods

5.1.1 Reagents and Materials

HPLC grade methanol (MeOH) was purchased from Sigma Aldrich.
Phosphate buffer salts, $NaH_2PO_4.H_2O$ (>99%) and $Na_2HPO_4.7H_2O$ (98-102%) were purchased from Sigma.
Phosphoric Acid (>85%) was obtained from Sigma.
$NaNO_2$ (99.99%) purchased from Sigma was used to prepare standard solutions.
Amicon Ultra – 0.5mL, 3000MWCO centrifugal filters were obtained from Millipore.
2,3-diaminonapthalene (DAN) was purchased from Sigma
β-octlyglucopyranoside (OG) was purchased from Sigma

5.1.2 Miscellaneous equipment

A Hettich Mikro120 centrifuge was used for the immunoaffinity protocol.
A Gilson GV Lab vortex mixer was used mix sample and standard solutions.
A Mettler pH meter was used for mobile phase preparation

5.1.3 HPLC Instrumentation

A Waters HPLC modular system was used and comprised of the following:
1) 600E Powerline multisolvent delivery system with 100μL heads
2) 600E system controller
3) 717plus autosampler
4) 486 UV absorbance detector
5) 474 Fluorescence detector.
The instrument was controlled by Empower software.

5.1.4 HPLC Conditions

Mobile phase consisted of 15mM phosphate buffer in 55% MeOH, pH7.5
Excitation wavelength: 375nm
Emission wavelength: 415nm
Injection volume: 20μL
Flow rate: 1mL/minute
Column: Waters ACE 5 C18 250x4.6mm
All mobile phases were vacumn filtered through 0.45μM filters and then sonicated in a water bath for 5 minutes before pumping through the system.

5.1.5 Sample preparation

Whole SF was diluted by a factor of five with Milli-Q water.
For the isolation of MVs, please refer the method that was developed in chapter 3 (Figure 3.23)
MVs were burst by adding with 1% (w/v) β-octlyglucopyranoside (OG) and mixing end-over-end overnight at 4ºC
The lyased vesicles were passed through a "3kDa cut-off "centrifugal filter as per the manufacturer's instructions in order to remove proteins and lipids which would interfere with the fluorescence derivitisation [31, 32] in addition to fouling the column.

5.1.6 Preparation of Standards

A 2mM (69mg/L) NO_2^- stock solution was prepared from the sodium salt. From this a 2μM working standard was prepared. Using this working standard a series of standards were prepared by serial dilution – 0nM, 31.25nM, 62.5nM, 125nM, 250nM, 500nM, 1000nM.

5.1.7 Reaction of NO_2^- with DAN to yield NAT

A modified version of the method developed by Li *et al.* [32] was employed (details in the Discussion section).

200µL of standard/ultrafiltered sample was incubated at room temperature with 20µL 1µg/mL DAN followed by the addition of 10µL of 2.8M NaOH. 20µL of this solution was directly injected onto the HPLC column.

5.2 Results

5.2.1 Establishment of linearity range and generation of a calibration curve

The method employed was that developed by Li *et al.* [32] except a final concentration of 0.1µg/mL DAN was used instead of 5µg/mL due to high blank values (see discussion). A series of nitrite standards were run - 0nM, 31.25nM, 62.5nM, 125nM, 250nM, 500nM, 1000nM. Linearity was excellent up to 250nM. Beyond that concentration, the linearity suffered adversely. This was possibly due to the DAN reagent being completely used up. Therefore, all standard curves were prepared in the 0-250nM range. Three injections for each standard were carried out and the mean and standard deviation were calculated. An example of a calibration curve may be seen in Figure 5.5.

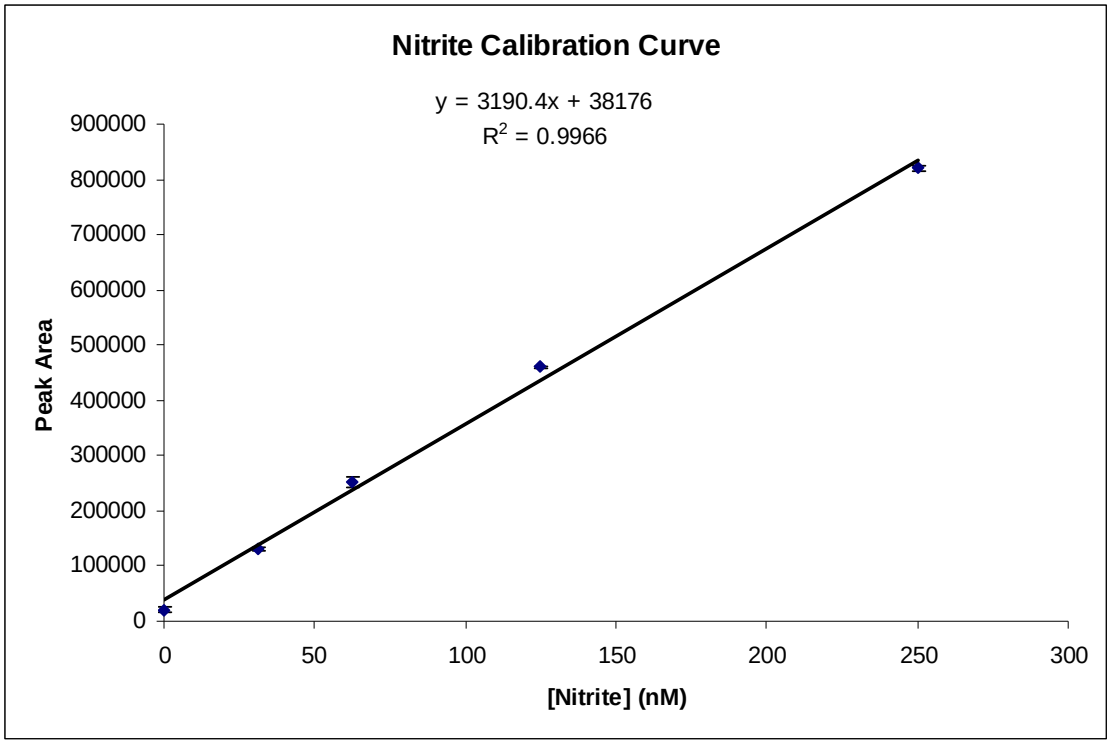

Figure 5.5*: A typical calibration curve generated from standard NO_2^- (0-250nM). Three injections per standard were carried out and the mean and standard deviation were plotted. Also included is the R^2 value. The chromatography conditions were: Mobile phase: 15mM phosphate buffer in 55% MeOH, pH7.5; Excitation wavelength: 375nm; Emission wavelength: 415nm; Injection volume: 20µL; Flow rate: 1mL/minute; Column: Waters ACE 5 C18 250x4.6mm*

5.2.2 Establishment if the Microcon ultracentrifugation filters are a source of NO_2^-

Prior to performing a HPLC experiment on any biofluid, it is important to remove proteins and other high molecular weight species that may interfere with the analysis or as discovered in chapter 2, irreversibly bind to the stationary phase. Initially, a C18 Waters Sep-Pak filter was selected as the means to remove proteins etc. However the formic acid present, which acts as an ion-pairing reagent in order to increase the hydrophobicity of the proteins, interfered with the subsequent fluorescent derivitisation of NO_2^-.

Therefore these unwanted species were removed using an ultra-filtration device with a 3kDa molecular weight "cut-off". However, centrifuge filters are known to be a source of nitrite. This is due to the possible presence of azide which may be added to preserve the cellulose or other filter matrix [11]. Smith *et al.* [35] performed a study on ten commercially available filters from a number of manufacturers. One of the filters studied was the 3kDa cut-off filter that was used in this experiment. They pre-washed the filter three times prior to analysis and found that the $[NO_2^-]$ was $0.7 \pm 0.1\mu M$. Li *et al.* [32] also found that some filters may contain nitrite and/or nitrate and therefore the filters should be washed four times with distilled water prior to use. A filter study was therefore performed in order to establish NO_2^- levels, and determine the amount of washing required. Chromatograms from this study are displayed in Figure 5.6. After the fourth wash, further washing did not reduce $[NO_2^-]$ below ~15nM. Therefore, all filter devices were washed four times before sample filtration.

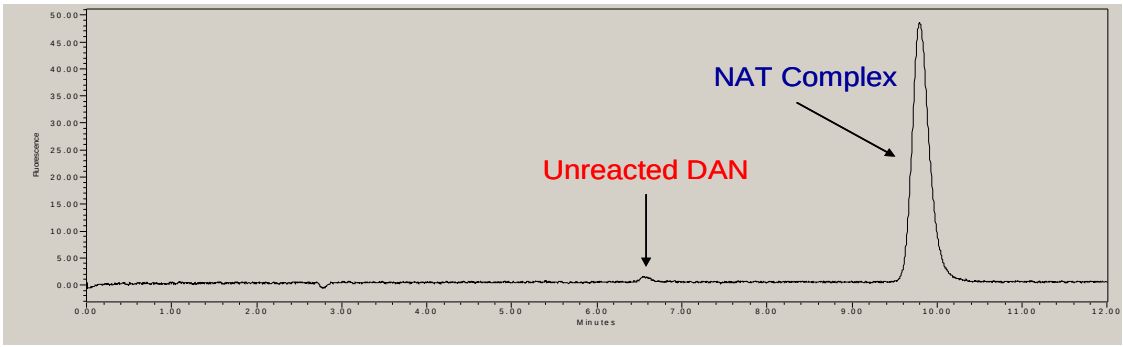

Wash 1: [NO_2^-] = 204nM

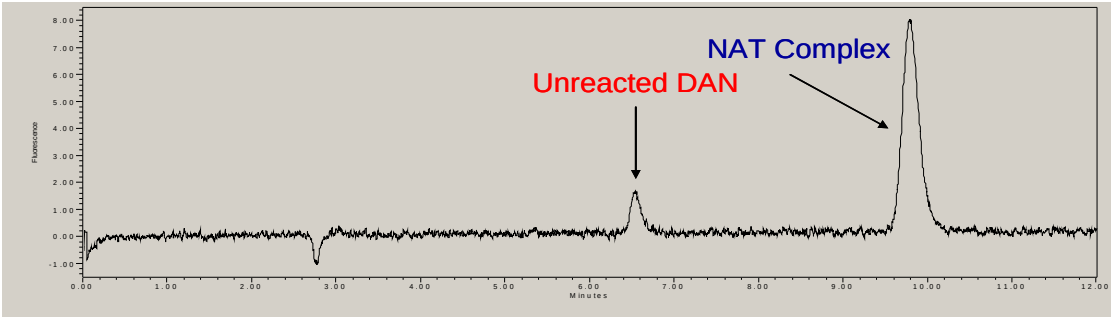

Wash 2: [NO_2^-] = 23nM

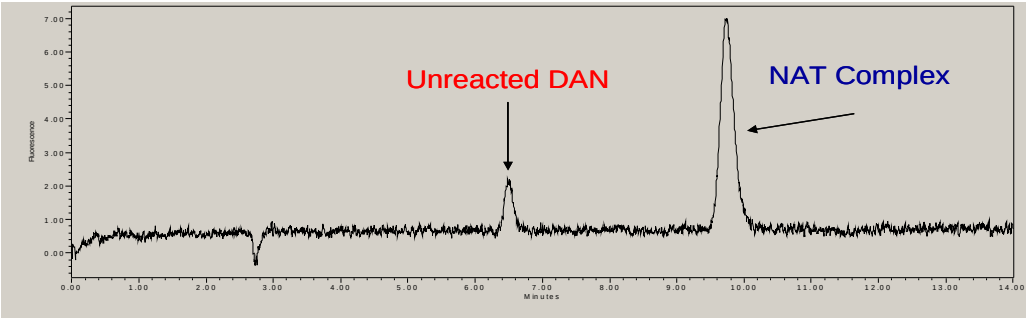

Wash 3: [NO_2^-] = 17nM

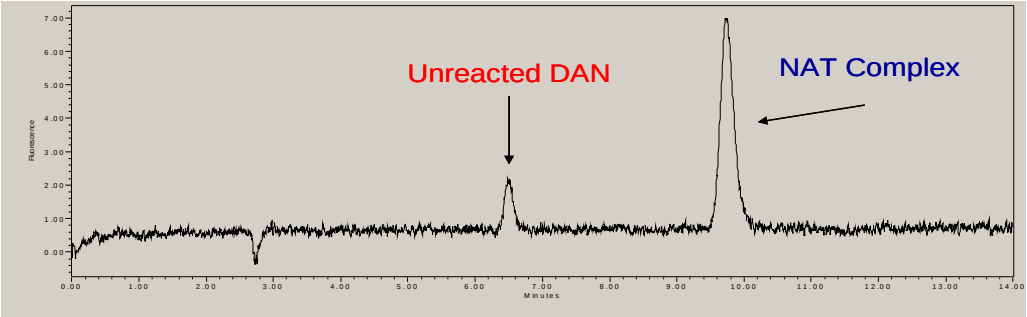

Wash 4: [NO_2^-] = 15nM

Figure 5.6: *Chromatograms resulting from a series of consecutive washes through a Microcon ultracentrifugation device. The unreacted fluorescent DAN and the NAT complex (i.e. NO_2^-) are indicated. The chromatography conditions were: Mobile phase: 15mM phosphate buffer in 55% MeOH, pH7.5; Excitation wavelength: 375nm; Emission wavelength: 415nm; Injection volume: 20µL; Flow rate: 1mL/minute; Column: Waters ACE 5 C18 250x4.6mm*

5.2.3 Establishment if β-octylglucopyranoside (OG) releases further NO_2^- from the filtration device

As 1% (w/v) OG is used to lyase the MVs, it was deemed this would be an appropriate blank. Therefore, following four washes with Milli-Q water, a 1% (w/v) OG solution was filtered and the eluate was analysed employing the established method with three injections. A chromatogram is shown in Figure 5.7.

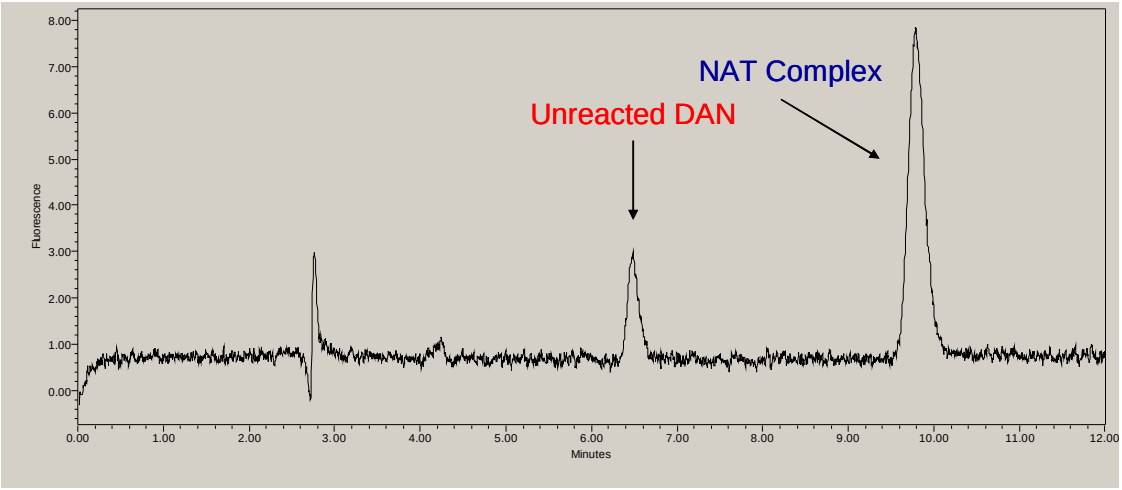

1% OG Blank: [NO_2^-] 19nM

Figure 5.7: *Chromatogram of 1% (w/v) OG which is used as a control blank. Unreacted fluorescent DAN, and the NAT complex (i.e. NO_2^-) are indicated. The chromatography conditions were: Mobile phase: 15mM phosphate buffer in 55% MeOH, pH7.5; Excitation wavelength: 375nm; Emission wavelength: 415nm; Injection volume: 20µL; Flow rate: 1mL/minute; Column: Waters ACE 5 C18 250x4.6mm*

As the water only blank contained 15nM NO_2^- and the OG blank value was 19nM NO_2^-, it was concluded that OG does not contribute to further release of NO_2^- from the filtration devices.

5.2.4 Determination of $[NO_2^-]$ in whole synovial fluid

One OA and one RA synovial fluid sample were taken, diluted by a factor of five with Milli-Q water and filtered to remove proteinaceous material. Dilution was necessary to ensure nitrite concentrations would fall within the calibration curve. Following fluorescence derivitisation, the samples were analysed by HPLC. Chromatograms from both patient samples are shown in Figure 5.8.

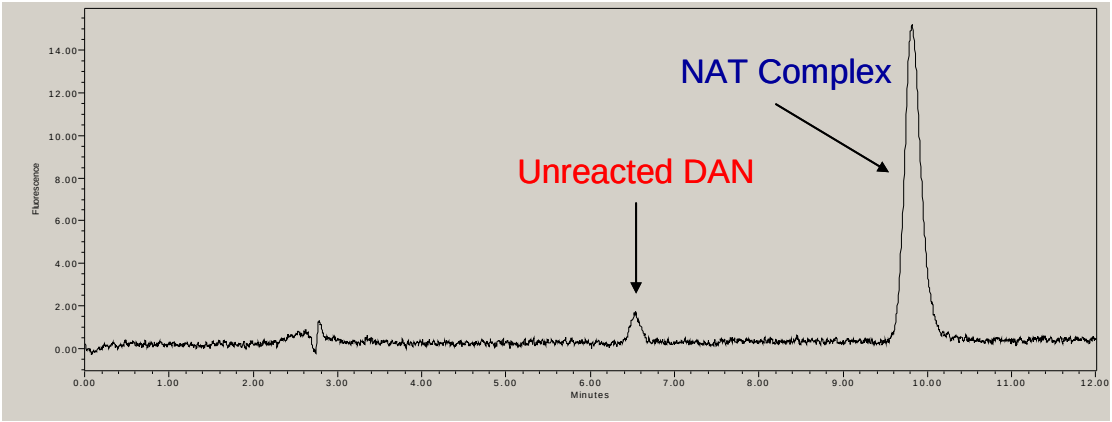

OA whole SF diluted by a factor of 5: $[NO_2^-]$ 54nM

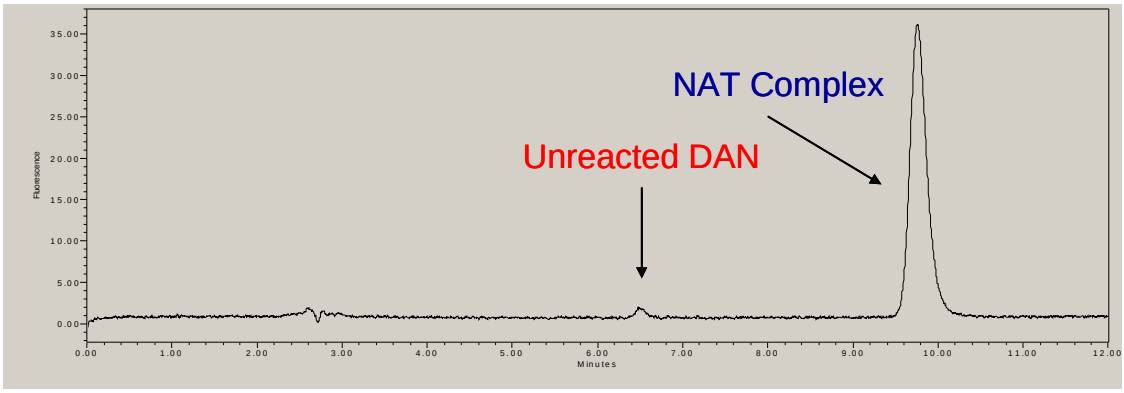

RA whole SF diluted by a factor of 5: $[NO_2^-]$ 144nM

Figure 5.8: *Chromatogram of one OA and one RA whole synovial sample diluted in water by a factor of five. Unreacted fluorescent DAN, and the NAT complex (i.e. NO_2^-) are indicated. The chromatography conditions were: Mobile phase: 15mM phosphate buffer in 55% MeOH, pH7.5; Excitation wavelength: 375nm; Emission wavelength: 415nm; Injection volume: 20μL; Flow rate: 1mL/minute; Column: Waters ACE 5 C18 250x4.6mm*

From Figure 5.8 it can be seen that [NO_2^-] in the diluted OA sample is 54nM, while that in the RA sample is 144nM. This means that [NO_2^-] in whole synovial fluid for the OA and RA patient sample is 270nM and 720nm respectively. These concentrations are similar to those found in the literature (~ 100-4000nM [11]). The nitrite concentration in the RA sample is three times that of the OA sample.

5.2.5 Determination of [NO_2^-] in 200,000g CHAPS Pellet

Reconstituted 200,000g CHAPS pellets from one OA and one RA samples were treated with 1% (w/v) OG and mixed end-over-end overnight at 4ºC. Following filtration, derivitisation with DAN took place, and each sample was analysed by HPLC. Chromatograms for this analysis are shown in Figure 5.9.

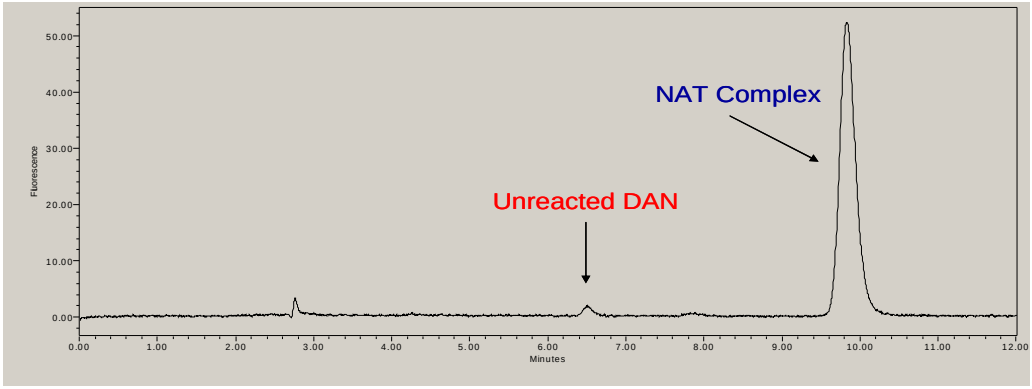

OA 200,000g CHAPS Pellet: [NO_2^-] 225nM

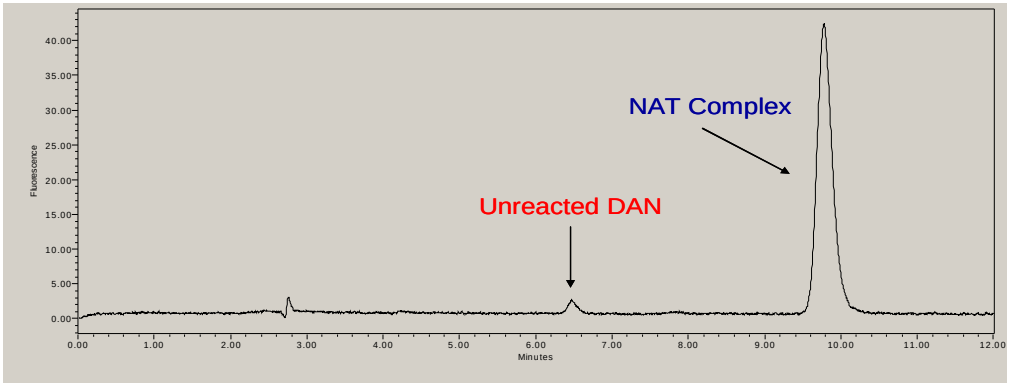

RA 200,000g CHAPS Pellet: [NO_2^-] 174nM

Figure 5.9: *Chromatogram of one OA and one RA 200,00g CHAPS pellets. Unreacted fluorescent DAN, and the NAT complex (i.e. NO_2^-) are indicated. The chromatography conditions were: Mobile phase: 15mM phosphate buffer in 55% MeOH, pH7.5; Excitation wavelength: 375nm; Emission wavelength: 415nm; Injection volume: 20µL; Flow rate: 1mL/minute; Column: Waters ACE 5 C18 250x4.6mm*

Analysis of the 200,000g CHAPS pellets clearly demonstrates that NO_2^- is present in both OA and RA microvesicles at concentrations of 225nM and 174nM respectively.

Finally, the crude 200,000g supernatant samples, corresponding to the CHAPS pellets above, were also analysed, and yielded nitrite concentrations of 95nM for OA and 259nM for RA. It was noted that the level of NO_2^- is higher in the MV fraction than in the SN fraction for the OA sample while the converse is true in the case of RA. However, this is not offered as a hypothesis. Clearly, a large cohort of patient samples would need to be analysed before making any quantitative claims relating to the distribution of NO_2^- between the pellet and the SN. However, the analysis did accomplish the original qualitative aim of the study by establishing that NO_2^- is associated with SF MVs following vesicle solubilisation with OG.

5.3 Discussion

As outlined in the introduction to this chapter, interest in the role that NO plays in the body has received considerable attention (Ford [24] quoted some 10^4 publications in the last two decades). Previously believed to be a metabolite of NO activity, NO_2^- is now appreciated as a source of NO under hypoxic conditions [15]. However, given its short half life in the presence of heme proteins, many studies were undertaken to ascertain how the reduction of NO_2^- to NO might be realised before being scavenged by heme proteins. Also from the introduction, the hypothesis that SF MVs could harbour NO_2^- and thus act as possible NO-producing sites was ventured. Therefore a novel study was undertaken to establish this possibility.

It was believed that the concentration of nitrite ($[NO_2^-]$) in MV would be very low and so a sensitive method of analysis would therefore be needed. A literature search established that a HPLC method based on fluorescence detection offered the greatest sensitivity. One such method was developed by Li *et al*. [32] However, it was found in this project that the blank (water) yielded a high NO_2^- concentration. It was established that the Millipore micron filtration device (employed to remove proteins, due to the fluorescence quenching effect they exert) was the source of this exogenous NO_2^-. Therefore, prior washing with water was necessary to bring the blank value within acceptable levels. However, when applied to the analysis of the 200,000g pellet, the magnitude of this black value became unacceptable i.e. the $[NO_2^-]$ in the sample was less than three times the $[NO_2^-]$ in the blank. Further washing with water was ineffective, as was washing with 0.1M NaOH (as recommended by the supplier). A publication by Gharavi *et al*. [36] also employed Li's method, except a final concentration of 0.1μg/mL DAN was used instead of 5μg/mL. This was found to be successful in significantly reducing the blank value to 15nM (Figure 5.6). A linear range of 0-250nM NO_2^- was established with R^2=0.9966. Concentrations greater than 250nM, adversely affected the R^2 value, most likely due to total consumption of the DAN fluorescent agent at higher concentrations.

The detergent employed to rupture the MV membranes was 1% (w/v) OG, and therefore this was the blank used. This did not contribute to further NO_2^- from the filtration device

(Figure 5.7) after washing with Milli-Q water. One OA and one RA sample were analysed and the [NO_2^-] was measured in the whole SF (Figure 5.7) and the 200,000g pellet (Figure 5.8) of each. As only one patient sample was analysed representing each pathology, it was not possible to infer a meaningful hypothesis based on the quantitative data obtained. However, the aim of this study was to establish the presence of NO_2^- in MVs. This was achieved and it was confirmed that NO_2^- is present in MVs. Advancing a hypothesis concerning the implication of this on the other hand may ignite interest to further study.

Studies by Feelish *et al.* [15, 29] have established that the presence of NO_2^- under hypoxic conditions lead to NO formation. This is particularly pertinent in the joint environment where hypoxic conditions exist. Under these conditions, the formation of NO by reduction of NO_2^- may be a more realistic model than the formation of NO by the classic iNOS pathway, (Figure 5.1) where O_2 was seen to be a critical co-factor in this metabolic pathway. A caveat to this suggestion was recognised by Ford [24] and Vitturi *et al.* [23] and related to the conundrum; how can NO be produced from NO_2^- and survive being rapidly scavenged by ferrous heme? Various schemes were offered by the authors, but each encountered objections on kinetic grounds. On three occasions in their publication Vitturi *et al.* [23] alluded a protective micro-environment; *"Compartmentalization of nitrite reduction away from excess ferrous heme is one potential strategy by which the kinetic barriers discussed above are bypassed"……"..under physiological conditions might require special spatial localization conditions…"* and *"Emerging data are shedding some insights…For example, subcellular compartmentalization of distinct nitrite-reducing activities have been reported in the liver"*. However, there was no suggestion that MVs may offer this micro-environment. Two factors support this proposition that MVs are plausible NO-producing sites. The first is a result of this current study which established that NO_2^- is associated with MVs and the second is that there is a mode of entry for NO_2^- into the vesicle (Figure 5.3).

The discussion thus far has centred on the tenet that NO_2^- which is present in SF MVs is a precursor to the formation of NO. However, the converse may be true i.e. NO initially present in vesicles may have undergone oxidation to NO_2^-. In light of the discussion thus

far, the presence of hemoglobin would ensure this. From the MS data in chapter 3, hemoglobin subunits alpha and beta were found to be associated with MVs. This possibility depends on the oxygen tension is the micro-locality i.e. the presence of deoxygenated versus oxygenated hemoglobin [23]. In deoxygenated conditions the reduction of NO_2^- to NO is favoured, while in an oxygenated environment, oxidation of NO to NO_2^- and finally to NO_3^- is the case. That NO_2^- was found in MVs and these vesicles in turn were in a hypoxic setting, any hemoglobin present was likely to be deoxygenated. Therefore, how is oxidation of NO to NO_2^- achieved? Another protein species that was identified by MS was ceruloplasmin. Shiva *et al*. [37] termed this protein "*a NO oxidase and nitrite synthase"*. Ceruloplasmin is a 132 kDa protein containing six copper centres [38] and the redox reaction proceeds as follows;

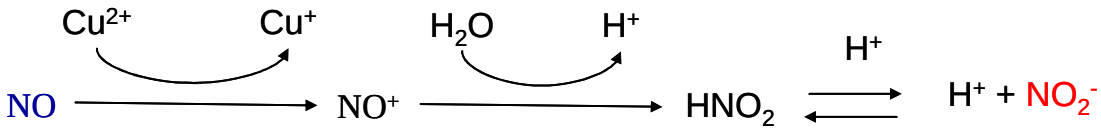

5.4 Conclusion

This study established for the first time that NO_2^- is present in MVs. It was not possible to determine the type of vesicle that harbour this anion, but some potentially interesting speculations have been proposed that may account for questions that were raised in the literature. In particular, it may be that MVs afford a sub-cellular microenvironment that is compatible to the chemistry of NO and/or NO_2^-. Potentially fruitful future work could establish if there are unique protein nitrosylation reactions taking place inside vesicles that may not occur in the cytoplasm of the cell or in the ECM. The hypothesis that different vesicle types may possess unique biochemical sites is plausible and future study into MVs is needed. A potentially useful starting point may be directed towards the isolation of homogeneous vesicle types. In that way it would be easier to classify and establish the true purpose of MVs in the body.

5.5 References

References

(1) Moncada, S.; Higgs, A. The L-Arginine-Nitric Oxide Pathway. *The New England Journal of Medicine* **1993**, *329*, 2002-2012.

(2) Furchgott, R. F.; Zawadzki, J. V. The Obligatory Role of Endothelial-Cells in the Relaxation of Arterial Smooth-Muscle by Acetylcholine. *Nature* **1980**, *288*, 373-376.

(3) Ignarro, L. J.; Buga, G. M.; Wood, K. S.; Byrns, R. E.; Chaudhuri, G. Endothelium-Derived Relaxing Factor Produced and Released from Artery and Vein is Nitric-Oxide. *Proceedings of the National Academy of Sciences of the United States of America* **1987**, *84*, 9265-9269.

(4) Jang, D.; Murrell, G. A. C. Nitric Oxide in Arthritis. *Free Radical Biology and Medicine* **1998**, *24*, 1511-1519.

(5) Bredt, D. S.; Hwang, P. M.; Glatt, C. E.; Lowenstein, C.; Reed, R. R.; Snyder, S. H. Cloned and Expressed Nitric-Oxide Synthase Structurally Resembles Cytochrome-P-450 Reductase. *Nature* **1991**, *351*, 714-718.

(6) Xie, Q. W.; Cho, H. J.; Calaycay, J.; Mumford, R. A.; Swiderek, K. M.; Lee, T. D.; Ding, A. H.; Troso, T.; Nathan, C. Cloning and Characterization of Inducible Nitric-Oxide Synthase from Mouse Macrophages. *Science* **1992**, *256*, 225-228.

(7) Lamas, S.; Marsden, P. A.; Li, G. K.; Tempst, P.; Michel, T. Endothelial Nitric-Oxide Synthase - Molecular-Cloning and Characterization of a Distinct Constitutive Enzyme Isoform. *Proceedings of the National Academy of Sciences of the United States of America* **1992**, *89*, 6348-6352.

(8) Abramson, S. B.; Amin, A. R.; Clancy, R. M.; Attur, M. The role of nitric oxide in tissue destruction. *Best Practice & Research Clinical Rheumatology* **2001**, *15*, 831-845.

(9) Vuolteenaho, K.; Moilanen, T.; Knowles, R. G.; Moilanen, E. The role of nitric oxide in osteoarthritis. *Scandinavian Journal of Rheumatology* **2007**, *36*, 247-U5.

(10) Tzeng, E.; Billiar, T. R.; Robbins, P. D.; Loftus, M.; Stuehr, D. J. Expression of Human Inducible Nitric-Oxide Synthase in a Tetrahydrobiopterin (H4b)-Deficient Cell-Line - H4b Promotes Assembly of Enzyme Subunits into an Active. *Proceedings of the National Academy of Sciences of the United States of America* **1995**, *92*, 11771-11775.

(11) Ellis, G.; Adatia, I.; Yazdanpanah, M.; Makela, S. K. Nitrite and Nitrate Analyses: A Clinical Biochemistry Perspective. *Clinical Biochemistry* **1998**, *31*, 195-220.

(12) J. MacMicking; Qi. Xie, C. N. Nitric Oxide and Macrophage Function. *Annual Review of Immunology* **1997**, *15*, 323-350.

(13) Wollheim F.A. In *Pathogenesis of osteoarthritis;* MC Hochberg, Ed.; Rheumatology; Mosby: 2003; Vol. 1, pp 1801.

(14) Everett, S. A.; Dennis, M. F.; Tozer, G. M.; Prise, V. E.; Wardman, P.; Stratford, M. R. L. Nitric oxide in biological fluids: analysis of nitrite and nitrate by high-performance ion chromatography. *Journal of Chromatography A* **1995**, *706*, 437-442.

(15) Feelisch, M. The chemical biology of nitric oxide — an outsider's reflections about its role in osteoarthritis. *Osteoarthritis and Cartilage* **2008**, *16*, S3-S13.

(16) R. Korhonen, A. Lahti, H. Kankaanranta, E Moilanen Nitric oxide production and signaling in granulocytic inflammation. *Current Drug Targets - Inflammation & Allegry* **2005**, *4*, 471.

(17) Boudko, D. Y. Bioanalytical profile of the l-arginine/nitric oxide pathway and its evaluation by capillary electrophoresis. *Journal of Chromatography B* **2007**, *851*, 186-210.

(18) Daiber, A.; Bachschmid, M.; Kavakli, C.; Frein, D.; Wendt, M.; Ullrich, V.; Munzel, T. A new pitfall in detecting biological end products of nitric oxide-nitration, nitrosylation and nitrite/nitrate artefacts during freezing. *Nitric Oxide-Biology and Chemistry* **2003**, *9*, 44-52.

(19) Abramson, S. B. Osteoarthritis and nitric oxide. *Osteoarthritis and Cartilage* **2008**, *16*, S15-S20.

(20) Squadrito, G. L.; Pryor, W. A. Oxidative chemistry of nitric oxide: the roles of superoxide, peroxynitrite, and carbon dioxide. *Free Radical Biology and Medicine* **1998**, *25*, 392-403.

(21) Bailey, S. M.; Landar, A.; Darley-Usmar, V. Mitochondrial proteomics in free radical research. *Free Radical Biology and Medicine* **2005**, *38*, 175-188.

(22) Denicola, A.; Radi, R. Peroxynitrite and drug-dependent toxicity. *Toxicology* **2005**, *208*, 273-288.

(23) Vitturi, D. A.; Patel, R. P. Current perspectives and challenges in understanding the role of nitrite as an integral player in nitric oxide biology and therapy. *Free Radical Biology and Medicine* **2011**, *51*, 805-812.

(24) Ford, P. C. Reactions of NO and Nitrite with Heme Models and Proteins. *Inorganic chemistry* **2010**, *49*, 6226-6239.

(25) Stadler, J.; Stefanovic-Racic, M.; Billiar, T.; Curran, R.; McIntyre, L.; Georgescu, H.; Simmons, R.; Evans, C. Articular chondrocytes synthesize nitric oxide in response to cytokines and lipopolysaccharide. *The Journal of Immunology* **1991**, *147*, 3915-3920.

(26) Rediske, J. J.; Koehne, C. F.; Zhang, B.; Lotz, M. The inducible production of nitric oxide by articular cell types. *Osteoarthritis and Cartilage* **1994**, *2*, 199-206.

(27) Jedlicková, V.; Paluch, Z.; Alusík, S. Determination of nitrate and nitrite by high-performance liquid chromatography in human plasma. *Journal of Chromatography B* **2002**, *780*, 193-197.

(28) Hines, I. N.; Grisham, M. B. Divergent roles of superoxide and nitric oxide in liver ischemia and reperfusion injury. *Journal of Clinical Biochemistry and Nutrition* **2011**, *48*, 50-56.

(29) Feelisch, M.; Fernandez, B. O.; Bryan, N. S.; Garcia-Saura, M. F.; Bauer, S.; Whitlock, D. R.; Ford, P. C.; Janero, D. R.; Rodriguez, J.; Ashrafian, H. Tissue Processing of Nitrite in Hypoxia - an intricate interplay of nitric oxide-generating and scavenging systems. *Journal of Biological Chemistry* **2008**, *283*, 33927-33934.

(30) Garner, A.; Smith, D. A.; Hooper, N. Visualization of detergent solubilization of membranes: Implications for the isolation of rafts. *Biophysical Journal* **2008**, *94*, 1326-1340.

(31) Fernández-Cancio, M.; Fernández-Vitos, E. M.; Centelles, J. J.; Imperial, S. Sources of interference in the use of 2,3-diaminonaphthalene for the fluorimetric determination of nitric oxide synthase activity in biological samples. *Clinica Chimica Acta* **2001**, *312*, 205-212.

(32) Li, H.; Meininger, C. J.; Wu, G. Rapid determination of nitrite by reversed-phase high-performance liquid chromatography with fluorescence detection. *Journal of Chromatography B: Biomedical Sciences and Applications* **2000**, *746*, 199-207.

(33) N. Gharavi; A.O.S. El-Kadi Measurement of nitric oxide in murine Hepatoma Hepa1c1c7 cells by reversed phase HPLC with fluorescence detection. *Journal of Pharnacy & Pharmaceutical Sciences* **2003**, *6*, 302.

(34) Jobgen, W. S.; Jobgen, S. C.; Li, H.; Meininger, C. J.; Wu, G. Analysis of nitrite and nitrate in biological samples using high-performance liquid chromatography. *Journal of Chromatography B* **2007**, *851*, 71-82.

(35) Smith, C. C. T.; Stanyer, L.; Betteridge, D. J. Evaluation of methods for the extraction of nitrite and nitrate in biological fluids employing high-performance anion-exchange liquid chromatography for their determination. *Journal of Chromatography B* **2002**, *779*, 201-209.

(36) Gharavi, N.; El-Kadi, A. Measurement of nitric oxide in murine Hepatoma Hepa1c1c7 cells by reversed phase HPLC with fluorescence detection. *Journal of Pharmacy and Pharmaceutical Sciences* **2003**, *6*, 302-307.

(37) Shiva, S.; Wang, X.; Ringwood, L.; Xu, X.; Yuditskaya, S.; Annavajjhala, V.; Miyajima, H.; Hogg, N.; Harris, Z.; Gladwin, M. Ceruloplasmin is a NO oxidase and nitrite synthase that determines endocrine NO homeostasis. *Nature Chemical Biology* **2006**, *2*, 486-493.

(38) Hellman, N.; Gitlin, J. Ceruloplasmin metabolism and function. *Annual Review of Nutrition* **2002**, *22*, 439-458.